Tasmanian Geological Survey Record UR2018/04

THE EARLY CARBONIFEROUS TEBRAKUNNA DYKE SWARM, AND OTHER LATE PALAEOZOIC MAFIC-INTERMEDIATE DYKES OF EASTERN TASMANIA

by J. L. Everard, M. P. McClenaghan and D. Phillips

Department of State Growth

Tasmanian Government

Mineral Resources Tasmania

PO Box 56

Rosny Park Tasmania 7018

Phone (03) 6165 4800

Fax (03) 62338338

Email info@mrt.tas.gov.au

Internet www.mrt.tas.gov.au

September 2018

Refer to this document as:
Everard, J. L., McClenaghan, M. P. and Phillips, D. (2018). The Early Carboniferous Tebrakunna Dyke Swarm, and other late Palaeozoic mafic-intermediate dykes of eastern Tasmania. Geological Survey Record 2018/04. Mineral Resources Tasmania.

Cover photo:
Dolerite dyke intruding granite at Grant Point, near St Helens.

Tasmanian Geological Survey Record UR2018/04

THE EARLY CARBONIFEROUS TEBRAKUNNA DYKE SWARM, AND OTHER LATE PALAEOZOIC MAFIC-INTERMEDIATE DYKES OF EASTERN TASMANIA

by J. L. Everard, M. P. McClenaghan and D. Phillips

Mineral Resources Tasmania
Department of State Growth

Tasmanian Government

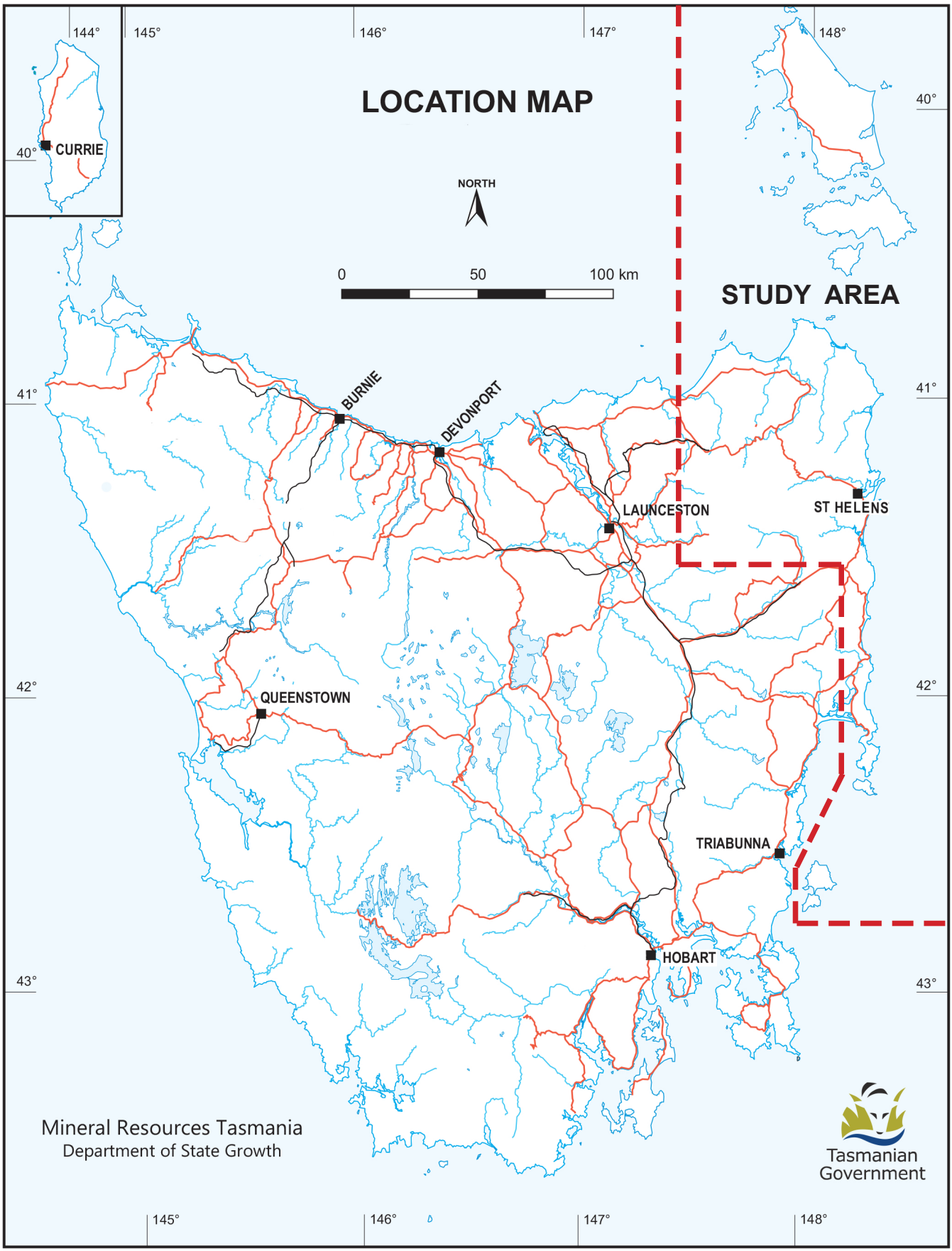
LOCATION MAP
NORTH
0
50
100 km
STUDY AREA
CURRIE
BURNIE
DEVONPORT
LAUNCESTON
ST HELENS
QUEENSTOWN
TRIABUNNA
HOBART
144°
145°
146°
147°
148°
40°
41°
42°
43°
Mineral Resources Tasmania
Department of State Growth
Tasmanian Government

Contents

List of figures

List of tables

Abstract

Dolerite dykes are widespread in eastern Tasmania, from Maria Island to the Furneaux Islands and beyond, and intrude both Devonian granites and mid-Palaeozoic Mathinna Supergroup turbidites. They are most abundant in the far northeast, north of St Helens, where a swarm of more than 20 NE- to NNE-trending mainly tholeiitic dolerite dykes comprise the Tebrakunna Dyke Swarm. Individual dykes, which are clearly resolvable on aeromagnetic imagery, can be traced for up to 6 km, are up to at least 30 m wide, and are typically subvertical with chilled margins. Elsewhere, mafic dykes are less common and more variable in orientation and composition. In the Freycinet Peninsula area, a NNW-trend predominates and alkalic compositions are more common. In the southern Furneaux Islands there are cross-cutting NE- to ENE- and NW-trending dykes of various composition.

Typically the dykes are aphyric or sparsely plagioclase-phyric, with a subophitic or intergranular groundmass of variably sericitised plagioclase, variably uralitised clinopyroxene, rare usually altered olivine, and iron – titanium oxides partly replaced by titanite. Interstitial quartz is present in many samples. Biotite, hornblende, apatite, epidote and sulphides are mostly minor to accessory constituents of some samples.

Most of the dykes (including alkalic types) show characteristic tholeiitic fractionation trends with total iron (FeO_{tot}), TiO_2 and incompatible elements all increasing with decreasing Mg#. Major- and trace-element data and Pearce Element Ratio analysis suggests that the main fractionating phases were clinopyroxene, plagioclase and olivine. Other dykes with higher SiO_2 content (ranging up to andesite) and relatively lower FeO_{tot}, CaO and TiO_2 at given Mg# form a "calc-alkaline" group. Petrographically, basaltic members of this suite differ only subtly from the other dykes, for instance in containing a greater proportion of groundmass quartz, but andesitic and more felsic samples may display obvious disequilibrium textures, and in some dykes mingling of mafic and felsic material may be apparent in outcrop.

Almost all the dykes display negative Nb anomalies on primitive mantle normalised diagrams, which is interpreted to indicate derivation from subduction-modified mantle. Some of the calc-alkaline dykes have been contaminated by assimilation of granitic wall rocks, which probably occurred concurrently with fractional crystallisation (AFC).

New ^{39}Ar-^{40}Ar dating of plagioclase separates yielded a plateau age of 334.2 ± 7.0 Ma and a total gas age of 330.2 ± 2.8 Ma for two samples from the Tebrakunna Dyke Swarm, and a similar total gas age of 333.0 ± 3.5 Ma for a dyke from Flinders Island. Although these are considered minimum ages, their consistency suggests that most of the dykes were emplaced in the Early Carboniferous, up to 40 Myr after the youngest eastern Tasmanian granites (~374 Ma). A fourth sample, from Freycinet Peninsula, yielded a total gas age of 258.1 ± 2.5 Ma, which although geologically possible, may be much younger than the emplacement age.

Introduction

Pre-Jurassic dolerite dykes are a widespread but volumetrically minor component of the pre-Late Carboniferous basement of eastern Tasmania. Mostly brief descriptions of particular occurrences are scattered throughout many papers, reports and unpublished theses (e.g., Reid and Henderson, 1928; Thomas, 1943; Blake, 1947; Walker, 1957; Groves et al., 1977; Cocker, 1977, 1980; McClenaghan et al., 1982; Hunns, 1982; Baillie, 1986; Everard, 2001; Worthing and Woolward, 2010). McClenaghan (1984) reviewed the dykes from a broader perspective, and suggested a petrogenetic relationship to the Devonian granodiorites and the Hogans Road Diorite.

Many of the dykes are found in the area of the Blue Tier 1:50 000 map sheet (McClenaghan and Williams

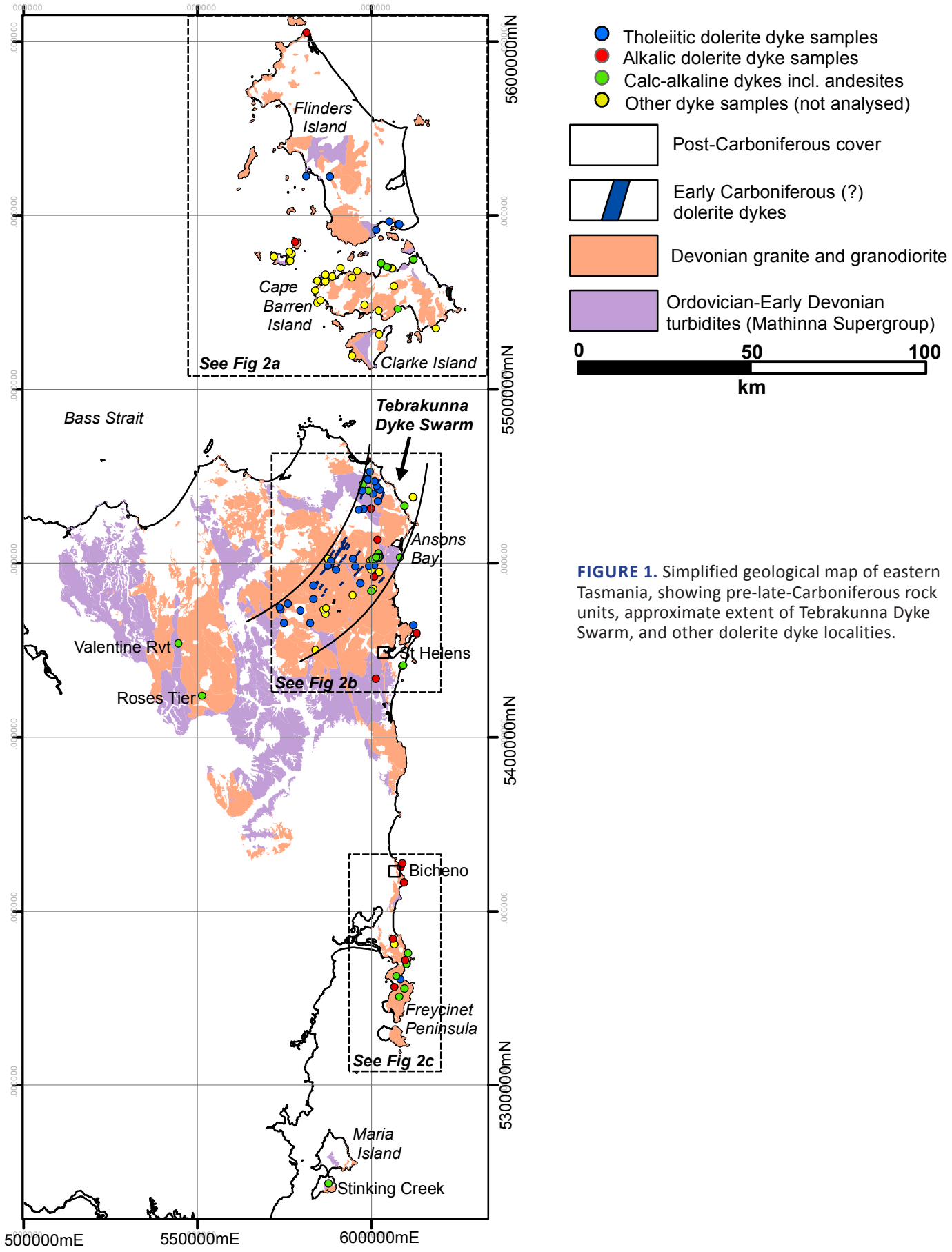

FIGURE 1. Simplified geological map of eastern Tasmania, showing pre-late-Carboniferous rock units, approximate extent of Tebrakunna Dyke Swarm, and other dolerite dyke localities.

1983), for which no explanatory notes were produced. Others occur on Freycinet Peninsula, near Bicheno and on the islands of the Furneaux Group, areas covered by only limited or reconnaissance geological mapping. The purpose of this report is to collate and integrate previous published and unpublished information on the dykes and present new information on their petrology and age. A short summary, partly based on an earlier version of this report, is given by Everard and McClenaghan (2014).

All map coordinates in this report refer to the Geocentric Datum of Australia 1994 (GDA94) and quoted strikes are with respect to true north.

Geological setting

The Palaeozoic rocks of eastern Tasmania and the Furneaux Group (of islands) are the southern extension of the Lachlan Orogen of mainland Australia. They are dominated by the Mathinna Supergroup, a quartz-rich turbidite sequence of Early Ordovician to Early Devonian age, the basement of which is not exposed, which was folded during the Middle Devonian Tabberabberan Orogeny at ~389 Ma and intruded by granites between ~400 Ma and ~374 Ma. In Tasmania, the Tabberabberan Orogeny and granite emplacement were probably the result of the juxtaposition of the Eastern and Western Tasmanian terranes (Black et al., 2010). The older, pre-deformation intrusions are mainly granodiorites, whereas the younger intrusions range from granodiorite to alkali feldspar granite. The granites were emplaced at high levels with narrow contact aureoles (Black et al., 2005; McClenaghan, 2006).

By the earliest Permian, the granites had been unroofed, and a Permian glacio-marine and Triassic fluvial shelf sequence, the Parmeener Supergroup, was deposited throughout most of Tasmania, followed by voluminous intrusion of Jurassic dolerite at ~183 Ma (Burgess et al., 2015). Following continental rifting in the Cretaceous and Early Cenozoic, uplift and erosion resulted in the removal of much this younger cover in northeastern Tasmania. Basaltic volcanism was widespread in the Cenozoic, with peaks of activity at ~47 Ma and ~16 Ma in northeastern Tasmania (Brown, 1982; Sutherland and Wellman, 1986; Everard et al., 2014 and references therein).

Distribution and trend

Dolerite dykes crop out in a 400-km-long zone parallel to the east coast of Tasmania, from Maria Island (Clarke and Baillie, 1984) in the south, to at least as far north as Hogan Island, ~90 km northwest of Flinders Island in Bass Strait (Hope et al., 1974) (Fig. 1).

The dykes are, however, most common in far northeast Tasmania, north of St Helens, on the Blue Tier and Eddystone 1:50 000 map sheets (McClenaghan and Williams, 1983; Baillie, 1984). The Tebrakunna Dyke Swarm is herein defined as that set of about twenty NE- to NNE-trending subparallel dolerite dykes that crop out between a point ~3 km east of Gardens Lagoon (~603000mE, 5444000mN) and a point ~1 km north of Old Chum Dam (~588000mE, 5455000mN). The designated type locality (strictly speaking, of the Tebrakunna Dolerite) is a large dyke cropping out near the bridge on Tebrakunna Road over the Great Musselroe River (~589100mE, 5450900mN). The Tebrakunna Dyke Swarm, as thus defined, is about 17 km wide and can be traced for about 50 km from the northeast coast near Mt William, southwest to at least as far as the Pyengana area. The trend of individual dykes swings from about 20° (from true north) in the Mt William area to 35-40° in the type area, and about 60° near Pyengana (Figs 1, 2b).

The number of known dykes falls off rapidly to the southwest. Associated magnetic anomalies (Fig. 3b), however, suggest that the main swarm continues for more than 80 km in an arcuate pattern toward Roses Tier (where a mapped dyke segment may have strike of about 70°) and the Mt Scott areas (McClenaghan et al., 1993). These are the most westerly known dykes.

Elsewhere, dolerite dykes are rarer, show a greater dispersal of strike, and are not necessarily members of the same suite. In the St Helens area, the strike of six dykes ranges from 005° to 080°; the general northeast trend is similar to, but more dispersed than the Tebrakunna Dyke Swarm immediately to the north. About fifteen known dykes between Freycinet Peninsula and Bicheno vary in strike between 100° and 180°, but with a strong mode near 160° (Figs 2c, 4c). This is particularly evident in the Friendly Beaches area, where reconnaissance mapping indicates a swarm of subparallel NNW-trending dykes (Jennings, 1984; Bacon, 1984, 1991).

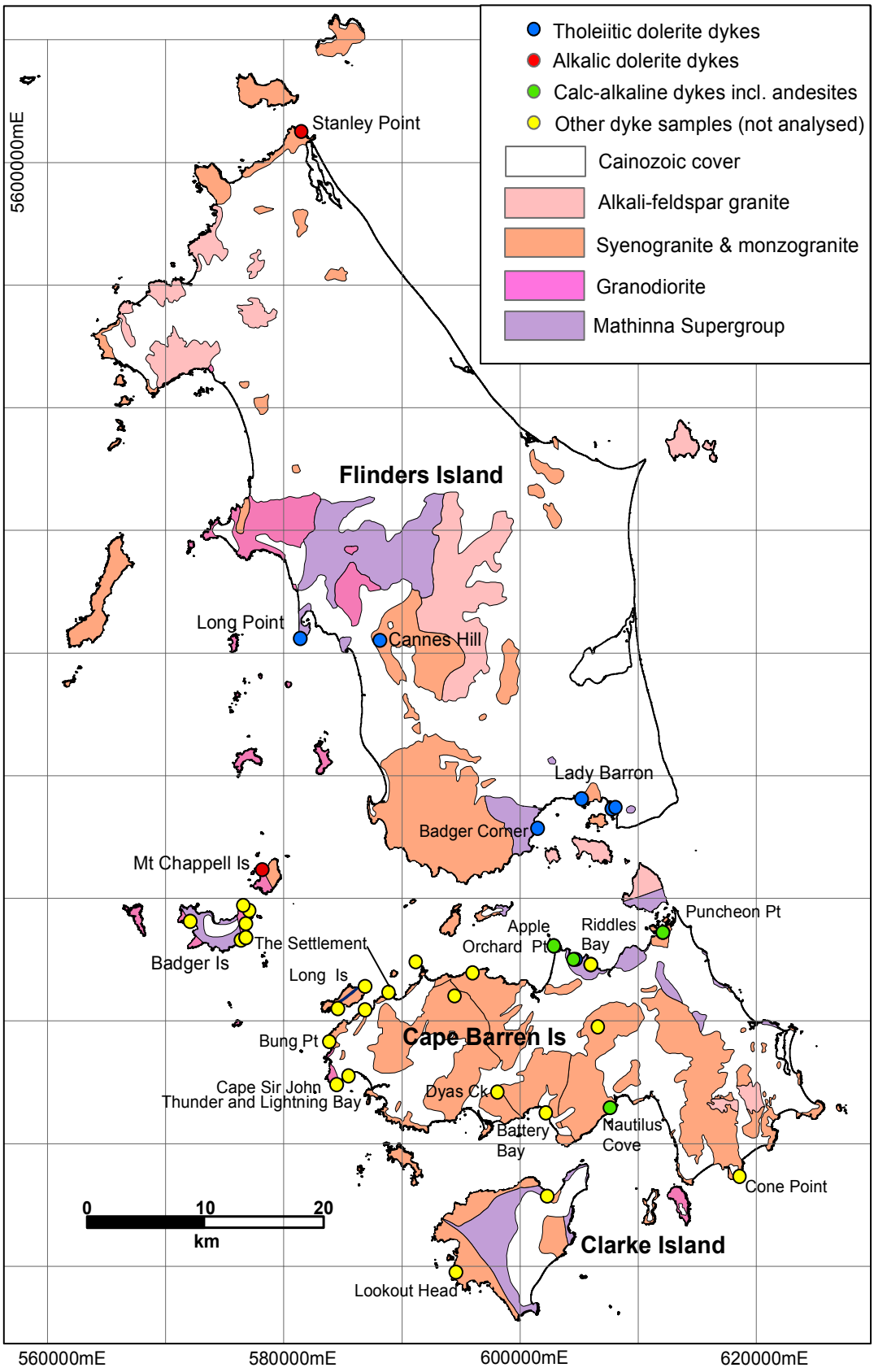

FIGURE 2a. Simplified geological maps showing location of dolerite dyke samples: Furneaux Islands area.

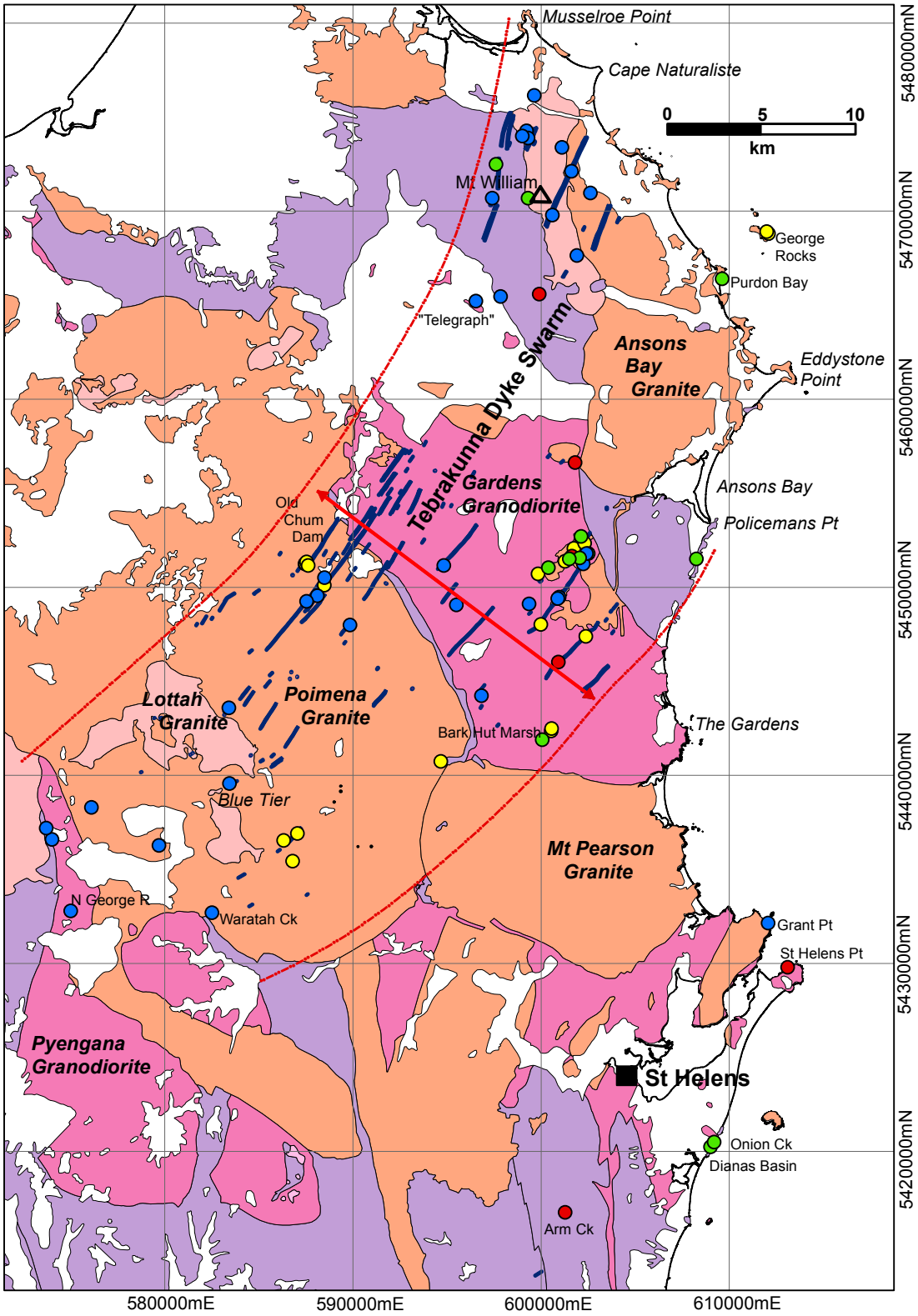

FIGURE 2b. Simplified geological maps showing location of dolerite dyke samples: St Helens-Blue Tier-Eddystone Point area.

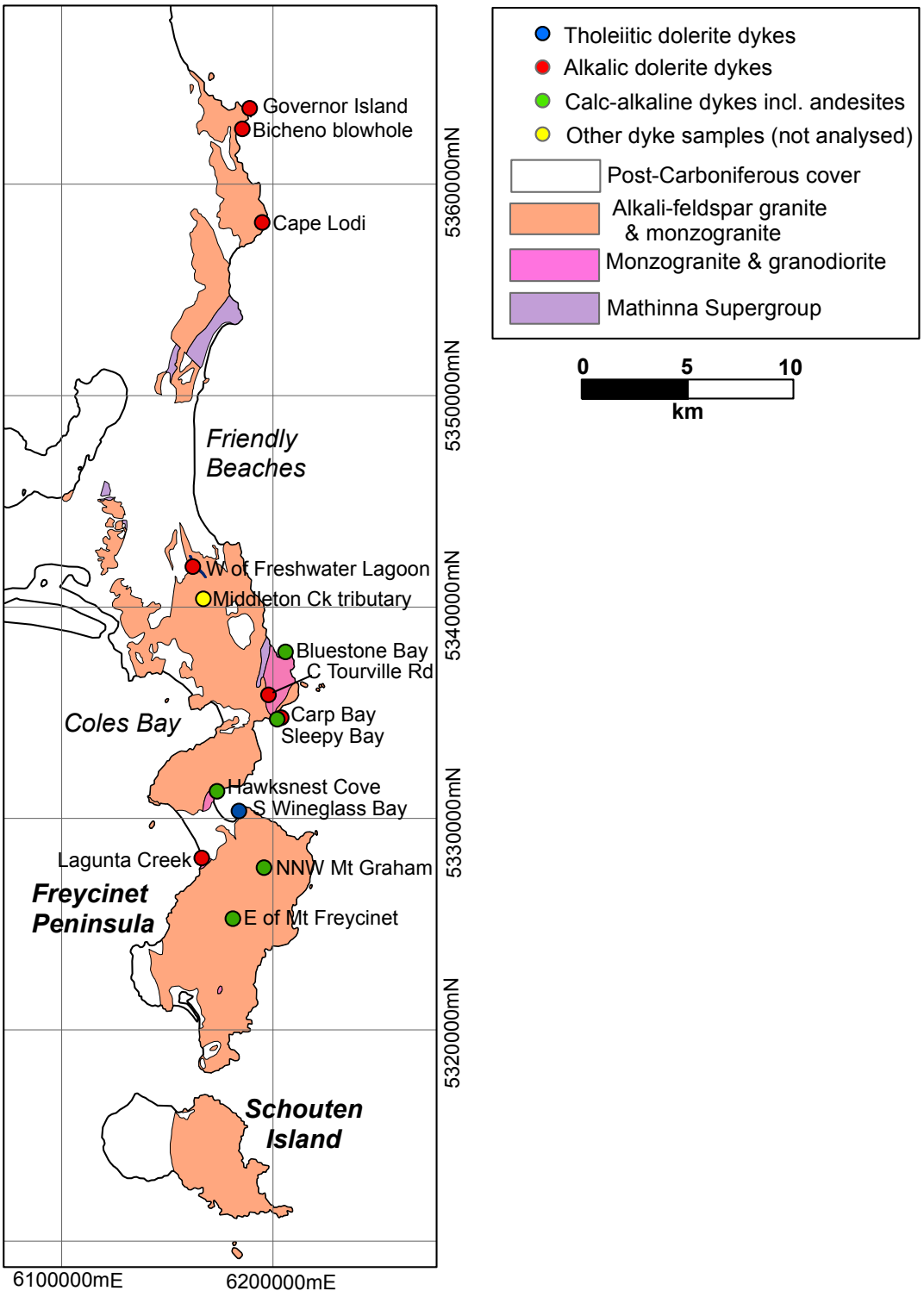

FIGURE 2c. Simplified geological maps showing location of dolerite dyke samples: Freycinet Peninsula-Bicheno area.

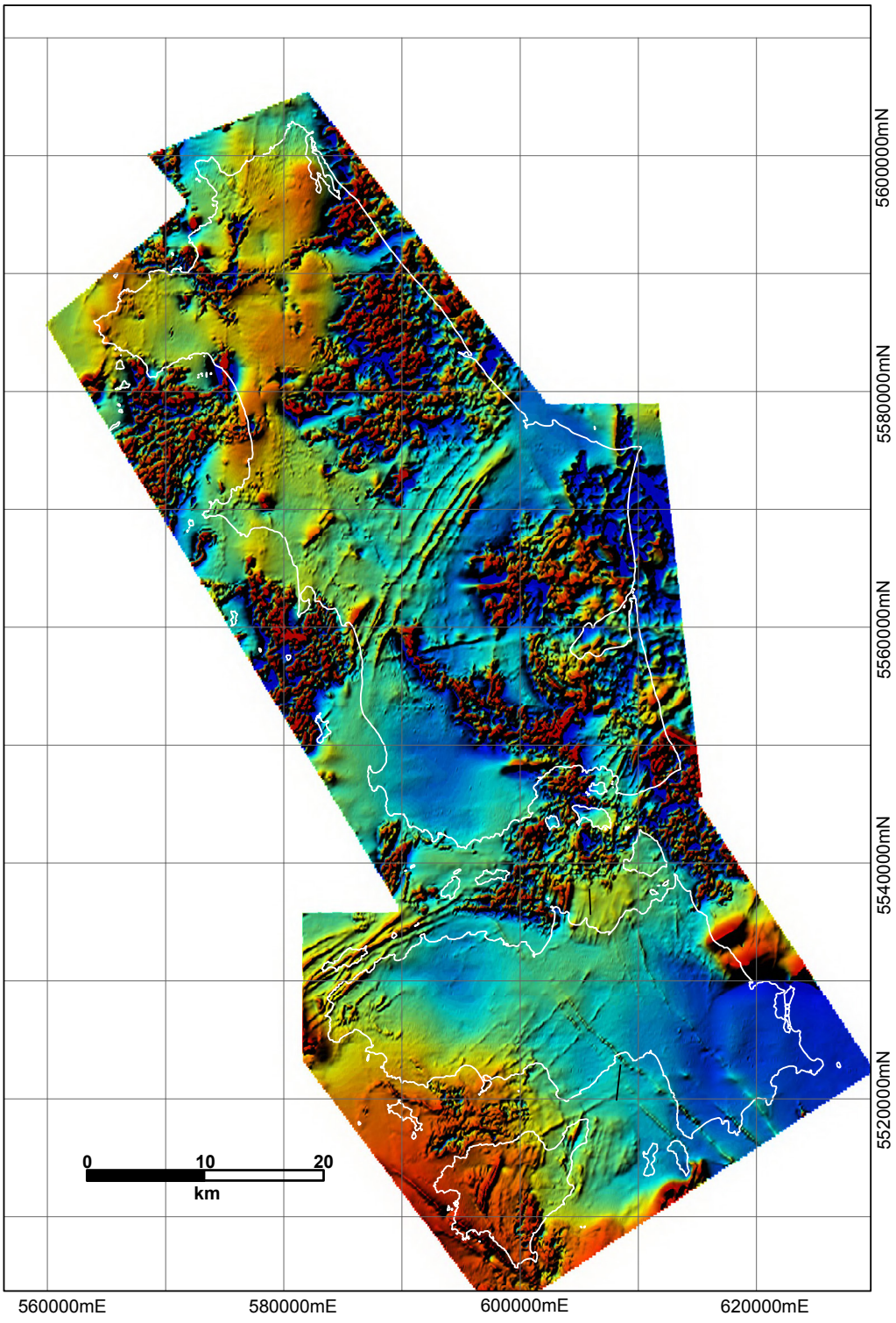

FIGURE 3a. Colour images of total magnetic intensity (TMI) derived from MRT 2007 northeast Tasmania airborne survey: Furneaux Islands area.

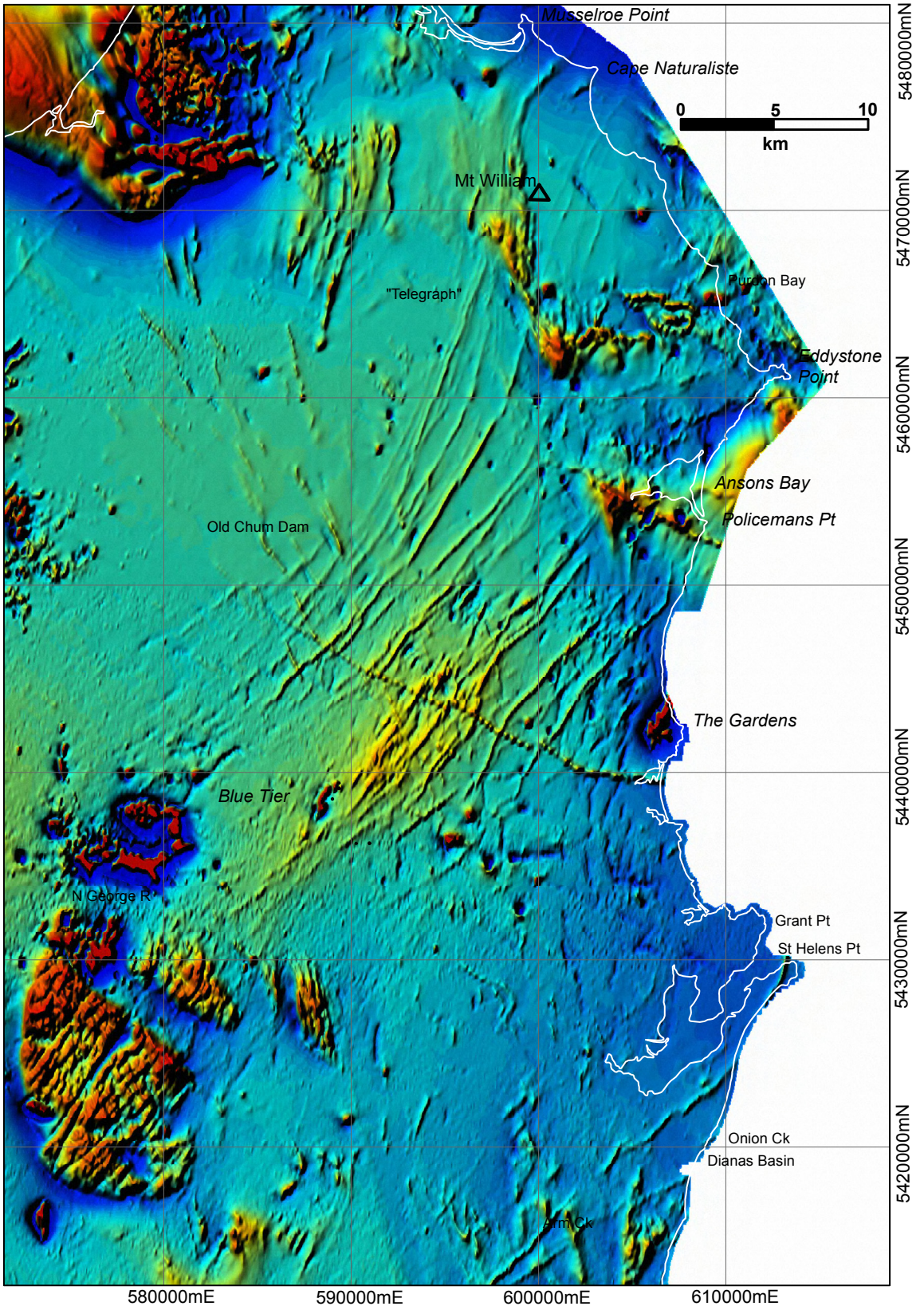

FIGURE 3b. Colour images of total magnetic intensity (TMI) derived from MRT 2007 northeast Tasmania airborne survey: St Helens-Blue Tier-Eddystone Point area.

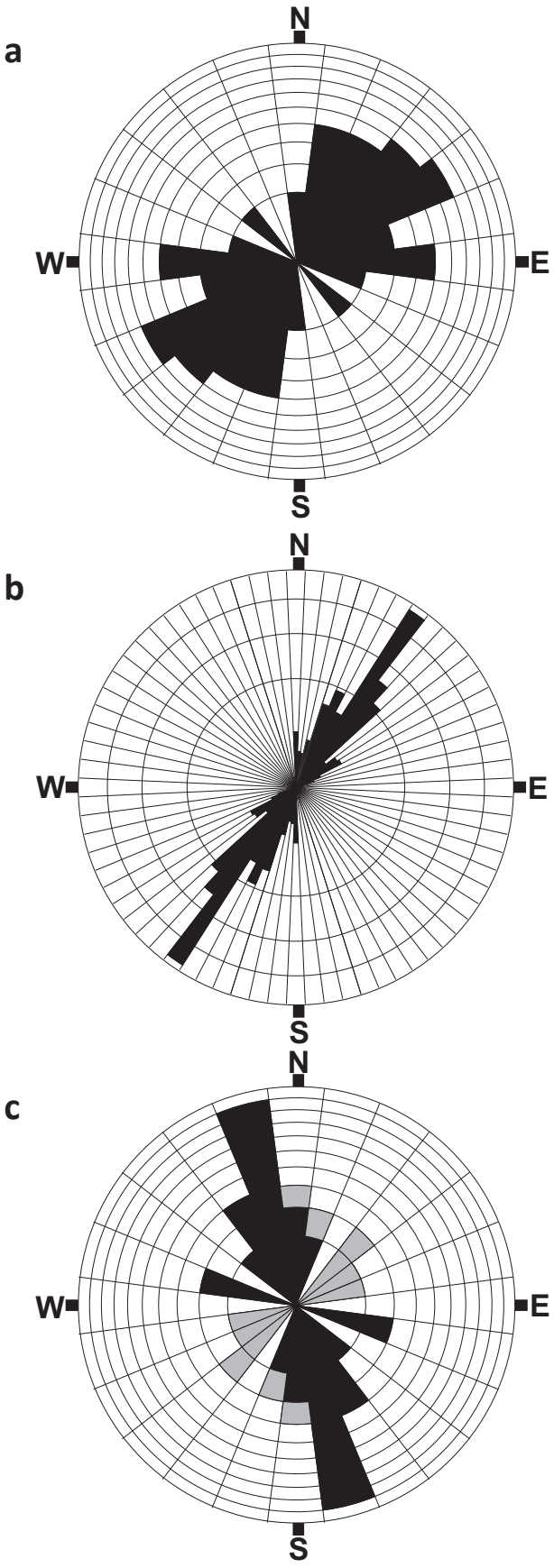

FIGURE 4. Rose diagrams showing measured strike of dolerite dykes.
a. Furneaux Islands; each segment represents one dyke, with strikes divided into 15° intervals;
b. Tebrakunna Dyke Swarm in Blue Tier-Eddystone Point area; each segment represents 10 km of strike of dykes on 1:25 000 geological maps, with strikes divided into 5° intervals;
c. dykes in Bicheno-Freycinet Peninsula area and Maria Island (black) and in St Helens area (grey); with strikes divided into 15° intervals.

In several instances, there is a clear strong local control by joints in the country rock (usually granite). At Arm Creek, northwest of Scamander, a dyke has intruded along a NE-trending sinistral wrench fault displacing the Mathinna Supergroup (Worthing and Woolward, 2010).

Dykes in the Furneaux Islands vary widely in orientation, although a northeast trend is most common amongst the limited field measurements (Figs 2a, 4a). However, aeromagnetic imagery (Fig. 3a) suggests that several distinct swarms may be present in this area. On eastern Cape Barren Island, there appear to be cross-cutting sets of NE- to NNE-trending and NW-trending dykes; this is supported by the limited field evidence available. The former set possibly extends to near Lady Barron on Flinders Island. In the northwest of Cape Barren Island, on Long Island and in the Franklin Sound area, a set of strong ENE-trending linear magnetic anomalies probably represents a set of dolerite dykes mapped by Cocker (1977, 1980), for which there is little petrological information. On central Flinders Island, several parallel, slightly arcuate NE- to NNE-trending (~015-040°) linear aeromagnetic anomalies mostly lie over Cenozoic cover, but one coincides with a dolerite outcrop at Cannes Hill, near Whitemark (Methorst 2008; and Appendix).

Several N-S striking dolerite dykes up to 15 cm wide, and an E-W trending dyke 0.6 m wide, were reported at the northeast point of Hogan Island (Hope et al., 1974).

The dykes of the Furneaux Islands, the St Helens, Bicheno and Friendly Beaches areas, Freycinet Peninsula and Maria Island can at present only be considered to be possible outliers of the Tebrakunna Dyke Swarm.

Field characteristics

Outcrop of the dykes is usually poor. The main Tebrakunna Dyke Swarm crosses a section of the coast that is dominated by long sandy beaches, and coastal exposures are rare, although some good outcrop has been observed in streams and steep hillsides. On the Blue Tier and Eddystone map sheets (McClenaghan and Williams, 1983; Baillie, 1984), individual dykes have been followed and mapped for up to 6 km largely on the basis of bands of abundant float of dark brown rounded fine- to medium-grained dolerite boulders. These are considered likely to overlie in situ rock at shallow depth, as locally outcrop is also present. Bands of abundant dolerite float are easily visible and contrast with the pale grey quartz-rich soil derived from poorly exposed granite, the usual country rock. In areas of Mathinna Supergroup rocks, rounded dolerite boulders contrast with the mote angular float of the country rocks, and are easy to follow.

The width of the dykes is often uncertain, but the extent of a band of dolerite float suggested a width of up to 50 m for a dyke on the Blue Tier sheet. McClenaghan et al. (1982) reported widths of 1 to 30 m from the southeast part of the Ringarooma map sheet (in Brown et al., 1977) and Baillie (1986) reported widths up 30 m on the Eddystone map sheet. The lack of deviation where the dykes trend across areas of topographic relief indicates that they are vertical or very steep.

There are better coastal exposures of dykes outside the main swarm, in the Bicheno area, Freycinet Peninsula and the Furneaux islands, where they tend to be narrower. The width of a well-exposed coastal outcrop at St Helens Point is 14 m, whereas another dyke on Grants Point is only 1.6–2 m wide (Fig. 5e); both are vertical or nearly so. Steeply dipping dykes are exposed at Bicheno (2.5–4 m) and Cape Lodi (~1 m). There are some well-exposed dykes on Freycinet Peninsula at Cape Tourville Road (8–10 m), Carp Bay (~10m) and Lagunta Creek (~6.5 m) (Fig. 5a). Near Lady Barron on Flinders Island, two dykes are 10–15 m wide and ~0.5 m wide (Fig. 5f), and a dyke at Riddles Bay, Cape Barren Island is ~6 m wide.

Where contacts with the country rocks are exposed, the dykes show chilled contact zones and steep boundaries. No coeval volcanics are known, nor is their preservation likely as the Carboniferous was a period of widespread erosion in Tasmania, resulting in exhumation of Devonian granites.

Distinguishing features

The dolerite dykes of the Tebrakunna Dyke Swarm and its possible outliers should be clearly distinguished from other mafic to intermediate intrusions in the region.

A suite of Cretaceous shoshonite dykes, stock-like intrusions and rare lavas, centred on the Cape Portland (Jennings and Sutherland, 1969), can be distinguished from the dolerites by both petrographic criteria (e.g., strongly porphyritic textures and the presence of magmatic hornblende) and geochemistry (e.g., high K_2O/Na_2O).

Compared to Jurassic dolerite, in which igneous minerals are little altered, the pre-Jurassic dolerite dykes generally show a higher rank and grade of metamorphism (e.g., partial replacement of pyroxenes by fine-grained amphibole and chlorite, turbid alteration of feldspar, replacement of iron-titanium oxides by titanite etc.). In hand specimen, this is often expressed by a distinctly greenish tint. In addition, pigeonite and orthopyroxene are common in Jurassic dolerite, but have not been reported in the older dykes. Jurassic dolerite typically occurs as larger intrusions, and in much of northeast Tasmania is restricted to thick subhorizontal sill remnants capping mountains or, on the north coast near Cape Portland and Waterhouse, major downthrown fault blocks associated with small outcrops of Permo-Triassic sedimentary rocks. Jurassic intrusions into the basement rocks (Devonian granite and Mathinna Supergroup) are very rare in northeast Tasmania, and potential examples may need careful assessment to distinguish them from pre-Jurassic dykes.

Minor fine-grained diorite or granodiorite dykes with abundant biotite and/or hornblende may appear very dark in the field, and superficially resemble dolerite dykes. Thin section examination may be necessary to distinguish them. In the St Helens area, several small quartz-plagioclase-hornblende porphyry (or "spessartite") dykes (Cocker, 1977, p. 138–139; McClenaghan et al., 1987, 1992) are petrographically and geochemically distinct (e.g., more felsic), and probably closely related to the Devonian granodiorites. A similar plagioclase-hornblende-phyric dyke occurs at Roses Tier. Near Puncheon Point on Cape Barren Island, black, very biotite-rich microgranodiorite dykes intrude granite.

Mafic enclaves and schlieren within the Devonian granites also should not be confused with the dolerite dykes, although they may have a distant petrogenetic relationship with them.

Rubbly flow remnants of Cainozoic basalt may be distinguished from dolerite float by features such as the presence of vesicles or amygdales, fresh olivine phenocrysts or mantle xenoliths, but in some cases thin section examination may also be required for confirmation.

Classification

As discussed below, geochemistry is used to empirically classify the dykes into three groups:

- A tholeiitic group, which comprises most of the samples from the main Tebrakunna Dyke Swarm, and is also present in the Furneaux islands but relatively uncommon in the central east coast (i.e., south of St Helens)
- An alkalic group, characterised by higher total alkalis, prevalent in the central east coast and notably Freycinet Peninsula, but uncommon elsewhere
- A calc-alkaline and generally more felsic group, present in most areas but less common than the other types.

Magnetic properties

The dykes vary from weakly to strongly magnetic, with magnetic susceptibility ranging over more than two orders of magnitude (Tables 1, 2; all tables can be found after References, following p. 63). Measurements were made using a hand-held susceptibility meter ("Kappameter", Model KT-5), with a sensor diameter of about 65 mm. Data was gathered both in the field from multiple readings of natural outcrops, and in the laboratory from hand specimens. Field measurements have the advantage that short range natural variability can be detected and more meaningful average, minimum and maximum values calculated, but measured values may differ from the true values due to uneven surfaces or weathering effects. Laboratory measurements can usually be taken from smooth sawn surfaces of fresh material, but low values may be obtained if the specimen is too small; for this reason some values are given as minimum estimates (>) in Table 1.

The highest measured magnetic susceptibilities are from hand specimens of dykes at St Helens Point (sample SHP, 40.1×10^{-3} SI), Onion Creek south of St Helens (NJ447, 28.7×10^{-3} SI) and from the centre of a dyke at Lagunta Creek, Freycinet Peninsula (LC3, 24.6×10^{-3} SI). These are from alkalic dykes (see Geochemistry section), apart from the Onion Creek dyke which is assigned to the calc-alkaline group. There is, however, no clear relationship between magnetic susceptibility and geochemistry.

FIGURE 5. Field photographs of dolerite dykes.
a. Lagunta Creek, Freycinet Peninsula; stepped western contact of large dyke;
b. Lagunta Creek: detail showing plagioclase megacrysts and irregular margins, truncating aplite veinlets in host monzogranite;
c. Bluestone Bay: irregular contacts of 2.5–4-m-wide dyke;
d. near Bicheno blowhole: tapering fingers of dyke following joints in host granite;
e. Grant Point: vertical 1.6-m-wide dyke within Grant Point Granite;
f. White Beach, Flinders Island: vertical 0.5-m-wide dyke intruding Lady Barron Granite;
g. Yellow Beaches, Flinders Island: western contact of large dyke with chilled margin and cross-cutting aplite vein originating in host granite;
h. Stanley Point, Flinders Island: vertical view of 0.7-m-wide alkali dolerite dyke (photo: M. J. Vicary).


e


f


g


h

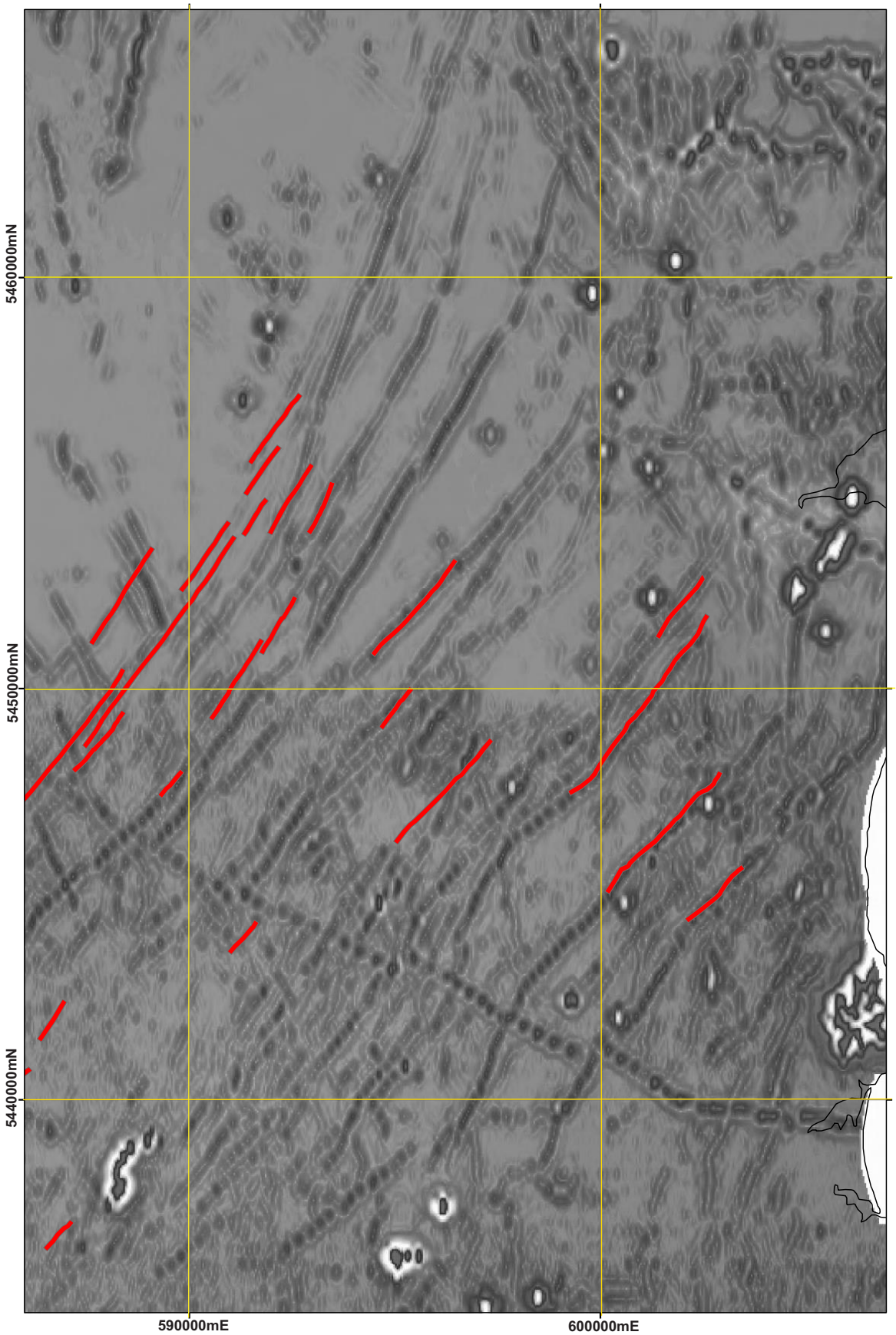

FIGURE 6. Grey-scale image (1:125 000) of The Gardens- Ansons River area, based on the first vertical derivative of total magnetic intensity (MRT 2007 northeast Tasmania airborne survey). Previously mapped dolerite dykes are superimposed as red lines. The "bulls-eye" magnetic anomalies are mostly known or inferred Cainozoic basalt plugs.

More detailed magnetic susceptibility measurements for some of the dykes from the Tebrakunna Dyke Swarm on the Blue Tier 1:50 000 map sheet are listed in Table 2. The fine-grained dolerite and andesite dykes (mean ~0.5 × 10^{-3} SI) typically have lower values than the coarser-grained dolerites (~7 × 10^{-3} SI). Both are higher than for the granitic country rocks of the area (mostly less than 0.25 × 10^{-3} SI), and thus the dykes show as generally well-defined linear features on aeromagnetic images.

On the Blue Tier map sheet, many magnetic lineaments correspond to dykes previously mapped from ground observations. In some cases, the lineaments extend beyond the mapped dyke on the same trend, or connect segments of mapped dyke (Fig. 6). There are also numerous magnetic lineaments without a corresponding mapped dyke. This suggests that there are many unexposed and unmapped dykes, with little or no surface expression. As discussed above, aeromagnetic data from the Furneaux islands suggests the presence of several poorly documented dyke sets with contrasting trends.

Some magnetic lineaments probably represent different dyke suites, or have other sources. South and west of Gladstone, a set of NNW-trending magnetic lineaments coincides with outcropping olivine nephelinite at one location (500 m N of Ogilvies Bridge) and is thus probably due to feeder dykes related to Neogene volcanism. Northeast of Gladstone, a set of close-spaced N- to NNE-trending lineaments is due to magnetic horizons within the Mathinna Supergroup. Broader W- to WNW-trending lineaments near The Gardens, Ansons Bay and Waterhouse are poorly understood, but may be caused by mafic material ("megaschlieren") within Devonian granites.

A ground traverse by proton precession magnetometer, approximately at right angles to the strike of several mapped dykes, was trialled across an area of poor outcrop east of Eddystone Road (Fig. 7). Two positive anomalies correspond to dykes depicted on the Eddystone 1:50 000 and Naturaliste 1:25 000 maps, although the smaller, eastern dyke may be ~100 m further west than mapped.

Petrography

Detailed petrographic descriptions of 136 available samples are given in the Appendix and tabulated in Table 3, and only a summary of the main features is given here.

Tholeiitic and alkalic dykes

Typical dykes are dark grey to bluish- or greenish-grey, massive and usually aphyric. Rarely, plagioclase megacrysts (exceptionally up to 140 × 50 mm as at Lagunta Creek, Freycinet Peninsula; Fig. 5b) may be conspicuous in outcrop. Many other samples contain smaller phenocrysts or microphenocrysts of plagioclase (≤ 10 mm) (e.g., Fig. 8e) and subordinate clinopyroxene, usually euhedral and grading downward in grain size to the groundmass. Some plagioclase phenocrysts are relatively rounded or embayed, and may be xenocrysts, or have crystallised at depth and undergone decompression melting. Probable or possible olivine microphenocrysts, usually wholly replaced by chlorite, are present in about 15 (~10% of) samples, generally the more mafic ones. Relict cores of fresh olivine were noted in only a few samples (e.g., NJ406 and NJ407, tholeiitic dykes from the main Tebrakunna Dyke Swarm).

The groundmass of typical samples from the interior of dykes consists of a medium- to coarse grained, ophitic (Fig. 8c, g, j) to intergranular (Fig. 8f, h) intergrowth of variably altered plagioclase and clinopyroxene, together with opaque minerals (probably both ilmenite and magnetite) and commonly but not invariably minor interstitial quartz. In thin section, clinopyroxene is typically very pale pinkish-brown (and therefore probably slightly titaniferous augite) where fresh (Fig. 8c, g, j), but is usually partly (Fig. 8c, e, h) or wholly replaced (Fig. 8d) by a pale yellow-green pleochroic aggregate of actinolite and chlorite ("uralite"). Dark brown hornblende is noted in a few samples, usually at the margins of tremolite-actinolite (Fig. 8l), or less commonly as discrete grains. Small amounts of red-brown biotite flakes are present in the groundmass of some samples. Plagioclase is commonly zoned, may be clear and fresh, or turbid and partly sericitised. In most samples it is less altered than clinopyroxene, although in a few (e.g., LC3, Fig. 8g; MBT30, MNET36) the reverse is true. Opaque minerals may be fresh or, more commonly, incipiently to wholly replaced by fine-grained turbid titanite. Other minerals noted include accessory apatite, rare epidote (as a replacement of plagioclase) and sulphides.

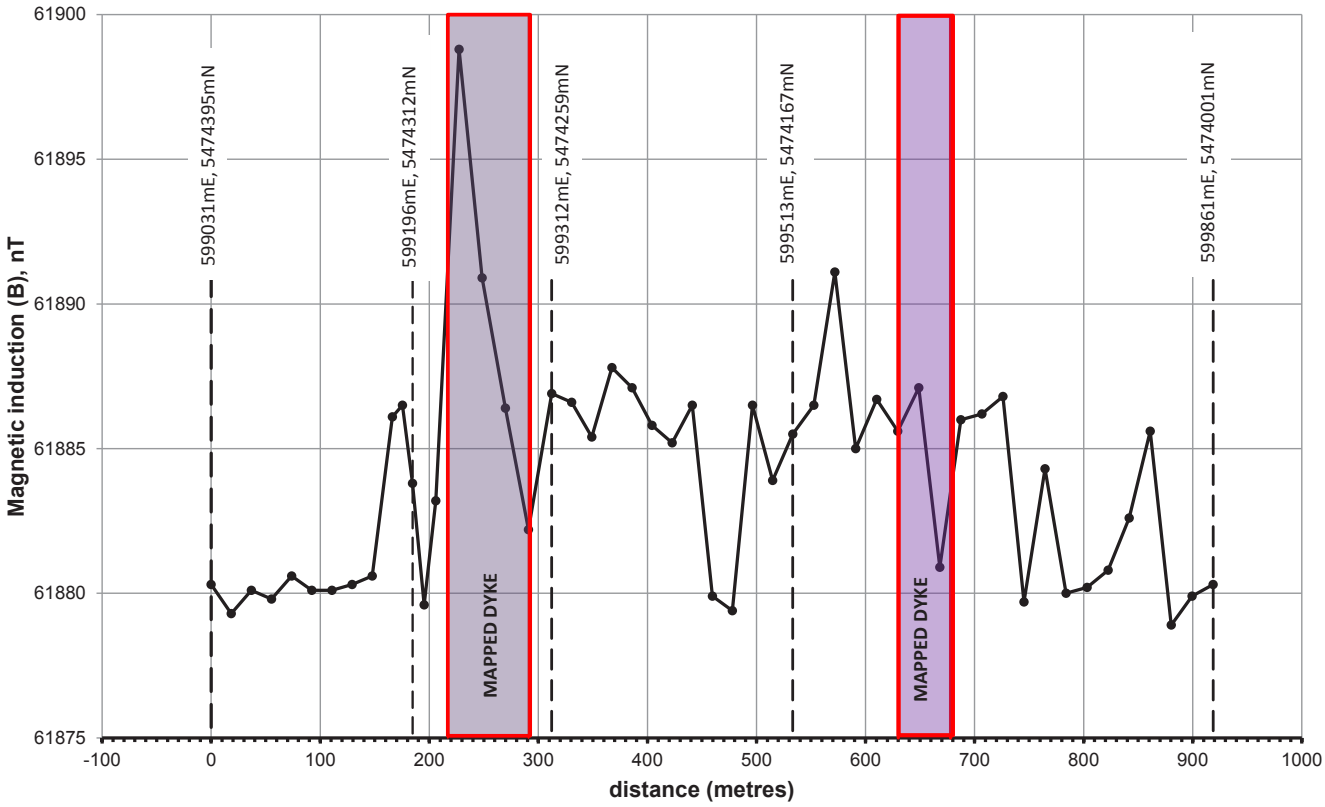

FIGURE 7. Ground magnetometer profile east of Musselroe Road, showing location of dykes from 1:25 000 map. Proton precession magnetometer, with GPS control locations.

Plagioclase laths are usually randomly oriented in medium- and coarse-grained samples (although crudely aligned in MNET17, MNET32 and MBT44). Samples collected from near chilled contacts (e.g., NJ453, Fig. 8a; MBT73) may contain narrow aligned plagioclase microphenocrysts, defining a fluidal texture, together with subordinate equant euhedral clinopyroxene microphenocrysts, in a very fine-grained groundmass.

A strongly fractionated fine-grained tholeiitic dyke in the Tebrakunna Road area (samples MNET37, MNET38) has an unusual micropoikilitic texture (Fig. 8b). Tabular plagioclase grains with very abundant inclusions of pale pink titaniferous augite prisms form a locally micrographic intergrowth with zoned alkali feldspar, polycrystalline quartz and large acicular opaque grains.

Calc-alkaline dykes

The basaltic members of this group (generally with ~50–54% SiO_2) are petrographically similar to the tholeiitic and alkalic dykes, with textures ranging from ophitic (Fig. 8l) to intergranular (Fig. 8m), although small amounts of quartz and sometimes minor biotite are more common in the groundmass. A few scattered, embayed xenocrysts of quartz and feldspar with reaction coronas may be present.

More felsic calc-alkaline bodies have distinct petrographic characteristics. In the Ansons Bay area, several small bodies, up to 200 m across, have been mapped as andesite (McClenaghan and Williams, 1983). They contain small phenocrysts of quartz, plagioclase, chlorite and less commonly alkali feldspar and biotite in a fine-grained quartzofeldspathic groundmass with actinolite and minor clinopyroxene or biotite (Tables 3, 4). Many of the phenocrysts, particularly quartz, are strongly resorbed and surrounded by reaction coronas (Fig. 8q, r, s). These andesites (typically with 57–59% SiO_2) may be dolerites contaminated by assimilation of granitic country rock. Dykes at Onion Creek near Scamander (NJ447) and from Nautilus Cove on Cape Barren Island (BA4) are similar, although slightly more mafic.

The most felsic members of this group contain abundant quartz and feldspar xenocrysts in a quartzofeldspathic groundmass with abundant biotite and disequilibrium textures. These are obvious “hybrid rocks” formed by incomplete digestion of granitic material by a mafic magma. Some contain distinctive zones of more and less felsic material. These have been sampled at Hawksnest Cove (FY32, FP1; Fig. 8o) and Sleepy Bay (FP22) on Freycinet Peninsula, at Dianas Basin near St

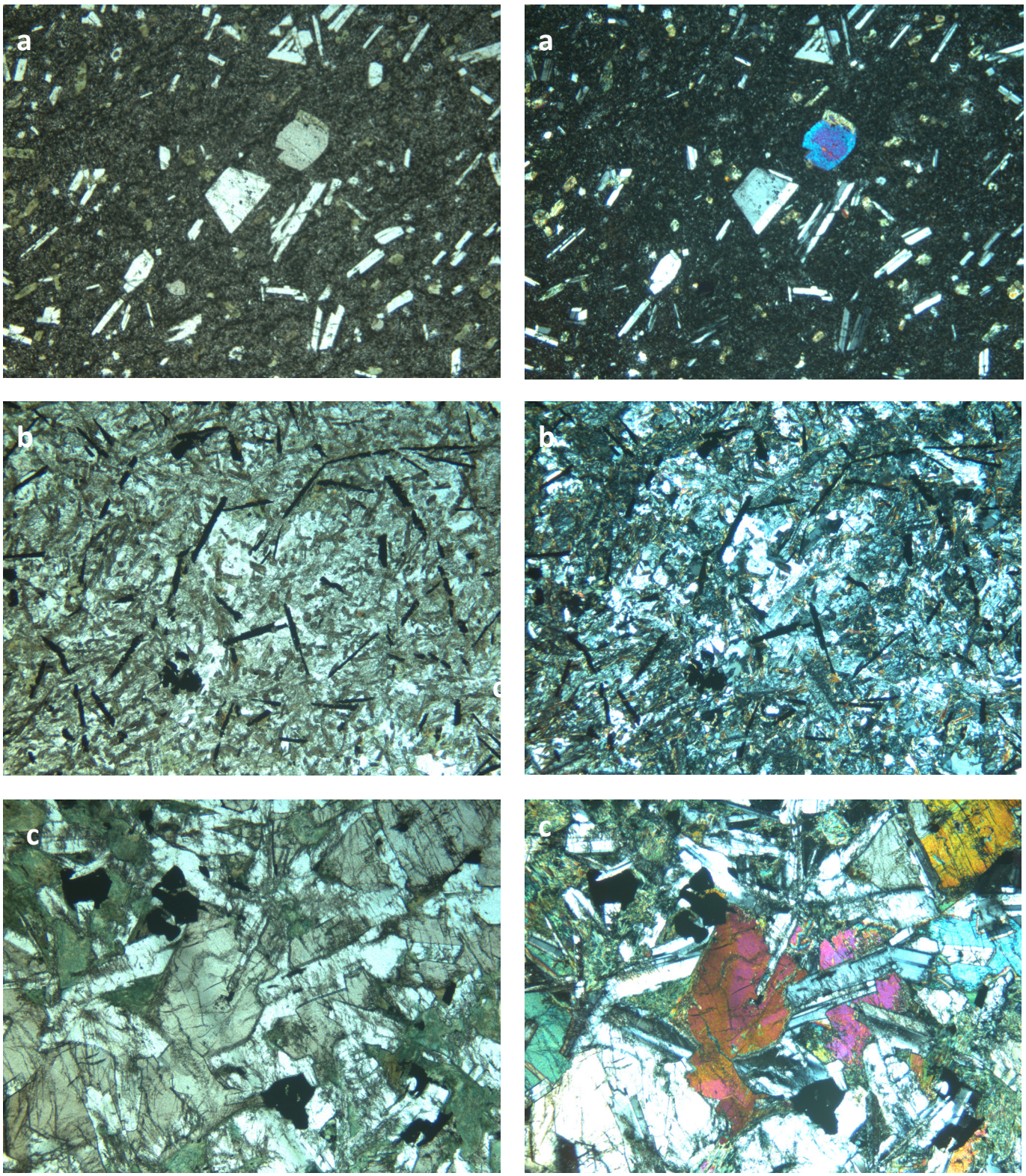

FIGURE 8. Photomicrographs of representative samples, in plane polarised light (left) and crossed nicols (right); field of view ~4.5 × 3.4 mm unless otherwise stated (see Table 3 and Appendix for detailed descriptions).
a. NJ453, chilled tholeiitic dyke, near Tebrakunna Road. Aligned plagioclase and augite microphenocrysts in a very fine-grained groundmass;
b. MNET38, tholeiitic dyke, near Tebrakunna Road. Plagioclase subhedra, micropoikilitically enclosing titaniferous augite prisms and acicular opaques, with micrographic intergrowth of alkali feldspar and quartz;
c. 77/907, tholeiitic dyke, Airport Beach, Flinders Island. Very coarse-grained ophitic intergrowth of plagioclase and titaniferous augite, partly replaced by actinolite.

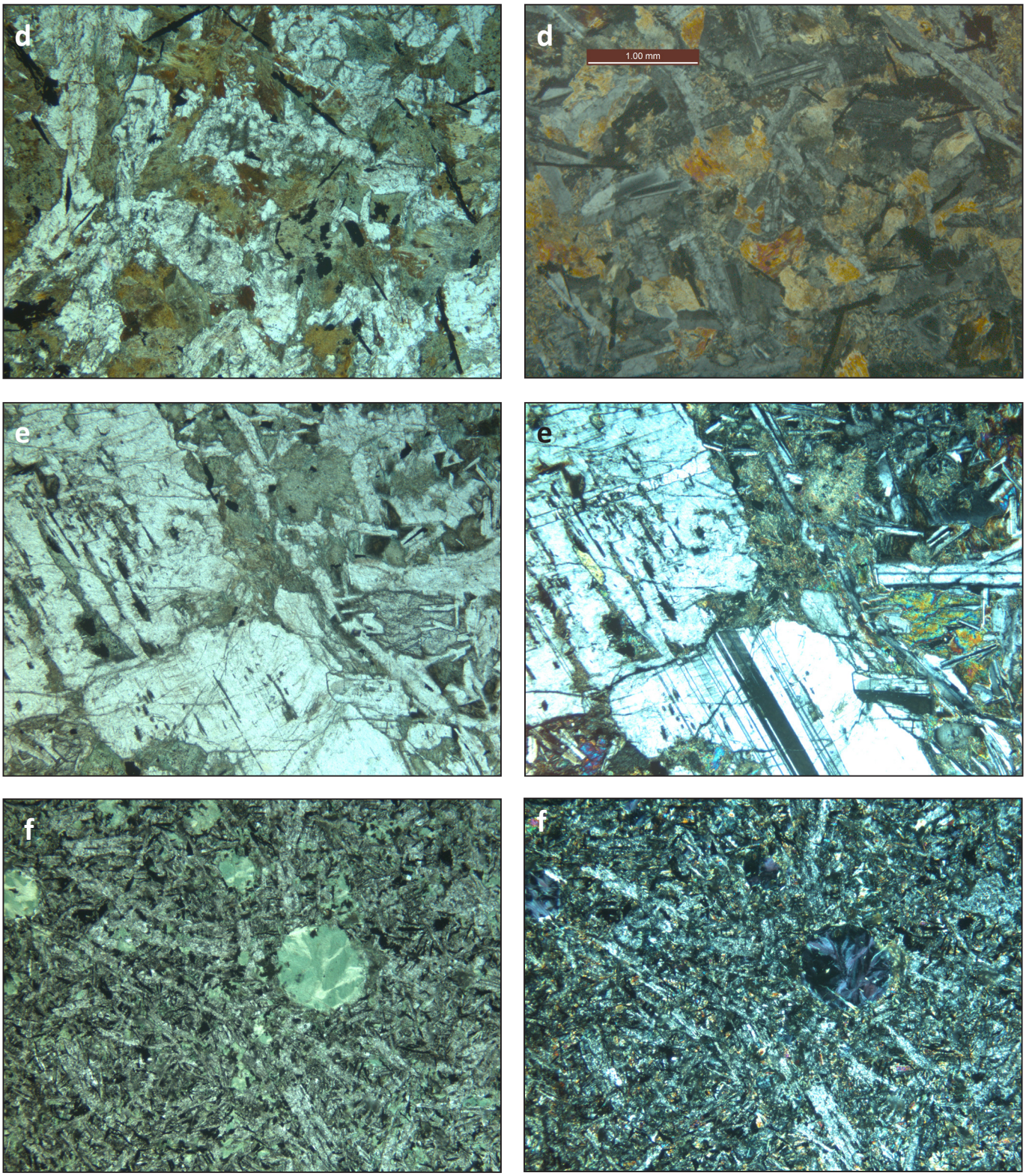

FIGURE 8 cont. Photomicrographs of representative samples, in plane polarised light (left) and crossed nicols (right); field of view ~4.5 × 3.4 mm unless otherwise stated (see Table 3 and Appendix for detailed descriptions).
d. NJ423, tholeiitic dyke, Mt William area. Coarse-grained ophitic intergrowth of plagioclase, former augite completely replaced by actinolite, and minor biotite (brown);
e. NJ425, tholeiitic dyke, Forester Kangaroo Drive, Mt William area. Part of a large fresh plagioclase phenocryst, in a medium-grained ophitic groundmass of plagioclase and augite, largely replaced by actinolite;
f. LC1, alkalic dyke, Lagunta Creek, Freycinet Peninsula; chilled margin. Very fine-grained intergranular texture with chlorite amygdales and possible pseudomorphs after olivine, and groundmass chlorite.

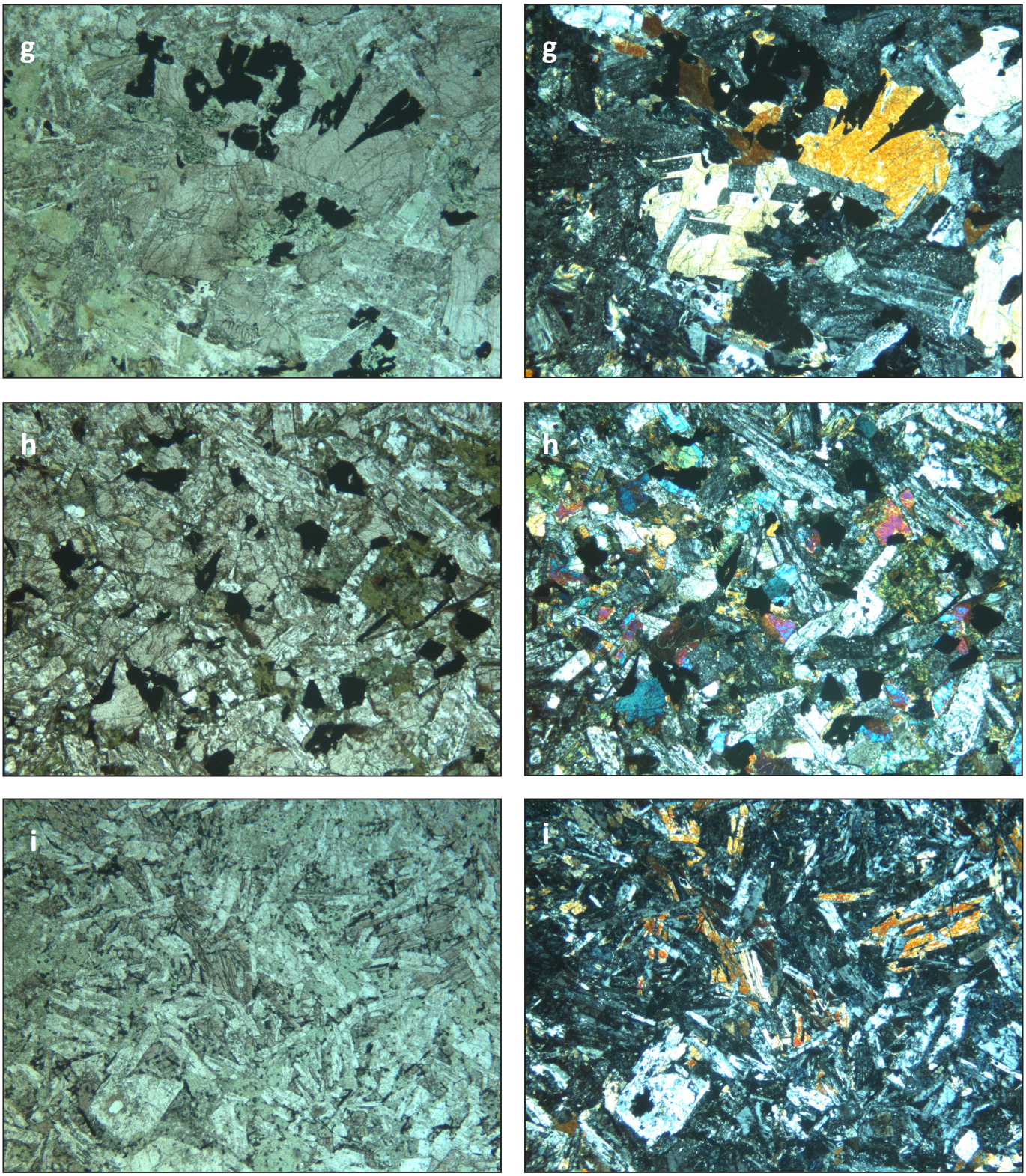

FIGURE 8 cont. Photomicrographs of representative samples, in plane polarised light (left) and crossed nicols (right); field of view ~4.5 × 3.4 mm unless otherwise stated (see Table 3 and Appendix for detailed descriptions).
g. LC3, alkalic dyke, Lagunta Creek, Freycinet Peninsula. Interior of dyke, with coarse-grained subophitic intergrowth of fresh titaniferous augite and largely albitised plagioclase;
h. NJ480, alkalic dyke, Arm Creek, Upper Scamander. Coarse-grained consertal intergrowth of augite, partly replaced by brown-green actinolite, and plagioclase;
i. BD2A, alkalic dyke, near Bicheno Blowhole. Medium-grained, seriate to slightly subophitic intergrowth of mainly plagioclase, augite and chlorite

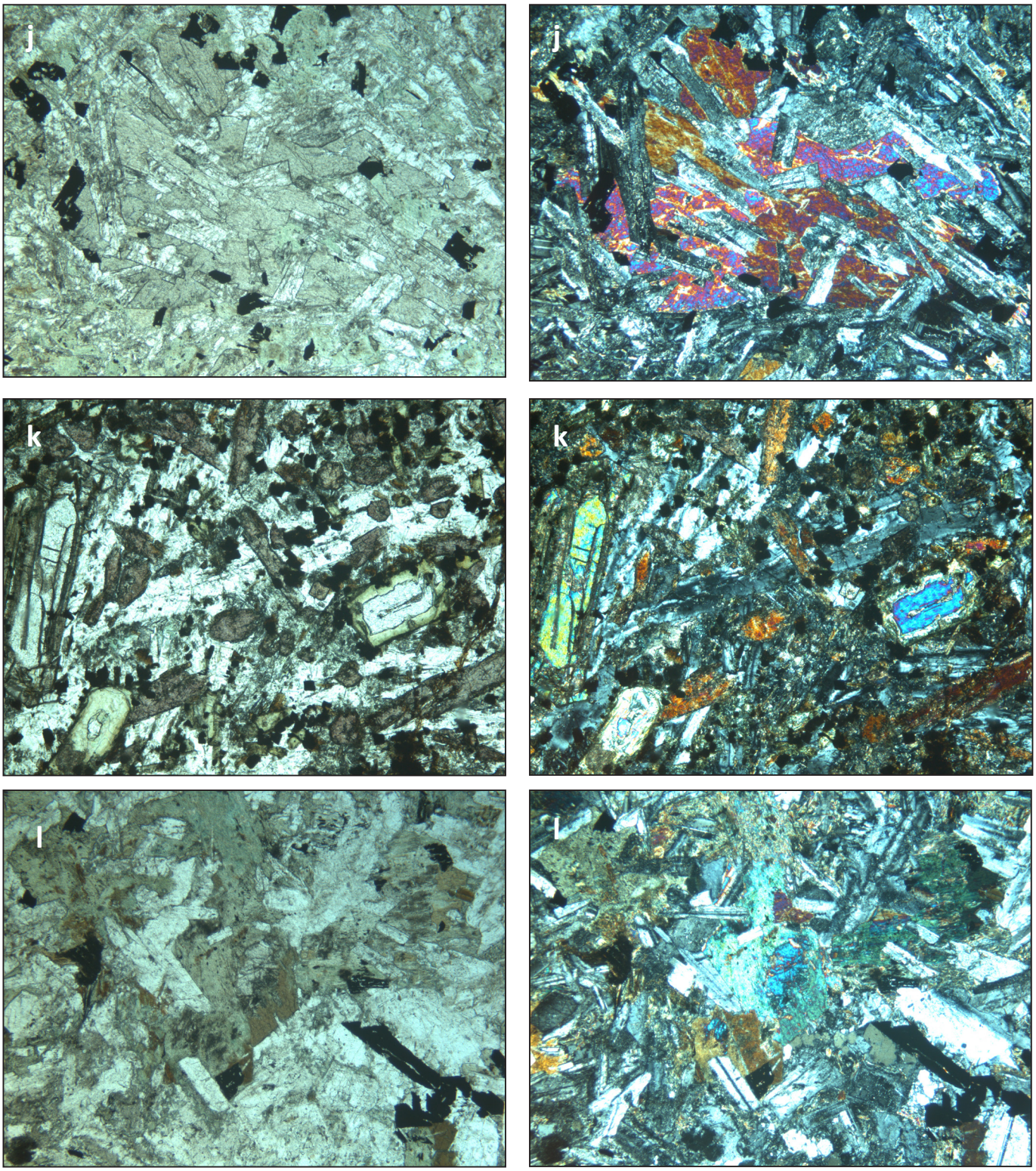

FIGURE 8 cont. Photomicrographs of representative samples, in plane polarised light (left) and crossed nicols (right); field of view ~4.5 × 3.4 mm unless otherwise stated (see Table 3 and Appendix for detailed descriptions).
j. MBT74, alkalic dyke, Ansons Bay Road. Coarse-grained ophitic texture; partly altered plagioclase, mostly fresh augite and opaques;
k. R014365, alkali dolerite, Stanley Point, Flinders Island. Partly altered olivine microphenocrysts (left, centre right), titaniferous augite (deep pink) with narrow margins of kaersutitic amphibole (brown), plagioclase and opaques. Intergranular texture. Field of view ~1.8 × 1.3mm;
l. SMD, calc-alkaline dyke, South Maria Island. Coarse-grained subophitic intergrowth of plagioclase, largely altered augite and minor brown hornblende (centre).

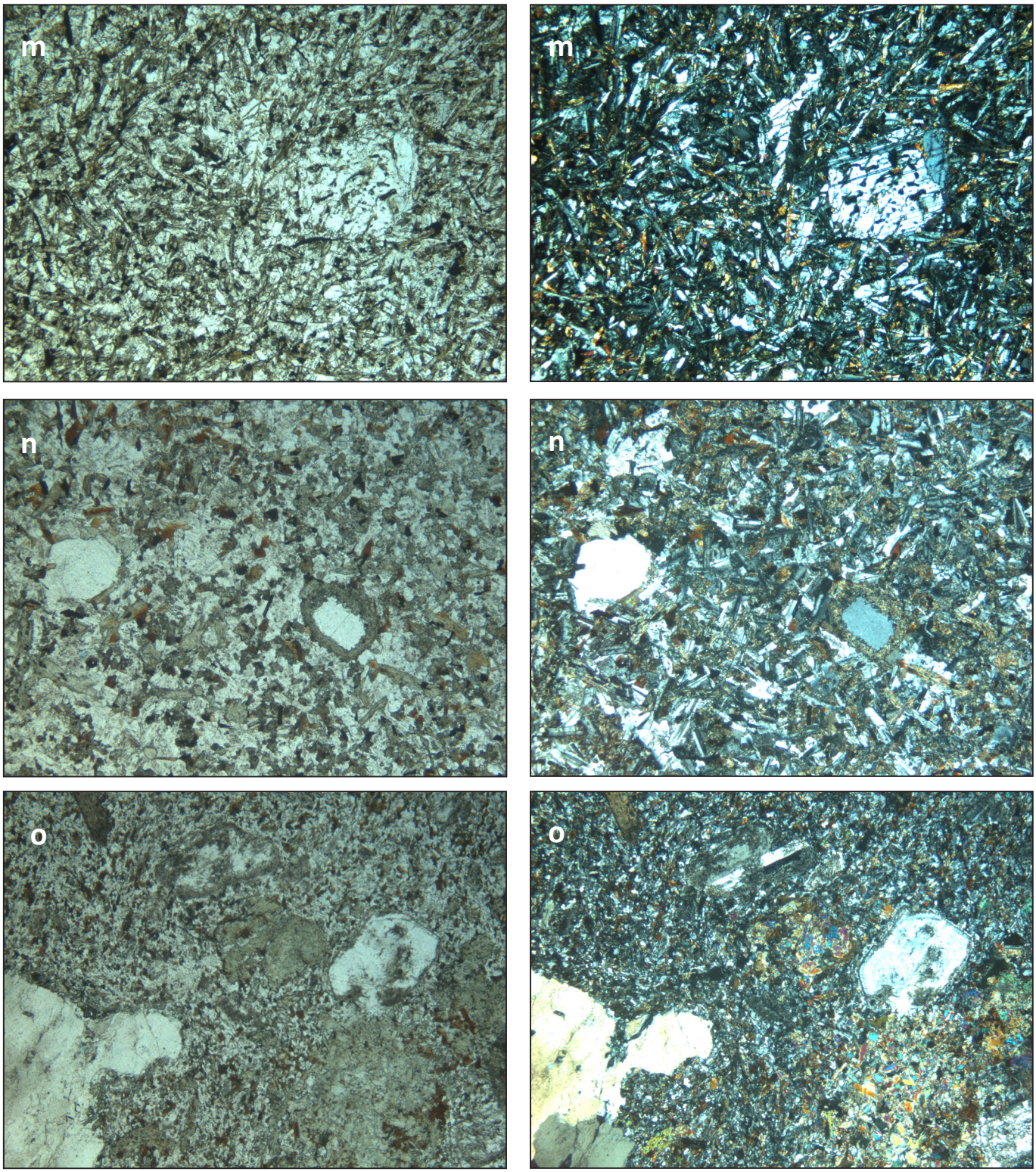

FIGURE 8 cont. Photomicrographs of representative samples, in plane polarised light (left) and crossed nicols (right); field of view ~4.5 × 3.4 mm unless otherwise stated (see Table 3 and Appendix for detailed descriptions).
m. FY31, calc-alkaline dyke, near Mt Freycinet. Plagioclase phenocrysts with abundant inclusions in a fine-grained intergranular groundmass;
n. NJ511, calc-alkaline dyke, Policemans Point. Corroded xenocrysts of quartz with reaction coronas of actinolite and biotite, in a fine-medium grained groundmass of plagioclase, quartz, actinolite, biotite and opaques;
o. FY32, calc-alkaline dyke, Hawksnest Cove, Freycinet Peninsula. Disequilibrium textures, with corroded xenocrysts of quartz (lower left), plagioclase (upper centre) and alkali feldspar (right), reaction rims and aggregates of fine-grained actinolite (centre) and a fine-grained quartzofeldspathic groundmass with abundant biotite and actinolite.

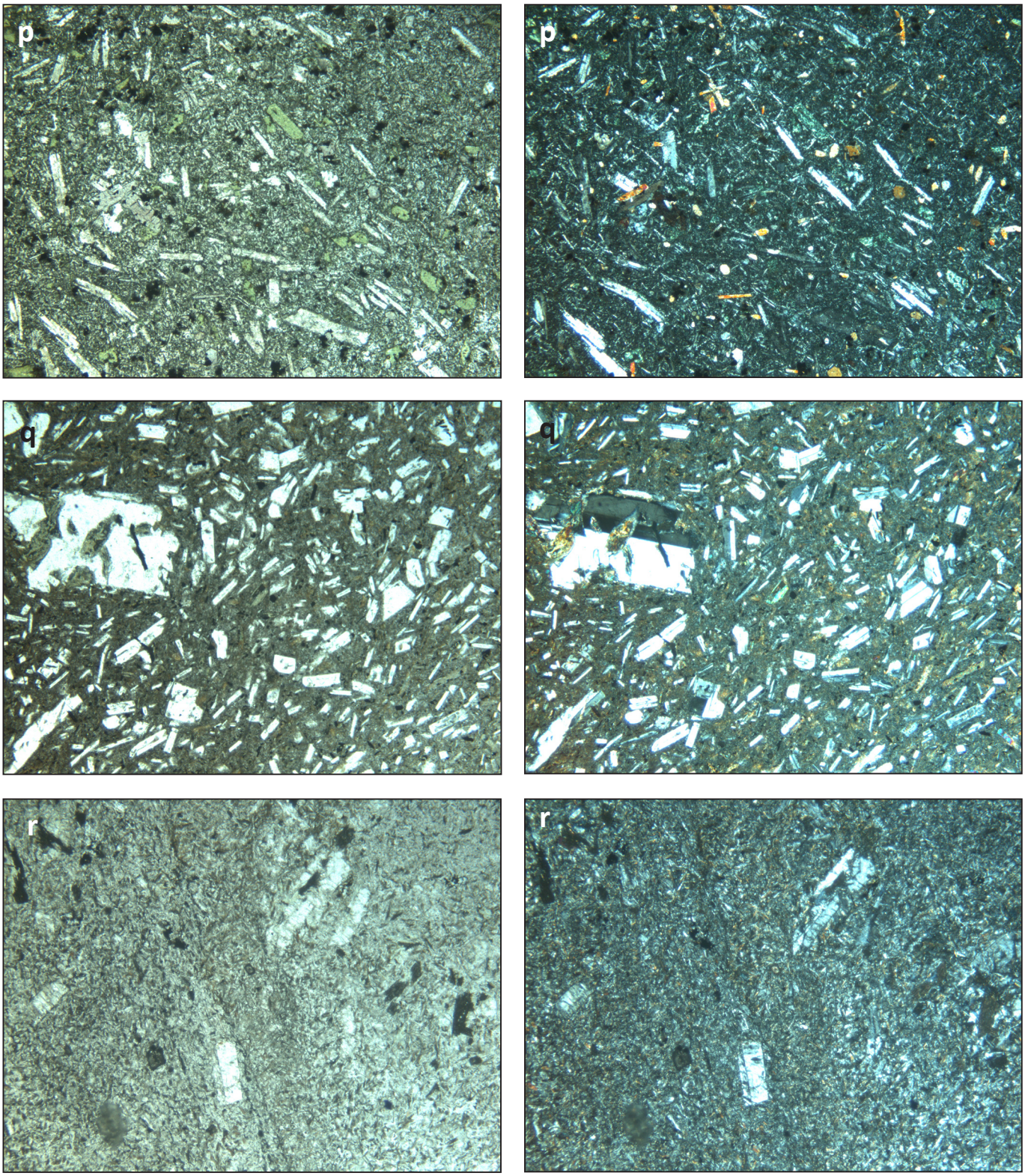

FIGURE 8 cont. Photomicrographs of representative samples, in plane polarised light (left) and crossed nicols (right); field of view ~4.5 x 3.4 mm unless otherwise stated (see Table 3 and Appendix for detailed descriptions).
p. BA3, calc-alkaline dyke, Apple Orchard Point, Cape Barren Island. Aligned microphenocrysts of plagioclase, augite and chloritized olivine in a very fine-grained groundmass;
q. MBT98, andesite, near Big Creek. Plagioclase microphenocrysts and laths in a chilled very fine-grained groundmass;
r. MBT75, andesite, near Gripe Creek. Microphenocrysts of plagioclase and secondary titanite in an uneven fine- to very fine-grained groundmass.

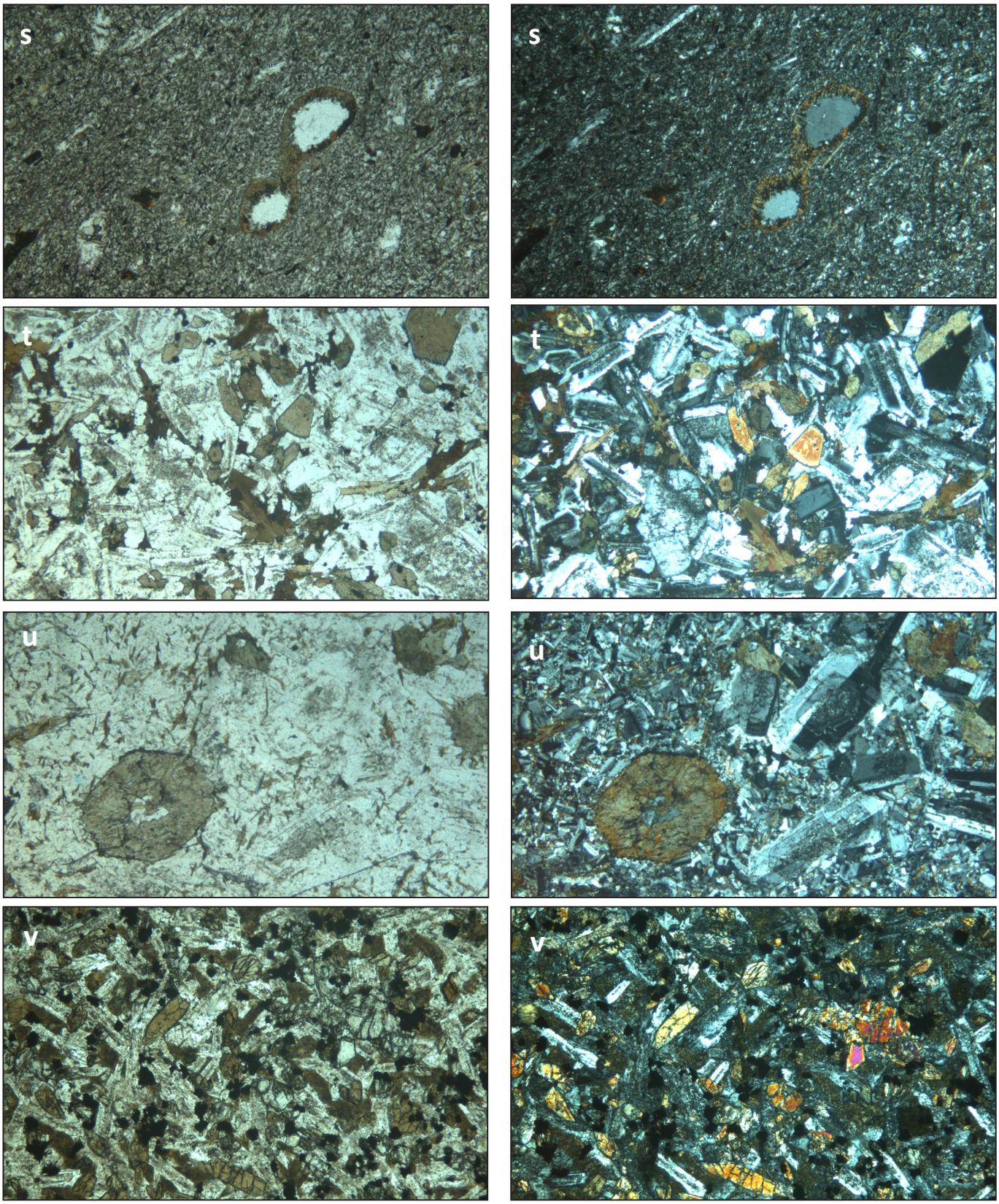

FIGURE 8 cont. Photomicrographs of representative samples, in plane polarised light (left) and crossed nicols (right); field of view ~4.5 × 3.4 mm unless otherwise stated (see Table 3 and Appendix for detailed descriptions).
s. MNET12, andesite, NE of Pretty Marsh. Phenocrysts and xenocrysts of feldspar and quartz, with biotite-rich reaction haloes, in a fine-grained foliated quartzofeldspathic groundmass containing also chlorite, actinolite and augite;
t. R1084, hornblende-biotite microdiorite, Roses Tier. Euhedral brown hornblende, ragged biotite, strongly zoned plagioclase and orthoclase, and minor quartz. Field of view ~1.8 × 1.3 mm;
u. BA35, hornblende-biotite microgranodiorite, Puncheon Point, Cape Barren Island. Seriate texture, with euhedral hornblende, strongly zoned plagioclase and orthoclase, and minor biotite, grading down to a groundmass with also abundant quartz;
v. GR6, possible basanite, George Rocks. Field of view ~1.8 × 1.3 mm. Augite microphenocryst (centre right) and an intergranular groundmass of plagioclase, augite, hornblende (brown) and opaques.

Helens (NJ446) and within the main Tebrakunna Dyke Swarm at Purdon Bay (NJ364B), Gripe Creek (MBT167) and Policemans Point (NJ511, Fig. 8n).

Petrographically unusual dykes

A few dykes have atypical mineralogy and geochemistry and may be representative of other suites. A dyke from the Roses Tier area (R1084, Fig. 8t) consists of plagioclase, orthoclase, hornblende, subordinate biotite and minor quartz, and may be a microdiorite related to the granodiorites of the Scottsdale Batholith. Samples from George Rocks (GR6, PE11), north of Eddystone Point, are also unusual in containing abundant hornblende (Fig. 8v).

Some of the dykes from the Furneaux islands are also unusual and distinctive. A dyke from northern Flinders Island (FLD4, Fig. 8k), consisting mainly of plagioclase, partly altered olivine, titaniferous augite and kaersutitic amphibole has strongly alkalic trace element chemistry and is clearly distinct from the other dykes. As noted above, a hornblende microgranodiorite dyke from near Puncheon Point on Cape Barren Island (samples BA35 and 43940; Fig. 8u) also clearly belongs to a different suite.

Mineral Chemistry

Limited data on the composition of minerals in the dolerites has been published previously. These are from a tholeiitic dyke (MR136) in the Blue Tier area (McClenaghan et al., 1982; McClenaghan, 1984), an alkalic dyke (MBT74) near Ansons Bay (McClenaghan, 1984) and an unanalysed but probably tholeiitic dyke (EE6) near Musselroe Bay (Baillie, 1986).

New data

Three samples were chosen for additional reconnaissance electron microprobe analyses: a tholeiitic dyke (NJ407) and an andesite (MNET5) from the main Tebrakunna Dyke Swarm (NJ407) and an alkalic dyke (LC1) from Lagunta Creek, Freycinet Peninsula.

Pyroxenes

Clinopyroxenes from NJ407, MNET5 and MBT74 (Table 5a) are all common quadrilateral pyroxenes and classify as augites in the nomenclature of Morimoto (1988), with a fairly restricted range of Mg# (100*Mg/(Mg + FeII)) of 66–78 (Fig. 9). The non-quadrilateral components TiO_2 (0.98–3.91%) and Al_2O_3 (1.42–5.61%) are however significant, and all but one of the analyses qualifies as aluminian (Al > 0.10 as cations), although only two as titanian (Ti > 0.10) (Morimoto, 1988). Na_2O (≤0.45%) and Fe_2O_3 (inferred from stoichiometry) are low.

There are no systematic differences in pyroxene composition between the three samples. They tend to be more calcic than similar augites analysed from Jurassic dolerites (Hall et al., 1988; Everard, 1987; Humphrys 2007; A. W. McNeill, unpublished data), although their much higher TiO_2 and Al_2O_3 content (relative to ≤2.0% and mostly ≤0.6%, respectively, in the Jurassic dolerites) is more diagnostic. They, however, do compositionally overlap in both quadrilateral and minor components with clinopyroxenes in tholeiitic and moderately alkalic Cainozoic basalts (e.g., Everard, 1989; Ming Zhang, unpublished data).

Feldspars

The alkalic dolerite at Lagunta Creek (Table 5b) contains labradorite megacrysts (sample LC1E) of composition ~An_{65}, but the turbid plagioclase in the groundmass is albite to oligoclase ($An_{3.5}$ to $An_{14.7}$) consistent with greenschist facies metamorphism.

Plagioclase compositions in the other dolerite samples, all from the Tebrakunna Dyke Swarm, vary widely, but are predominantly labradorite. Thus in tholeiitic dykes they range from $An_{58.7–70.0}$ (NJ407), $An_{50.3-77.7}$ (MR136) and $An_{36.9–67.7}$ (EE6), whereas two analyses from alkalic dyke MBT74 are oligoclase ($An_{26.1}$) and labradorite ($An_{65.0}$).

In andesite MNET5, both microphenocryst and groundmass plagioclase are labradorite ($An_{53.3–62.4}$), but orthoclase (~$Or_{94}Ab_5$) is also present in the groundmass (Table 5b).

Olivine

Fresh olivine is rare in these dykes. A single analysis of a phenocryst from sample NJ407 has composition ~$Fo_{82.7}$. (Table 5f). The host rock has Mg# of 65.3 (at Fe_2O_3/FeO = 0.20), implying an equilibrium olivine composition of ~$Fo_{86.3}$, assuming a crystal-liquid Fe-Mg distribution coefficient for olivine of 0.3 (Roeder and Emslie, 1970). Given the assumptions involved, the phenocryst probably crystallised in equilibrium with a liquid near the composition of the host rock, and is not a xenocryst. The presence of minor CaO (0.26%) suggests that it crystallised at relatively low pressure in a sub-volcanic environment.

Biotite

Biotite, where present, is only a minor phase in tholeiitic and alkalic dykes (Table 5c). Two analyses from sample

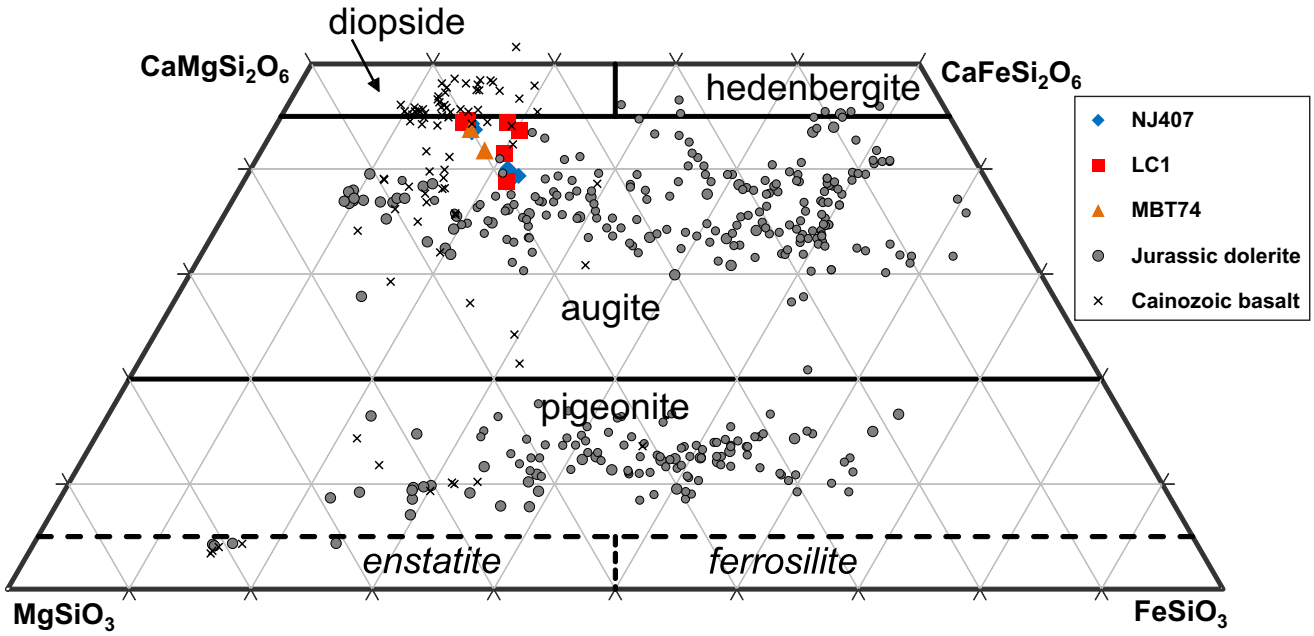

FIGURE 9. Electron microprobe analyses of clinopyroxene from dolerite dykes plotted on the pyroxene quadrilateral, with classification of Morimoto (1988). Pyroxene analyses from Tasmanian Jurassic dolerite and Cainozoic basalts also shown for comparison (see text for data sources).

NJ407 are trioctahedral micas lying close to the phlogopite-annite join, although with significant TiO_2 (≤ 4.7%, or 0.268 atoms per formula unit). An analysis from sample MR136 (McClenaghan, 1984) is similar, although more aluminous (i.e., with significant solid solution to the eastonite-siderophyllite join), and with lower TiO_2. As Mg# ranges from 50.2 to 61.2, these biotites are dominated by the phlogopite end-member (Rieder et al., 1998).

Three analyses from andesite MNET5 differ mainly in their lower Mg# (40.6–41.9), and are thus annite-dominant.

Amphibole

Analyses from samples LC1 and NJ407 (Table 5e) are both calcic amphiboles with low Al_2O_3 (≤ 2.01%), Na_2O (≤ 0.25%) and TiO_2 (≤ 0.06%) and classify as ferro-actinolite and actinolite respectively (nomenclature of Leake et al., 1997). The analysis from LC1 has much lower Mg# (48.7) than that of relict clinopyroxene from the same sample (64.7–77.9), suggesting that it is derived from alteration of fine-grained, more iron-rich groundmass clinopyroxene. The analysis from NJ407 has high Mg# (76.3), comparable to that of clinopyroxene platelets. Another microprobe analysis (not tabulated) from sample NJ407 is probably a mixture of tremolite-actinolite, clinopyroxene and biotite.

In contrast, two amphibole analyses from sample MR136 (McClenaghan, 1984) contain much higher Al_2O_3 (≤ 8.33%) and Na_2O (≤ 1.26%). They are probably magnesiohornblende (Mg# ~61–64), although low Ca in one analysis suggests some intergrown chlorite.

An analysis of groundmass amphibole from andesite MNET5 has much lower Mg# (27.2) and is a ferro-hornblende, although slightly deficient in Ca, with tetrahedral Aliv balanced by octahedral Al^{vi},Ti and partial occupancy of the A sites.

The "amphibole" analyses presented by Baillie (1986) from sample EE6 (85/274) are probably mixtures of tremolite-actinolite, clinopyroxene, epidote and possibly other minerals.

Chlorite

Two similar analyses of chlorite from sample LC1 (Table 5d) are near-stoichiometric without postulating any FeIII, and since Mg# ~53 are pycnochlorites in the nomenclature of Hey (1954). Microphenocryst and groundmass chlorite from andesite MNET5 is slightly more aluminous and iron-rich (Mg# ~44), and are brunsvigites.

Other minerals

Also analysed from sample LC1 (Table 5f) were near-stoichiometric prehnite, and clinozoisite with significant

FeIII (~0.46 atoms/per formula unit), i.e., substitution toward epidote.

Near-stoichiometric analyses of ilmenite were reported from samples MBT74 and MR136 by McClenaghan (1984). Ilmenite and titanite were evident during electron microprobe study of samples LC1 and NJ407, and pyrite in LC1, but were not analysed.

Geochemistry

Chemical analyses have been previously published of dolerites from Freycinet Peninsula (Spry, 1962; Everard, 2001), the St Helens area (Cocker, 1977; McClenaghan et al., 1992), the eastern part of the Ringarooma map sheet (McClenaghan et al., 1982) and the Eddystone map sheet (Baillie, 1986). Thirteen samples from the Coles Bay, Bicheno and Eddystone areas were analysed in 1973 by P. L. F. Collins (unpublished). Numerous previously unpublished analyses have also been obtained by the present authors over the past three decades. Samples collected from the Furneaux islands by D. J. Jennings, T. Methorst and M. Vicary were also analysed.

Where possible, powders and/or hand specimens from older collections have been re-analysed on a new XRF machine, acquired by MRT in 2009, on which improved accuracy and precision, and lower detection limits, for many trace elements is possible. For 19 analyses, the original samples have been lost, or insufficient material was left. In some cases, the locality was re-sampled; otherwise the original analyses have been used.

The following discussion is based on 98 XRF analyses (Table 6), of which 79 had trace elements analysed or re-analysed on the "new" machine. For six selected samples, a more complete set of trace elements was also determined by solution inductively coupled plasma mass spectroscopy (ICPMS) at the University of Tasmania (Table 7). Sample locations presented in Table 1 and plotted in Figures 1 and 2.

Major elements

On a total alkali-silica plot (Fig. 10a), most of the dykes cluster around 48–52% SiO_2 and 3–4% total alkalis, but a smaller number are more felsic (with SiO_2 ranging up to ~67%) and/or have higher alkalis. If the empirical boundary between tholeiitic and alkali basalts of Macdonald and Katsura (1964) is superimposed, most dykes fall into the tholeiitic field, but a few with relatively low SiO_2 are high in alkalis and are thus chemically equivalent to alkali basalts. It is noteworthy that majority of these alkalic dolerites are from outside the main Tebrakunna Dyke Swarm; most are from the Freycinet Peninsula-Bicheno region (Fig. 2c). Note also that only a handful of samples fall into the alkalic field if the alternative subdivision of Irvine and Baragar (1971) is adopted.

Plots of major elements against Mg# (molar 100*Mg/(Mg + FeII), Table 6) can used to further subdivide the dykes. This parameter quantifies the usual fractionation trends of mafic magmas. On a plot of total iron (FeOtot) against Mg# (Fig. 10f), most of the dykes define a coherent linear trend of progressive iron enrichment. This is usually considered a typical tholeiitic trend, but it is also shown by those dykes with higher alkalis, which on this diagram overlap with, and cannot be distinguished from, the clearly tholeiitic dykes. A third group of dykes plots at lower FeO_{tot} values in a dispersed pattern below the other two groups, and is herein referred to as the calc-alkaline group. A similar pattern is seen in a plot of TiO_2 against Mg# (Fig. 10d): the calc-alkaline group has lower TiO_2 at given Mg#.

A plot of Mg# against SiO_2 (Fig. 10c) shows that the calc-alkaline dykes have consistently higher SiO_2 (generally > 52% and up to 66.6%), than the tholeiitic and alkalic dykes (generally < 52% SiO_2). We consider below whether some of these relatively felsic dykes have been contaminated by the addition of crustal material such as granitic melt, rather than being simply derived from the more mafic dykes by closed system processes such as crystal fractionation.

This subdivision into three groups is arbitrary and some dykes are transitional in character. Two samples from Grants Point, near St Helens, probably belong to the tholeiitic group but have slightly higher SiO_2 (~53%) than usual. A dyke from Apple Orchard Point, Cape Barren Island (sample BA3) has relatively low SiO_2 (~50%) but otherwise more resembles the calc-alkaline dykes.

A plot of CaO against Mg# (Fig. 10g) shows that CaO decreases with fractionation in the tholeiitic dykes, whereas the data for the other groups is more dispersed. In particular, the third, calc-alkaline group tends to have lower CaO at any given Mg#. Alumina also decreases with fractionation (Fig. 10e), but with no clear distinction between the groups. The more incompatible element oxides, Na_2O, K_2O and P_2O_5 (Figs. 10h, i, j), tend to increase with fractionation, but data are scattered. It is noteworthy that some alkalic dykes, mainly from Freycinet Peninsula, have relatively high P_2O_5, as is

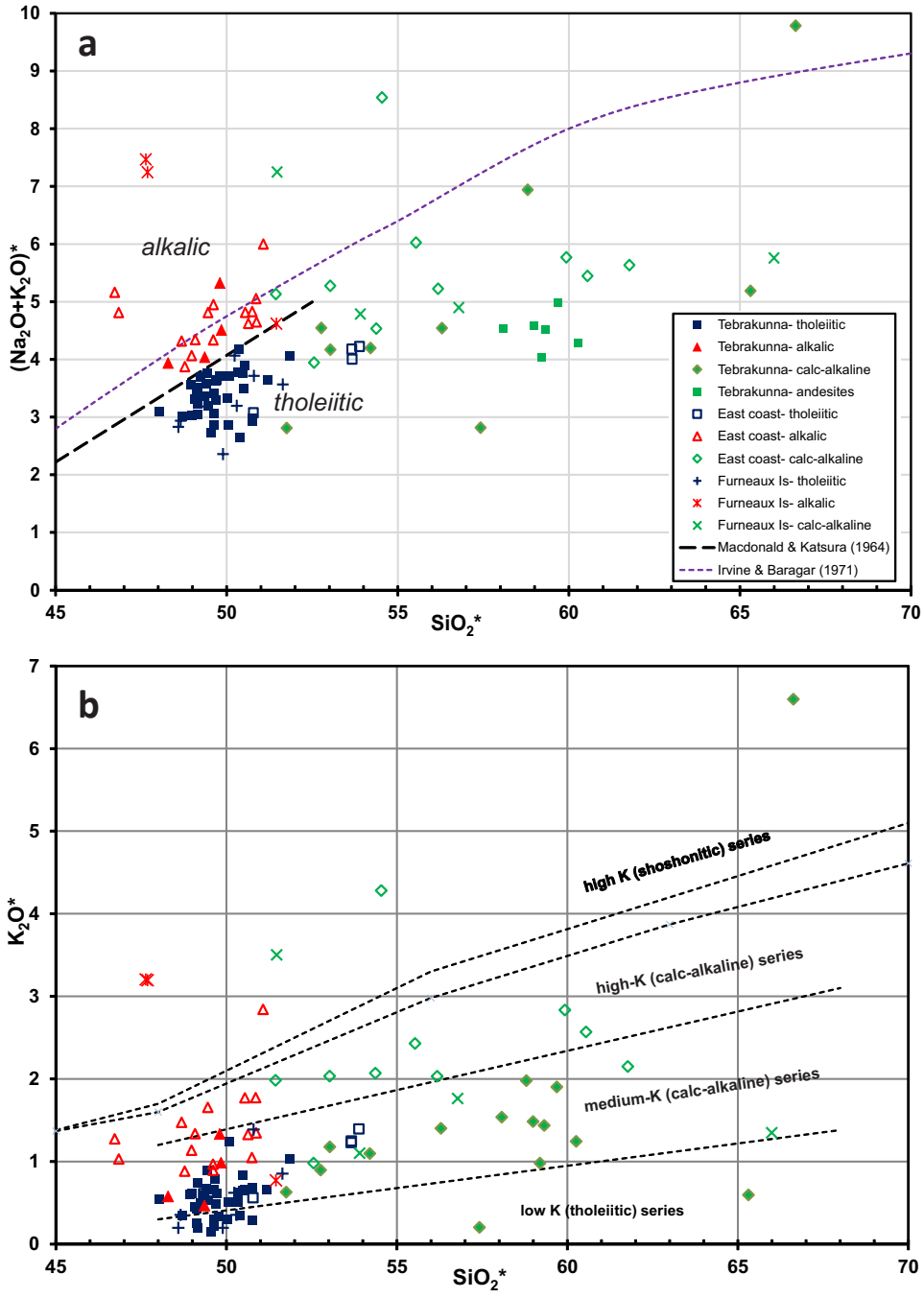

FIGURE 10. Major element plots, with per cent oxides recalculated to 100% anhydrous and CO_2-free.
a. total alkalis ($Na_2O + K_2O$) – SiO_2; **b.** K_2O - SiO_2, with series fields after Le Maitre et al. (1989) and Rickwood (1989).

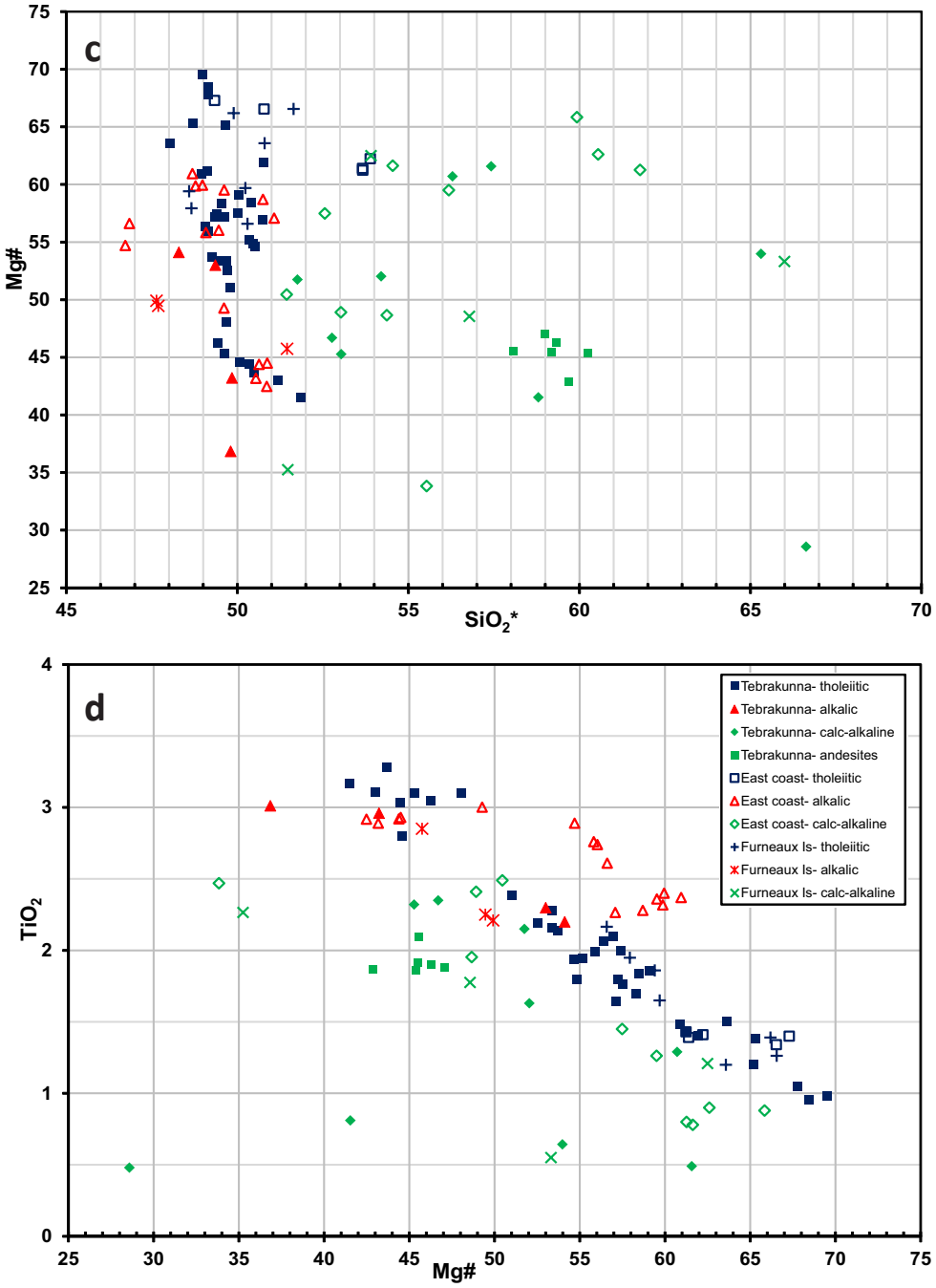

FIGURE 10 cont. Major element plots, with per cent oxides recalculated to 100% anhydrous and CO_2-free. **c.** Mg# – SiO_2; **d.** TiO_2 – Mg#. Mg# is molar 100MgO/(MgO + FeO) calculated at Fe_2O_3(%)/FeO(%) = 0.20.

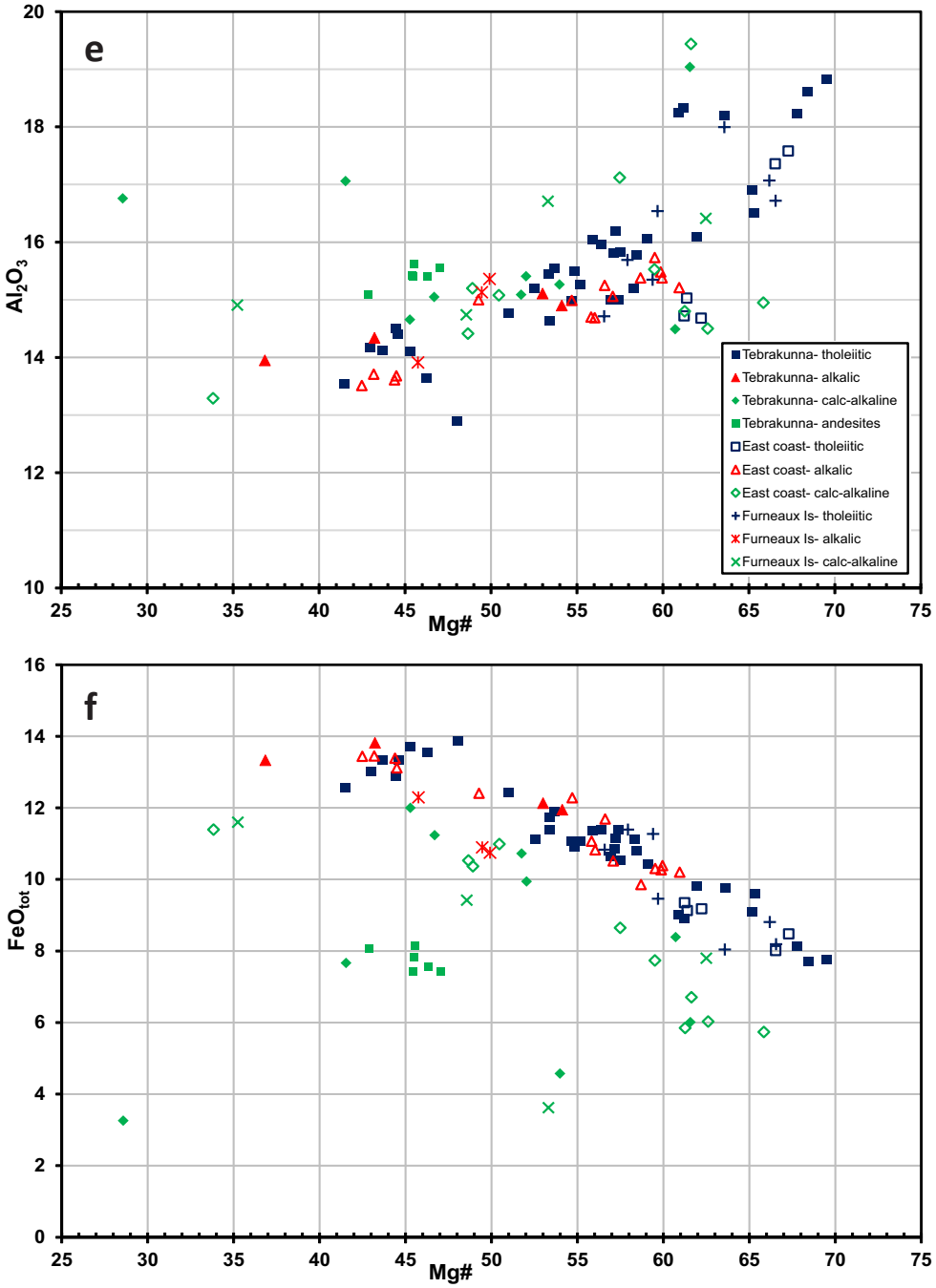

FIGURE 10. cont. Major element plots, with per cent oxides recalculated to 100% anhydrous and CO_2-free. **e.** Al_2O_3 – Mg#; **f.** Total iron as FeO – Mg#.

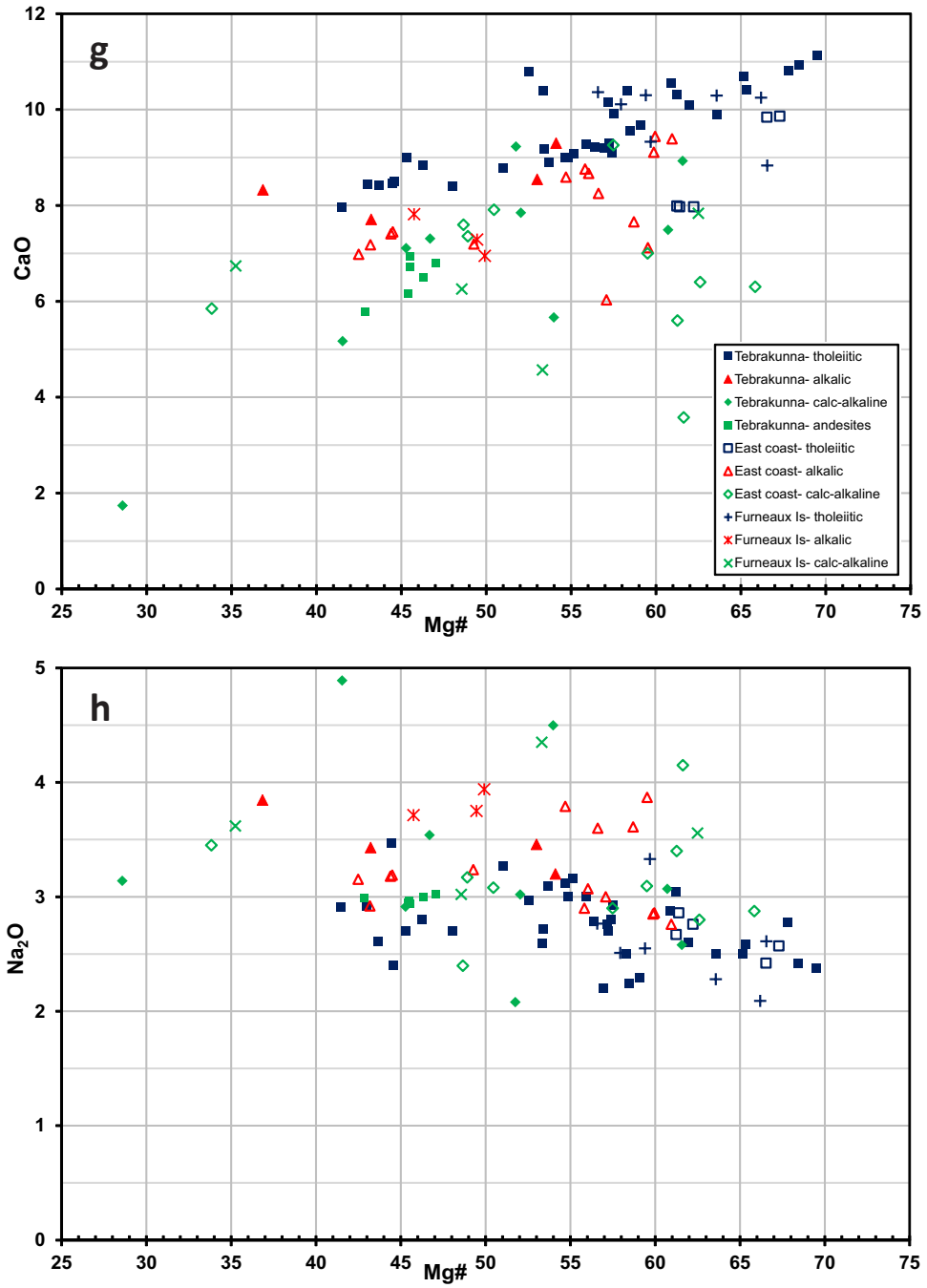

FIGURE 10 cont. Major element plots, with per cent oxides recalculated to 100% anhydrous and CO_2-free. **g.** CaO – Mg#; **h.** Na_2O – Mg#.

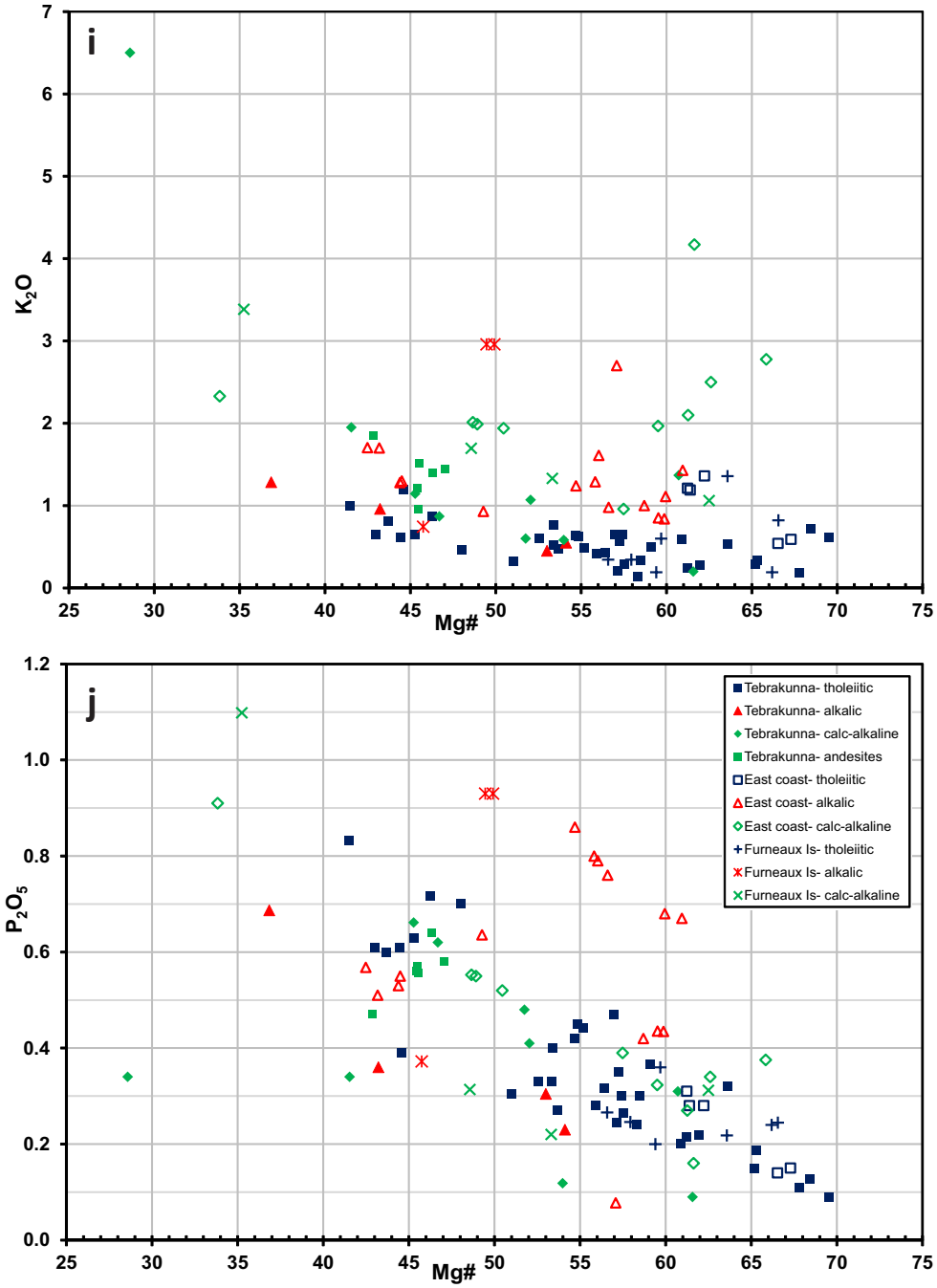

FIGURE 10 cont. Major element plots, with per cent oxides recalculated to 100% anhydrous and CO_2-free. **i.** K_2O – Mg#; **j.** P_2O_5 – Mg#.

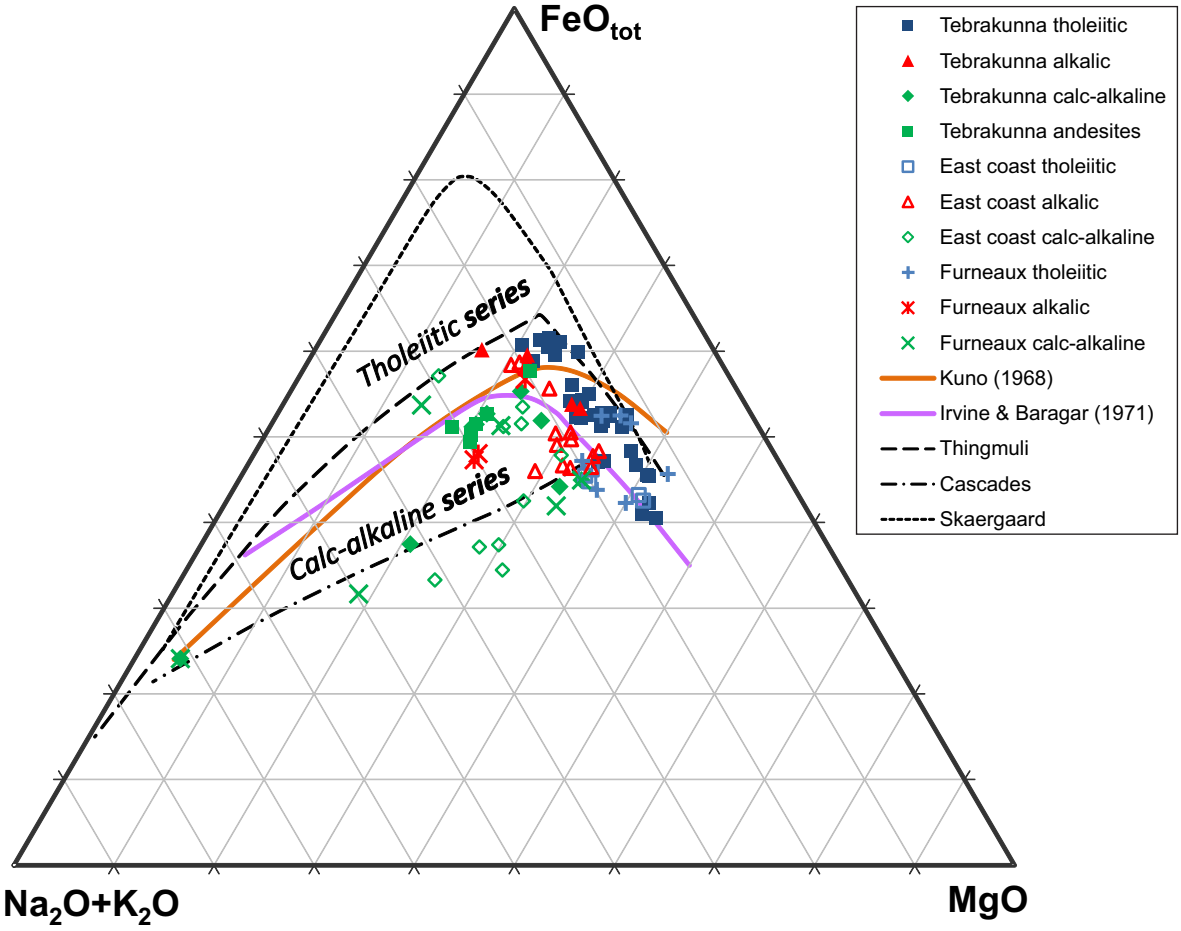

FIGURE 11. AFM (total alkalis-total iron-magnesia) plot, showing boundaries of tholeiitic and calc-alkaline series after Kuno (1968) and Irvine and Baragar (1971). Tholeiitic trends for Skaergaard (Wager and Brown, 1968) and Thingmuli (Carmichael, 1964) and calc-alkaline trend for Cascades (Carmichael, 1964) also shown.

typical of alkaline magmas, but others have similar or lower levels to the tholeiites. This is further discussed below in relation to trace elements.

On a plot of K_2O against SiO_2 (Fig. 10b), the tholeiitic dykes fall into the low-K (tholeiitic) and medium-K calc-alkaline fields of Le Maitre (2002). The alkalic and contaminated dykes are more dispersed, but mostly fall into the medium-K and high-K calc-alkaline fields, with a few with very high K_2O falling into the shoshonite field of Rickwood (1989).

On an AFM (total alkali-total iron-magnesia) diagram (Fig. 11) tholeiitic dykes show a clear iron-enrichment trend and mostly plot in the tholeiitic field of Irvine and Baragar (1971), although in the alternative plot of Kuno (1968) they straddle the boundary with the calc-alkaline field. The alkalic dykes are displaced toward the alkali apex and plot more ambiguously, whereas the calc-alkaline dykes show no clear trend and mostly plot in the calc-alkaline field.

Although classical CIPW norms are of limited use for these rocks and are not presented in full in Table 6, it may be worth noting that almost all of the calc-alkaline dykes are quartz (Q) normative, whereas about one third of the tholeiitic dykes are Q-normative and two thirds are ol-hy normative, and most of the alkalic group are also ol-hy normative. The only truly alkalic dykes, in the sense of silica-undersaturation (i.e., ol-ne normative) are the dykes at Lagunta Creek, Freycinet Peninsula (samples LC1 and LC3) and Stanley Point, Flinders Island (FLD4). As discussed below, the latter also has alkalic trace element geochemistry and clearly belongs to a different suite.

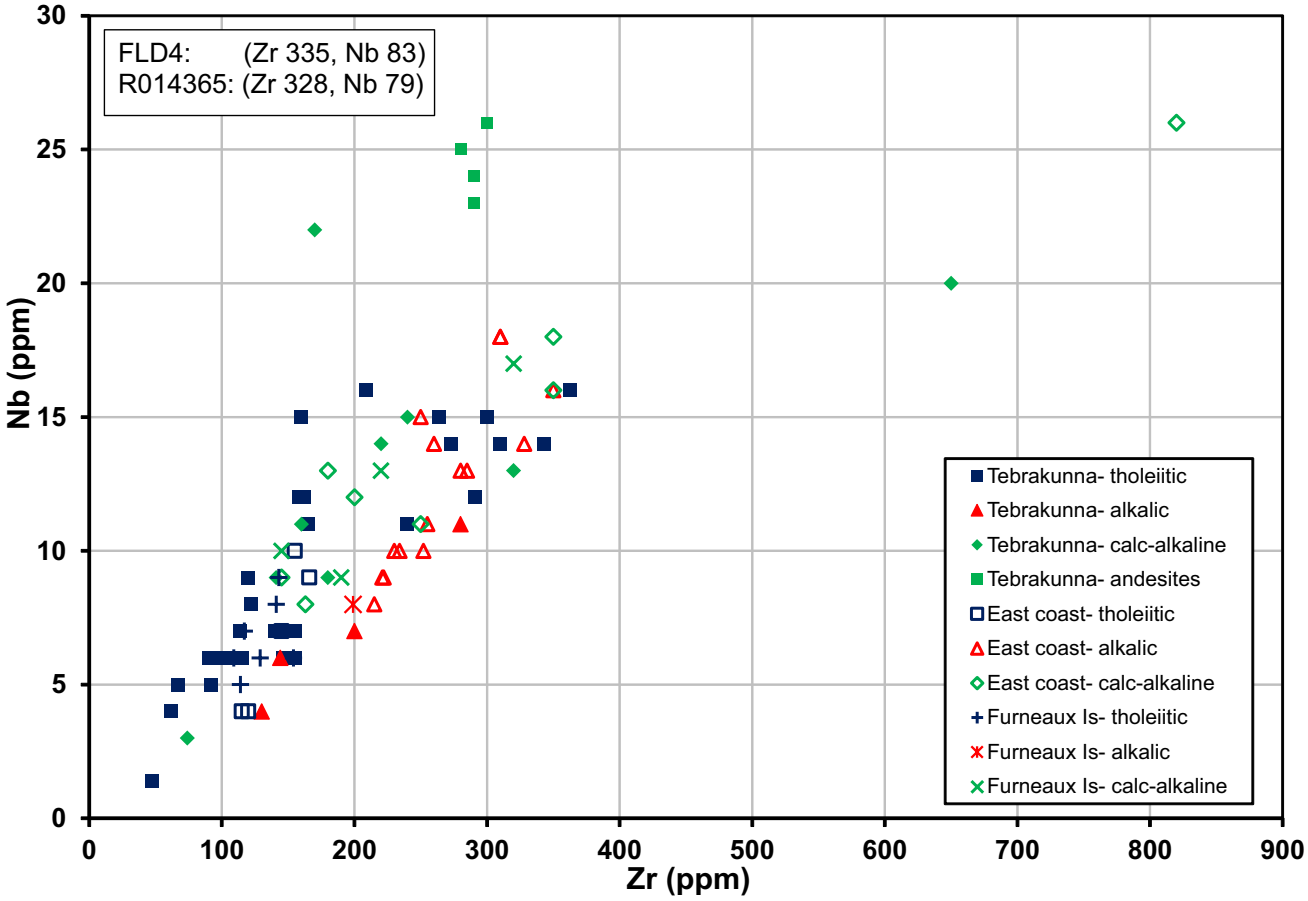

FIGURE 12. Nb-Zr plot for dolerite dykes.

Pearce element ratios

In order to test which minerals where involved in crystal fractionation, the Pearce Element Ratio (PER) analysis technique (Russell and Stanley, 1990) has been applied to the major element data.

The first requirement of the technique is that the samples must be related to a common parent system that at one time was homogeneous, i.e., they are cogenetic. This is assumed to be true for the tholeiitic and alkalic dykes, due to their similar mode of occurrence and relatively uniform petrographic character.

The second requirement is to identify an element that did not participate in the material transfer process that caused the geochemical variation. This is termed a conserved element and is used as a standardising denominator of the PERs. Highly incompatible elements that are not involved in likely fractionating minerals are the best possibilities for conserved elements, particularly if they are also immobile during alteration and weathering. If two elements are plotted against each other and lie on a line that passes through the origin then they are likely to be conserved elements (Stanley and Madeisky, 1993). Plots of Nb vs Zr (Fig. 12) and P_2O_5 vs Zr (not shown) come closest to this condition, particularly if the calc-alkaline dykes are not considered. As Zr is a relatively abundant trace element, easily determined by XRF with good relative precision, it is the preferred conserved element denominator, and is expressed as molar values (i.e., 10000*Zr (ppm)/91.22).

The numerators are derived from the major element oxide weight per cent values, converted to molar Al, Fe, Mg, Ca and Na. They are divided by Zr to calculate three vectors:

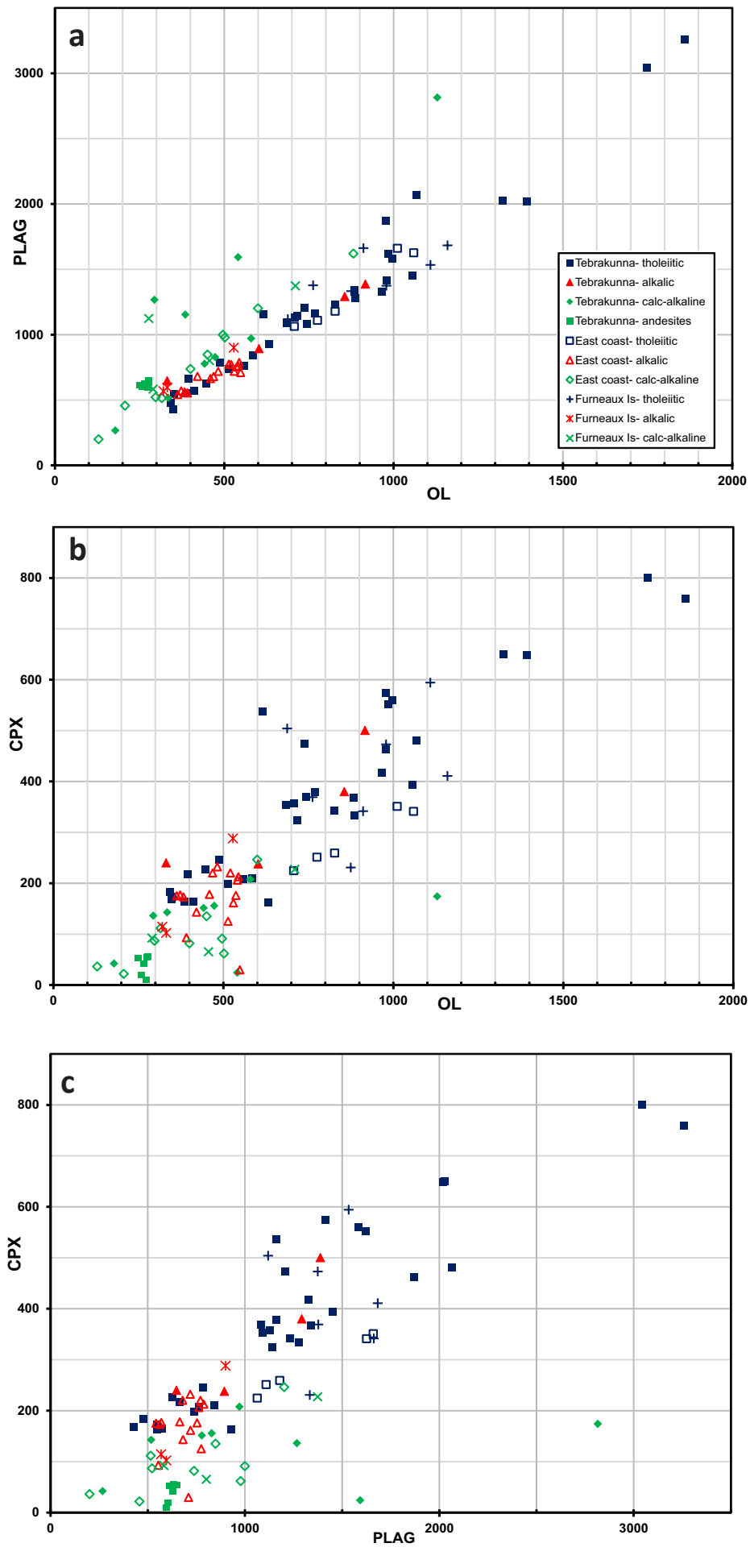

FIGURE 13. Pearce Element Ratio plots of vectors.
a. olivine and plagioclase;
b. olivine and clinopyroxene;
c. plagioclase and clinopyroxene.
Samples MR146 and 63095 plot along trends, off scale to the upper right. See text for discussion.

$OL = [-Ca/2 - Na/4 + (Fe_{tot} + Mg)/2 + Al/4]/Zr$

$PLAG = (Na/2 + Al/2)/Zr$

$CPX = (Ca + Na/2 - Al/2)/Zr$

related to olivine, plagioclase and clinopyroxene fractionation respectively.

On a Pearce Element Ratio assemblage test plot of PLAG against OL (Fig. 13a), samples from both the tholeiitic and alkalic groups define a coherent linear trend at an angle between the directions expected for olivine and plagioclase fractionation. A cruder trend is evident for the calc-alkaline dykes, which are expected to have been affected by other processes, additional to crystal fractionation. This diagram does not indicate whether clinopyroxene is a fractionating phase, as its vector is perpendicular to the diagram.

On a similar plot of CPX against OL (Fig. 13b), the samples from the tholeiitic dykes show a moderately coherent linear trend, but the correlation is poor for the alkalic dykes and absent for the calc-alkaline dykes. In the latter case, the assumption that they are related to a common homogeneous parent is likely to be invalid, as they are thought to contain various amounts of possibly different crustal contaminants. In this diagram, the fractionation vector for plagioclase is perpendicular to the diagram. Note that CPX has negative values (not plotted) for two strongly calc-alkaline samples (NJ446 from Dianas Basin and NJ364B, a granite-dolerite hybrid rock from Purdon Bay), due mainly to very low CaO values.

On a plot of PLAG against CPX (Fig. 13c), the tholeiitic dykes also show a moderately coherent linear trend, but again the correlation is poor for the alkalic dykes and absent for the calc-alkaline dykes. In this case, the vector for olivine is perpendicular to the diagram.

Overall, the trends shown on these diagrams (Fig. 13a–c) are consistent with the interpretation that much of the composition variation shown by the tholeiitic dykes is due to fractionation of olivine, clinopyroxene and plagioclase. Other factors, such as variable degrees of partial melting or element mobility may have affected the alkalic dykes, whereas in the calc-alkaline dykes any fractionation trends have been largely obscured by processes such as assimilation and/or mixing with felsic magmas.

However, in each of the diagrams the same four dykes (all from the tholeiitic group and from the main Tebrakunna Dyke Swarm) have the largest values of OL, PLAG and CPX, due to their low values of the chosen conserved element, zirconium, which forms the denominator. Therefore, the apparent mutual correlation in Figure 13a–c may be spurious at high values, particularly as two of these samples (63095 from the Mt William area, with 48 ppm Zr, and MR146 from Spinel Creek near Weldborough with only 26 ppm Zr) are old analyses.

This raises the issue of criticisms of the Pearce Element Ratio technique made by Rollinson (1993) and other authors referred to therein. Although a detailed exposition of the argument is outside the scope of this report, it can be shown that the correlation coefficient of two ratios (x/z and y/z) with a common denominator is not necessarily zero, even if x, y and z are uncorrelated and unrelated. Thus, spurious correlations may exist between the ratios OL, CPX and OL due to even small variations in their common denominator Zr.

Compatible trace elements

The highly compatible trace elements Ni (Fig. 14e) and Cr (Fig. 14c) both decline strongly with fractionation (i.e., correlate positively with Mg#), although all three groups (tholeiitic, alkalic and calc-alkaline dykes) show considerable scatter. The overall trend is consistent with fractionation of olivine and clinopyroxene.

In contrast, vanadium (Fig. 14b) increases with fractionation in the tholeiitic dykes and most of the alkalic dykes, whereas in the more felsic calc-alkaline dykes, data is more dispersed and at lower levels. Scandium (Fig. 14a) shows similar behaviour, but the data are more scattered. These trends are similar to those of titanium.

Cobalt (Fig. 14d) shows no clear trends with fractionation. Levels are ~40 ppm, regardless of Mg#, in most tholeiitic and alkalic dykes, but are again generally lower in the calc-alkaline dykes.

High field strength trace elements (HFSE)

Most incompatible high field strength elements (e.g., Zr, Nb, Ti, P, La, Ce and Nd) vary over considerable ranges, and pairs of these elements show good to fair mutual correlations (e.g., Fig. 12). These elements also tend to show negative correlations with Mg#, and thus much of their variation is probably due to fractionation (Figs 10c, 10j, 14m).

The only dyke with a clearly alkalic trace element signature is from near Stanley Point, at the northern tip of Flinders Island (samples FLD4, R014365). With

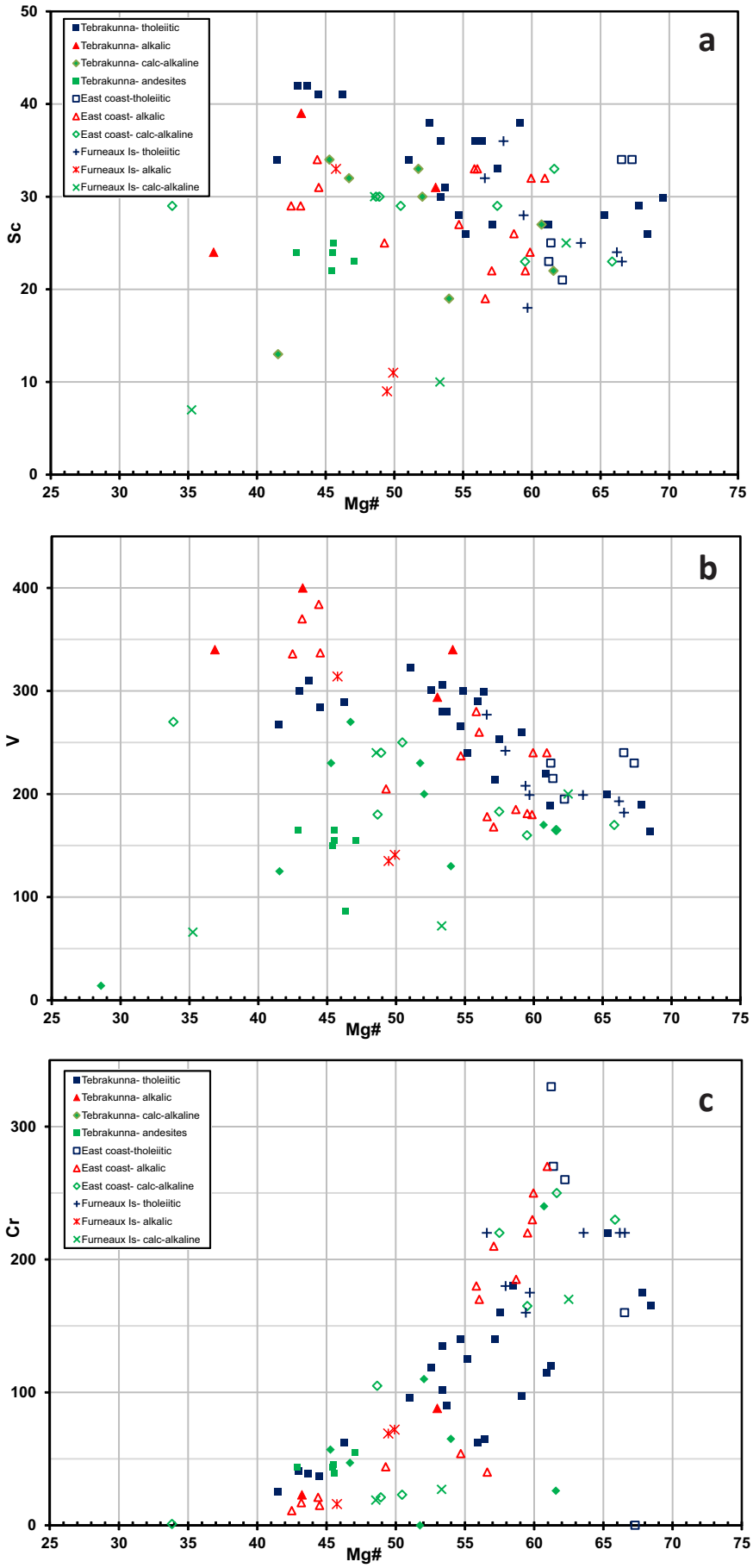

FIGURE 14.
Trace element plots.
a. Sc–Mg#
b. V–Mg#
c. Cr–Mg#.

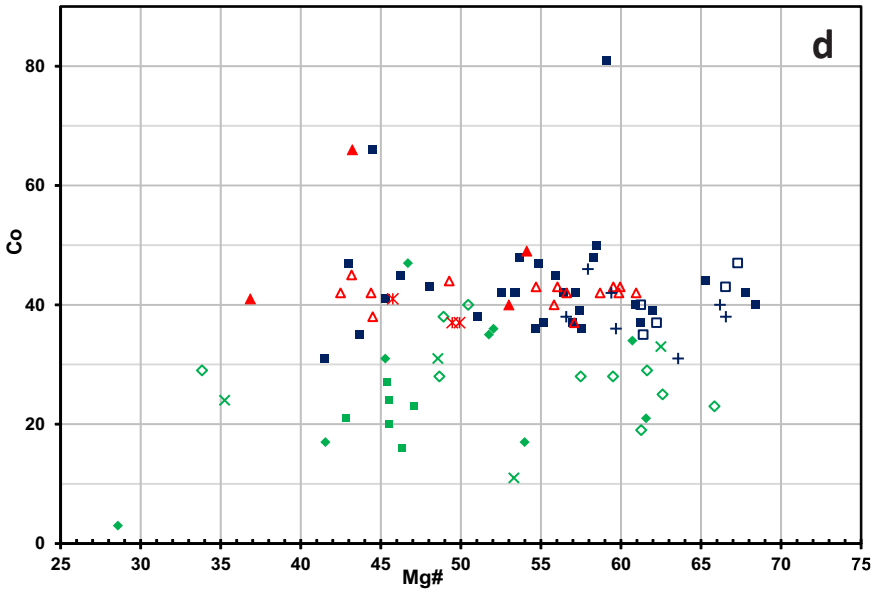

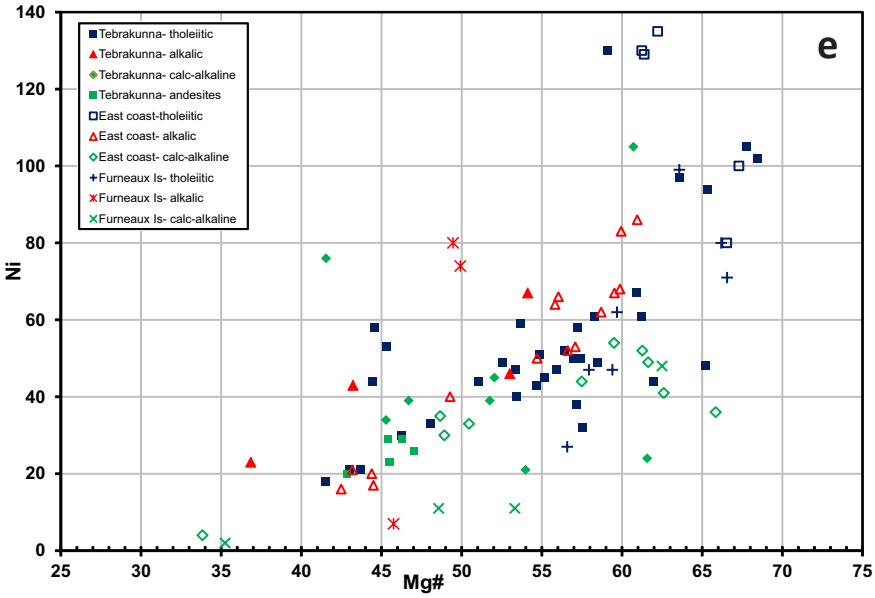

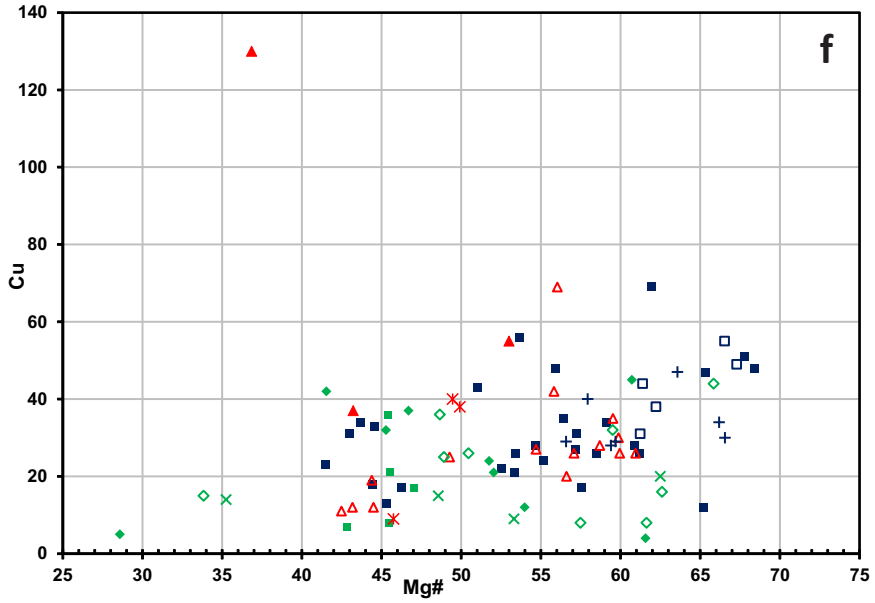

FIGURE 14. (continued)
Trace element plots.
d. Co–Mg#
e. Ni–Mg#
f. Cu–Mg#.

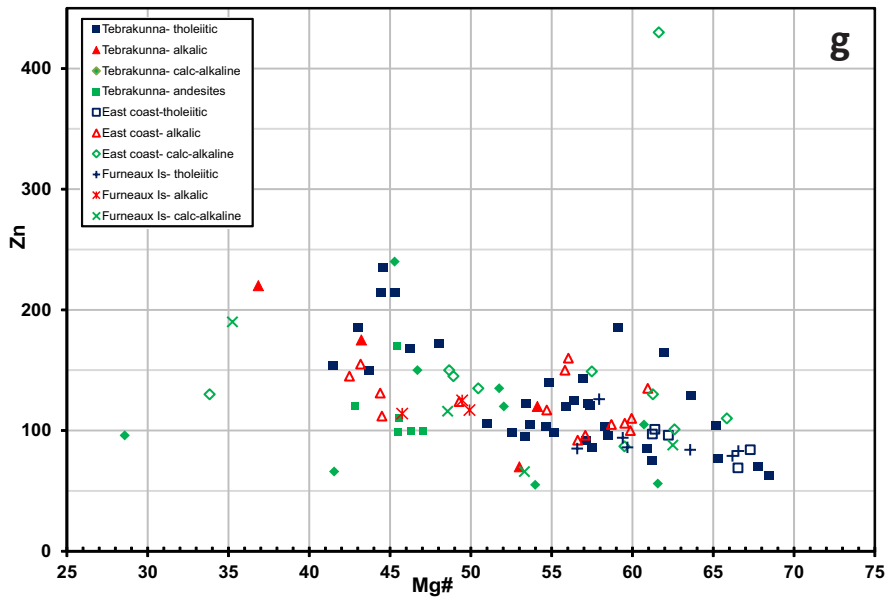

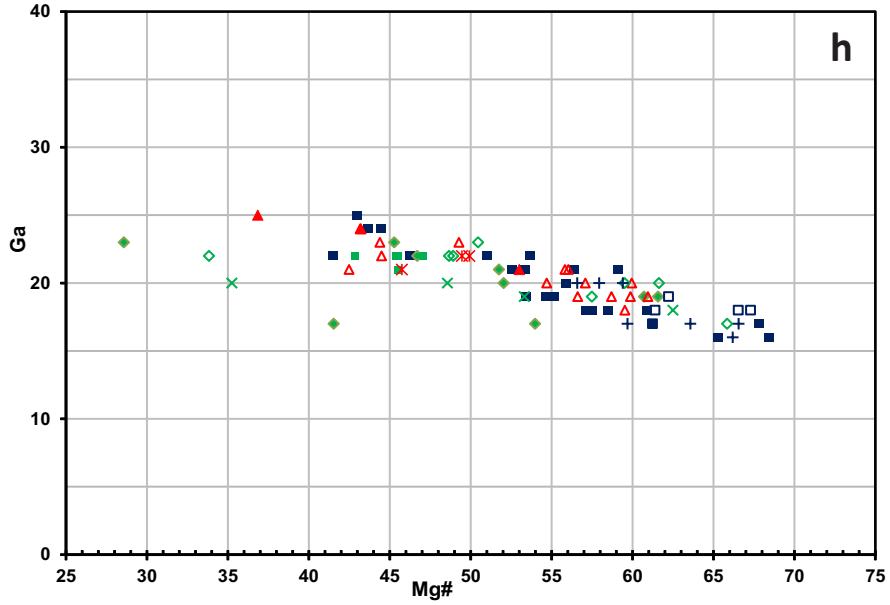

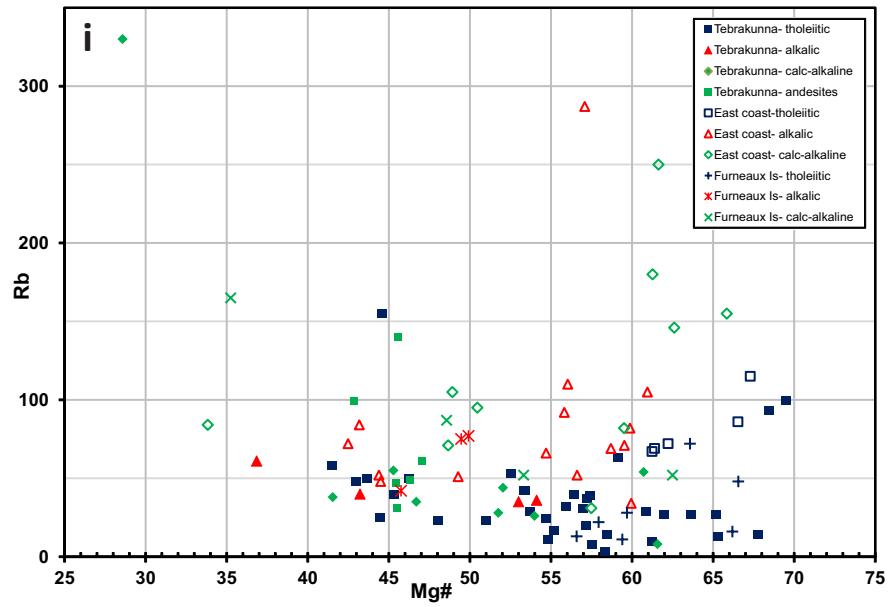

FIGURE 14. (continued) Trace element plots.
g. Zn–Mg#
h. Ga–Mg#
i. Rb–Mg# .

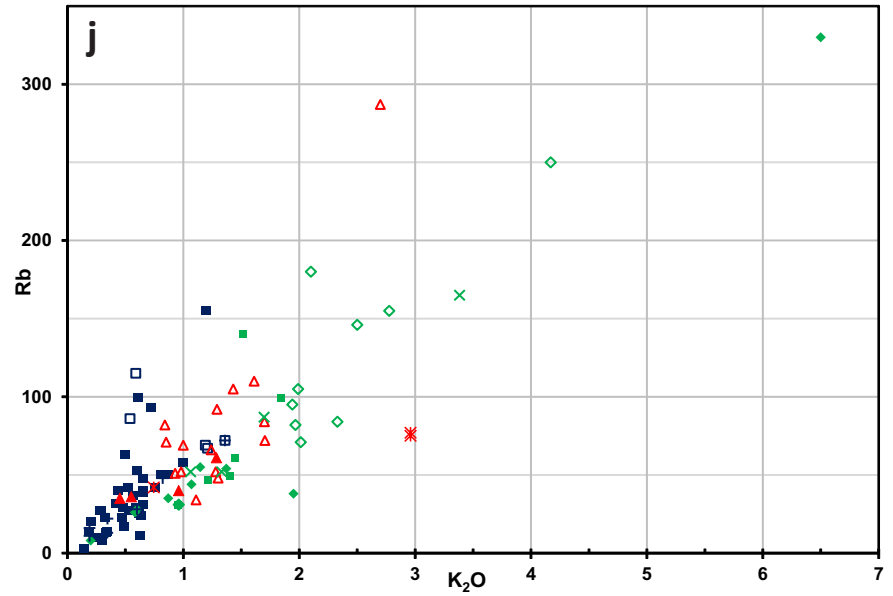

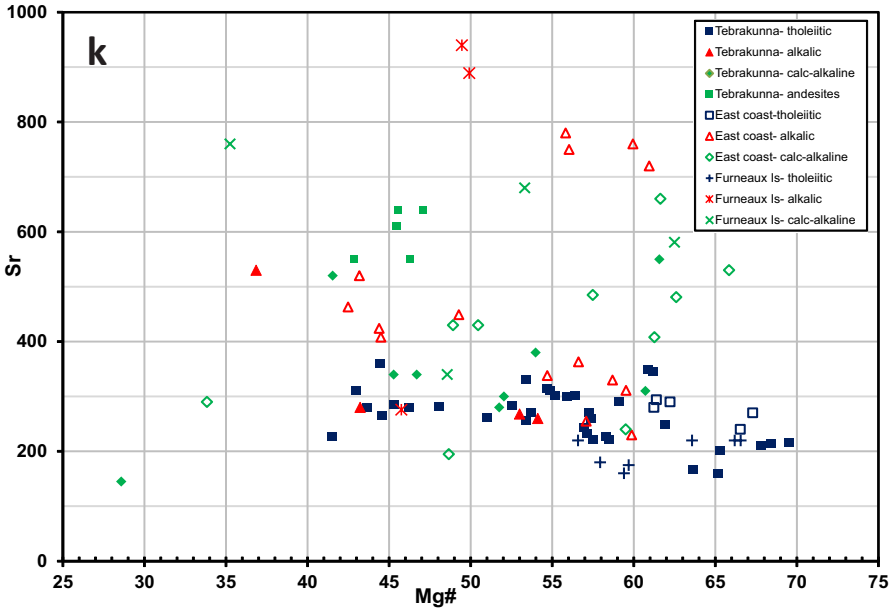

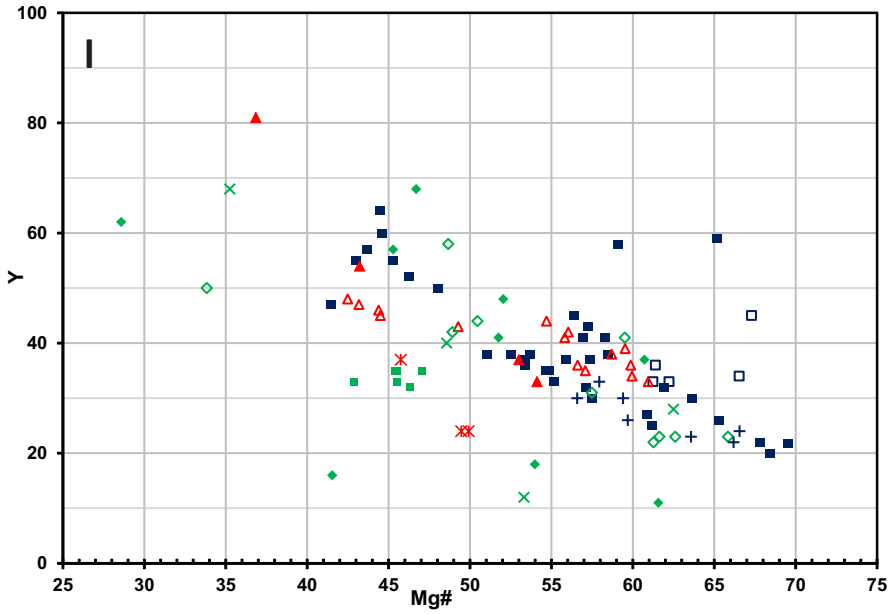

FIGURE 14. (continued)
Trace element plots.
j. Rb–K_2O
k. Sr–Mg#
l. Y–Mg#.

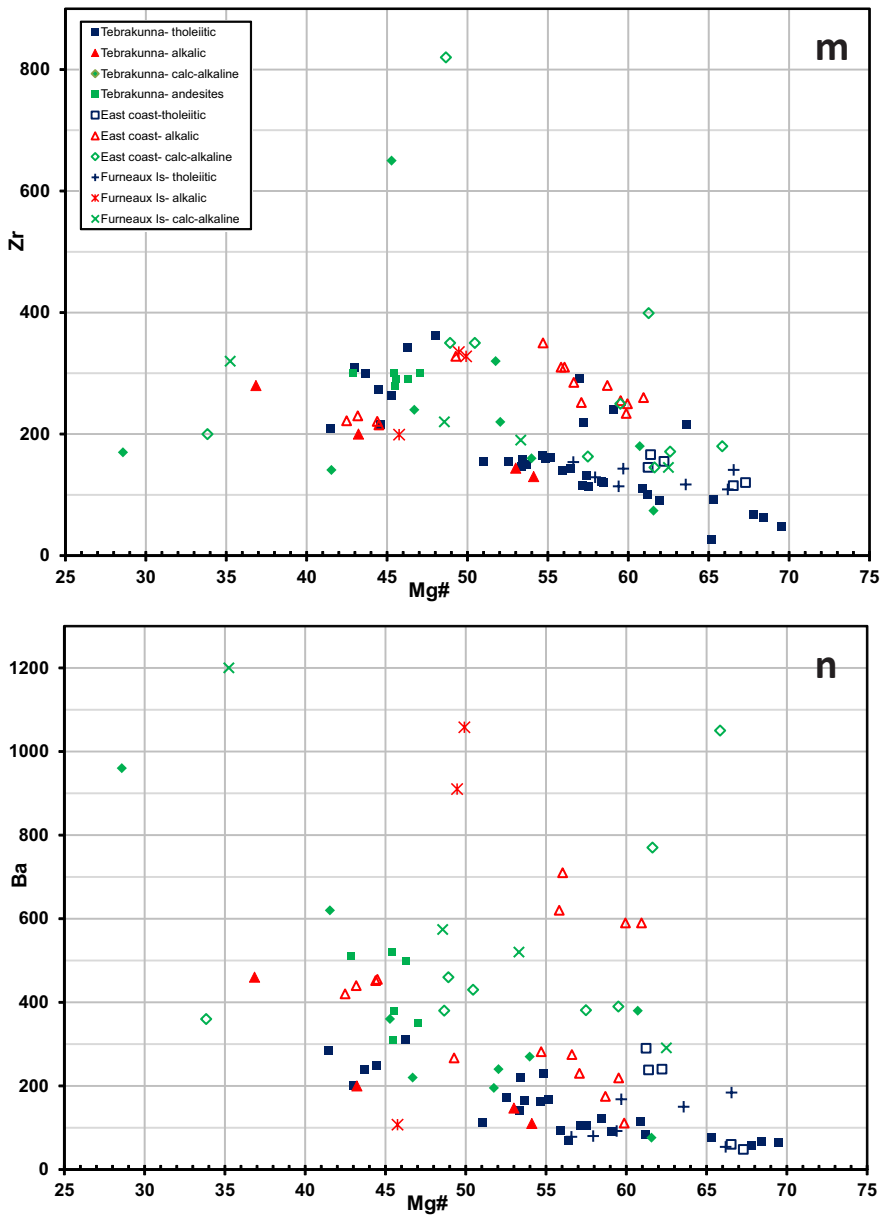

FIGURE 14. (continued) Trace element plots.
m. Zr–Mg#
n. Ba–Mg#.

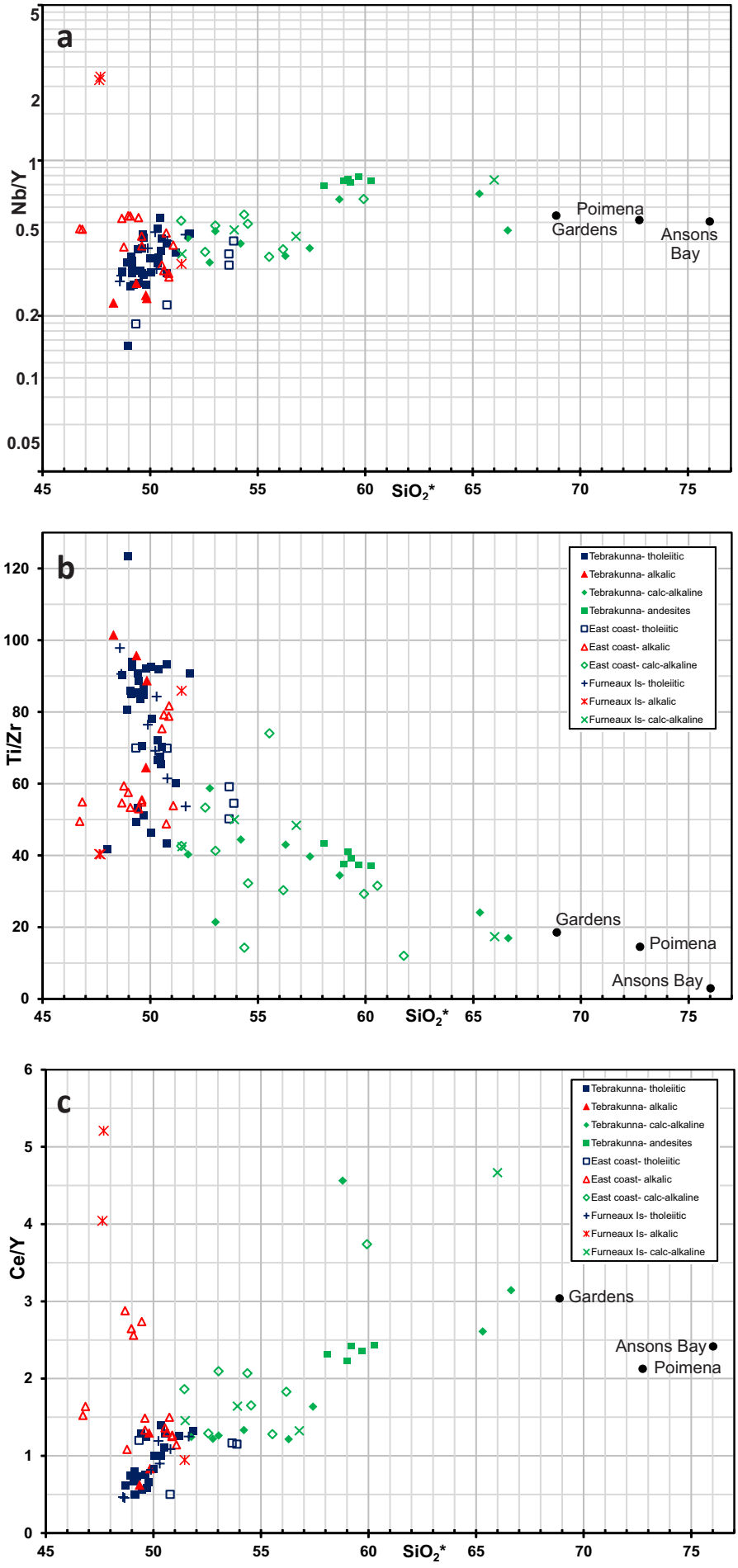

FIGURE 15. Plots of **a.** Nb/Y–SiO_2; **b.** Ti/Zr–SiO_2; **c.** Ce/Y–SiO_2 for the dolerite dykes; the mean compositions of the Gardens Granodiorite, Poimena Granite and Ansons Bay Granite (Geoscience Australia data) are also shown.

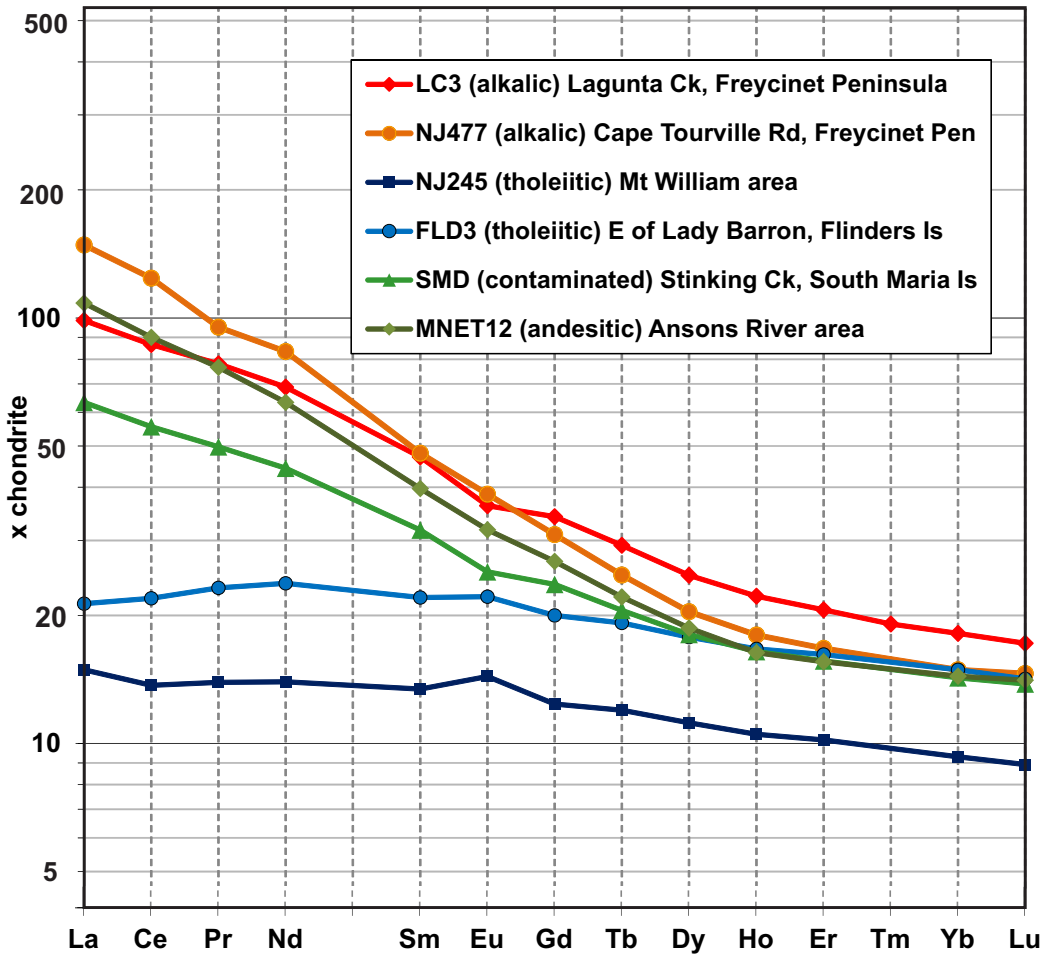

FIGURE 16. Rare earth element plots of selected dolerite samples, normalised to average CI chondritic meteorites (Boynton, 1984), based on ICPMS data.

this exception, those dykes classified as alkalic, on the basis of major elements, lack the relative enrichment in Nb (e.g., Nb/Y >1) typical of within-plate alkali basalts, and in most respects, their trace element signature is little different from the tholeiitic dykes. A few alkalic dykes from Freycinet Peninsula (Lagunta Creek, Cape Bay, Cape Tourville) have slightly higher Nb/Y ratios (0.36–0.44) than most of the clearly tholeiitic dykes. Most of the calc-alkaline dykes also have moderately high Nb/Y (up to 0.8), although some do not (Fig. 15a).

The calc-alkaline dykes have generally lower Ti/Zr ratios than the other groups, further decreasing with increasing SiO_2 (Fig. 15b). This could indicate either fractionation of a Ti-bearing phase, or assimilation of felsic material with low Ti/Zr.

Rare earth elements (REE)

Complete REE data were obtained by ICPMS for six samples, broadly representative of the compositional range and geographic distribution of the dykes (Fig. 16).

Two representative samples of the tholeiitic group (NJ245 from the main Tebrakunna Dyke Swarm, and FLD3 from Flinders Island) display relatively flat, weakly LREE enriched ((La/Yb)N ~1.4–1.6) patterns at ~10–25 × chondrite. For both samples, LREE are nearly flat, whereas the HREE display a slight negative slope. The small positive Eu anomaly in sample NJ245 may indicate slight accumulation of plagioclase, consistent with abundant plagioclase phenocrysts observed in thin section.

A representative sample of a calc-alkaline dolerite (SMD from Maria Island), and an andesite (MNET12) from the Ansons Bay area, have similar HREE contents, but are more enriched in LREE than the tholeiitic dykes. Together with their higher SiO_2 contents (51.4% and 58.0%), this is consistent with contamination by granitic melt.

Two alkalic dolerites (LC3 and NJ477 from Freycinet Peninsula) are also strongly LREE-enriched. This is

probably a primary feature, perhaps reflecting a lower degree of partial melting of mantle, as their lower SiO_2 (44.2% and 47.6%) suggests that they are unlikely to be have been significantly contaminated by granitic or other crustal material.

In the absence of complete REE data, the ratio Ce/Y can be used to estimate degree of LREE- enrichment of other samples, since Y^{3+} has similar behaviour in magmas to the HREE, particularly Ho^{3+} (e.g. Bau, 1996) The average chondritic meteorite or model primitive mantle has Ce/Y ~0.39, analogous to (La/Yb)N = 1 (Sun and McDonough, 1989). The dolerite dykes range in Ce/Y from ~0.45 to 5.2 (Fig. 15c) and are thus all likely to be LREE-enriched relative to chondrite. The tholeiitic group and some alkalic dykes tend to have relatively low values (0.45–1.32) and these are likely to display only weak LREE-enrichment. Some of the alkalic dykes from Freycinet Peninsula (Lagunta Creek, Carp Bay and Cape Tourville) have distinctly higher Ce/Y (1.52–2.88) (as is also evident in the ICPMS data), and are also relatively high in Nb/Y and P_2O_5.

The highest ratio (Ce/Y = 4.0–5.2) is from a dyke near Stanley Point, Flinders Island (samples FLD4, R014365) which probably belongs to a different suite. However, many members of the calc-alkaline group also have relatively high values (1.2–4.6). If the calc-alkaline dykes were derived from the tholeiitic dykes by simple contamination or assimilation of felsic material, the latter must have had higher Ce/Y and Nb/Y, and lower Ti/Zr. This is broadly true of the granitic host rocks (Fig. 15) and is further discussed below in relation to petrogenesis.

Large ion lithophile elements (LILE)

Rubidium (3–330 ppm) (Fig. 14i), barium (54–1200 ppm) (Fig. 14n) and to a lesser extent strontium (145–940 ppm) (Fig. 14k) vary over wide ranges and display crude positive correlations with K_2O (e.g., Fig. 14j). The highest values are in calc-alkaline dykes and a few alkalic dykes, but some of these dykes are low in these elements. Although these elements are normally considered highly incompatible (except for Sr in plagioclase and Ba in potash feldspar), most plots are scattered. Fractionation trends have probably been masked by element mobility during metamorphism and weathering.

Virtually all high (>10 ppm) lead values are from contaminated, relatively felsic dykes, notably those from Onion Creek near St Helens (sample NJ446, 63 ppm) and a dolerite-granite hybrid rock from Purdon Bay (NJ364B, 48 ppm). This probably reflects a granitic or other crustal component. In alkalic and tholeiitic dykes, lead is at or below 10 ppm, excluding three older analyses of doubtful accuracy.

Caesium also varies widely, from below detection limit (<3 ppm) to 62 ppm in a calc-alkaline dyke (FP11) from Freycinet Peninsula, although in most samples it is below 10 ppm. It shows no clear correlation with other elements or dyke type. This erratic behaviour is probably due to its very high mobility.

Other elements

Copper data (Fig. 14f) are very scattered, with one anomalously high value (135 ppm in sample MBT143 from near Ansons Bay). The remainder range from 4–69 ppm and perhaps tend to decline with fractionation.

Zinc (Fig. 14g) appears to behave as a weakly incompatible element, increasing with fractionation, but the data are quite scattered, particularly for the calc-alkaline group of dykes. It is anomalously high (430 ppm) in a calc-alkaline dyke (NJ446) from near Dianas Basin; remaining data range from 55–240 ppm.

Gallium (Fig. 14h) shows a clear but small increase with fractionation (from ~16 to ~25 ppm), with more scatter in the calc-alkaline dykes. It correlates negatively with Al_2O_3, which shows the opposite fractionation trend.

Arsenic is weakly anomalous in some dykes, with maxima (58 and 34 ppm) in two tholeiitiic dykes from south of Musselroe Bay. Antimony and bismuth (maximum values of both, 4 ppm) are close to detection limit and show no clear association with each other or arsenic.

Molybdenum has a maximum of only 9 ppm in a calc-alkaline dyke (FY31) from near Mt Freycinet. Only nine samples returned values greater than 2 ppm; it is probably significant that all are from calc-alkaline or alkalic dykes.

Tin is weakly anomalous (>10 ppm) in six samples, but is probably significant that five are old (1973–1974) MRT analyses, from a time when laboratory contamination is known to have sometimes occurred. The highest tin value (41 ppm) is however, from a recent recrushing and analysis of a sample (FP21) from Freycinet Peninsula, belonging to the contaminated group of dykes. The earlier analysis of the same sample returned 58 ppm Sn, suggesting that the anomaly is real. The dyke may have assimilated granitic country rock, which is known to locally contain elevated tin values.

Tungsten has an apparent maximum value of 14 ppm from sample R1084 near Roses Tier, possibly due to laboratory contamination, as other samples returned 3 ppm or less.

Thorium and uranium tend to be highest in calc-alkaline felsic dykes, particularly "hybrid" rocks with obvious petrographic evidence of interaction with granite, such as NJ364B (Purdon Bay), MBT167 (Gripe Creek) and FY32 (Hawksnest Cove). In tholeiitic and alkalic dykes, and some calc-alkaline dykes, these elements are generally close to or below XRF detection limits of 2 and 1 ppm respectively.

Spider diagrams

Incompatible element spider diagrams, in which trace and minor element data are normalised to model primitive mantle and plotted in order of decreasing mantle incompatibility (Sun and McDonough, 1989), are plotted for six representative samples for which comprehensive analytical data (including ICPMS) are available (Fig. 17a). Caution is needed in interpreting the LILE, due to element mobility. In particular, all six samples are very enriched (at hundreds to thousands of times above mantle levels) in Cs, a highly mobile element. As this is unlikely to be a primary magmatic feature, that element is not plotted.

Although relative abundances are lower in the two tholeiitic dykes than in the other types, all six samples (Fig. 17a) show jagged patterns with large positive Pb anomalies and distinct negative Nb and Ta anomalies, relative to adjacent elements of similar incompatibility. Weak to moderate negative Ti anomalies are also present. This is a crust-like signature, and might have been acquired by high level assimilation, or by partial melting of mantle previously contaminated by crustal material.

The two samples from the calc-alkaline group (MNET12 and SMD) also show moderate positive K anomalies, consistent with assimilation of granitic material, but larger positive K (and Rb) anomalies are also present in sample NJ245, from the tholeiitic group.

Less complete diagrams are plotted for other samples for which adequate XRF data are available (Fig. 18a, b, c). XRF data for Pb, Th and U are not used, as they are close to detection limit for many samples. These diagrams show some features similar to those seen in the ICPMS data: in particular most of the dykes show a negative Nb anomaly. This is well-developed in all the dykes from the central east coast (Maria Island to Grant Point), including in relatively low-SiO_2, alkalic dykes from Freycinet Peninsula (e.g., from Lagunta Creek, Fig. 18b) which lack direct evidence for crustal contamination. This perhaps suggests that relative Nb depletion is not necessarily due to high level contamination, and might be a primary, perhaps subduction-related signature. Negative Nb anomalies tend to be less pronounced or even absent in some dykes from the main Tebrakunna Dyke Swarm (e.g., from the Mt William area), due to higher Nb/K (Fig. 18a). These are mostly tholeiitic dykes, but similar relatively high Nb/K is seen in also some calc-alkaline andesitic dykes (e.g., MBT165, MBT97 and MBT98, Ansons River area, Fig. 18c). Some tholeiitic dykes from Flinders Island (e.g., FLD2 and FLD3, Lady Barron, Fig.18a) show a similar pattern.

Weak to moderate negative Ti anomalies are also present in many calc-alkaline dykes. These are probably crustal signatures, due to either local high level contamination (e.g., from granitic country rocks) or are indicative of a crustally contaminated mantle source.

Spider diagrams are plotted from the mean compositions of the tholeiitic, alkalic and calc-alkaline groups, utilising XRF data (Fig. 19). Only those samples for which all the plotted elements were determined were used, and the Stanley Point dyke FLD4 was excluded when calculating the mean of the alkalic dolerites. Separate averages were calculated for basaltic (13 samples), andesitic (5 samples) and clearly contaminated or "hybrid" (5 samples) members of the calc-alkaline group.

The mean compositions of each group are subparallel and remarkably similar, with large negative Nb and smaller negative Sr and Ti anomalies. The alkalic and calc-alkaline groups have higher absolute levels of incompatible elements, relative to the tholeiitic group, except that the calc-alkaline groups (especially the hybrid rocks) have similar or greater depletion in Ti.

Overall, the patterns are similar to that of average upper continental crust (Taylor and McLennan, 1981) but with more marked negative Ti and P anomalies (Fig. 19a).

Averages for the alkalic and calc-alkaline groups are also plotted, normalised against the mean composition of the tholeiitc dykes (Fig. 19b). The basaltic and andesitic calc-alkaline groups plot parallel to, and slightly below average upper continental crust for the most incompatible elements (Rb, Ba, Nb. K), but have higher levels for the less incompatible elements (REE, Sr, P, Zr, Ti and Y). Thus the calc-alkaline dykes cannot be modelled by simple assimilation of average upper continental crust by the tholeiitic group.

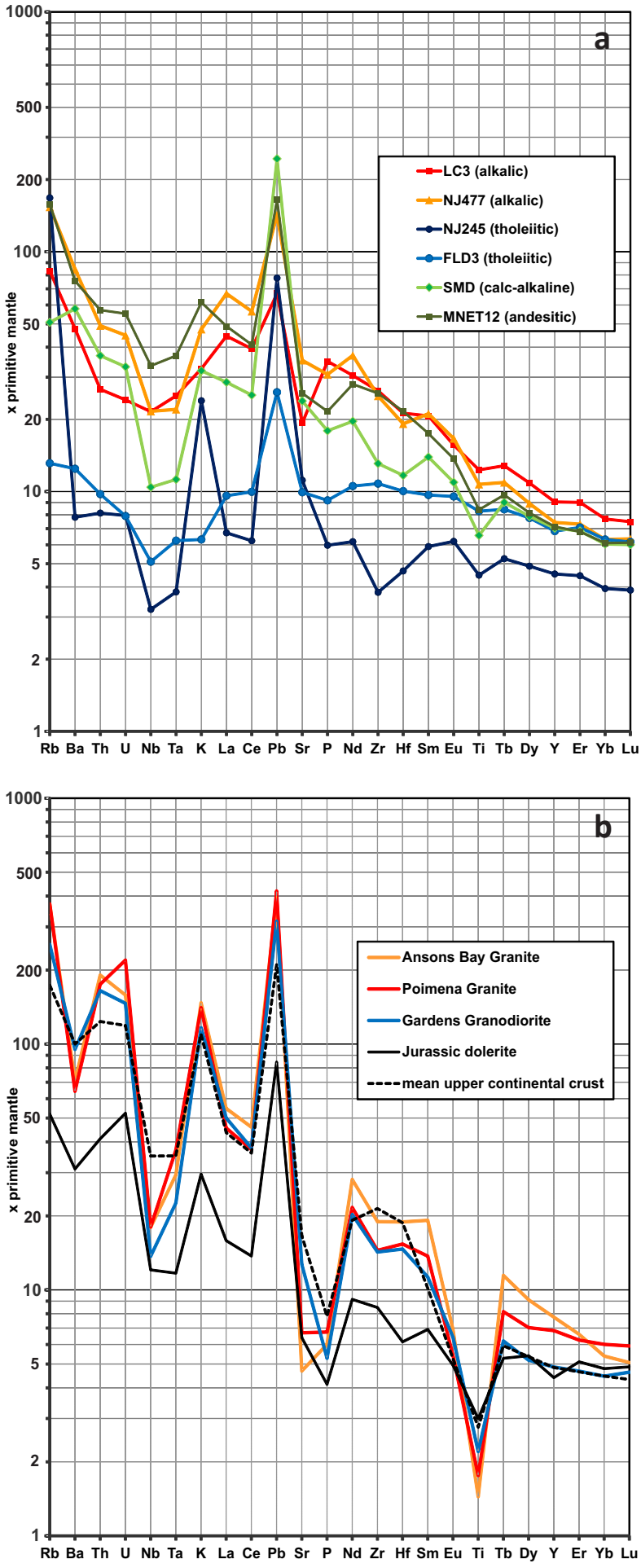

FIGURE 17. Incompatible element spider diagrams, normalised to model primitive mantle (Sun & McDonough,1989) with elements arranged in decreasing order of mantle incompatibility, based on ICPMS data.
a. selected dolerite samples;
b. for comparison, average compositions of Ansons Bay Granite (n= 4), Poimena Granite (n = 5), Gardens Granodiorite (n=4) (MRT/Geoscience Australia, unpublished data), Jurassic Dolerite chilled margins (Hergt et al., 1989) and mean upper continental crust (Taylor & McLennan, 1981).

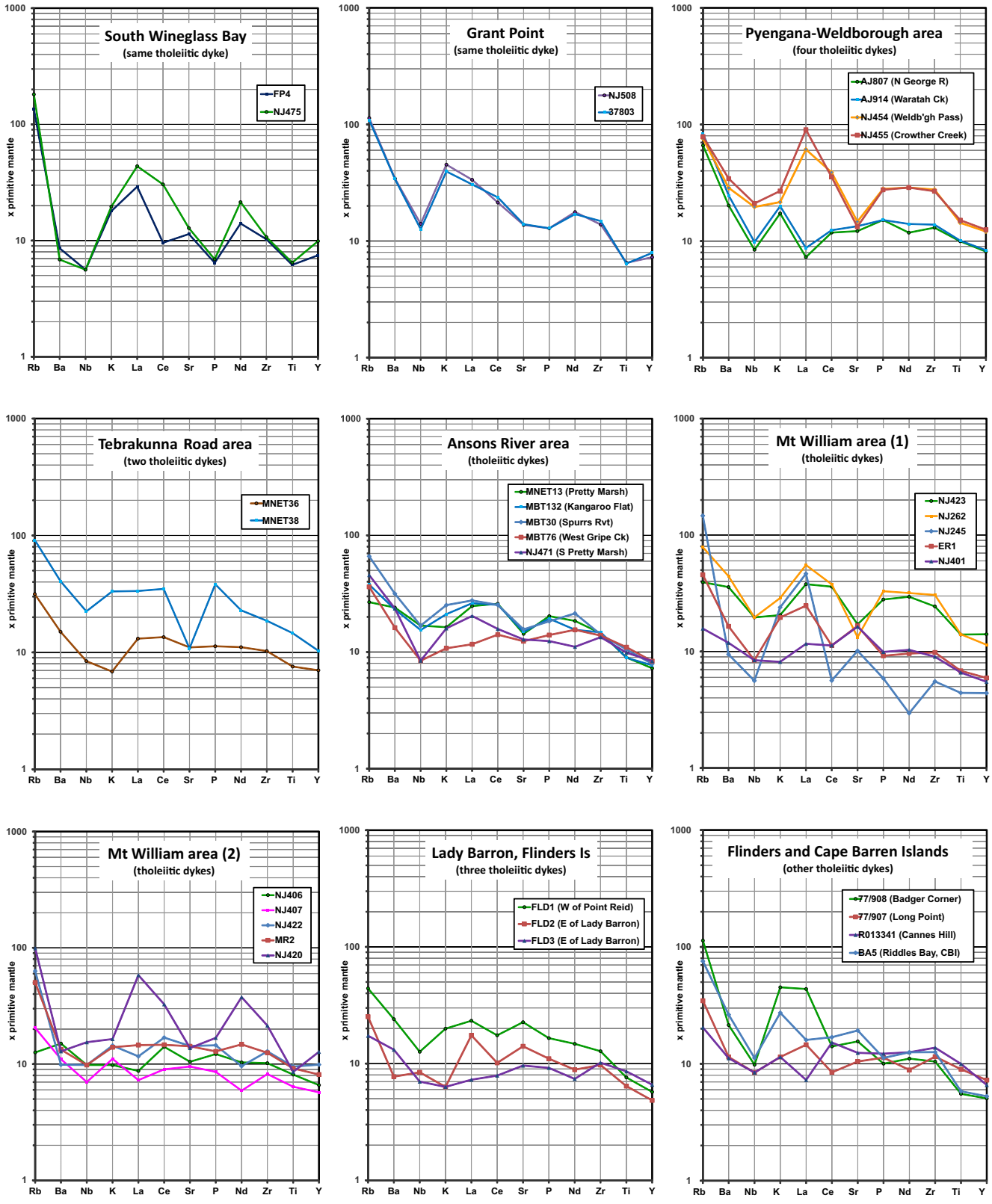

FIGURE 18a. Incompatible element spider diagrams, normalised to model primitive mantle (Sun and McDonough,1989) with elements arranged in decreasing order of mantle incompatibility. Based on XRF data: tholeiitic dykes.

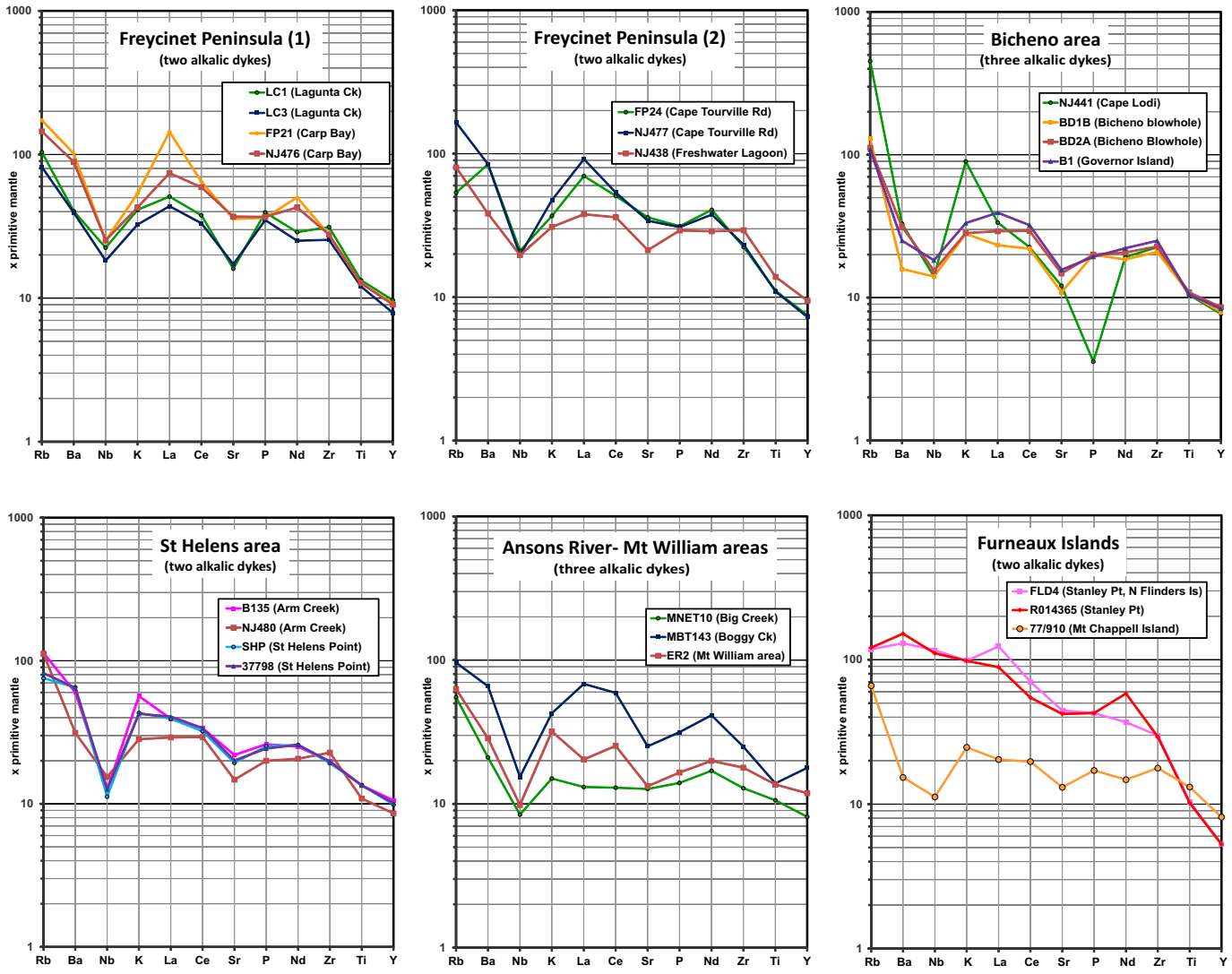

FIGURE 18b. Incompatible element spider diagrams, normalised to model primitive mantle (Sun and McDonough,1989) with elements arranged in decreasing order of mantle incompatibility. Based on XRF data: alkalic dykes.

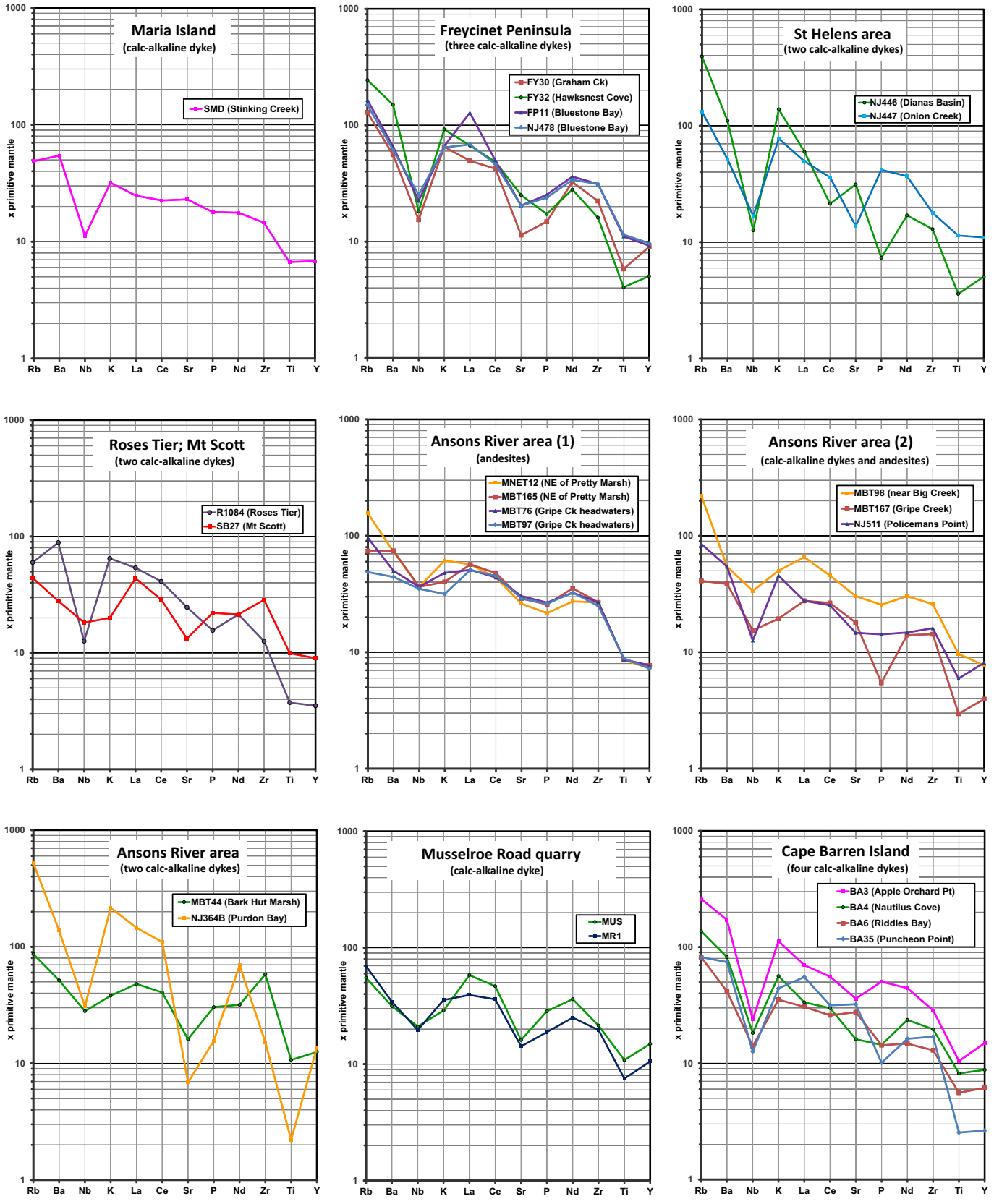

FIGURE 18c. Incompatible element spider diagrams, normalised to model primitive mantle (Sun and McDonough,1989) with elements arranged in decreasing order of mantle incompatibility. Based on XRF data: calc-alkaline dykes, including andesites.

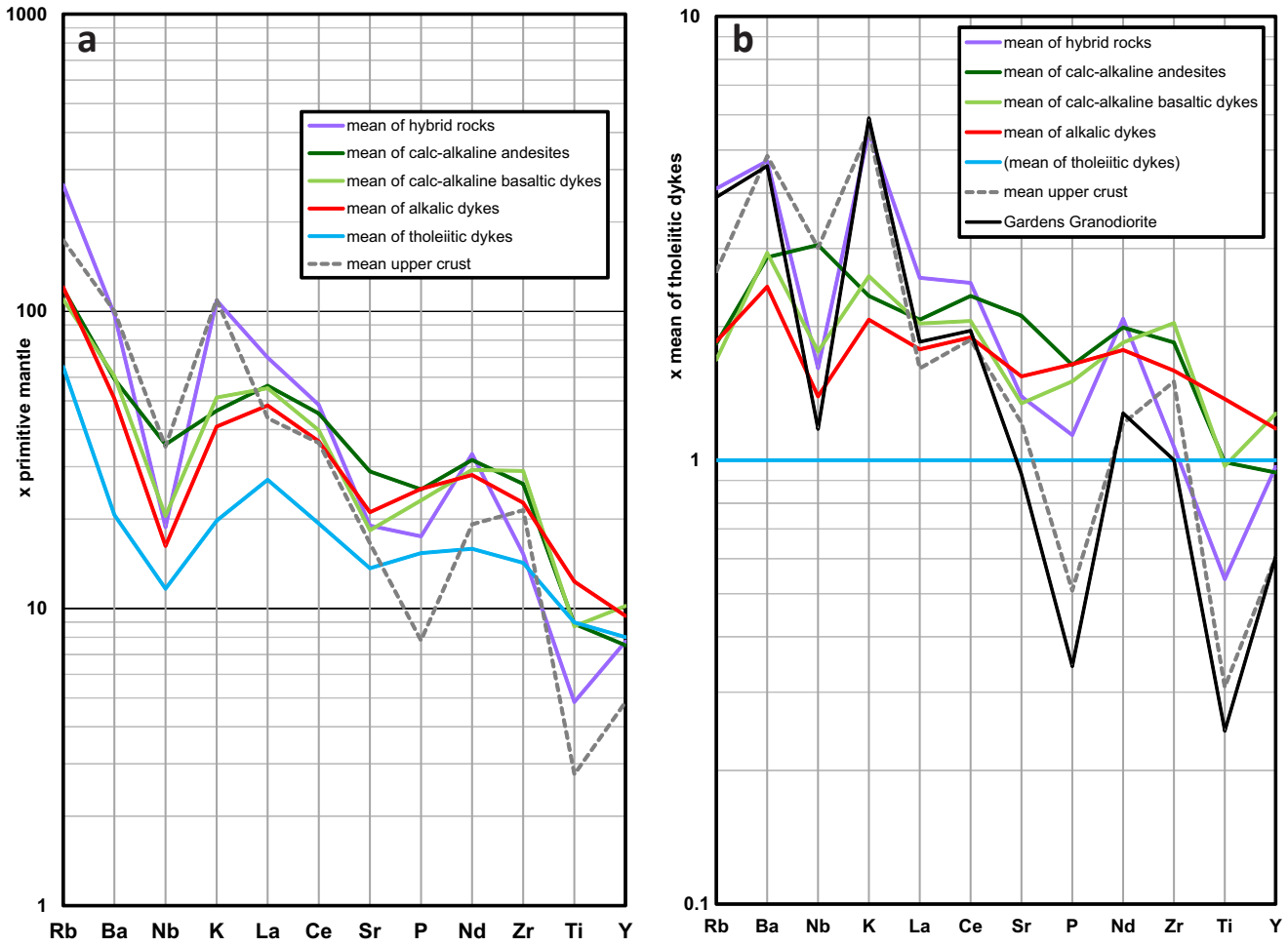

FIGURE 19. Incompatible element spider diagrams, based on averaged XRF data, for tholeiitic, alkalic, calc-alkaline basaltic, andesitic and "hybrid" dykes, with average Poimena Granite and average upper continental crust (Taylor and McLennan, 1981) also shown: **a.** normalised to model Primitive Mantle (Sun and McDonough, 1989); **b.** normalised to average composition of tholeiitic dykes. See text for discussion.

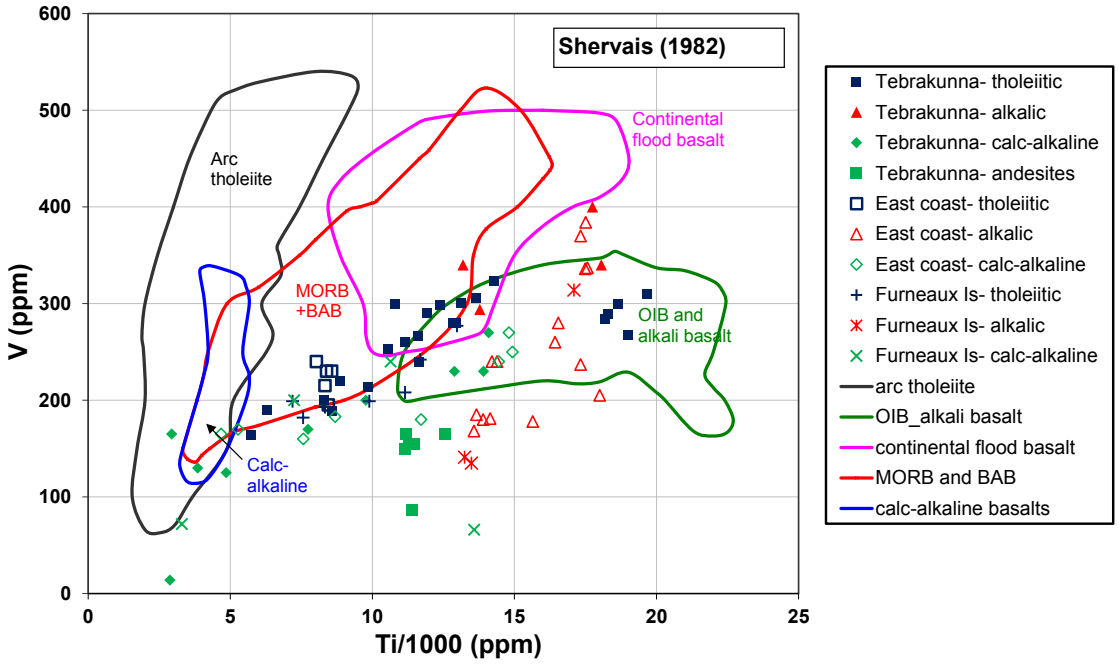

FIGURE 20. Ti–V plot of dolerite dykes, with fields for lavas from various tectonic settings shown after Shervais (1982) (MORB- mid-ocean ridge basalt, BAB- back arc basalt, OIB- ocean island basalt).

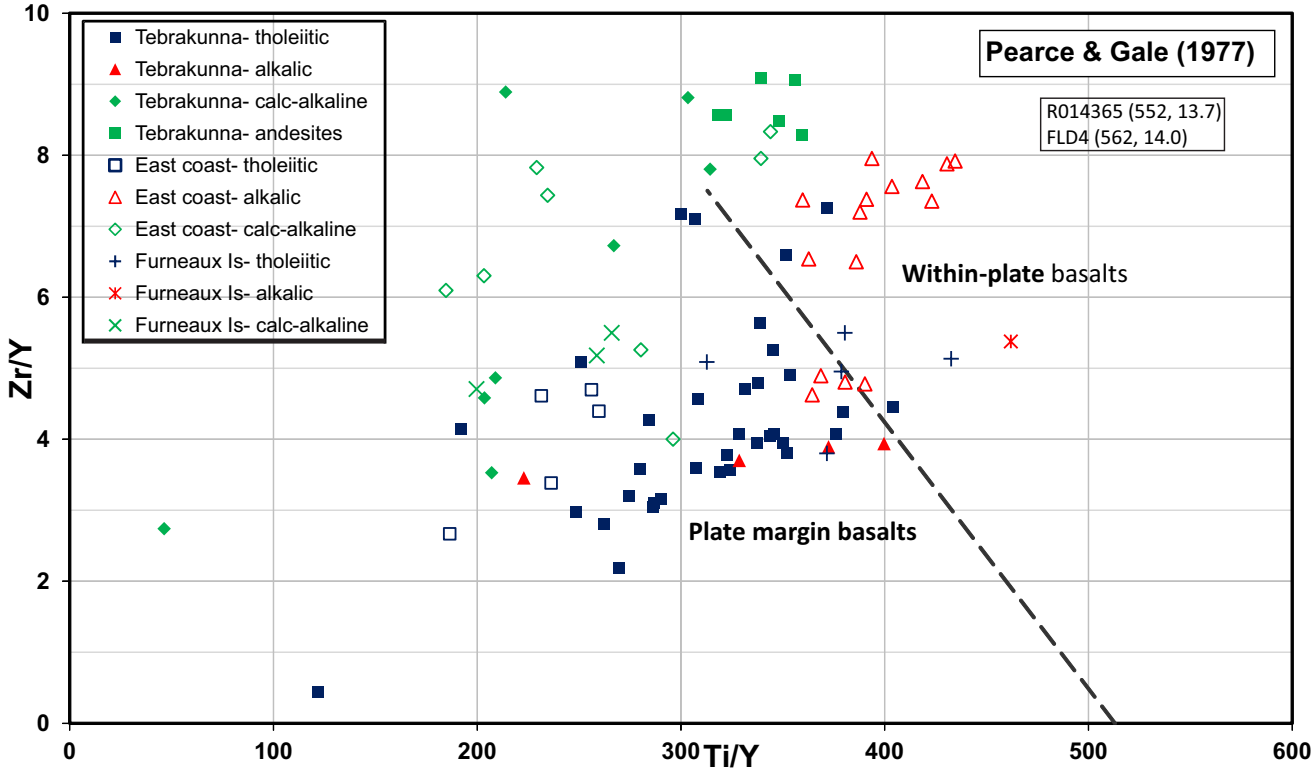

FIGURE 21. Ti/Y–Zr/Y plot of dolerite dykes, with fields for within-plate basalt and plate margin basalts shown after Pearce and Gale (1977).

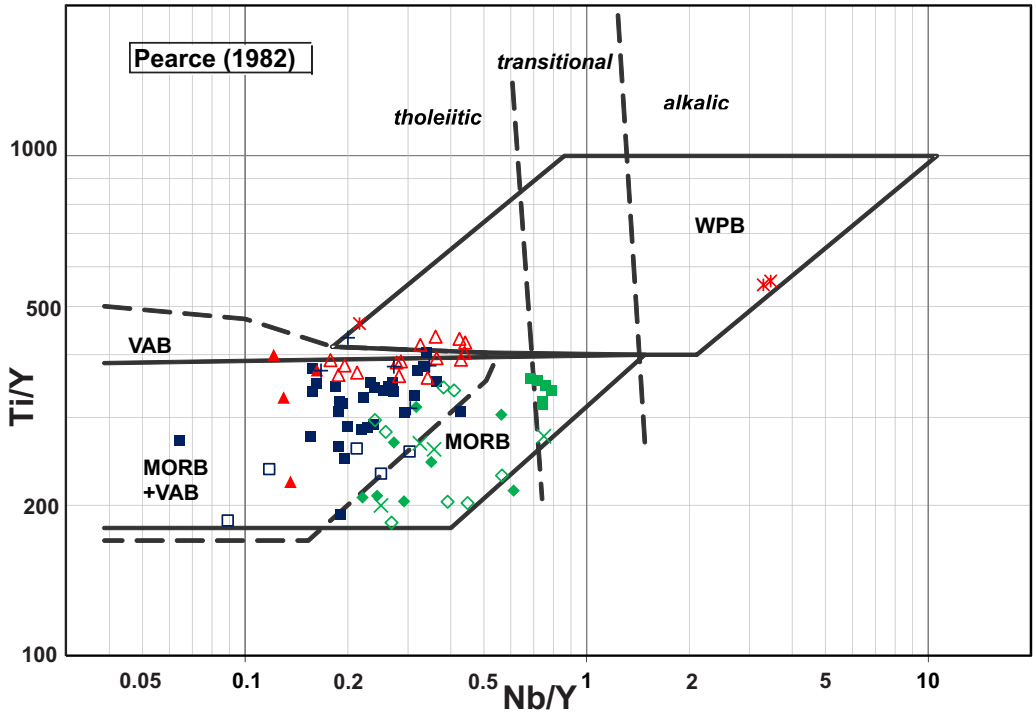

FIGURE 22. Ti/Y–Nb/Y of dolerite dykes, with fields for within-plate basalt (WPB), volcanic arc basalt (VAB) and mid-ocean ridge basalt (MORB) shown after Pearce (1982).

Tectonomagmatic discrimination diagrams

Binary or ternary diagrams of mostly immobile incompatible elements were devised and widely used, particularly in the 1970s and 1980s, to assist in determining the tectonic setting of ancient rocks (e.g., Pearce and Cann, 1973; Floyd and Winchester, 1975; Shervais, 1982; Meschede, 1986). Many of the diagrams were based on limited datasets, and they have tended to become less popular as petrogenetic models have become more sophisticated. Nevertheless, data from the eastern Tasmanian dykes were trialled on a selection of these diagrams. Some of the results are ambiguous or need to be interpreted with caution.

On the Ti-V diagram (Fig. 20) of Shervais (1982), almost all the dykes lack the low Ti/V ratios characteristic of arc tholeiites. The tholeiitic dykes plot mostly within the CFB (continental flood basalt) or MORB/BAB (mid-ocean ridge basalt/back arc basin) fields, whereas the alkalic and calc-alkaline dykes tend to have still higher Ti/V, and are scattered around or below the OIB (ocean island basalt)/alkali basalt field.

On the Zr/Y-Ti/Y diagram (Fig. 21) of Pearce and Gale (1977), most of the tholeiitic dykes plot in the plate margin field, defined by arc basalts and mid-ocean ridge basalts (MORB). This is not necessarily definitive, as these ratios are also low in many low-Ti intraplate basalts and dolerites (including Tasmanian Jurassic dolerite). The alkalic and calc-alkaline dykes are scattered, with many falling into the within-plate field.

On the Nb/Y-Ti/Y diagram (Fig. 22) of Pearce (1982), most of the dykes plot in the fields of MORB or VAB (volcanic arc basalt), which overlap and cannot be discriminated on this diagram. However, most of the dykes fall clearly outside the WPB (within plate basalt) field on account of their low Ti/Y. Also, all the tholeiitic and alkalic dykes and most of the calc-alkaline group plot as tholeiitic basalts on account of their low Nb/Y. The outstanding exception is sample FLD4 from Stanley Point, Flinders Island, which clearly belongs to a different suite and plots as a within-plate alkali basalt.

The dykes plot quite ambiguously on the Nb-Zr-Y diagram (Fig. 23) of Meschede (1986), mostly in either

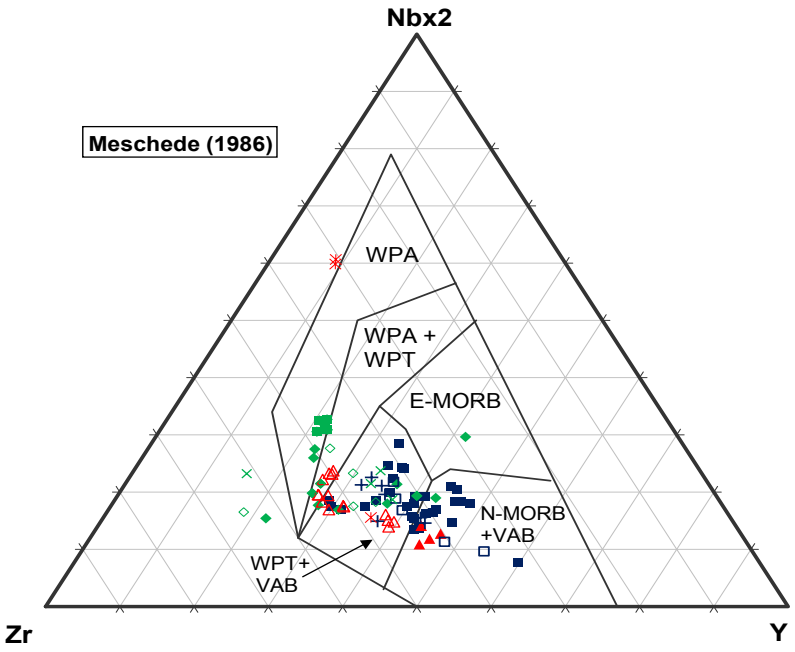

FIGURE 23. Nb–Zr–Y of dolerite dykes, with fields for lavas from various tectonic settings shown after Meschede (1986) (WPA- within plate alkali basalt, WPT- within plate tholeiite, VAB- volcanic arc basalt, N-MORB and E-MORB- normal and enriched mid-ocean ridge basalt).

the N-MORB/VAB or WPB/VAB fields, although some alkalic or calc-alkaline dykes plot in the unequivocal within-plate fields. Again, sample FLD4 plots as a within-plate alkali basalt.

Overall, the dolerites appear to be more resemble plate margin, possibly MORB or back-arc basin basalts, than within plate basalts. However, uncritical application of these diagrams may be misleading due to anomalous features of the dolerites, such as their relative depletion in Nb and Ti.

Isotopic data

Sun and Higgins (1996) measured neodymium isotope ratios for samples of dykes from Onion Creek (41701) and Grant Point (MSH172) respectively, which are herein assigned to the calc-alkaline group on the basis of major and trace element analyses. The reported εNd values (at 370 Ma) of +0.4 and +0.6 respectively are close to CHUR (i.e., Bulk Earth) and well below typical mantle values, and provide further evidence for crustal assimilation. They are also similar to some Tasmanian Cretaceous suites at Port Cygnet and Cape Portland (Bottrill et al. 2014), but well above εNd values for Jurassic dolerite (–6.4 to –4.9; Hergt et al., 1989). There are no strontium isotope data, nor any isotope data from the tholeiitic or alkalic dykes.

Age

Field constraints

The dykes of the Tebrakunna Dyke Swarm intrude the Mathinna Supergroup and all granite types in northeast Tasmania, ranging from granodiorites (e.g., the Gardens and Pyengana Granodiorites), through monzogranites and syenogranites (e.g., the Poimena and Ansons Bay Granites) to alkali feldspar granites (e.g., the Lottah and Mt William Granites). Assuming that there is only one generation of dolerite dykes, the maximum age of the Tebrakunna Dyke Swarm is constrained by the ~374–400 Ma U-Pb SHRIMP ages of the granites (Black et al., 2005), particularly the 377.8 ± 2.4 Ma Lottah Granite, the youngest body known to be intruded by them.

Several dykes have chilled margins against the Bicheno Granite, which has a SHRIMP age of 381.4 ± 2.7 Ma (Black et al., 2005) and the granites of Freycinet Peninsula, which are 379.3 ± 1.9 Ma and older (Kositcin and Everard, 2013). Near the Friendly Beaches, a minimum age for the dolerite dykes there is suggested by their absence within Permian strata. There are no direct numerical constraints on the age of dolerite dykes from the Furneaux islands, where none of their country rocks have been dated directly.

In the Blue Tier area, a few dykes have central zones of dolerite with margins of quartz feldspar porphyry (Brown et al., 1977). Another composite dyke of garnetiferous quartz feldspar porphyry and minor dolerite extends southeast from the Boobyalla Granite for at least 12 km, cross-cutting both the Mathinna Supergroup and several granite plutons (Baillie et al., 1978). At Yellow Beaches on Flinders Island, a thick (15–20 m) dolerite dyke is cut by a narrow (25–30 mm) aplite or quartz-feldspar porphyry vein originating in, but not extending far into, the host Lady Barron Granite (Baillie, 1986) (Fig. 5g). These, and similar relationships elsewhere, have been cited as evidence that the dolerite dykes are coeval with the granites, but an alternative interpretation is that injection of hot mafic magma has reheated previously solidified granite above its solidus temperature, causing localised partial melting.

Previous geochronology

Because of metamorphism and alteration, the dykes are difficult targets for K/Ar dating. McClenaghan and Higgins (1993) made an indirect attempt to do so by dating biotite separated from granite country rock collected from within 0.3 m of two dolerite dykes, near Ansons Bay Road (~600200mE, 5445000mN) and at Grants Point (~611900mE, 5432000mN). This was based on the premise that the intrusion of the dolerite would have reheated the granite and reset its biotite by expelling any radiogenic argon.

Biotite from the Gardens Granodiorite close to the Ansons Bay Road dyke yielded a K/Ar age of 386 ± 4.2 Ma. In comparison, biotite from the same pluton, collected away from the dykes, yielded four K/Ar ages of 394 ± 2.8 to 380 ± 8 Ma (weighted mean 389.2 Ma). Biotite from the Grant Point Granite, adjacent to the dyke, yielded an age of 388 ± 2.6 Ma, in comparison to 390 ± 2.8 Ma from a sample (MSH173) collected about 100 m away (McClenaghan and Higgins, 1993).

Although both biotite ages from near the dykes are slightly younger than those away from them, the differences are not significant. This may suggest that the dolerites were intruded before the granites had cooled below the closure temperature, or alternatively that they failed to reset the biotite in the host granite. It should be noted that the Gardens Granodiorite and Grant Point Granite are both considered to have

been emplaced essentially contemporaneously during the George River intrusive phase, which has yielded a weighted mean biotite K/Ar age of 392.2 ± 1.2 Ma (McClenaghan et al., 1992; McClenaghan and Higgins, 1993).

New $^{40}Ar/^{39}Ar$ dating

Here we present four new $^{40}Ar/^{39}Ar$ dates from plagioclase extracted from two samples of the Tebrakunna Dyke Swarm and two outlying dolerite dykes from the Furneaux Group and the Freycinet Peninsula (Table 8 and Fig. 24; see Table 1 for sample locations). Full analytical data are presented in Table 9.

The most robust age is a $^{40}Ar/^{39}Ar$ plateau age of 334.2 ± 7 Ma (2σ) from a tholeiitic dyke (sample NJ245) from the northern part of the main swarm near Mt William. The other three samples failed to give plateau ages, but $^{40}Ar/^{39}Ar$ total gas ages (analogous to K/Ar ages) can be calculated. A dyke from southwest of Ansons Bay (MNET2) yielded 330.2 ± 5.6 Ma. The large dyke from Yellow Beaches, east of Lady Barron on Flinders Island (FLD3), yielded 333.0 ± 7.0 Ma.

Due to slight alteration of the samples, these are interpreted as minimum ages, but they are within error. Together, they suggest that both the Tebrakunna Dyke Swarm and at least some of the dolerite dykes on Flinders Island are coeval and were intruded at or before ~334 Ma (Early Carboniferous). Although, at face value, this is up to ~40 Myr after termination of granite emplacement in eastern Tasmania (~374 Ma), the latter is based on SHRIMP ages from zircon, which Black et al. (2005) showed are typically about 10 Myr older than the previously reported K-Ar and Rb-Sr ages. This was attributed to higher closure temperatures of the U-Pb system in zircon and earlier closure during slow cooling of the granites. It is therefore likely that the interval between the intrusion of the granites and the dykes is less than 40 Myr. As these new $^{40}Ar/^{39}Ar$ dates are minimum ages, it remains possible that some of the dykes are essentially coeval with the granites.

The fourth sample, part of a large plagioclase megacryst from the dyke at Lagunta Creek, Freycinet Peninsula, yielded a distinctly younger total gas age of 258.1 ± 5.0 Ma (late Permian), also interpreted as a minimum age. Although possible from the local field relationships, a Permian age would imply that this dyke is markedly younger than similar dykes in the Friendly Beaches area, and it seems likely that its true age is considerably greater.

Discussion

Comparison with Victoria

Mafic to intermediate rocks, including dykes, are widespread in the southern Lachlan Fold Belt of mainland Australia. However, all well-documented examples appear to differ in composition and/or age to the Tebrakunna Dyke Swarm, the extrapolation of which would not intersect mainland Australia, if Tasmania was in an essentially modern relative position in the Early Carboniferous.

The Melbourne Zone, to which the Mathinna Supergroup of Tasmania is most commonly correlated (e.g. Powell and Baillie, 1992), contains the ~150-km-long NNW-trending Woods Point Dyke Swarm. This comprises mainly calc-alkaline hornblende-bearing rocks ranging from peridotite to monzonite, including lamprophyric types, locally with hydrothermal alteration and gold mineralisation (Marsden, 1988). To the east, the Tabberabbera Dyke Swarm is of similar age and consists mainly of quartz diorite, hornblende porphyrite and quartz feldspar porphyry (Marsden, 1988). Both swarms are late Middle Devonian in age, shortly post-dating the Tabberabberan Orogeny in Victoria, and thus appreciably older than the Tebrakunna Dyke Swarm, which has dominantly tholeiitic affinities and in which hornblende is minor or absent.

Numerous north-south and NNW-trending “magnetic dykes”, parallel to major strike-slip faults, are interpreted in the Tabberabbera Zone (e.g., Vandenberg et al., 2000, p. 282), but no petrological information on these inferred dykes seems to be available.

Soesoo and Nicholls (1999) reported “at least three geochemically distinct groups” of dykes in the Tambo River area within the southern Omeo Zone. The more basaltic members of their second group (e.g., their analysis TA16) have some resemblance to some of the tholeiitic dykes of the Tebrakunna Dyke Swarm, although the Tambo dykes are more depleted in HREE. More importantly, the age of the Tambo dykes, although poorly constrained, is Early Devonian.

Soesoo and Nicholls (1999) noted a change in the chemistry of mafic rocks in eastern Victoria, from incompatible-element depleted, calc-alkaline or tholeiitic compositions with arc-like signatures in the Early and Middle Devonian, to incompatible element-enriched, transitional or weakly alkalic compositions and intra-plate signatures in the Late Devonian/Early

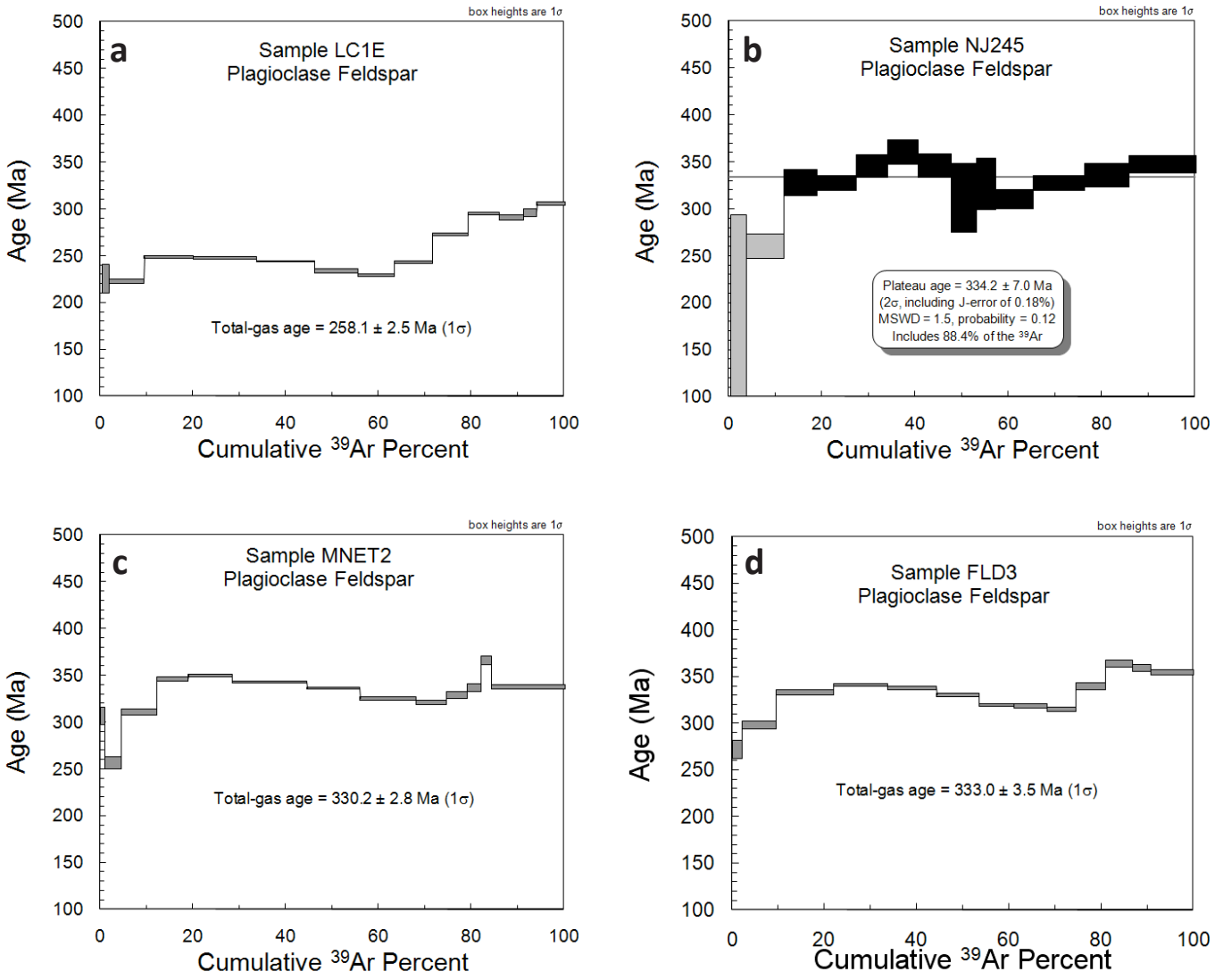

FIGURE 24. $^{40}Ar/^{39}Ar$ step-heating age spectra for plagioclase feldspar separates.
a. Phenocryst from sample LC1, alkalic dyke, Lagunta Creek, Freycinet Peninsula;
b. Sample NJ245, tholeiitic dyke from Tebrakunna Dyke Swarm, Mt William National Park;
c. Sample MNET2, coarse-grained dolerite, Tebrakunna Dyke Swarm, Gripe Creek-Big Creek area;
d. Sample FLD3, tholeiitic dyke, east of Lady Barron, Flinders Island.

Carboniferous. They attributed this to a change in tectonic setting following ocean closure in the Early Devonian, whereby foundering of a detached lithospheric slab resulted in mafic-intermediate magmatism with subduction-like signatures. Later, lateral influx of less depleted asthenospheric mantle resulted in a change to transitional to alkalic magmatism. Such a model, however, does not seem appropriate for Tasmania, where magmatism with subduction-like signatures, exemplified by the Tebrakunna Dyke Swarm, probably persisted until the Early Carboniferous (~334 Ma), well after the Tabberaberran Orogeny (~389 Ma) and the termination of related granite emplacement (~373 Ma).

A minor occurrence of early Jurassic (191 Ma) alkali dolerite dykes has been reported from the Freestone Creek area, in the southern Tabberabbera Zone (Soesoo et al., 1999; Soesoo, 2006). These have strongly potassic and HFSE-enriched compositions that resemble the unusual and undated alkali dolerite dyke at Stanley Point, Flinders Island.

Petrogenesis

The Early Carboniferous age of at least the majority of the dykes, and field evidence such as chilled margins, indicates that they were intruded well after emplacement of the granites, and precludes any direct petrogenetic relationship with them. Although the dykes may represent the final manifestation of the Tabberabberan Orogeny, which was caused (in Tasmania) by the amalgamation of the eastern and western Tasmanian terranes (Black et al., 2010), they were clearly emplaced in an intra-plate tectonic environment and cannot be arc-derived magmas.

However, nearly all the dykes display arc-like characteristics, such as relative depletion in Nb and Ti (e.g., Figs 17a, 19a). An alternative interpretation is that this represents a crustal signature, since negative Nb, Ta and Ti anomalies, together with positive Pb, K, Th and U anomalies, are also displayed by average upper continental crust (e.g., Taylor and McLennan, 1981) (Figs 17b, 19a). To assess the possibility that the dykes were contaminated by assimilation of their country rock, mean compositions of three large granite plutons which are transected by the Tebrakunna Dyke Swarm, the Ansons Bay and Poimena Granites and the Gardens Granodiorite, were calculated (Geoscience Australia unpublished ICPMS data). All show a similar primitive-mantle normalised signature (Fig. 17b), qualitatively similar to but with larger anomalies than those of the dykes. There is some petrographic and field evidence, particularly from the andesites and the more felsic of the calc-alkaline dykes, that high-level assimilation of granitic material has occurred. Direct assimilation, however, appears unlikely to be an important process in the petrogenesis of the more mafic tholeiitic and alkalic dykes, which are in low in SiO_2 and lack obvious xenocrysts. Yet most of these dykes also have markedly negative Nb anomalies, the magnitude of which does not correlate with SiO_2 (Fig. 15a). A possible partial explanation is that the contaminant was a haplogranitic minimum melt, consisting of essentially normative quartz and alkali feldspar (Q, Or and Ab) and that HFSE such as Nb, Ta, REE, Zr and Ti were mostly retained in accessory minerals within the host granites, rather than incorporated into the dykes.

An alternative hypothesis is that dolerite dykes were derived by partial melting of mantle that had itself been contaminated by crustal material during an earlier subduction event. The Jurassic Tasmanian and Ferrar dolerites also display a crustal incompatible element signature (Fig. 17b), very similar to that of the Early Carboniferous dykes, but are remarkably uniform and lack petrographic evidence for crustal contamination. Hergt et al. (1989) showed that the crustal trace element signature of Tasmanian dolerite could be explained if it were derived by the partial melting (~30%) of a depleted mantle that had been contaminated by the addition of ≤ 3% continental sediment during an earlier episode of subduction.

We suggest that the dominantly tholeiitic dykes of the Tebrakunna Dyke Swarm have tapped partial melts of similar “contaminated” lithospheric mantle. Partial melting may have been a result of upwelling and influx of hot asthenospheric mantle, caused either by the foundering of a subducted slab (e.g., Soesoo and Nicholls, 1999), or by edge-related effects (e.g., King and Anderson, 1998), following the amalgamation of the eastern and western Tasmanian terranes.

It is uncertain whether the addition of subducted sediment to the lithospheric mantle was a relatively local event resulting from subduction immediately prior to the Tabberabberan Orogeny (e.g., Black et al., 2010), or caused by the continental-scale subduction that occurred along the eastern margin of Gondwana for most of the Palaeozoic (e.g., Cox, 1978), to which the Tasmanian/Ferrar Jurassic dolerite mantle source has been attributed. However, the less negative εNd of the Tebrakunna Dyke Swarm, relative to the Jurassic dolerite, suggests the former.

The alkalic dykes may simply represent lower degree partial melts, or addition of alkali-rich haplogranitic melt to the magma.

Although a few of the more felsic calc-alkaline dykes are clearly the result of direct magma mingling with partially remelted country rocks, most of the calc-alkaline dykes are higher in some HFSE (e.g., Zr, P_2O_5 and REE) than both the tholeiitic dykes and potential upper crustal contaminants (e.g., mean upper crust, or mean local granite; Fig. 19). The andesitic dykes, in particular, also have less negative Nb anomalies, and higher Nb/Y than the tholeiitic (and alkalic) dykes (Fig. 15a). Thus the calc-alkaline dykes (especially the andesites) cannot be modelled by simple addition of average upper crust or average granite to the average composition of the tholeiitic dykes.

Concurrent assimilation and fractional crystallisation (AFC), whereby a magma continuously changes composition by simultaneously fractionating crystals and assimilating wall rock, is a more realistic scenario, and may account for the high levels of HFSE in the calc-alkaline dykes. The equations derived by Powell (1984) show that AFC can result in concentrations of incompatible elements that exceed those of either the initial melt or the assimilant, and are even greater those that could have been produced by ideal fractional crystallisation, with the greatest enrichment being shown by the most incompatible elements (see also Rollinson, 1993, p. 127–130). For example, the average Nb content of the calc-alkaline andesites (25.4 ppm) could have been produced from the average composition of the tholeiitic dykes (8.3 ppm Nb) by assimilation/fractional crystallisation with the host Gardens Granodiorite (9.8 ppm Nb), assuming a bulk distribution coefficient for Nb of 0.01 and a assimilation/fractional crystallisation ratio (r) of 0.5, by 49% crystallisation (F= 0.51); or for r = 0.2, 62% crystallisation (F = 0.38).

Conclusion

- The Tebrakunna Dyke Swarm of northeast Tasmania consists dominantly of NNE-trending tholeiitic dolerite dykes and was emplaced in the Early Carboniferous, at or shortly before ~335 Ma.
- Mafic to intermediate dykes in the Furneaux Islands, Freycinet Peninsula and elsewhere near the east Tasmanian coast have more variable trends and compositions, but at least some were also emplaced at ~335 Ma.
- The younger age of the majority of the dykes precludes any direct role for them in the petrogenesis of Devonian granites, although the latter contain field and chemical evidence for a mafic, mantle-derived component.
- The more mafic dykes display typical tholeiitic major and trace element trends attributable to the fractionation of olivine, clinopyroxene and plagioclase.
- Most dykes are characterised by marked negative Nb and smaller Ti anomalies on primitive-mantle normalised spider diagrams, probably indicating derivation from subduction-modified lithospheric mantle. It is uncertain, however, whether metasomatism by LILE-enriched slab-derived fluid was a local mid-Late Devonian event related to collision of the eastern and western Tasmanian terrains and granite generation, or earlier, possibly Cambrian, continental-scale event that also provided the source for the Jurassic Tasmanian-Ferrar dolerite magmatism.
- A more felsic “calc-alkaline” suite can be defined, the more felsic members of which contain clear field, petrographic and chemical evidence for assimilation of granitic or other crustal material by mafic magmas. However, simple addition of granitic material cannot alone account for the HFSE characteristics of the andesitic calc-alkaline dykes, and concurrent assimilation-crystal fractionation (AFC) processes were probably involved.
- A few amphibole-bearing microdioritic or microtonalitic dykes, and rare strongly alkalic dykes belong to other suites and require further investigation.

Possible further work

- Further field work, sampling and laboratory studies of the dykes in the Furneaux islands, with their contrasting trends, are needed to define their petrological and age relationships.

- Detailed geological mapping in remote areas of the Freycinet Peninsula and in the Furneaux islands would probably result in the discovery of more dykes.
- Further isotope analysis, particularly of the tholeiitic and alkalic dykes, could help constrain petrogenetic models. In particular, Nd and Sr isotope ratios may help define mantle sources and the relative roles of anomalous or subduction-modified mantle and contamination by continental crust.
- Geochronology of petrographically or geochemically unusual dykes, such as at those at Stanley Point, Puncheon Point and Roses Tier, may return appreciably different ages to the main Tebrakunna Dyke Swarm, and help define previously unrecognised suites.
- Although the mineral chemistry of major rock-forming silicates in typical dykes is known at the reconnaissance level, the composition of opaque and accessory phases, and those in unusual dykes, has not been investigated.

Acknowledgements

The University of Tasmania is thanked for lending thin sections of samples collected by J. D. Cocker. Ralph Bottrill (MRT) and Karsten Goemann (Central Science Laboratory, University of Tasmania) are thanked for assisting with electron microprobe analyses. Richie Woolley (MRT) performed and interpreted semi-quantitative x-ray diffraction of selected samples. Other laboratory staff over many years, too numerous to mention, cut thin sections and prepared samples for X-ray fluorescence. June Pongratz prepared the manuscript for publication.

References

Bacon C. A. 1984. The Mt Paul Coalfield. Tasmania Department of Mines Unpublished Report 1984/17.

Bacon C. A. 1991. The Coal Resources of Tasmania. Geological Survey Bulletin 64, Tasmania Department of Resources and Energy.

Baillie P. W. 1984. Geological Atlas 1:50,000 series. Sheet 25 (8516S). Eddystone. Tasmania Department of Mines.

Baillie P. W. 1986. Geological Survey Explanatory Report. Sheet 25 (8516S). Eddystone. Tasmania Department of Mines.

Baillie P. W.;Turner N.J.; Cox S.F. 1978. Geological Atlas 1:50,000 Series, Sheet 24 (8416S). Boobyalla. Tasmania Department of Mines.

Bau M. 1996. Controls on the fractionation of isovalent trace elements in magmatic and aqueous systems: evidence from Y/Ho, Zr/Hf and lanthanide tetrad effect. *Contributions to Mineralogy and Petrology* **123**: 323–333.

Black L. P., McClenaghan M. P., Korsch R. J., Everard J. L. & Foudoulis C. 2005. The significance of Devonian-Carboniferous igneous activity in Tasmania, as derived from U-Pb SHRIMP dating of zircon. *Australian Journal of Earth Sciences* **52**: 807–829.

Black L. P.; Everard J. L.; McClenaghan M. P.; Korsch R. J.; Calver C. R.; Fioretti A. M.; Brown A. V.; Foudoulis C. 2010. Controls on Devonian-Carboniferous magmatism in Tasmania, based on inherited zircon age patterns, Sr, Nd, and Pb isotopes, and major and trace element geochemistry. *Australian Journal of Earth Sciences* **57**: 933–968.

Blake F. 1947. The Furneaux Group of islands (with accompanying maps, plans 700A, 700B). Tasmania Geological Survey typed reports, 1947, 52–82.

Bottrill R. S.; Everard J. L.; Taheri J. 2014. Cretaceous igneous rocks. In: Corbett K. D.; Quilty P. G.; Calver C.R. 2014. The Geological Evolution of Tasmania. *Geological Society of Australia Special Publication* **24**: 453–462.

Boynton W.V. 1984. Geochemistry of the rare earth elements: meteorite studies. In: Henderson P. (ed.) *Rare earth element geochemistry*: 63–114. Elsevier.

Brown A. V. 1982. Whole rock K/Ar ages of basalts. In: McClenaghan, M. P. et al. Geology of the Ringarooma-Boobyalla area. *Geological Survey of Tasmania Bulletin* 61: 178.

Brown A. V.; McClenaghan M. P.; Moore W. R.; Turner N. J.; McClenaghan J.; Williams P. R.; Baillie P. W.; Corbett K. D.; Corbett E. B.; Cox S. F.; Groves D. I.; Pike G. P. 1977. Geological Atlas 1:50,000 series. Sheet 25 (8415N). Ringarooma. Tasmania Department of Mines.

Burgess S. D.; Bowring S. A.; Fleming T. H.; Elliot D. H. 2015. High-precision geochronology links the Ferrar large igneous province with early-Jurassic ocean anoxia and biotic crisis. *Earth and Planetary Science Letters* **415**: 90–99.

Carmichael I. S. E. 1964. The petrology of Thingmuli, a Tertiary volcano in eastern Iceland. *Journal of Petrology* **5**: 436–460.

Clarke M. J.; Baillie P. W. 1981. Geological Atlas 1:50,000 series. Sheet 77 (8512N), Maria. Tasmania Department of Mines.

Clarke M. J.; Baillie P. W. 1984. Geological Survey Explanatory Report. Sheet 77 (8512N), Maria. Tasmania Department of Mines.

Cocker J. D. 1977. Petrogenesis of Tasmanian granitoids. PhD thesis, University of Tasmania (unpublished).

Cocker J. D. 1980. Regional geology of the southern Furneaux Group. *Papers and Proceedings of the Royal Society of Tasmania* **114**: 49–68.

Cox K. G. 1978. Flood basalts, subduction and the break-up of Gondwanaland. *Nature* **274**: 47–49.

Everard J. L. 1987. Petrology of the Jurassic dolerite. In Turner N. J. & Calver C. R. Geological Survey Explanatory

Report. Geological Atlas 1: 50,000 series. Sheet 49 (8514N). St Marys. p. 123–148

Everard J. L. 1989. Petrology of the Tertiary basalt. In: Seymour D. B. (Ed.). Geological Survey Explanatory Report. Sheet 36 (8015N). St Valentines, p. 79–142. Tasmania Department of Mines.

Everard J.L. 2001. Intrusive relationships of granite and dolerite at Lagunta Creek, Freycinet Peninsula. *Papers and Proceedings of the Royal Society of Tasmania* **135**: 63–74.

Everard J. L.; McClenaghan M. P. 2014. Tebrakunna Dyke Swarm and other Late Palaeozoic dolerite dykes, Eastern Tasmania. In: Corbett K. D.; Quilty P. G.; Calver C.R. 2014. The Geological Evolution of Tasmania. *Geological Society of Australia Special Publication* **24**: 319–321.

Everard J. L.; Baillie P. W.; Beyer E. E.; Doyle R. B.; O'Reilly S. Y.; Zhang M. 2014. Palaeogene-Neogene basaltic volcanism. In: Corbett K. D., Quilty P. G. & Calver C.R. 2014. The Geological Evolution of Tasmania. *Geological Society of Australia Special Publication* **24**: 463–494.

Floyd P. A.; Winchester J. A. 1975. Magma-type and tectonic setting discrimination using immobile elements. *Earth and Planetary Science Letters* **27**: 211–218.

Groves D. I.; Cocker J. D.; Jennings D. J. 1977. The geology, geochemistry and mineralisation of the Blue Tier Batholith. *Geological Survey of Tasmania Bulletin* 53.

Hall R. P.; Hughes D. J.; Joyner L. 1988. Fe-enrichment in tholeiitic pyroxenes: complex two-pyroxene assemblages in Mesozoic dolerites, southern Tasmania. *Geological Magazine* **125**: 573–582.

Hergt J. M.; Chappell B. W.; McCulloch M. T.; McDougall I.; Chivas A. R. 1989. Geochemical and isotopic constraints on the origin of the Jurassic dolerites of Tasmania. *Journal of Petrology* **30**: 841-833.

Hey M. H. 1954. A new review of the chlorites. *Mineralogical Magazine* **30**: 277.

Hope J.; Brown G.; McIntosh B.S. 1974. Natural history of the Hogan Group. 1. Physical environment and vertebrate fauna. *Papers and Proceedings of the Royal Society of Tasmania* **107**: 65–72.

Humphrys M. 2007. The origin of felsic segregations and massive granophyres in Jurassic dolerite intrusions. BSc Honours thesis, University of Tasmania (unpublished).

Hunns S.R. 1982. The geology and geochemistry of the Bicheno garnet-cordierite-biotite granite. BSc Honours thesis, University of Tasmania (unpublished).

Irvine T. N.; Baragar W. R. A. 1971. A guide to the chemical classification of the common volcanic rocks. *Canadian Journal of Earth Sciences* **8**: 523–548.

Jennings D. J. 1984. Mt Paul Coalfield- geological sketch map. Tasmania Department of Mines Plan 5043.

Jennings D. J.; Sutherland F. L. 1969. Geology of the Cape Portland area, with special reference to the Mesozoic (?) appinitic rocks. *Tasmania Department of Mines Technical Reports* **13**: 45–81.

King S. D.; Anderson D. L. 1998. Edge-driven convection. *Earth and Planetary Science Letters* **160**: 289–296.

Kositcin N., Everard J. L. 2013. New SHRIMP U-Pb zircon ages from Tasmania. Tasmanian Geological Survey Record 2013/02, Geoscience Australia Record 2013/22.

Kuno H. 1968. Differentiation of basalt magmas. In: Hess H.H.; Poldervaart A. (eds). *Basalts: The Poldervaart Treatise on Rocks of Basaltic Composition, Vol. 2*: 623–688. Interscience, New York.

Le Maitre R.W. (ed.) 2002. *A Classification of Igneous Rocks and Glossary of Terms, 2nd Edition*. Cambridge University Press (236 pp.)

Le Maitre R. W.; Bateman P.; Dudek A.; Keller J.; Lameyre Le Bas M. J.; Sabine P. A.; Schmid R.; Sorensen H.; Streckeisen A.; Woolley A. R.; Zanettin B. 1989. *A Classification of Igneous Rocks and Glossary of Terms*. Blackwell, Oxford.

Leake B.E. (Comp.). 1997: Nomenclature of amphiboles: Report of the Subcommittee on Amphiboles of the International Mineralogical Association, Commission on New Minerals and Mineral Names. *American Mineralogist* **82**: 1019–1037.

McClenaghan M. P. 1984. The petrology, mineralogy and geochemistry of the Pyengana and Gardens granodiorites, the Hogans Road diorite and the dolerite dykes of the Blue Tier batholith. Tasmania Department of Mines Unpublished Report 1984/04.

McClenaghan M. P. 2006. The geochemistry of Tasmanian Devonian-Carboniferous granites and implications for the composition of their source rocks. *Tasmanian Geological Survey Record* 2006/06.

McClenaghan M.P.; Higgins N.C. 1993. The age and intrusive relationships of granitoids of the Blue Tier Batholith, north-east Tasmania. *Mineral Resources Tasmania Report* **1993/33**.

McClenaghan M. P.; Williams P. R. 1983. Geological Atlas 1:50,000 series. Sheet 33 (8515N). Blue Tier. Tasmania Department of Mines.

McClenaghan M. P.; Turner N. J.; Baillie P. W.; Brown A. V.; Williams P. R.; Moore W. R. 1982. Geology of the Ringarooma-Boobyalla area. *Geological Survey of Tasmania Bulletin* **61**.

McClenaghan M. P.; Turner N. J.; Williams P. R. 1987. Geological Atlas 1:50,000 series. Sheet 41 (8515S). St Helens. Tasmania Department of Mines.

McClenaghan M. P.; Turner N. J.; Everard J. L. 1992. Geological Survey Explanatory Report. Sheet 41 (8515S). St Helens. Tasmania Department of Mines.

McClenaghan M. P.; Everard J. L.; Goscombe B. D.; Findlay R. H.; Calver C. R. 1993. Geological Atlas 1:50,000 series. Sheet 40 (8415S). Alberton. Tasmania Department of Mines.

Macdonald G. A.; Katsura T. 1964. Chemical composition of Hawaiian lavas. *Journal of Petrology* **5**: 82–133.

McDougall I.; Green D. C. 1982. Cretaceous K/Ar ages from north-eastern Tasmania. Appendix 3. In McClenaghan M.P.; Turner N.J.; Baillie P.W.; Brown A.V.; Williams P.R.; Moore W. R. 1982. Geology of the Ringarooma-Boobyalla area. *Geological Survey of Tasmania Bulletin* **61**.

Marsden M. A. H. 1988. Middle Devonian igneous activity. In: Douglas J. G.; Ferguson J. A. *Geology of Victoria*, p. 149–151. Geological Society of Australia, Victorian Division.

Meschede M. 1986. A method of discriminating between different types of mid-ocean ridge basalts and continental tholeiites with the Nb-Zr-Y diagram. *Chemical Geology* **56**: 207–218.

Methorst T. 2008. Gravity survey of Flinders Island. BSc Honours thesis, University of Tasmania (unpublished).

Morimoto N. 1988. Nomenclature of pyroxenes. *American Mineralogist* **73**: 1123–1133.

Pearce J.A. 1982. Trace element characteristics of lavas from destructive plate boundaries. In: Thorpe R.S. (ed.).

Andesites: 525–548. Wiley, Chichester.

Pearce J.A.; Cann J.R. 1973. Tectonic setting of basic volcanic rocks determined using trace element analyses. *Earth and Planetary Science Letters* **19**: 290–300.

Pearce J.A.; Gale G.H. 1977. Identification of ore-deposition environment from trace element geochemistry of associated igneous host rocks. *Geological Society Special Publication* **7**: 14–24.

Powell C. McA.; Baillie P. W. 1992. Tectonic affinity of the Mathinna Group in the Lachlan Fold Belt. *Tectonophysics* **214**: 193–209.

Powell R. 1984. Inversion of the assimilation and fractional crystallization equations: characterization of contaminants from isotope and trace element relationships in volcanic suites. *Journal of the Geological Society of London* **141**: 447–452.

Reid A. M.; Henderson Q. J. 1928. Blue Tier tin field. *Geological Survey of Tasmania Bulletin* **28**.

Rickwood P. C. 1989. Boundary lines within petrologic diagrams which use oxides of major and minor elements. *Lithos* **22**: 247–263.

Rieder M. (comp.). 1998. Nomenclature of the micas. *Canadian Mineralogist* **36**: 905–912.

Roeder P. R.; Emslie R. F. 1970. Olivine-liquid equilibrium. *Contributions to Mineralogy and Petrology* **29**: 275–289.

Rollinson H. R. 1993. *Using Geochemical Data: Evaluation, Presentation, Interpretation*. Longman.

Russell J. K.; Stanley C. R. (eds). 1990. Theory and application of Pearce Element Ratios to geochemical data analysis. *Short Course Notes Geological Association of Canada* **8**.

Shervais J.W. 1982. Ti-V plots and the petrogenesis of modern and ophiolitic lavas. *Earth and Planetary Science Letters* **59**: 101–118.

Soesoo A. 2006. Mesozoic alkali basalts and felsic rocks in eastern Victoria, Australia. In: Hanski E.; Mertanen S.; Rämö T.; Vuollo J (Eds). *Dyke Swarms- Time Markers of Crustal Evolution*: 131–146. Taylor & Francis, London.

Soesoo A.; Nicholls A. 1999. Mafic rocks spatially associated with Devonian felsic intrusions of the southern Lachlan Fold Belt: a possible mantle contribution to crustal evolution processes. *Australian Journal of Earth Sciences* **46**: 725–734.

Soesoo A.; Bons P. D.; Elburg M. A. 1999. Freestone dykes- an alkali-rich Jurassic dyke population in eastern Victoria. *Australian Journal of Earth Sciences* **46**: 1–9.

Spry A. H. 1962. Igneous activity. In: Spry A.; Banks M.R. (eds). The Geology of Tasmania. *Journal of the Geological Society of Australia* **9**: 255–284.

Stanley C. R.; Madeisky H. E. 1993. Pearce Element Ratio analysis: applications in lithogeochemical exploration. *Short Course Notes Mineral Deposit Research Unit, University of British Columbia* **8**.

Sun S.-S.; McDonough W. F. 1989. Chemical and isotopic systematics of oceanic basalts: implications for mantle composition and processes; In: Saunders A. D.; Norry M. J. (eds). Magmatism in the Ocean Basins. *Geological Society of London Special Publication* **42**: 313–346.

Sun S.-S.; Higgins N. C. 1996. Neodymium and strontium isotope study of the Blue Tier Batholith, NE Tasmania, and its bearing on the origin of tin-bearing alkali feldspar granites. *Ore Geology Reviews* **10**: 339–365.

Sutherland F. L.; Kershaw R. C. 1971. The Cainozoic geology of Flinders Island. *Papers and Proceedings of the Royal Society of Tasmania* **105**: 151–176.

Sutherland F. L.; Wellman P. 1986. Potassium-argon ages of Tertiary volcanic rocks, Tasmania. *Papers and Proceedings of the Royal Society of Tasmania* **120**: 77–86.

Taylor S. R.; McLennan S. M. 1981. The composition and evolution of the continental crust: rare element evidence from sedimentary rocks. *Philosophical Transactions of the Royal Society* **A301**: 381–399.

Thomas D. E. 1943. Tin deposits of the Blue Tier district. Tasmania Department of Mines Unpublished Reports 1943, 35–73.

Vandenberg A. H. M.; Willman C. E.; Maher S.; Simons B. A.; Cayley R. A.; Taylor D. H.; Morand V. J.; Moore D. H.; Radojkovic A. 2000. The Tasman Fold Belt System in Victoria: Geology and mineralisation of Proterozoic to Carboniferous rocks. *Geological Survey of Victoria Special Publication*.

Wager L. R.; Brown G. M. 1968. *Layered Igneous Rocks.* Oliver & Boyd, London.

Walker K. R. 1957. The geology of the St Helens –Scamander area, Tasmania. *Papers and Proceedings of the Royal Society of Tasmania* **91**: 23–40.

Worthing M. A. & Woolward I. R. 2010. Explanatory Report for the Dublin Town (5840), Brilliant (5841), Falmouth (6040) and Beaumaris (6041) geological map sheets. 1:25 000 Scale Digital Geological Map Series. Explanatory Report 3. Mineral Resources Tasmania.

Zwingmann H.; Sutherland F. L.; Graham I.; Forsyth S. M.; Everard J. L.; Wartho J.-A. 2004. New K-Ar and Ar-Ar ages for NE Tasmanian basalts: implications for volcanic evolution following Tasman rifting. *Geological Society of Australia Abstracts* **73**: 141.

TABLE 1 Sample locations

Field No.	Reg. No.[1]	Analysis No.	Coll.[2]	mEgda94	mNgda94	Locality	Description	Type[3]	HS	TS	SiO_2%	χ (x 10^{-3} SI)
SMD	R004379	20040097	JLE	587720	5271680	Stinking Ck, South Maria Island	dolerite	C	Y	Y	51.44	0.47
LC1	R004436	910748	JLE	606640	5328110	Mouth of Lagunta Ck, Freycinet Peninsula	dolerite, chilled margin	A	Y	Y	45.52	>6.91
LC3	R004438	910749	JLE	606640	5328110	Mouth of Lagunta Ck, Freycinet Peninsula	dolerite, dyke centre	A	Y	Y	44.58	24.6
FY30	R004464	20010133	JLE	609580	5327660	2 km NNW of Mt Graham	dolerite	C	Y	Y	54.42	0.63
FY31	R004465	20010134	JLE	608110	5325250	E of Mt Freycinet	dolerite	C	Y	Y	52.88	>14.0
FP4	73/542	735804	PLFC	608310	5330380	SE headland of Wineglass Bay	dolerite	T		Y	47.20	>0.37
NJ475	R014324	20130001	JLE	608400	5330340	SE headland of Wineglass Bay	dolerite	T	Y	Y	47.78	
CB20	43964		JDC	608410	5330280	SE headland of Wineglass Bay	dolerite	T		Y		
CB21	43965		JDC	608510	5330280	SE headland of Wineglass Bay	dolerite	T		Y		
FY32	R004466	20010135	JLE	607360	5331270	Hawksnest Cove, Wineglass Bay	biotite microtonalite (hybrid)	C	Y	Y	58.71	>0.17
FP1	73/541	735803	PLFC	607310	5331280	Hawksnest Cove, Wineglass Bay	biotite microtonalite (hybrid)	C		Y	58.90	
NJ476	R014325	20130002	JLE	610400	5334750	Point between Sleepy and Carp Bays	dolerite	A	Y	Y	47.35	1.77
FP21	73/544	735806	PLFC	610510	5334680	Point between Sleepy and Carp Bays	dolerite	A		Y	48.80	>0.45
FP22	73/545	735807	PLFC	610210	5334680	Sleepy Bay	biotite microtonalite (hybrid)	C		Y	60.30	
NJ477	R014326	20130003	JLE	609800	5335830	Cape Tourville Road	dolerite	A	Y	Y	47.23	2.11
FP24	73/546	735808	PLFC	609810	5335680	Cape Tourville Road	dolerite	A		Y	47.82	8.93
NJ478	R014327	20130004	JLE	610600	5337860	East headland of Bluestone Bay	dolerite	C	Y	Y	50.32	>0.64
FP11	73/543	735805	PLFC	610510	5337880	East headland of Bluestone Bay	dolerite	C		Y	51.90	0.51
CB1	43960		JDC	~610600	~5337900	East headland of Bluestone Bay	dolerite					0.64
CB5	43961		JDC	~610600	~5337900	East headland of Bluestone Bay	dolerite					>0.47
CB6	43962		JDC	~610600	~5337900	East headland of Bluestone Bay	dolerite					0.60
CB7	43963		JDC	~610600	~5337900	East headland of Bluestone Bay	dolerite	C		Y		
NJ438	R013353	20080419	JLE	606220	5341900	~1km W of Freshwater Lagoon	dolerite	A	Y	Y	47.63	
NJ442	R013371		JLE	606710	5340370	Middleton Creek tributary	dolerite	A	Y	Y		
NJ440	R013369		JLE	609500	5358170	Cape Lodi	dolerite	A	Y	Y		>0.50
NJ441	R013370	20080421	JLE	609500	5358180	Cape Lodi	dolerite	A	Y	Y	48.52	0.97
B15a	43955		JDC	~609600	~5358100	Cape Lodi	dolerite	A		Y		
B15b	43956		JDC	~609600	~5358100	Cape Lodi	dolerite	A		Y		
B36	43958		JDC	~609600	~5358100	Cape Lodi	dolerite	A		Y		
BD1B	R004446	991036	JLE	608560	5362600	Bicheno blowhole	dolerite, chilled margin		Y	Y	46.44	>0.49
BD2A	R004447	991037	JLE	608560	5362600	Bicheno blowhole	dolerite, dyke centre	A	Y	Y	47.30	0.64
B51	43959		JDC	608610	5362680	Bicheno blowhole	dolerite					>0.37
B1	73/604	736628	PLFC	608910	5363580	The Gulch, Bicheno	dolerite	A		Y	47.50	0.37
B33	43957		JDC	608910	5363380	Governor Island, Bicheno	dolerite	A		Y		
B135	R014210	20080226	MW	601290	5416740	Arm Creek, Upper Scamander	dolerite	A	Y	Y	48.86	
NJ480	R014329	20130005	JLE	601280	5416750	Arm Creek, Upper Scamander	dolerite	A	Y	Y	48.49	>14.2
NJ446	R013375	20100105	JLE	609014	5420240	Coast 1.2 km N of Dianas Basin outlet	biotite microdiorite	C	Y	Y	53.13	0.37
NJ447	R013376	20100106	JLE	609200	5420490	Onion Ck 1.5 km N of Dianas Basin	dolerite (quartz monzodiorite)	C	Y	Y	53.27	28.7
41701	41701		JDC	~609600?	~5420800?	Dianas Basin	dolerite				54.65	
SHP	C108645	20010257	JLE	613110	5429780	St Helens Point	dolerite	A	Y	Y	49.11	40.1
37798	37798		JDC	613410	5429780	St Helens Point	dolerite				49.14	
611463			JDC	613210	5429680	St Helens Point	dolerite				48.30	
MSH91	R010796		MPM	612010	5432180	Grants Point	dolerite	T		Y		
MSH172	R001907	850179	MPM	612110	5432180	Grants Point	dolerite				51.99	
NJ508	R014359	20160204	JLE	612070	5432132	Grants Point	dolerite	T	Y	Y	52.57	1.01
37803	37803	20040039	JDC	612110	5432280	Grants Point	dolerite				52.00	
R1084	R001084	910631	MPM	551410	5411780	Near Cascade Creek, Roses Tier	biotite-hbl microdiorite	C		Y	57.95	

TABLE 1 Sample locations (continued)

Field No.	Reg. No.[1]	Analysis No.	Coll.[2]	mEgda94	mNgda94	Locality	Description	Type[3]	HS	TS	SiO_2%	χ (x 10^{-3} SI)
SB27	R006211	20130175	MPM	544710	5426880	S of Valentine Rvt, ~1.5km ESE of Mt Scott	dolerite	C		Y	49.35	
AJ807	R004327	910743	JLE	575010	5432780	North George River	dolerite	T	Y	Y	48.16	0.75
AJ914	R004328	910744	JLE	582510	5432680	E tributary, Waratah Creek, Pyengana	dolerite	T	Y	Y	48.72	0.89
NJ455	R013384	20100111	JLE	583450	5439560	Crowther Ck, 1.3 km NNW of Poimena	dolerite	T	Y	Y	50.14	0.76
NJ454	R013383	20100110	JLE	579700	5436260	450m W of hairpin bend, Weldborough Pass	dolerite	T	Y	Y	49.30	0.61
JR66		742538	JM	579610	5436280	Tasman Hwy W of Weldborough Pass	dolerite				48.80	
JR26	74/518		JM	579610	5436280	Tasman Hwy W of Weldborough Pass	dolerite			Y		
MR30	72/393	735113	MPM	574010	5436580	upper Cascade River	dolerite				48.50	
MR146	74/461a	741650	MPM	576110	5438280	Spinel Ck, S of Weldborough	dolerite				48.40	
MR136	74/437	741647	MPM	573710	5437180	Mt Paris Dam Rd	dolerite			Y	47.10	
MBT210	R006143		MPM	586798	5435434	E of Lottah (loc. 1876)	dolerite			Y		
MBT219	R006152		MPM	586329	5436526	E of Lottah (loc. 1922)	dolerite			Y		
MBT220	R006153		MPM	587056	5436900	E of Lottah (loc. 1926)	dolerite			Y		
JR65		742537	JM	583410	5443580	Rocky Ck, Blue Tier	dolerite				49.80	
JR13	74/510		JM	583410	5443580	Rocky Ck, Blue Tier	dolerite	T		Y		
MBT225	*R006158*		*MPM*	*587900*	*5437810*	*S of Sun Flats Rd (loc. 1977)*	*Jurassic dolerite*			*Y*		
MNET38	R001100	20080234	MPM	588117	5449540	S of Tebrakunna Rd, loc. 100, float	dolerite, fine-gr	T		Y	50.02	0.68
MNET37	R001099		MPM	588485	5450098	S of Tebrakunna Rd	dolerite			Y		
MNET36	R001098	20080233	MPM	588500	5450506	S of Tebrakunna Rd, loc. 98, float	dolerite	T		Y	48.07	5.6
NJ453	R013382		JLE	587462	5451240	N of Tebrakunna Road	dolerite			Y		
MNET35	R001097		MPM	587478	5451250	N of Tebrakunna Road	dolerite			Y		
MNET34	R001096		MPM	587543	5451342	N of Tebrakunna Road	dolerite			Y		
MNET33	R001095		MPM	587631	5451150	N of Tebrakunna Road	dolerite			Y		
MNET17	R001079		MPM	600542	5442348	Bark Hut Marsh area	dolerite			Y		
MNET32	R001094		MPM	600561	5442481	Bark Hut Marsh area	dolerite			Y		
MBT44	75/579	20080319	MPM	600067	5441892	Bark Hut Marsh	dolerite	C	Y	Y	51.63	
MBT74	75/856	760573	MPM	600928	5446013	E of Last R bridge, Ansons Bay Rd, loc 629	dolerite	A		Y	46.00	
MNET16	R001078		MPM	602384	5447381	Sampsons Ck area	andesite			Y		
MNET13	R001075	20080231	MPM	600966	5449468	Pretty Marsh Hill	dolerite	T		Y	48.78	12.84
MBT71	75/845	760570	MPM	600890	5449394	near Pretty Marsh Hill, loc 553	dolerite	T		Y	48.70	
MBT132	76/858	20080334	MPM	602245	5451237	near Kangaroo Flat, locs 612, 1224	dolerite	T	Y	Y	48.74	
MBT73	75/846		MPM	599997	5448013	near Janeys Ck, loc. 590	chilled dolerite		Y	Y		
MBT30	75/512	20080318	MPM	596841	5444231	tributary of Spurrs Rvt	dolerite	T	Y	Y	47.66	
MBT176	R006109		MPM	594683	5440733	NW of Cliffords Rd, loc.1640	dolerite			Y		
MBT76	75/858	20080325	MPM	602421	5451788	near Gripe Ck, loc 680	dolerite	T	Y	Y	48.20	
MBT82	75/891		MPM	602323	5452335	Gripe Ck, loc. 712	dolerite		Y	Y		
MNET10	R001072	20080229	MPM	601644	5451644	Big Creek	dolerite	A		Y	47.76	13.23
NJ471	R014320	20110318	JLE	599372	5449103	1 km S of Pretty Marsh	dolerite	T	Y	Y	47.65	19.70
MNET2	R001064		MPM	602129	5452649	Gripe Creek	dolerite			Y		
MNET4	R001066		MPM	601756	5452056	Big Creek	dolerite			Y		
MBT143	77/466	20080335	MPM	601818	5456624	near Boggy Ck trib, loc 1280	dolerite	A	Y	Y	47.98	
MNET12	R001074	20080230	MPM	600400	5451031	NE of Pretty Marsh	andesite	C		Y	57.99	0.488
MBT165	77/780	20080338	MPM	600420	5450942	NE of Pretty Marsh, loc 1546	andesite	C	Y	Y	58.63	
MBT75	75/857	20080324	MPM	602512	5451789	near Gripe Ck, loc 664	andesite	C	Y	Y	57.54	
MNET5	R001067		MPM	602507	5451796	near headwaters of Gripe Ck	andesite	C		Y		
MBT77	75/859	760574	MPM	602416	5451787	near Gripe Creek, loc 684	andesite	C		Y	57.80	
MNET9	R001071		MPM	602348	5451723	near headwaters of Gripe Ck	andesite	C		Y		
MBT97	76/682	20080330	MPM	602058	5451555	near Big Creek, loc 943	andesite	C	Y	Y	57.44	
MNET11	R001073		MPM	601277	5451373	W of Big Ck	andesite	C		Y		
MBT98	76/681	20080331	MPM	601510	5451503	near Big Creek, loc 945	chilled andesite	C	Y	Y	57.07	
MNET14	R001076		MPM	599846	5450708	Pretty Marsh	andesite	C		Y		
MBT167	77/782	20080339	MPM	602137	5452698	Gripe Ck. loc 1563	granite/dolerite hybrid	C	Y	Y	63.97	

TABLE 1 Sample locations (continued)

Field No.	Reg. No.[1]	Analysis No.	Coll.[2]	mEgda94	mNgda94	Locality	Description	Type[3]	HS	TS	SiO_2%	χ (x 10^{-3} SI)
NJ511	R014362	20160206	JLE	608257	5451495	coast ~2km S of Policemens Point	andesite	C	Y	Y	55.00	0.47
MBT144	*77/583*		*MPM*	*608363*	*5459623*	*Eddystone Rd near Reeves Ck, loc. 1309*	*Jurassic dolerite*			*Y*		
BT22		783151	PRW	594838	5451152	trib of Big Boggy Ck, S of Fraser Rd	dolerite				47.60	
BT28		783153	PRW	587549	5449242	near start of Ripdoodle Rd	dolerite				48.00	
BT30		783154	PRW	595502	5449058	SW of Wild Pig Hill	dolerite				47.90	
BT31		783155	PRW	589848	5447988	just E of upper Great Musselroe R	dolerite				48.60	
NJ364A	R013303		JLE	609630	5466390	N end of Purdon Bay	chilled granite/ dolerite hybrid		Y			>0.10
NJ364B	R013304	20080286	JLE	609630	5466390	N end of Purdon Bay	granite/dolerite hybrid	C	Y	Y	65.64	0.09
NJ423	R013317	20080225	JLE	602630	5470960	2.7 km E of Mt William	dolerite	T	Y	Y	49.36	0.69
NJ262	R013280	20080200	JLE	601910	5467630	3.7 km SSE of Mt William	dolerite	T	Y	Y	48.10	0.85
ER2	73/636	736631	PLFC	599910	5465580	5 km S of Mt William	dolerite	A		Y	48.50	0.45
NJ245	R013279	20080199	JLE	601620	5472110	Forester Kangaroo Drive	dolerite	T	Y	Y	47.88	0.57
MW1	73/634	736627	PLFC	600610	5469780	1 km SSE of Mt William	dolerite	T		Y	47.50	>0.52
MW2	73/633	736628	PLFC	599310	5470680	Foot of Mt William on west	dolerite	C		Y	55.70	>0.23
ER1	73/635	736630	PLFC	597910	5465480	6 km SSW of Mt William	dolerite	T		Y	47.30	3.12
NJ401	R013312	20080220	JLE	597850	5465450	Farm track, "Telegraph"	dolerite	T	Y	Y	47.63	>3.94
NJ406	R013313	20080221	JLE	596530	5465230	Eddystone Rd opposite "Telegraph"	dolerite	T	Y	Y	48.56	4.69
NJ407	R013314	20080222	JLE	596540	5465210	Eddystone Rd opposite "Telegraph"	dolerite	T	Y	Y	47.23	7.71
MUS	C108643	20010259	JLE	597610	5472480	Musselroe Road	dolerite	C	Y	Y	51.20	>0.70
MR1	73/605	736624	PLFC	597710	5472580	Quarry, Musselroe Road	dolerite	C		Y	52.50	0.55
EA11	85/262	802656	PWB	597410	5470680	2.5 km W of Mt William	dolerite			Y	49.01	
NJ420	R013315	20080223	JLE	599230	5474260	~ 4 km S of Musselroe Bay	dolerite	T	Y	Y	48.63	0.72
NJ422	R013316	20080224	JLE	599640	5476140	~ 4 km S of Musselroe Bay	dolerite	T	Y	Y	47.60	1.21
MR2	73/606	736625	PLFC	599310	5473880	Musselroe Road	dolerite	T		Y	47.30	0.81
MR3	73/632	736626	PLFC	599010	5473980	Musselroe Road	dolerite	T		Y	48.10	
EE6	85/274		PWB	~598400	~5474700	~4 km S of Poole (Musselroe Bay)	dolerite			Y		
63095	63095		PAK	601110	5473380	2.8 km NNE of Mt William	dolerite				48.29	
GR6	43954		JDC	612000	5468900	George Rocks	alkali dolerite (Cainozoic?)			Y		
PE11	85/281		PWB	612000	5468900	George Rocks	alkali dolerite (Cainozoic?)			Y		
FLD1	R006525	990882	JLE	605210	5548080	W of Pt Reid, Lady Barron	dolerite	T	Y	Y	48.55	>0.49
FLD3	R006527	990884	JLE	607810	5547280	E of Lady Barron	dolerite	T	Y	Y	47.02	>3.59
285	43942		JDC	~607800	~5547300	E of Lady Barron township	dolerite					
286	43943		JDC	~607800	~5547300	E of Lady Barron township	aplite, feldspathic			Y		0.16
FLD2	R006526	990883	JLE	608110	5547380	E of Lady Barron	dolerite	T	Y	Y	48.20	1.39
77/908	77/908	20070303	DJJ	601510	5545680	Badger Corner Rd foreshore	dolerite	T	Y	Y	49.75	
R013341	R013341	20080434	TCM	588160	5561017	Cannes Hill, Flinders Island	dolerite	T	Y	Y	48.93	5.08
77/907b	77/907b	20070302	DJJ	581410	5561180	Airport Beach-Long Pt	dolerite	T	Y	Y	47.30	
FLD4	R006528	990885	JLE	581510	5602480	~900m ESE of Stanley Pt, Flinders Is	alkali dolerite	A	Y	Y	44.17	13.3
R014365	R014365	20170188	MJV	581564	5602456	~900m ESE of Stanley Pt, Flinders Is	alkali dolerite	A	Y	Y	44.01	7.19
BA3	R011908	20050175	JLE	602870	5536120	S side of Apple Orchard Pt, C Barren Is	dolerite	C	Y	Y	49.73	>4.58
BA5	R011910	20050177	JLE	604710	5534980	Riddles Bay, Cape Barren Is	dolerite	T	Y	Y	49.72	>0.49
BA6	R011911	20050178	JLE	604560	5534990	Riddles Bay, Cape Barren Is	dolerite	C	Y	Y	52.03	≥ 0.49
BA4	R011909	20050176	JLE	607630	5522900	W of Nautilus Cove, C Barren Is	dolerite	C	Y	Y	54.67	>0.27
BA35	R011928	20050192	JLE	612100	5537190	SE of Puncheon Point, C Barren Is	hbl-bte micro-granodiorite	C	Y	Y	65.09	0.30
R014343	R014343		DJJ	618600	5517300	E side of Cone Point, C Barren Is	alkali dolerite		Y	Y		
R014344	R014344		DJJ	584500	5524800	E dyke, Cape Sir John, C Barren Is	dolerite		Y	Y		0.45
R014345	R014345		DJJ	584000	5425000	W dyke, Cape Sir John, C Barren Is	dolerite		Y	Y		0.45
26	43940		JDC	~612110	~5537200	SE of Puncheon Point, C Barren Is	hbl-bte micro-granodiorite			Y		
1	43933		JDC	~588900	~5532300	east of settlement, Cape Barren Is	dolerite			Y		
8	43934		JDC	~585500	~5525500	Thunder and Lightning Bay, C Barren Is	dolerite			Y		

TABLE 1 Sample locations (continued)

Field No.	Reg. No.[1]	Analysis No.	Coll.[2]	mEgda94	mNgda94	Locality	Description	Type[3]	HS	TS	SiO_2%	χ (x 10^{-3} SI)
10	43935		JDC	~596000	~5533900	west of Whittling Office Bay, CBI	dolerite			Y		
35	43936		JDC	~602200	~5522500	Battery Bay, Cape Barren Is	dolerite			Y		
116	43937		JDC	~594500	~5532000	SE flank of Petticoat Ridge, C Barren Is	dolerite			Y		
201	43938		JDC	~598100	~5524200	near Dyas Ck, Cape Barren Is (?)	dolerite			Y		
22	43939		JDC	~606000	~5534600	near Dover Point, Cape Barren Is (?)	dolerite			Y		
69	43941		JDC	~606600	~5529500	N flank of Phils Hill, Cape Barren Is (?)	dolerite			Y		
3	43944		JDC	~586900	~5530900	near pier, The Settlement, C Barren Is	dolerite					>10.5
5	43945		JDC	~583900	~5528300	near Bungs Pt, Cape Barren Is	dolerite					>0.60
21	43946		JDC	~606000	~5534600	near Dover Point, Cape Barren Is (?)	dolerite					>0.85
24	43947		JDC	~602900	5536100	Apple Orchard Pt, Cape Barren Is	dolerite					>0.20
152	43948		JDC	~586900	~5532800	eastern Long Island	dolerite			Y		
154	43949		JDC	~584600	~5531000	western Long Island	dolerite			Y		
276	43950		JDC	~591200	~5534800	Neds Reef, north of Cape Barren Is	dolerite					>0.22
C9	43951		JDC	~594600	~5509500	Western Clarke Island	dolerite			Y		
C45	43952		JDC	~602300	~5515700	Kangaroo Bay, Clarke Is (?)	dolerite			Y		
C46	43953		JDC	~602300	~5515700	Kangaroo Bay, Clarke Is (?)	dolerite			Y		
77/910	77/910	20070305	DJJ	~578200	~5542300	N coast of Mt Chappell Is	dolerite	A	Y	Y	49.66	
A4	43966		JDC	~576800	~5537900	eastern Badger Is	dolerite			Y		
A5	43967		JDC	~577100	~5539000	eastern Badger Is	dolerite			Y		
A7	43968		JDC	~576600	~5539400	eastern Badger Is	dolerite			Y		
A17	43969		JDC	~572100	~5538100	western Badger Island	dolerite			Y		
A20	43970		JDC	~576400	~5536600	S of Lucy Pt, Badger Is	dolerite			Y		
A25	43971		JDC	~576800	~5536800	Lucy Pt, Badger Is	dolerite					
A27	43972		JDC	~576800	~5536800	Lucy Pt, Badger Is	dolerite			Y		

[1] Registration numbers of the form R004379 and 73/542 are from the Mineral Resources Tasmania collection, those of the form 43964 are from the University of Tasmania collection.

[2] JLE- J. L. Everard, MPM- M. P. McClenaghan, JDC- J. D. Cocker, PLFC- P. L. F. Collins, DJJ- D. J. Jennings, JM- J. McClenaghan, MW- M. Worthing, PWB- P. W. Baillie, PRW- P. R. Williams, TCM- T. C. Methorst, PAK- P. A. Kitto, MJV-M. J. Vicary.

[3] T- tholeiitic, A- alkalic; C- calc-alkaline.

TABLE 2 Field magnetic susceptibility (x 10^{-3} SI)

Field Stn/ Field No	Sample Reg No.[1]	Location	mE	mN	Description	Type	Comment	Magnetic susceptibility			Standard deviation	No. of readings
			GDA94					Mean	Min	Max		
NJ476	R014325	Carp Bay	610402	5434753	dolerite	alkalic		1.55	0.87	3.54	0.80	10
NJ478	R014327	Bluestone Bay	610602	5337863	dolerite	calc-alkaline		0.59	0.48	0.72	0.07	10
NJ480	R014329	Arm Creek	601282	5416753	dolerite	alkalic		11.89	8.35	14.80	2.98	5
SHP	C108645	St Helens Point	613112	5429783	dolerite	alkalic		26.39	7.32	34.90	7.00	20
MNET38	R001100	S of Tebrakunna Road	588117	5449540	dolerite	tholeiitic	fine-gr	0.68	0.49	1.00	0.16	8
MNET33	R001095	N of Tebrakunna Road	587631	5451150	dolerite		coarse-gr	1.51	0.49	4.76	1.21	13
MNET36	R001098	S of Tebrakunna Road	588500	5450506	dolerite	tholeiitic	coarse-gr	5.63	0.67	8.39	2.85	11
MNET37	R001099	S of Tebrakunna Road	588485	5450098	dolerite		coarse-gr	0.79	0.64	0.95	0.16	3
MNET17	R001079	Bark Hut Marsh area	600542	5442348	dolerite		coarse-gr	0.58	0.45	0.63	0.07	5
MNET32	R001094	Bark Hut Marsh area	600561	5442481	dolerite		coarse-gr	0.66	0.51	0.86	0.12	7
MNET13	R001075	Pretty Marsh Hill	600966	5449468	dolerite	tholeiitic	coarse-gr	12.84	10.20	17.00	1.90	13
-	-	Pretty Marsh Hill	601082	5449652	dolerite		coarse-gr	9.03	5.45	13.70	2.96	13
MNET12	R001074	NE of Pretty Marsh	600400	5451031	andesite	calc-alkaline	fine-gr	0.49	0.35	0.85	0.18	10
MNET4	R001066	Big Creek	601756	5452056	dolerite		coarse-gr	12.15	0.99	19.10	5.33	10
MNET10	R001072	Big Creek	601644	5451644	dolerite	alkalic	coarse-gr	13.23	7.50	16.20	2.80	10
-	-	400 m E of Big Creek	601990	5451606	dolerite		fine-gr	0.51	0.32	0.82	0.15	12
MNET11	R001073	W of Big Creek	601277	5451373	andesite	calc-alkaline	fine-gr	0.49	0.35	0.77	0.13	12
MNET5	R001067	near headwaters of Gripe Ck	602507	5451796	andesite	calc-alkaline	fine-gr	0.36	0.30	0.39	0.04	5
MNET9	R001071	near headwaters of Gripe Ck	602350	5451723	andesite	calc-alkaline	fine-gr	0.63	0.41	1.11	0.25	10
MNET2	R001064	Gripe Creek	602129	5452649	dolerite		coarse-gr	14.33	5.39	25.30	6.19	10
-	-	N side of Gripe Creek	602140	5452702	dolerite		coarse-gr	7.93	4.26	11.70	3.42	4
MNET29	R001091	tributary of Big Boggy Ck	600705	5457702	dolerite		coarse-gr	0.70	0.55	0.81	0.09	7
-	-	small tributary of Ansons R	602494	5453159	dolerite		coarse-gr	12.33	10.70	13.60	1.48	3
NJ364	R013303	N end of Purdon Bay	609632	5466393	hybrid	calc-alkaline	chilled margin	0.15	0.11	0.19	0.03	10
NJ364	R013304	N end of Purdon Bay	609632	5466393	hybrid	calc-alkaline	centre, dark zones	0.13	0.09	0.18	0.02	10
NJ364	R013304	N end of Purdon Bay	609632	5466393	hybrid	calc-alkaline	centre, light zones	0.07	0.06	0.08	0.01	5
NJ262	R013280	3.7 km SSE of Mt William	601912	5467633	dolerite	tholeiitic		0.63	0.56	0.81	0.08	10
NJ423	R013317	2.7 km E of Mt William	602632	5470963	dolerite	tholeiitic		0.70	0.61	0.82	0.08	6
NJ245	R013279	Forester Kangaroo Drive	601592	5472133	dolerite	tholeiitic		0.52	0.30	0.76	0.14	10
NJ401	R013312	Farm track, "Telegraph"	597852	5465453	dolerite	tholeiitic		4.12	3.20	5.35	0.73	10
NJ406	R013313	Eddystone Rd near "Telegraph"	596532	5465233	dolerite	tholeiitic		8.91	3.44	19.80	5.32	10
NJ410	-	Eddystone Rd near "Telegraph"	597742	5472483	dolerite			0.55	0.42	0.66	0.07	20
NJ422	R013316	~4 km S of Musselroe Bay	599642	5474143	dolerite	tholeiitic		0.74	0.56	1.08	0.15	10

[1] see Table 1 for magnetic susceptibility measurements on individual samples.

TABLE 3 Summary of petrography

Field No.	Other ID	Locality	CA	Type	Phenocrysts	Groundmass		Mineralogy					
						Grain size	Texture	Plag	Cpx	hbl	bte	Q	Other
SMD	R004379	South Maria Island	Y	C	-	cgr	subophitic	S	M	m		m	act
LC1	R004436	Lagunta Ck	Y	A	plag ≤ 140mm; ol (altered)	vfgr	intergranular	A	M			-	act, chl
LC3	R004438	Lagunta Ck	Y	A	plag ≤ 140mm; ol (altered)	cgr	subophitic	P	F		tr?	-	act, chl, ep, serpentine
FY30	R004464	Mt Graham	Y	C	plag ≤ 2mm; qtz (xenos)	mgr	seriate	S	S			m	act, chl, cc
FY31	R004465	Mt Freycinet	Y	C	plag ≤ 2.5mm; ol(?)	fgr	intergranular	S	P			r?	cc
FP4	73/542	SE Wineglass Bay	Y	T	-	mgr	intergranular/ subophitic	S	P				act
NJ475	R014324	SE Wineglass Bay	Y	T	plag ≤ 4mm	mgr	intergranular/ subophitic	P	M				act, chl, prehnite
CB20	43964	SE Wineglass Bay		T	plag megacryst ≥ 25mm	mgr	intergranular/ subophitic	S	A				act
CB21	43965	SE Wineglass Bay		T	plag ≤ 10mm	f-mgr	intergranular/ seriate	S	A				act
FY32	R004466	Hawksnest Cove	Y	C	Qtz ≤ 3mm, plag, ksp (xenos)	fgr	porphyritic/ microgranular	S	-		ab	ab	act, ksp?
FP1	73/541	Hawksnest Cove	Y	C	Qtz ≤ 3mm, plag, ksp (xenos)	fgr	porphyritic/ microgranular	S	-		ab	ab	act, ksp?
NJ476	R014325	Sleepy/Carp Bays	Y	A	plag ≤ 3mm	cgr	seriate/consertal	P	M		m		act, cc
FP21	73/544	Sleepy/Carp Bays	Y	A	plag ≤ 3mm	cgr	seriate/consertal	P	M		m		act, cc
FP22	73/545	Sleepy Bay	Y	C	Qtz ≤ 3mm, plag ≤ 2.5mm (xenos)	fgr	porphyritic, microgranular	P	-		ab	ab	act, ksp
NJ477	R014326	Cape Tourville Rd	Y	A	-	cgr	consertal	P	A		m	-	act
FP24	73/546	Cape Tourville Rd	Y	A	-	cgr	consertal	P	A		m	-	act
NJ478	R014327	Bluestone Bay	Y	C	plag ≤ 3mm	m-fgr	intergranular	S	P		c	m	act
FP11	73/543	Bluestone Bay	Y	C	plag ≤ 3mm	m-cgr	intergranular	P	A		c	m	act
CB7	43963	Bluestone Bay		C	plag; qtz xenocryst (~2 mm)	m-cgr	intergranular	M	A		c	r	act
NJ438	R013353	Freshwater Lagoon	Y	A	-	cgr	subophitic	P	P				act, chl
NJ442	R013371	Middleton Ck trib	-	A	-	cgr	ophitic	A	P				act, chl, ep
NJ440	R013369	Cape Lodi	-	A	plag ≤ 5mm, ol? (chl)	m-cgr	intergranular	P	M				chl
NJ441	R013370	Cape Lodi	Y	A	plag ≤ 3mm, xenos ≤ 14mm; ol? (chl)	m-cgr	intergranular	P	M				chl, ep, cc, hydrogrossular?
B15a	43955	Cape Lodi		A	plag ≤ 2mm, ol(?) ≤ 0.5mm	mgr	intergranular	M	A				chl
B15b	42956	Cape Lodi		A	plag ≤ 1mm, sparse	f-vfgr	chilled, fluida	M	A				chl, act
B36	43958	Cape Lodi		A	plag xeno (12mm)	mgr	intergranular	P	P				chl
BD2A	R004447	Bicheno blowhole	Y	A	plag ≤ 10mm, ol(?, sparse)	mgr	seriate; subophitic	P	F				chl
B1	73/604	The Gulch, Bicheno	Y	A	ol(?)	mgr	intergranular/ subophitic	P	F				chl, prehnite, cc
B33	43957	Governor Is		A	plag ≤ 3mm, Kspar xeno (10mm)	mgr	intergranular/ subophitic	P	F				chl
B135	R014210	Arm Ck	Y	A	-	cgr	consertal	P	P			m	act, chl, ep, prehnite
NJ480	R014329	Arm Ck	Y	A	-	cgr	consertal	P	P			m	act, chl, ep, prehnite
NJ446	R013375	Dianas Basin	Y	C	plag xenocrysts (1-3mm)	fgr	porphyritic/ microgranular	A	-		ab	c?	
NJ447	R013376	Onion Ck	Y	C	plag ≤ 0.5mm	fgr	intergranular	P	M			m	act, cc
SHP	C108645	St Helens Pt	Y	A	-	cgr	consertal	P	P			m	chl, prehnite, act, ep, cc
MSH91	R010796	Grants Pt		T	Q xenos ≤ 2mm; cpx (altered)	fgr	intergranular	S	P				act, sericite
NJ508	R014359	Grants Pt	Y	T	Q ≤ 3mm; plag ≤ 1.5mm (xenos); cpx	fgr	intergranular	S	P				act, sericite
R1084	R001084	Cascade Ck, Roses Tier		C	plag, ksp ≤ 4mm, corroded	c gr	consertal	S	-	ab	c	m	ksp
SB27	R006211	Valentine Rvt (Mt Scott)	Y	C	plag ≤ 3 x 0.5mm; ol? (talc)	f-mgr	intergranular	S	M			m	act
AJ807	R004327	N George River	Y	T	plag ≤ 1.5 mm, cpx(?)	f-mgr	intergranular	P	A			r	act

TABLE 3 Summary of petrography (continued)

Field No.	Other ID	Locality	CA	Type	Phenocrysts	Groundmass		Mineralogy					
						Grain size	Texture	Plag	Cpx	hbl	bte	Q	Other
AJ914	R004328	Waratah Ck, Pyengana	Y	T	-	m-cgr	ophitic/subophitic	S	P				act
NJ455	R013384	Crowther Ck	Y	T	-	mgr	intergranular	S	A		m	tr	act
NJ454	R013383	Weldborough Pass	Y	T	-	mgr	consertal/ subophitic	P	M			tr	act
JR26	74/518	Weldborough Pass			-	cgr	consertal/ subophitic	P	A			tr	act
MR136	74/437	Mt Paris Dam Rd			cpx?, ≤ 1 mm, altered	fgr	intergranular	S	A	m	m		act
MBT210	R006143	E of Lottah			-	cgr	subophitic	S	A	tr			act
MBT219	R006152	E of Lottah			-	m-cgr	subophitic	P	A				act
MBT220	R006153	E of Lottah			-	m-cgr	ophitic	P	A	tr			act
JR13	74/510	Rocky Ck		T	plag ≤ 2 mm, ol (altered)	mgr	intergranular	S	A				act
MNET38	R001100	S of Tebrakunna Rd	Y	T	plag ≤1.5 mm	fgr	micropoikilitic	P	S			ab	act, chl, ksp
MNET37	R001099	S of Tebrakunna Rd			-	fgr	micropoikilitic	M	P			ab	act, chl, ksp
MNET36	R001098	S of Tebrakunna Rd	Y	T		cgr	subophitic/ophitic	S	P			r	
NJ453	R013382	N of Tebrakunna Rd			plag ≤ 3 mm	vfgr	chilled, fluidal	F	M				act, chl
MNET35	R001097	N of Tebrakunna Rd			plag ≤ 2.5 mm, sparse; cpx(?), alt	fgr	intergranular	M	P			tr	act, chl
MNET34	R001096	N of Tebrakunna Rd			plag ≤ 4 mm	cgr	subophitic	S	A				act
MNET33	R001095	N of Tebrakunna Rd			plag ≤ 4 mm; Qtz xenos	mgr	intergranular	M	A			ab	act, chl
MNET17	R001079	Bark Hut Marsh			plag ≤ 5 mm; cpx	mgr	intergranular, fluidal	S	S			r	act, chl
MNET32	R001094	Bark Hut Marsh			plag ≤ 4 mm, ol	mgr	intergranular	P	S			tr	act, chl
MBT44	75/579	Bark Hut Marsh	Y	C	plag	cgr	intergranular, fluidal	P	S			tr	act, chl
MBT74	75/856	E of Last R bridge	Y	A	-	cgr	ophitic	M	S				act, chl
MNET16	R001078	Sampsons Ck area			plag ≤ 1 x 0.2 mm	f-vfgr	intergranular	P	M			tr	act, chl?
MNET13	R001075	Pretty Marsh Hill	Y	T	-	cgr	subophitic	S	P			m	act, chl
MBT71	75/845	near Pretty Msh Hill	Y	T	plag ≤ 2.5 mm	cgr	consertal/ subophitic	S	P			tr	act, chl, ep (r]
MBT132	76/858	near Kangaroo Flat	Y	T	-	cgr	subophitic	P	S			m	act, chl
MBT73	75/846	near Janeys Ck			-	vfgr	chilled, fluidal	S	A				act
MBT30	75/512	trib of Spurrs Rvt	Y	T	-	cgr	consertal/ subophitic	M	P			m	act, chl, ep
MBT176	R006109	NW of Cliffords Rd			-	cgr	subophitic	M	P			m	act, chl
MBT76	75/858	near Gripe Ck	Y	T	-	cgr	subophitic	S	P			m	
MBT82	75/891	Gripe Ck			-	cgr	subophitic	S	M			-	act
MNET10	R001072	Big Creek	Y	A	-	cgr	ophitic	S	P		m	r	act, chl, ksp?
NJ471	R014320	S of Pretty Marsh	Y	T	plag ≤ 10 mm	vcgr	ophitic	S	P			r	act, chl
MNET2	R001064	Gripe Creek			-	cgr	ophitic	S	P		m	r	act
MNET4	R001066	Big Creek			-	mgr	ophitic	S	P			-	act, chl, cc
MBT143	77/466	near Boggy Ck trib	Y	A	plag ≤ 4 mm	f-mgr	intergranular	M	S			-	
MNET12	R001074	NE of Pretty Marsh	Y	C	plag ≤ 0.5 mm; Q; ksp (xenos)	vfgr	intergranular	S	m		m	ab	act, chl
MBT165	77/780	NE of Pretty Marsh	Y	C	plag 0.2 - 0.6 mm; Q	vfgr	intergranular	F	-			ab	act, chl
MBT75	75/857	near Gripe Ck	Y	C	plag ≤ 1 x 0.3 mm; opaques (alt)	vfgr	intergranular	F	m	tr	m	c	act, chl
MNET5	R001067	near Gripe Ck		C	plag ≤ 1 x 0.15 mm; Q xenos	fgr	intergranular	P	m		m	c	act, chl
MBT77	75/859	near Gripe Ck	Y	C	plag ≤ 0.6 mm	fgr	intergranular	P	-			c	act, chl
MNET9	R001071	near Gripe Ck		C	plag ≤ 1 mm; chl ≤ 0.7 mm	f-vfgr	intergranular	P	r?			c	chl
MBT97	76/682	near Big Creek	Y	C	plag, chl ≤ 1mm; Q xenos ≤ 0.2 mm	fgr	intergranular, fluidal	P	-			c	act, chl
MNET11	R001073	W of Big Ck		C	plag ≤ 1.5 mm; chl ≤ 1 mm	fgr	intergranular	P	-			c	act, chl
MBT98	76/681	near Big Creek	Y	C	plag ≤ 2 mm	fgr	vfgr chilled mesostasis	F	-			c?	act

TABLE 3 Summary of petrography (continued)

Field No.	Other ID	Locality	CA	Type	Phenocrysts	Groundmass		Mineralogy					
						Grain size	Texture	Plag	Cpx	hbl	bte	Q	Other
MNET14	R001076	Pretty Marsh		C	chl ≤ 1.5 mm; q xenocrysts	f-vfgr	intergranular	M	-			c	act, chl
MBT167	77/782	Gripe Ck	Y	C	-	cgr	consertal (granitic)/ intergranular (doleritic)	P	-		m?	ab	act
NJ511	R014362	S of Policemens Pt		C	Q, ksp, plag (xenocrysts)	f-mgr	intergranular	P	-		ab	c	act, bte, cc
NJ364B	R013304	N Purdon Bay	Y	C	xenocrysts of granitic origin	cgr	consertal	S	-		ab	ab	Ksp, muscovite
NJ423	R013317	E of Mt William	Y	T	-	cgr	consertal/ subophitic	P	A		m	-	
NJ262	R013280	SSE of Mt William	Y	T	-	cgr	consertal/ subophitic	P	M		m	m	
ER2	73/636	S of Mt William	Y	A	-	cgr	consertal/ subophitic	P	A		tr	-	act, chl
NJ245	R013279	Forester Kangaroo Drive	Y	T	plag ≤ 8 mm	mgr	ophitic	P	M	m		-	act
MW1	73/634	SSE of Mt William	Y	T	plag ≤ 8 mm	mgr	subophitic/ intergranular	P	M			-	act
MW2	73/633	Foot of Mt William	Y	C	-	cgr	consertal	P	A	m	m	c	act, chl
ER1	73-635	SSW of Mt William	Y	T	-	m-cgr	ophitic	S	P			-	
NJ401	R013312	Track, "Telegraph"	Y	T	plag ≤ 8 mm	cgr	subophitic	S	P			-	act, chl
NJ406	R013313	opposite "Telegraph"	Y	T	plag ≤ 5 x 1 mm	vcgr	subophitic	S	P			-	act, chl, prehnite, talc?
NJ407	R013314	opposite "Telegraph"	Y	T	plag ≤ 10 mm; ol (some fresh)	fgr	subophitic	S	P		tr	-	chl, act, talc?
MUS	C108643	Musselroe Rd	Y	C	plag ≤ 4 mm, sparse	mgr	intergranular	O	A			m	act, chl
MR1	73/605	Musselroe Rd quarry	Y	C	plag ≤ 4 mm, sparse	cgr	intergranular/ consertal	O	A		tr	m	act, chl
EA11	85/262	W of Mt William	Y		plag ≤ 4 mm, abundant; ol	f-mgr	porphyritic/ intergranular	O	A			-	chl
NJ420	R013315	S of Musselroe Bay	Y	T	plag ≤1.5mm, sparse	cgr	ophitic/subophitic	S	M		m	-	
NJ422	R013316	S of Musselroe Bay	Y	T	-	f-mgr	intergranular	P	M			-	
MR2	73/606	Musselroe Road	Y	T	plag megacryst 7mm	m-cgr	subophitic	P	M			-	
MR3	73/632	Musselroe Road	Y	T	plag ≤3mm	cgr	subophitic	P	M			-	
EE6	85/274	S of Musselroe Bay			plag, sparse	m-cgr	subophitic	P	A			-	
GR6	43954	George Rocks			cpx ≤ 1mm, sparse	fgr	intergranular	P	S	ab		-	
PE11	85/281	George Rocks			cpx ≤ 2mm, sparse	fgr	intergranular	M	S	ab		-	chl, act
FLD1	R006525	W of Pt Reid	Y	T	-	mgr	ophitic	M	P	m		-	chl, act, ep?
FLD3	R006527	E of Lady Barron	Y	T	-	vcgr	subophitic	S	P			-	chl, act
43943	43943	E of Lady Barron			plag ≤ 2mm; epidote	f-mgr	granular (plag, Kspar)	P	-			-	ksp, ep
FLD2	R006526	E of Lady Barron	Y	T	-	m-cgr	subophitic	P	S			-	chl, act
77/908	77/908	Badger Corne	Y	T	plag ≤ 4 x 2 mm	mgr	seriate/ subophitic	S	M		c	-	act, chl
R013341	R013341	Cannes Hill	Y	T	plag ≤ 7 x 1.5 mm	cgr	subophitic/ intergranular	P	P			-	chl, act
77/907b	77/907b	Long Pt	Y	T	plag 3 - 5 mm	vcgr	ophitic	S	P			-	chl, act
FLD4	R006528	ESE of Stanley Pt	Y	A	ol ≤ 1.5 mm	f-mgr	intergranular/ seriate	S	P	m		-	ksp?
R014365	R014365	ESE of Stanley Pt	Y	A	ol ≤ 1 mm, alt; plag ≤ 1mm	mgr	intergranular/ seriate	S	F	m			ksp?
BA3	R011908	Apple Orchard Pt	Y	C	plag ≤ 0.6 mm; cpx; ol? (alt)	fgr	microporphyritic (vfgr mesostasis)	S	S			-	chl, ksp?
BA5	R011910	Riddles Bay	Y	T	plag ≤ 3 mm (sparse); ol (?)	m-cgr	ophitic	S	S			-	chl, act, prehnite, cc
BA6	R011911	Riddles Bay	Y	C	-	mgr	consertal/ subophitic	M	P	m		m	chl, ep, act, cc
BA4	R011909	Nautilus Cove	Y	C	-	fgr	intergranular	M	A			c	chl, act?

TABLE 3 Summary of petrography (continued)

Field No.	Other ID	Locality	CA	Type	Phenocrysts	Groundmass		Mineralogy					
						Grain size	Texture	Plag	Cpx	hbl	bte	Q	Other
BA35	R011928	SE of Puncheon Pt	Y		hbl ≤ 7mm; plag ≤ 2mm; ol; titanite	m-cgr	seriate	S	-	ab	m	ab	ksp
R014343	R014343	Cone Point			-	f-mgr	intergranular/ seriate	S	P	M		-	altered olivine(?)
R014344	R014344	E dyke, Cape Sir John			-	m-c-gr	subophitic	S	M			-	act
R014345	R014345	W dyke, Cape Sir John			-	m-gr	subophitic/ intergranular	S	M			-	chl
26	43940	SE of Puncheon Pt			hbl ≤ 3mm; plag ≤ 2mm	f-mgr	seriate	P	-	ab	ab	c	act, chl
43933	43933	east of The Settlement			-	mgr	intergranular	S	P			-	sericite, prehnite, act
43934	43934	Thunder & Lightning B			-	cgr	subophitic	M	A			-	chl
43935	43935	Whittling Office Bay			qtz xenos ≤ 2.5mm; ol(?)	fgr	intergranular	P	P			m	act, chl
43936	43936	Battery Bay			plag ≤ 2.5mm; cpx (?)	mgr	seriate/ intergranular	P	P			c	chl, act
43937	43937	Petticoat Ridge			ol (after ol?); plag ≤ 3.5 mm	cgr	ophitic	S	S			-	chl, act
43938	43938	near Dyas Ck (?)			chl (after ol) ≤ 3.5mm; plag ≤ 3mm	m-cgr	subophitic	S	P			-	chl, act
43939	43939	Dover Point (?)				mgr	consertal/ subophitic	M	P			m	chl, act, ep?
43941	43941	Phils Hill (?)			plag ≤1mm; ol (chl); qtz xenos	f-mgr	intergranular	P	P			m	act, chl
43948	43948	E Long Is			-	cgr	consertal	P	P			m	
43949	43949	W Long Island			plag ≤ 4mm	m-cgr	ophitic/seriate	P	S			-	prehnite
43951	43951	W Clarke Is			plag ≤ 2mm; cpx ≤ 1mm	vfgr	microporphyritic (vfgr mesostasis)	P	S		c	-	act, chl
43952	43952	Kangaroo B, Clarke Is			qtz xenos ≤ 5mm; plag ≤ 0.6mm	fgr	feldspathic, turbid, minor cpx	M	P			-	ch, ep
43953	43953	Kangaroo B, Clarke Is			plag ≤ 2mm	fgr	plag laths, vfgr mesostasis	S	P			-	
77/910	77/910	Mt Chappell Is	Y	A	-	cgr	consertal	M	P			m	chl, act. ep
43966	43966	E Badger Is			-	mgr	intergranular/ subophitic	M	S			m	ep, chl
43967	43967	E Badger Is			-	f-mgr	intergranular/ subophitic	M	S			-	chl
43968	43968	E Badger Is			plag ≤ 3mm, sparse	fgr	intergranular	P	S			-	chl
43969	43969	W Badger Is			-	m-cgr	consertal/ intergranular	P	P			m	chl, act
43970	43970	S of Lucy Pt			-	m-cgr	consertal	M	S			tr	chl, act, ep
43972	43972	Lucy Pt, Badger Is			-	m-cgr	consertal	M	S			tr	chl, act, ep

T- tholeiitic, A- alkalic, C- contaminated, F- fresh, S- slightly altered, P- partly altered, M- mostly altered, A- completely altered, T- tholeiitic, A- alkalic, C- contaminated, F- fresh, S- slightly altered, P- partly altered, M- mostly altered, A- completely altered, f- fine-grained, m- medium-grained, c- coarse-grained, Q, Qtz- quartz, plag- plagioclase, ksp- K feldspar, ab- abundant, c- common, m- minor, r- rare, tr- trace, cpx- clinopyroxene, hbl- hornblende, act- (tremolite)-actinolite, bte- biotite, chl- chlorite, ep- epidote, cc- calcite.

TABLE 4 Semi-quantitative X-ray diffraction results

			Approximate wt%						
Field No	**Reg No**	**Rock type**	**35–50%**	**25–35%**	**15–25%**	**10–15%**	**5–10%**	**2–5%**	**<2%**
MNET 5	R001067	andesite		Chl	Quartz, Plag		Cpx, Amph	Kspar, Mica[1]	Ilm
MNET 11	R001073	andesite		Plag	Chl, Amph, Quartz		Cpx	Kspar	Ilm, Mica
MNET 12	R001074	andesite		Plag	Chl, Quartz, Amph		Cpx	Kspar	Mica, Ilm
MNET 14	R001076	andesite		Chl, Plag	Quartz, Amph		Cpx	Kspar	Mica, Ilm
MNET 16	R001078	dolerite		Chl, Plag	Amph	Cpx			Ilm, Quartz, Mica
Previous Results (Recalculated):									
MNET 2	R001064	dolerite	Plag	Chl		Amph	Cpx	Ilm	Quartz, Mica
MNET 4	R001066	dolerite		Plag, Chl		Amph	Cpx	MicaT, Ilm, Calcite	
MNET 9	R001071	andesite		Chl	Plag, Quartz	Amph	Cpx		Ilm, Kspar, Mica
MNET 10	R001072	dolerite	Plag		Chl	Cpx	Amph	Ilm, Quartz	Mica, ? [2]

[1] Trioctahedral; [2] very small peak at 12.1Å; possible mixed-layer mineral?
Peak overlap may interfere with identifications (e.g., clinopyroxene and K-Feldspar) and quantitative calculations.
Amorphous material (e.g. organic material; hydrous iron oxides) and minerals present in trace amounts may not be detected.
Plag- plagioclase, Cpx- clinopyroxene, Chl- chlorite, Amph- amphibole, Kspar- K- Feldspar, Ilm- ilmenite
Analyst: R.N. Woolley, 14 September 2016.

TABLE 5a Electron microprobe analyses – clinopyroxene

Sample	LC1						NJ407					
Analysis	**1b**	**1d**	**2c**	**3a**	**4a**	**5b**	**1d**	**1e**	**2a**	**3b**	**4b**	**5d**
SiO_2	48.13	49.59	51.61	47.04	49.64	46.01	47.97	48.74	47.60	49.37	48.12	48.79
TiO_2	2.14	2.07	0.98	3.54	2.05	3.91	2.03	1.90	2.24	1.94	2.28	1.84
ZnO	<0.09	<0.09	<0.10	<0.10	<0.09	<0.09	<0.10	<0.10	0.09	<0.09	<0.10	<0.10
Al_2O_3	3.17	3.17	1.42	4.89	3.61	5.46	3.61	3.65	5.61	4.99	5.45	3.68
V_2O_3	0.13	0.10	0.10	0.21	0.13	0.23	0.10	0.09	0.12	0.11	0.14	0.11
Cr_2O_3	<0.06	<0.06	<0.05	0.24	<0.05	0.17	<0.06	<0.05	0.36	0.19	0.53	<0.06
FeO	9.32	9.27	13.23	11.05	12.14	11.69	13.15	13.27	9.43	9.72	9.73	12.62
NiO	<0.06	<0.06	<0.06	<0.06	0.07	<0.06	<0.06	<0.06	<0.06	<0.06	<0.06	<0.06
MnO	0.20	0.24	0.35	0.24	0.32	0.25	0.39	0.38	0.25	0.24	0.23	0.31
MgO	13.47	13.71	13.61	11.99	12.97	11.68	12.89	12.73	13.05	13.27	13.06	13.02
CaO	20.94	21.01	18.56	20.24	19.53	19.71	18.27	18.21	20.31	20.04	20.04	18.69
SrO	<0.05	<0.05	<0.05	<0.05	<0.05	<0.05	<0.06	<0.06	<0.06	<0.06	<0.05	<0.06
BaO	<0.06	<0.06	<0.06	<0.06	<0.06	<0.07	<0.06	<0.07	<0.06	<0.06	<0.06	<0.06
Na_2O	0.35	0.40	0.19	0.43	0.37	0.44	0.45	0.42	0.43	0.44	0.41	0.42
K_2O	<0.02	<0.02	<0.02	0.02	0.02	<0.02	0.03	<0.02	<0.02	<0.02	<0.02	<0.02
P_2O_5	<0.04	<0.05	0.04	<0.04	<0.06	0.05	<0.04	0.05	<0.04	<0.04	<0.05	<0.05
SO_3	<0.04	<0.04	<0.04	<0.04	<0.05	<0.05	<0.05	<0.05	<0.05	<0.04	<0.04	<0.05
Cl	<0.02	<0.02	<0.02	<0.02	<0.02	<0.02	<0.02	<0.02	<0.02	<0.02	<0.02	<0.02
F	<0.04	<0.04	<0.04	<0.04	<0.04	<0.04	<0.04	0.06	<0.04	<0.04	<0.04	<0.04
TOTAL	97.86	99.58	100.10	99.90	100.84	99.60	98.89	99.47	99.49	100.31	99.98	99.49
mineral formulae on the basis of 4 cations, 6 oxygens												
Si	1.838	1.860	1.947	1.780	1.855	1.752	1.830	1.852	1.788	1.839	1.801	1.847
Aliv	0.143	0.140	0.053	0.218	0.145	0.245	0.162	0.148	0.212	0.161	0.199	0.153
Alvi	–	–	0.010	–	0.014	–	–	0.015	0.036	0.058	0.041	0.011
Ti	0.061	0.058	0.028	0.101	0.058	0.112	0.058	0.054	0.063	0.054	0.064	0.052
V	0.004	0.003	0.003	0.006	0.004	0.007	0.003	0.003	0.004	0.003	0.004	0.003
Cr	–	–	–	0.007	–	0.005	–	–	0.011	0.006	0.016	–
Fe3	0.080	0.049	–	0.039	0.040	0.049	0.093	0.053	0.065	0.018	0.039	0.065
Fe2	0.218	0.242	0.418	0.311	0.340	0.324	0.327	0.369	0.231	0.284	0.266	0.335
Zn	–	–	–	–	–	–	–	–	0.003	–	–	–
Mn	0.006	0.008	0.011	0.008	0.010	0.008	0.012	0.012	0.008	0.008	0.007	0.010
Ni	–	–	–	–	0.002	–	–	–	–	–	–	–
Mg	0.767	0.767	0.765	0.676	0.723	0.663	0.733	0.721	0.731	0.737	0.729	0.735
Ca	0.857	0.844	0.750	0.821	0.782	0.804	0.747	0.742	0.817	0.800	0.804	0.758
Na	0.026	0.029	0.014	0.032	0.027	0.033	0.033	0.031	0.031	0.032	0.030	0.031
K	–	–	–	0.001	0.001	–	0.001	–	–	–	–	–
T (Si + Aliv)	1.981	2.000	2.000	1.999	2.000	1.997	1.992	2.000	2.000	2.000	2.000	2.000
M (rest)	2.019	2.000	1.999	2.001	2.000	2.003	2.008	2.000	2.000	2.000	2.000	2.000
Mg#	77.89	76.04	64.70	68.50	68.01	67.19	69.17	66.18	75.99	72.15	73.29	68.69

TABLE 5b Electron microprobe analyses – feldspar

Sample	LC1			LC1E (megacryst)		NJ407								MNET5				
Analysis	1c	1e	2b	R1/1	R1/2	1a	1b	3a	3c	4a	4c	6a	7a	2a	3a	4e	1a	4d
SiO_2	66.94	68.22	64.89	51.91	51.88	51.48	50.73	52.32	51.08	52.33	51.33	51.44	53.21	52.62	54.87	54.27	65.53	65.86
TiO_2	0.04	<0.03	<0.03	0.08	0.11	0.04	0.04	0.09	0.07	0.05	0.07	0.06	0.09	0.04	<0.03	<0.03	<0.03	<0.03
Al_2O_3	20.36	20.17	22.40	30.82	30.72	30.46	31.01	30.01	31.14	30.25	30.88	30.76	29.82	29.99	28.50	29.39	18.81	18.57
V_2O_3	<0.03	0.06	<0.03	nd	nd	<0.03	<0.03	<0.03	<0.03	0.03	<0.03	<0.03	<0.03	<0.03	<0.03	<0.03	<0.03	<0.03
FeO	0.70	0.29	<0.05	0.19	0.28	0.29	0.40	0.81	0.71	0.41	0.52	0.42	0.68	0.29	0.40	0.49	<0.05	0.09
MnO	<0.05	<0.05	<0.05	0.00	0.07	<0.04	<0.05	<0.05	<0.05	<0.05	<0.05	<0.05	0.07	<0.05	<0.04	<0.05	<0.05	<0.05
ZnO	<0.09	<0.09	<0.09	<0.09	<0.09	<0.09	<0.09	<0.09	<0.09	<0.09	<0.09	<0.09	<0.09	<0.09	<0.09	<0.09	0.12	<0.09
NiO	0.06	<0.05	<0.05	nd	nd	<0.06	<0.06	<0.06	<0.06	<0.06	<0.06	<0.06	<0.06	<0.06	<0.05	<0.06	<0.06	<0.06
MgO	0.44	0.04	<0.02	0.08	0.10	0.16	0.15	0.20	0.15	0.23	0.12	0.28	0.15	0.10	0.05	0.04	<0.02	<0.02
CaO	0.86	0.73	3.11	13.16	13.33	13.34	14.04	12.55	13.91	13.22	13.45	13.12	12.01	12.53	10.93	11.78	0.02	0.05
SrO	0.10	0.14	0.07	nd	nd	<0.05	0.07	<0.05	<0.05	0.06	0.07	<0.05	0.05	0.18	0.20	0.17	0.07	<0.05
BaO	<0.06	<0.06	<0.06	0.06	nd	0.06	<0.06	<0.06	<0.06	<0.06	<0.05	<0.06	<0.06	<0.06	<0.06	<0.06	0.29	0.27
Na_2O	10.87	11.05	9.93	3.85	3.89	3.92	3.28	4.16	3.49	3.91	3.77	3.80	4.61	4.03	5.11	4.74	0.59	0.55
K_2O	0.13	0.10	0.09	0.21	0.24	0.04	0.04	0.06	0.07	0.07	0.09	0.12	0.06	0.14	0.19	0.16	15.59	15.67
P_2O_5	<0.04	<0.04	<0.05	0.06	0.01	<0.04	<0.05	<0.04	<0.04	<0.04	<0.05	<0.05	<0.04	<0.04	<0.04	<0.05	<0.05	<0.05
Cl	<0.02	<0.02	<0.02	nd	nd	<0.02	<0.02	0.03	0.02	<0.02	<0.02	<0.02	<0.02	<0.02	<0.02	<0.02	<0.02	<0.02
TOTAL	100.49	100.80	100.48	100.41	100.63	99.77	99.75	100.23	100.64	100.55	100.29	100.01	100.75	99.91	100.24	101.05	101.04	101.08
cations on basis of 8 oxygens[1]																		
Si	2.951	2.970	2.845	2.36	2.35	2.354	2.325	2.389	2.328	2.376	2.341	2.350	2.411	2.395	2.480	2.440	2.995	3.007
Al	1.058	1.035	1.158	1.65	1.64	1.642	1.675	1.615	1.673	1.619	1.660	1.657	1.593	1.609	1.518	1.557	1.014	0.999
Ca	0.040	0.034	0.146	0.64	0.65	0.653	0.689	0.614	0.679	0.643	0.657	0.642	0.583	0.611	0.529	0.568	0.001	0.002
Sr	0.003	0.004	0.002	0.00	0.00	–	0.002	–	–	0.002	0.002	–	0.001	0.005	0.005	0.004	0.002	0.000
Ba	–	–	–	0.00	0.00	0.001	–	–	–	–	–	–	–	0.000	0.000	0.000	0.005	0.005
Na	0.929	0.933	0.844	0.34	0.34	0.348	0.291	0.368	0.309	0.344	0.333	0.336	0.405	0.355	0.447	0.413	0.052	0.049
K	0.007	0.006	0.005	0.01	0.01	0.002	0.003	0.003	0.004	0.004	0.005	0.007	0.003	0.008	0.011	0.009	0.909	0.913
Si+Al	4.009	4.005	4.003	4.00	4.00	3.996	4.000	4.004	4.000	3.995	4.001	4.007	4.004	4.003	3.998	3.998	4.009	4.006
R	0.979	0.976	0.997	0.99	1.00	1.004	0.985	0.986	0.992	0.993	0.997	0.986	0.993	0.979	0.993	0.995	0.970	0.969
An%	4.13	3.51	14.68	64.59	64.53	65.05	70.00	62.29	68.49	64.76	65.89	65.17	58.71	62.40	53.32	57.07	0.12	0.26
Ab%	94.86	95.53	84.66	34.18	34.10	34.63	29.55	37.38	31.10	34.68	33.40	34.11	40.82	36.28	45.06	41.57	5.38	5.05
Or%	0.75	0.59	0.49	1.23	1.37	0.22	0.26	0.33	0.40	0.39	0.52	0.72	0.33	0.85	1.08	0.92	93.76	94.20
other%	0.26	0.37	0.18	0.00	0.00	0.10	0.19	0.00	0.00	0.17	0.19	0.00	0.13	0.47	0.53	0.45	0.74	0.50

[1] Fe, Mn, Zn, Ti, Mg, Ni, P, V attributed to minor impurities and excluded.

TABLE 5c Electron microprobe analyses – biotite

Sample	NJ407		MNET5			MR136#
Analysis	1c	6b[1]	R1d	R2b	R4b	40
SiO_2	37.26	37.93	37.64	37.98	37.00	37.16
TiO_2	4.70	3.33	2.72	3.03	2.46	1.73
Al_2O_3	12.71	12.08	13.45	12.91	13.43	16.34
V_2O_3	0.09	0.07	0.06	0.05	0.09	nd
Cr_2O_3	<0.05	<0.06	<0.05	<0.05	<0.05	0.12
FeO	20.46	18.38	23.30	23.59	23.65	16.91
MnO	0.12	0.07	0.25	0.23	0.25	nd
ZnO	<0.09	<0.10	<0.10	0.15	<0.10	nd
NiO	0.06	<0.06	<0.06	<0.06	<0.06	nd
MgO	11.57	12.66	9.13	9.05	9.58	14.93
CaO	<0.02	1.13	0.04	0.04	0.08	0.48
BaO	0.11	<0.06	0.61	0.47	0.47	nd
Na_2O	0.21	0.09	<0.05	0.05	0.05	nd
K_2O	9.34	8.87	8.67	8.79	7.49	8.29
P_2O_5	<0.05	0.78	0.04	<0.05	<0.04	nd
SO_3	0.07	<0.05	<0.04	0.05	0.07	nd
Cl	0.09	0.33	0.43	0.48	0.37	nd
F	<0.04	0.09	0.23	0.23	0.24	nd
TOTAL	100.66	99.66	100.22	100.73	98.90	95.96
Cations on the basis of 10(O), 2(OH)						
Si	2.830	2.931	2.910	2.926	2.890	2.771
Al^{iv}	1.137	1.069	1.090	1.074	1.110	1.229
Alvi	–	0.031	0.135	0.099	0.127	0.208
Fe	1.299	1.188	1.506	1.520	1.545	1.055
Mn	0.008	0.004	0.016	0.015	0.016	–
Zn	–	–	–	0.009	–	–
Ti	0.268	0.193	0.158	0.175	0.144	0.097
V	0.005	0.004	0.004	0.003	0.005	–
Ni	0.004	–	–	–	–	–
Mg	1.309	1.459	1.052	1.040	1.116	1.660
Ba	0.003	–	0.018	0.014	0.014	–
Na	0.031	0.013	–	0.007	0.007	–
K	0.904	0.875	0.855	0.864	0.747	0.789
Cl	0.012	0.043	0.056	0.063	0.048	–
F	–	0.022	0.057	0.056	0.058	–
(OH)	1.988	1.935	1.887	1.880	1.893	–
T	3.967	4.000	4.000	4.000	4.000	4.000
M	2.893	2.879	2.872	2.861	2.953	3.019
A	0.939	0.888	0.873	0.885	0.768	0.789
Mg#	50.19	55.12	41.12	40.62	41.94	61.15

[1] Ca and P attributed to apatite inclusions and excluded.

from McClenaghan (1984).

TABLE 5d Electron microprobe analyses – chlorite

Sample	LC1		MNET5			
Analysis	**3b**	**4d**	**R1b**	**R1c**	**R2c**	**R4c**
SiO_2	28.41	28.10	28.16	25.89	25.88	26.15
TiO_2	0.06	<0.03	0.11	0.04	0.08	0.04
Al_2O_3	17.63	17.72	18.79	20.15	19.77	20.12
V_2O_3	<0.03	<0.03	<0.03	0.04	0.05	<0.03
Cr_2O_3	<0.06	<0.06	0.15	<0.05	<0.05	<0.05
FeO	25.63	26.14	28.52	28.68	29.14	29.17
MnO	0.34	0.31	0.48	0.46	0.43	0.38
MgO	16.39	16.11	12.32	12.78	12.57	12.41
CaO	0.10	0.09	0.90	0.05	<0.02	0.04
Na_2O	0.04	<0.05	0.08	<0.04	0.04	<0.05
K_2O	0.04	<0.02	0.07	<0.02	0.05	0.02
Cl	<0.02	0.02	<0.02	<0.02	<0.02	<0.02
F	0.05	<0.04	0.09	0.05	<0.04	<0.04
TOTAL	100.14	99.94	100.92	99.40	99.25	99.61
Cations based on 10 (O), 8(OH)						
Si	2.963	2.941	2.957	2.768	2.783	2.792
Al^{iv}	1.037	1.059	1.043	1.232	1.217	1.208
Al^{vi}	1.130	1.127	1.284	1.308	1.287	1.324
Fe	2.235	2.287	2.505	2.565	2.619	2.604
Mn	0.030	0.028	0.043	0.041	0.039	0.034
Mg	2.547	2.514	1.928	2.037	2.014	1.975
Ca	0.011	0.011	0.101	0.006	-	0.004
Cl	-	0.024	-	-	-	-
F	0.109	-	0.029	0.016	-	-
(OH)	7.891	7.976	7.971	7.984	8.000	8.000
Total cations	9.954	9.966	9.873	9.960	9.963	9.942
Mg#	53.26	52.36	43.50	44.26	43.47	43.14

TABLE 5e Electron microprobe analyses – amphibole

Sample	LC1[1]	NJ407	MNET5	MR136[2]	
Analysis	4b	5g	4a	36	37
SiO_2	52.17	55.65	45.07	47.57	49.19
TiO_2	0.06	<0.03	0.91	0.51	0.58
Al_2O_3	2.01	1.43	6.57	8.33	6.45
V_2O_3	<0.03	0.03	0.08	nd	nd
Cr_2O_3	0.07	<0.06	<0.06	0.25	0.23
FeO	20.06	9.93	27.94	14.25	16.92
MnO	0.33	0.12	0.31	-	0.27
MgO	10.59	17.90	5.87	13.88	14.88
CaO	12.33	12.80	8.75	10.66	7.63
Na_2O	0.16	0.25	1.28	1.26	0.85
K_2O	0.07	0.04	0.33	0.18	0.14
P_2O_5	0.55	<0.04	<0.05	nd	nd
SO_3	0.04	<0.04	0.07	nd	nd
Cl	<0.02	<0.02	0.17	nd	nd
F	0.08	<0.04	0.16	nd	nd
TOTAL	100.49	100.27	99.31	96.89	97.14
Cations based on 22(O), 2(OH); minimum Fe					
	all ferrous	all ferrous	all ferrous	15eNK	15eNK
Si	7.815	7.855	7.080	6.996	7.223
Al^{iv}	0.185	0.145	0.920	1.004	0.777
Al^{vi}	0.171	0.094	0.296	0.439	0.340
Ti	0.007	–	0.108	0.056	0.064
Cr	0.008	–	–	0.029	0.027
V	–	0.004	0.010	nd	nd
Fe3	–	–	–	0.030	0.014
Mg	2.365	3.766	1.374	3.043	3.257
Fe2 (C]	2.450	1.136	3.212	1.402	1.298
Fe2 (B)	0.063	0.036	0.458	0.320	0.766
Mn (B)	0.042	0.014	0.041	–	0.034
Ca (B)	1.863	1.936	1.473	1.680	1.200
Na (B)	0.033	0.014	0.029	–	–
Na (A)	0.013	0.055	0.362	0.359	0.242
K (A)	0.013	0.006	0.066	0.034	0.026
Cl	–	–	0.045	nd	nd
F	0.040	–	0.078	nd	nd
T sites	8.000	8.000	8.000	8.000	8.000
C sites	5.000	5.000	5.000	5.000	5.000
B sites	2.000	2.000	2.000	2.000	2.000
A sites	0.025	0.061	0.428	0.393	0.268
Mg#	48.48	76.27	27.24	63.85	61.21

[1] LC1: P attributed to apatite and stoichiometric Ca subtracted

[2] from McClenaghan (1984)

TABLE 5f Electron microprobe analyses – other

	Olivine	Epidote	Prehnite
Sample	NJ407	LC1	LC1
Analysis	5a	2a	4c
SiO_2	39.82	38.11	43.51
TiO_2	0.03	0.06	<0.03
Al_2O_3	0.05	28.37	24.41
V_2O_3	<0.03	<0.03	0.04
FeO	16.02	7.16	1.31
NiO	0.09	<0.06	0.07
MnO	0.23	0.22	0.05
MgO	44.65	0.03	0.59
CaO	0.26	23.76	26.03
SrO	<0.05	0.18	<0.05
F	<0.04	0.06	<0.04
TOTAL	101.14	97.95	96.01
Cations on the basis of:			
	4(O)	12(O),(OH)	10(O),2(OH)
Si	0.994	2.955	2.988
Ti	0.001	0.003	–
Al	0.001	2.592	1.975
V	–	–	0.002
Fe^3	–	0.464	–
Fe^2	0.334	–	0.075
Mn	0.005	0.015	0.003
Ni	0.002	–	0.004
Mg	1.661	0.004	0.060
Ca	0.007	1.973	1.915
Sr	–	0.008	–
F	–	0.016	–
Total cations	3.005	8.014	7.023
Mg#	83.25		

TABLE 6. Whole rock chemical analyses (XRF)

Region	EAST COAST DYKES										
	Maria Is	Freycinet Peninsula									
Locality	Stinking Ck	Lagunta Creek		Graham Ck	Mt Freyc't	South Wineglass Bay		Hawksnest Cove		Carp Bay	
Field No.	SMD	LC1	LC3	FY30	FY31	FP4	NJ475	FY32	FP1	FP21	NJ476
other ID	R004379	R004436	R004438	R004464	R004465	73-542	R014324	R004466	73-541	73-544	R014325
Analysis No	20040097	910748	910749	20010133	20010134	735804	20130001	20010135	735803	735806	20130002
Type	C	A	A	C	C	T	T	C	C	A	A
SiO2 (%)	51.44	45.52	44.58	54.42	52.88	48.87	47.78	58.71	58.90	48.09	47.35
TiO2	1.45	2.89	2.61	1.26	1.95	1.34	1.40	0.88	0.90	2.74	2.76
Al2O3	17.12	14.99	15.25	15.53	14.42	17.36	17.58	14.95	14.50	14.69	14.70
Fe2O3	1.10	2.39	3.12	1.26	2.87	*8.90	*9.42	0.75	*6.70	2.25	*12.30
FeO	7.66	10.13	8.88	6.60	7.95	nd	nd	5.06	nd	8.80	nd
MnO	0.15	0.21	0.20	0.13	0.18	0.15	0.15	0.11	0.11	0.19	0.20
MgO	5.56	7.05	7.25	5.40	4.75	7.57	8.29	5.26	4.80	6.56	6.65
CaO	9.26	8.59	8.25	7.00	7.60	9.84	9.86	6.30	6.40	8.67	8.76
Na2O	2.90	3.79	3.60	3.09	2.40	2.42	2.57	2.88	2.80	3.07	2.90
K2O	0.96	1.24	0.98	1.97	2.01	0.54	0.59	2.78	2.50	1.61	1.29
P2O5	0.39	0.86	0.76	0.32	0.55	0.14	0.15	0.38	0.34	0.79	0.80
H2O+	1.83	3.31	3.37	2.49	1.94			1.66		2.06	
H2O-											
CO2	0.05	0.07	0.06	0.34	0.28		<0.35	0.09		0.10	<0.35
SO3	0.01	0.03	0.04	0.05	0.04	0.01		0.04		0.02	
LOI						2.71	1.68		1.60		1.68
TOTAL	99.88	101.07	98.95	99.87	99.82	99.85	99.47	99.84	99.55	99.65	99.39
LOI2	1.03	2.26	2.44	2.10	1.33			1.19		1.19	
FeOt	8.65	12.28	11.69	7.74	10.53	8.01	8.48	5.74	6.03	10.83	11.07
Mg#(0.20)	57.48	54.70	56.61	59.50	48.66	66.54	67.29	65.84	62.60	56.03	55.83
Li (ppm)									60		
F (ppm)											
S (%)	0.0			0.0	<0.01		0.1	0.0			0.1
Cl (ppm)	560	480	890	30	70	160	0	700		270	0
Sc	29	27	19	23	30	34	34	23		33	33
V	183	237	178	160	180	240	230	170		260	280
Cr	220	54	40	165	105	160	nd	230		170	180
Co	28	43	42	28	28	43	47	23	25	43	40
Ni	44	50	52	54	35	80	100	36	41	66	64
Cu	8	27	20	32	36	55	49	44	16	69	42
Zn	149	117	92	87	150	69	84	110	101	160	150
Ga	19	20	19	20	22	18	18	17		21	21
As	5	3	7	<3	4	<3	4	6	<10	4	9
Rb	31	66	52	82	71	86	115	155	146	110	92
Sr	485	338	363	240	195	240	270	530	481	750	780
Y	31	44	36	41	58	34	45	23	23	42	41
Zr	163	350	285	250	820	115	120	180	171	310	310
Nb	8	16	13	11	26	4	4	13		18	18
Mo	<1	3	2	1	9	<1	<1	<1		3	2
Sn	8	3	1	<2	<2	<2	2	2	13	41	93
Sb	<2	<2	<2	<2	<2	<2	<2	<2		<2	<2
Cs	5	6	7	5	7	26	<3	13		55	<3
Ba	381	282	275	390	380	60	48	1050		710	620
La	17	35	30	34	65	20	30	46		99	51
Ce	40	67	59	75	120	17	54	86		115	105
Nd	24	39	34	44	65	19	29	38		68	58
W	<2	<2	3	2	<2	2	<2	2		<2	<2
Pb	13	3	1	13	12	3	<2	11	17	10	9
Bi	2	2	3	1	2	1	1	1		2	2
Th	<2	<2	<2	11	9	<2	<2	16		2	2
U	<1	1	1	4	4	2	1	6		1	2
Partial CIPW norms at Fe2O3/FeO = 0.20											
Q	2.00	-	-	4.89	6.61	-	-	10.11	12.29	-	-
C	-	-	-	-	-	-	-	-	-	-	-
ne	-	4.43	3.06	-	-	-	-	-	-	-	-
hy	19.33	-	-	19.17	19.64	21.30	10.64	16.69	15.69	7.79	11.77
ol	-	17.84	19.37	-	-	1.99	11.28	-	-	10.03	8.07

[1] total iron as Fe2O3; Mg#(0.20)- molar 100*Mg/(Mg + Fe^{II}) calculated at Fe2O3/FeO = 0.20; FeOt- total iron as FeO; nd- not determined

TABLE 6. Whole rock chemical analyses (XRF) (continued)

	EAST COAST DYKES									
Region	**Freycinet Peninsula**						**Bicheno area**			
Locality	**Sleepy Bay**	**Cape Tourville Rd**		**Bluestone Bay**		**F'water Lag**	**Cape Lodi**	**Bicheno blowhole**		**Governor Is**
Field No.	**FP22**	**FP24**	**NJ477**	**FP11**	**NJ478**	**NJ438**	**NJ441**	**BD1B**	**BD2A**	**B1**
other ID	**73-545**	**73-546**	**R014326**	**73-543**	**R014327**	**R013353**	**R013370**	**R004446**	**R004447**	**73-604**
Analysis No	**735807**	**735808**	**20130003**	**735805**	**20130004**	**20080419**	**20080421**	**991036**	**991037**	**736628**
Type	**C**	**A**	**A**	**C**	**C**	**A**	**A**	**A**	**A**	**A**
SiO2 (%)	60.30	47.82	47.23	51.86	50.32	47.63	48.52	46.44	47.30	48.45
TiO2	0.80	2.40	2.37	2.41	2.49	3.00	2.26	2.32	2.36	2.28
Al2O3	14.80	15.38	15.21	15.20	15.08	15.00	15.06	15.48	15.73	15.38
Fe2O3	*6.40	2.32	*11.34	1.85	*12.21	4.12	1.57	1.39	1.56	1.73
FeO	nd	8.30	nd	8.70	nd	8.70	9.10	9.02	8.90	8.30
MnO	0.10	0.17	0.18	0.17	0.18	0.24	0.18	0.18	0.16	0.16
MgO	4.40	7.39	7.57	4.72	5.32	5.73	6.65	7.28	7.20	6.66
CaO	5.60	9.44	9.39	7.36	7.91	7.20	6.03	9.11	7.12	7.66
Na2O	3.40	2.86	2.76	3.17	3.08	3.24	3.00	2.85	3.87	3.61
K2O	2.10	1.11	1.43	1.99	1.94	0.93	2.70	0.84	0.85	1.00
P2O5	0.27	0.68	0.67	0.55	0.52	0.64	0.08	0.43	0.44	0.42
H2O+		1.97		1.85		2.97	3.62	4.33	4.23	3.87
H2O-										
CO2		0.10	<0.35	0.10	<0.35	0.20	0.60	0.07	0.05	0.40
SO3		0.03		0.01		0.02	0.01	0.09	0.17	0.01
LOI	1.50		1.20		0.45					
TOTAL	99.67	99.97	99.35	99.95	99.50	99.63	99.39	99.85	99.95	99.92
LOI2		1.15		0.99		2.21	3.21	3.40	3.29	3.34
FeOt	5.85	10.39	10.20	10.37	10.99	12.41	10.51	10.27	10.31	9.86
Mg#(0.20)	61.27	59.94	60.94	48.91	50.46	49.27	57.08	59.87	59.52	58.70
Li (ppm)	58									
F (ppm)										
S (%)			0.0		<0.02	0.0	0.0			
Cl (ppm)		270	300	670	300	80	190	330	310	170
Sc		32	32	30	29	25	22	24	22	26
V		240	240	240	250	205	168	180	181	185
Cr		250	270	21	23	44	210	230	220	185
Co	19	43	42	38	40	44	37	42	43	42
Ni	52	83	86	30	33	40	53	68	67	62
Cu		26	26	25	26	25	26	30	35	28
Zn	130	110	135	145	135	124	96	100	106	105
Ga		20	19	22	23	23	20	19	18	19
As	<10	3	6	3	10	5	4	7	6	4
Rb	180	34	105	105	95	51	287	82	71	69
Sr	408	760	720	430	430	449	255	230	311	330
Y	22	34	33	42	44	43	35	36	39	38
Zr	399	250	260	350	350	328	252	234	255	280
Nb		15	14	16	18	14	10	10	11	13
Mo		2	1	3	2	3	<1	1	1	1
Sn	11	<2	14	6	2	1	2	<2	1	3
Sb		<2	<2	<2	<2	<2	<2	<2	<2	<2
Cs		6	<3	62	<3	2	12	6	6	8
Ba		590	590	460	430	267	230	111	219	175
La		48	63	88	47	26	23	16	20	27
Ce		90	95	88	82	64	40	39	52	57
Nd		55	51	49	46	39	26	25	28	30
W		<2	<2	<2	2	<2	<2	<2	1	<2
Pb	11	6	9	16	16	3	3	<2	3	6
Bi		3	2	2	2	3	2	1	3	2
Th		2	<2	4	2	<2	<2	<2	<2	<2
U		1	1	2	<1	3	2	1	1	<1
Partial CIPW norms at Fe2O3/FeO = 0.20										
Q	13.34	-	-	2.07	-	-	-	-	-	-
C	-	-	-	-	-	-	-	-	-	-
ne	-	-	-	-	-	-	-	-	-	-
hy	15.52	8.95	4.61	18.43	16.85	20.48	5.88	7.98	2.53	9.19
ol	-	10.53	13.75	-	2.03	3.37	14.23	11.81	17.37	10.16

TABLE 6. Whole rock chemical analyses (XRF) (continued)

Region	EAST COAST DYKES										
	St Helens area										
Locality	Arm Creek		Dianas Basin	Onion Ck	St Helens Point		Grant Point			Roses Tier	Mt Scott
Field No.	B135	NJ480	NJ446	NJ447	SHP	37798	MSH172	37803	NJ508	R1084	SB27
other ID	R014210	R014329	R013375	R013376	C108645	265	R001907	266	R014359	R001084	R006211
Analysis No	20080226	20130005	20100105	20100106	20010257		850179	20040039	20160204	910631	20130175
Type	A	A	C	C	A	A	T	T	T	C	C
SiO2 (%)	48.86	48.49	53.13	53.27	49.11	48.84	51.99	52.00	52.57	57.95	49.35
TiO2	2.92	2.89	0.78	2.47	2.93	2.92	1.43	1.39	1.41	0.81	2.15
Al2O3	13.51	13.71	19.44	13.29	13.68	13.61	14.72	15.03	14.68	17.06	15.09
Fe2O3	3.27	*14.95	1.12	3.55	3.11	3.72	1.42	1.63	*10.20	2.42	*11.92
FeO	10.50	nd	5.70	8.20	10.32	10.04	8.07	7.66		5.49	nd
MnO	0.22	0.23	0.18	0.19	0.21	0.22	0.19	0.16	0.16	0.13	0.18
MgO	4.72	4.86	5.12	2.77	5.00	5.08	7.02	6.90	7.19	2.59	5.47
CaO	6.98	7.18	3.58	5.85	7.45	7.41	7.99	7.97	7.97	5.17	9.23
Na2O	3.15	2.92	4.15	3.45	3.19	3.18	2.67	2.86	2.76	4.89	2.08
K2O	1.70	1.70	4.17	2.33	1.30	1.28	1.21	1.19	1.36	1.95	0.60
P2O5	0.57	0.51	0.16	0.91	0.55	0.53	0.31	0.28	0.28	0.34	0.48
H2O+	3.05		1.88	2.63	2.63	2.63	2.50	2.47		0.59	
H2O-											
CO2	0.20	<0.35	0.10	0.80	0.23	0.15	0.22	0.28	0.55	0.09	1.47
SO3	0.04		<0.02	0.10	0.08	0.06		0.04		0.07	
LOI		1.93							0.94		1.93
TOTAL	**99.69**	**99.37**	**99.51**	**99.81**	**99.79**	**99.67**	**99.74**	**99.86**	**100.07**	**99.55**	**99.95**
LOI2	2.08		1.35	2.62	1.71	1.67		1.90	1.49	0.09	3.40
FeOt	13.44	13.45	6.71	11.39	13.12	13.39	9.35	9.13	9.18	7.67	10.73
Mg#(0.20)	42.48	43.18	61.63	33.83	44.50	44.39	61.23	61.39	62.23	41.54	51.75
Li (ppm)											
F (ppm)											
S (%)	0.1	0.2	0.04	<0.01	0.1			0.0	0.1	<0.01	0.1
Cl (ppm)	160	<100	200	300	270	330		160		70	0
Sc	29	29	33	29	31	34	23	25	21	13	33
V	336	370	165	270	337	384	230	215	195	125	230
Cr	11	17	250	1	15	21	330	270	260		nd
Co	42	45	29	29	38	42	40	35	37	17	35
Ni	16	21	49	4	17	20	130	129	135	76	39
Cu	11	12	8	15	12	19	31	44	38	42	24
Zn	145	155	430	130	112	131	97	101	96	66	135
Ga	21	24	20	22	22	23	17	18	19	17	21
As	5	5	<3	6	7	4	10	8	3	6	5
Rb	72	84	250	84	48	52	67	69	72	38	28
Sr	463	520	660	290	408	424	280	294	290	520	280
Y	48	47	23	50	45	46	33	36	33	16	41
Zr	222	230	145	200	215	221	145	166	155	141	320
Nb	9	10	9	12	8	9	7	9	10	9	13
Mo	1	1	<1	<1	1	1	<2	<1	<1	2	1
Sn	2	2	7	<2	2	2	<4	<2	<2	<2	2
Sb	<2	<2	<2	<2	<2	<2		<2		<2	<2
Cs	4	<3	29	<3	5	3		11		3	15
Ba	420	440	770	360	455	452	290	238	240	620	195
La	27	25	41	34	27	28	9	21	23	37	30
Ce	60	64	38	64	57	60		42	38	73	51
Nd	34	41	23	50	35	35		23	24	29	29
W	1	<2	<2	<2	1	<2		1	<2	14	<2
Pb	3	3	63	10	3	4	17	6	7	5	5
Bi	4	3	1	2	3	4	<5	1	<1	<1	2
Th	1	<2	7	3	1	<2	5	2	4	8	2
U	3	2	5	3	2	1	6	1	2	3	1
Partial CIPW norms at Fe2O3/FeO = 0.20											
Q	-	-	-	*6.78*	*0.36*	-	*2.90*	*2.14*	*2.40*	*4.67*	*5.90*
C	-	-	*2.02*	-	-	-	-	-	-	-	-
ne	-	-	-	-	-	-	-	-	-	-	-
hy	*20.90*	*21.93*	*0.19*	*16.01*	*21.40*	*21.78*	*24.25*	*23.61*	*23.84*	*14.47*	*21.43*
ol	*0.56*	*0.24*	*15.79*	-	-	*0.19*	-	-	-	-	-

TABLE 6. Whole rock chemical analyses (XRF) (continued)

	TEBRAKUNNA DYKE SWARM										
Region	**Pyengana area**			**Blue Tier area**						**Fraser Road area**	
Locality	N George R	Waratah Ck	Crowther Ck	Weldborough Pass		Mt Paris Rd	Rocky Ck	Cascade R	Spinel Ck		
Field No.	**AJ807**	**AJ914**	**NJ455**	**NJ454**	**JR66**	**MR136**	**JR65**	**MR30**	**MR146**	**BT30**	**BT22**
other ID	R004327	R004328	R013384	R013383		72/437		72/393	74/461A		
Analysis No	910743	910744	20100111	20100110	742538	741647	742537	735113	741650	783154	783151
Type	T	T	T	T	T	T	T	T	T	T	T
SiO2 (%)	48.16	48.72	50.14	49.30	48.80	47.10	49.80	48.50	48.40	47.90	47.60
TiO2	2.16	2.19	3.11	3.28	3.10	1.50	1.40	2.80	1.20	3.10	2.00
Al2O3	15.44	15.20	14.17	14.13	14.10	18.20	16.10	14.40	16.90	12.90	15.00
Fe2O3	2.19	2.44	1.92	3.05	1.80	1.50	1.80	1.70	2.00	2.20	3.00
FeO	9.40	8.94	11.30	10.60	12.10	8.40	8.20	11.80	7.30	11.90	8.70
MnO	0.21	0.22	0.22	0.23	0.24	0.19	0.20	0.23	0.16	0.26	0.20
MgO	6.19	5.86	4.67	4.92	5.40	8.10	7.60	5.10	8.10	6.10	7.30
CaO	10.40	10.79	8.44	8.42	9.00	9.90	10.10	8.50	10.70	8.40	9.10
Na2O	2.59	2.97	2.92	2.61	2.70	2.50	2.60	2.40	2.50	2.70	2.80
K2O	0.52	0.60	0.65	0.81	0.65	0.53	0.28	1.20	0.29	0.47	0.65
P2O5	0.33	0.33	0.61	0.60	0.63	0.32	0.22	0.39	0.15	0.70	0.30
H2O+	2.60	2.22	1.50	1.96	1.50	1.60	1.80	2.00	2.00	3.20	3.50
H2O-								0.47	0.27	0.28	0.39
CO2	0.21	0.29	<0.1	0.10							
SO3	0.02	0.02	0.22	<0.02							
LOI											
TOTAL	**100.42**	**100.79**	**99.87**	**100.01**	**100.02**	**99.84**	**100.10**	**99.49**	**99.97**	**100.11**	**100.54**
LOI2	1.77	1.52	0.47	0.88							
FeOt	11.38	11.14	13.02	13.35	13.72	9.75	9.82	13.33	9.10	13.88	11.40
Mg#(0.20)	53.37	52.54	42.99	43.67	45.29	63.60	61.95	44.59	65.18	48.04	57.39
Li (ppm)					40	20	25	40	30	20	32
F (ppm)					1200		1200				
S (%)			0.09	0.09							
Cl (ppm)	110	110	200	300	200		200				
Sc	36	38	42	42							
V	280	301	300	310							
Cr	102	119	41	39							
Co	42	42	47	35	41		39			43	39
Ni	47	49	21	21	53	97	44	58	48	33	50
Cu	21	22	31	34	13		69	33	12		
Zn	95	98	185	150	214	129	165	235	104	172	121
Ga	21	21	25	24							
As	7	5	<3	4							
Rb	42	53	48	50	40	27	27	155	27	23	39
Sr	257	283	310	280	286	167	249	265	160	282	260
Y	37	38	55	57	55	30	32	60	59	50	37
Zr	146	155	310	300	264	215	90	215	26	363	132
Nb	6	7	14	15	15		6			16	
Mo	<1	<1	2	2							
Sn	1	1	3	4	15		31	8	36		5
Sb	<2	<2	<2	<2							
Cs	4	6	17	39							
Ba	141	172	200	240							
La	5	6	42	62							
Ce	21	22	69	63							
Nd	16	19	39	39							
W	2	2	<2	<2							
Pb	<2	1	5	6							
Bi	3	2	4	3							
Th	<2	<2	<2	2							
U	2	<1	2	2							
Partial CIPW norms at Fe2O3/FeO = 0.20											
Q	-	-	*4.25*	*3.98*	*1.83*	-	-	*1.76*	-	*1.83*	-
C	-	-	-	-	-	-	-	-	-	-	-
ne	-	-	-	-	-	-	-	-	-	-	-
hy	*16.92*	*9.29*	*19.80*	*21.07*	*21.87*	*9.75*	*22.68*	*21.96*	*13.49*	*24.72*	*13.58*
ol	*2.66*	*5.89*	-	-	-	*13.51*	*1.29*	-	*8.24*	-	*8.75*

TABLE 6. Whole rock chemical analyses (XRF) (continued)

	TEBRUKUNNA DYKE SWARM										
Region	**Tebrakunna Rd area**				**Ansons Bay-Ansons River area**						
Locality					Bark Hut F	Sampsons	Pretty Marsh		Kangaroo F	Spurrs Rvt	W Gripe Ck
Field No.	**BT28**	**BT31**	**MNET36**	**MNET38**	**MBT44**	**MBT74**	**MNET13**	**MBT71**	**MBT132**	**MBT30**	**MBT76**
other ID			R001098	R001100	75/579	75/856	R001075	75/845	76/858	75/512	75/858
Analysis No	783153	783155	20080233	20080234	20080319	760573	20080231	760570	20080334	20080318	20080325
Type	T	T	T	T	C	A	T	T	T	T	T
SiO2 (%)	48.00	48.60	48.07	50.02	51.63	46.00	48.78	48.70	48.74	47.66	48.20
TiO2	1.70	2.10	1.64	3.17	2.32	2.20	1.95	1.80	1.94	2.28	2.38
Al2O3	15.20	15.00	15.82	13.55	14.66	14.90	15.26	15.50	14.99	14.63	14.77
Fe2O3	3.70	1.50	4.06	2.18	1.78	2.50	3.08	2.90	1.97	4.03	4.14
FeO	7.80	9.30	7.20	10.60	10.40	9.70	8.30	8.30	9.30	8.10	8.70
MnO	0.19	0.19	0.21	0.22	0.20	0.23	0.19	0.21	0.20	0.20	0.21
MgO	7.40	6.70	6.89	4.23	4.72	6.70	6.47	6.30	6.35	6.39	6.15
CaO	10.40	9.20	10.16	7.97	7.11	9.30	9.09	9.00	9.01	9.18	8.77
Na2O	2.50	2.20	2.76	2.91	2.91	3.20	3.16	3.00	3.12	2.72	3.27
K2O	0.14	0.65	0.21	1.00	1.15	0.55	0.49	0.63	0.64	0.76	0.32
P2O5	0.24	0.47	0.25	0.83	0.66	0.23	0.44	0.45	0.42	0.40	0.30
H2O+	2.80	3.00	2.36	2.95	2.10	3.10	2.58	2.50	2.96	3.39	2.73
H2O-	0.30	0.36									
CO2			0.20	0.20	0.30	0.34	0.10	0.13	0.30	0.10	0.10
SO3			0.00	0.01	0.05		0.00		0.08	0.03	0.01
LOI											
TOTAL	**100.37**	**99.27**	**99.81**	**99.83**	**99.98**	**98.95**	**99.88**	**99.42**	**99.99**	**99.87**	**100.07**
LOI2			1.76	1.97	1.24		1.76		2.22	2.59	1.87
FeOt	11.13	10.65	10.86	12.56	12.00	11.95	11.07	10.91	11.07	11.73	12.43
Mg#(0.20)	58.31	56.96	57.16	41.48	45.28	54.11	55.16	54.85	54.66	53.40	51.02
Li (ppm)	36	38				25		15			
F (ppm)											
S (%)					0.2				0.1	0.0	0.0
Cl (ppm)			100	170	50		170		170	130	
Sc			27	34	34		26		28	30	34
V			214	267	230	340	240	300	266	306	323
Cr			140	25	57		125		140	135	96
Co	48	37	42	31	31	49	37	47	36	42	38
Ni	61	50	38	18	34	67	45	51	43	40	44
Cu			27	23	32		24		28	26	43
Zn	103	143	92	154	240	120	98	140	103	122	106
Ga			18	22	23		19		19	19	22
As			6	5	6		5		5	4	4
Rb	3	31	20	58	55	36	17	11	24	42	23
Sr	227	244	233	228	340	260	302	310	314	330	261
Y	41	41	32	47	57	33	33	35	35	36	38
Zr	122	291	115	209	650	130	162	160	165	158	155
Nb	8	12	6	16	20	4	12	15	11	12	6
Mo			<1	1	7		<1		<1	<1	<1
Sn			1	1	<2		<2		1	2	<2
Sb			<2	<2	<2		<2		<2	<2	<2
Cs			2	3	<3		2		3	4	1
Ba			105	284	360	110	168	230	162	221	113
La			9	23	33		17		18	19	8
Ce			24	62	72		46		45	45	25
Nd			15	31	43		25		21	29	21
W			<2	<2	<2		1		1	<2	1
Pb			<2	6	11		1		3	<2	6
Bi			2	3	3		3		3	2	4
Th			<2	1	4		<2		<2	<2	<2
U			1	2	1		1		1	2	1
Partial CIPW norms at Fe2O3/FeO = 0.20											
Q	-	*2.49*	-	*5.32*	*5.47*	-	-	-	-	-	-
C	-	-	-	-	-	-	-	-	-	-	-
ne	-	-	-	-	-	-	-	-	-	-	-
hy	*18.92*	*24.25*	*15.57*	*18.66*	*22.76*	*0.16*	*16.47*	*18.54*	*16.36*	*17.61*	*15.75*

TABLE 6. Whole rock chemical analyses (XRF) (continued)

	TEBRUKUNNA DYKE SWARM										
Region	Ansons Bay - Ansons River area										
Locality	Big Ck	S Pretty M	Boggy Ck	NE of Pretty Marsh		Gripe Creek headwaters			Near Big Ck	Gripe Ck	Pol'mans Pt
Field No.	**MNET10**	**NJ471**	**MBT143**	**MNET12**	**MBT165**	**MBT75**	**MBT77**	**MBT97**	**MBT98**	**MBT167**	**NJ511**
other ID	R001072	R014320	77/466	R001074	77/780	75/857	75/859	76/682	76/681	77/782	R014362
Analysis No	20080229	20110318	20080335	20080230	20080338	20080324	760574	20080330	20080331	20080339	20160206
Type	A	T	A	C	C	C	C	C	C	C	C
SiO2 (%)	47.76	47.65	47.98	57.99	58.63	57.54	57.80	57.44	57.07	63.97	55.00
TiO2	2.30	2.14	3.01	1.87	1.86	1.88	1.90	1.92	2.10	0.64	1.29
Al2O3	15.11	15.54	13.95	15.09	15.42	15.55	15.40	15.40	15.63	15.26	14.49
Fe2O3	3.92	*13.23	6.81	2.64	1.38	1.82	0.51	0.91	1.28	0.75	*9.32
FeO	8.60	nd	7.20	5.70	6.20	5.80	7.10	7.00	7.00	3.90	nd
MnO	0.21	0.21	0.23	0.15	0.13	0.15	0.14	0.15	0.15	0.08	0.14
MgO	6.50	6.56	3.70	2.88	2.94	3.14	3.10	3.10	3.24	2.55	6.16
CaO	8.55	8.91	8.33	5.79	6.17	6.79	6.50	6.72	6.93	5.66	7.49
Na2O	3.46	3.09	3.85	2.99	2.95	3.02	3.00	2.97	2.94	4.50	3.07
K2O	0.45	0.48	1.29	1.85	1.21	1.45	1.40	0.95	1.51	0.58	1.37
P2O5	0.30	0.27	0.69	0.47	0.56	0.58	0.64	0.57	0.56	0.12	0.31
H2O+	2.52		2.50	1.97	2.21	2.10	1.80	2.46	1.36	1.57	
H2O-											
CO2	0.20	<0.35	0.20	0.40	0.10	0.10	0.15	0.10	0.00	0.00	0.73
SO3	0.02	0.12	0.04	0.00	0.02	0.01		0.01	0.01	0.02	
LOI		1.79									0.56
TOTAL	**99.90**	**99.99**	**99.76**	**99.77**	**99.77**	**99.93**	**99.44**	**99.71**	**99.78**	**99.60**	99.93
LOI2	1.76	1.68	1.91	1.74	1.62	1.55		1.79	0.58	1.13	1.29
FeOt	12.13	11.90	13.33	8.07	7.44	7.43	7.56	7.82	8.15	4.57	8.39
Mg#(0.20)	53.00	53.68	36.85	42.86	45.41	47.05	46.31	45.49	45.54	53.98	60.71
Li (ppm)							35				
F (ppm)											
S (%)		0.1	0.1	<0.01	0.1	0.0		<0.01	0.1	0.1	0.1
Cl (ppm)	150	60	30	200	160	140		90	250	50	
Sc	31	31	24	24	22	23		24	25	19	27
V	294	280	340	165	150	155	86	155	165	130	170
Cr	88	90	<5	44	44	55		46	39	65	240
Co	40	48	41	21	27	23	16	20	24	17	34
Ni	46	59	23	20	29	26	29	23	23	21	105
Cu	55	56	130	7	36	17		8	21	12	45
Zn	70	105	220	120	170	100	100	99	110	55	105
Ga	21	22	25	22	22	22		21	22	17	19
As	7	<3	3	13	6	15		14	7	6	<3
Rb	35	29	61	99	47	61	49	31	140	26	54
Sr	268	270	530	550	610	640	550	610	640	380	310
Y	37	38	81	33	35	35	32	33	35	18	37
Zr	144	150	280	300	300	300	290	280	290	160	180
Nb	6	6	11	26	26	26	23	25	24	11	9
Mo	<1	<1	2	3	2	2		2	2	<1	<1
Sn	2	<2	3	<2	<2	4		2	<2	2	3
Sb	<2	<2	2	<2	<2	2		<2	<2	<2	
Cs	3	3	<3	8	6	<3		3	18	3	
Ba	147	165	460	510	520	350	500	310	380	270	380
La	9	14	47	39	39	35		35	45	19	19
Ce	23	28	105	78	85	78		80	81	47	45
Nd	23	15	56	37	48	44		44	41	19	20
W	2	2	<2	3	<2	<2		<2	2	3	<2
Pb	1	4	6	11	6	3		4	3	8	9
Bi	3	2	4	1	1	1		1	1	<1	<1
Th	<2	<2	<2	2	4	<2		2	<2	18	4
U	1	1	<1	2	1	<1		1	1	6	2
Partial CIPW norms at Fe2O3/FeO = 0.20											
Q	-	-	-	*15.38*	*18.14*	*14.81*	*15.85*	*16.67*	*13.72*	*19.45*	*6.01*
C	-	-	-	-	-	-	-	-	-	-	-
ne	-	-	-	-	-	-	-	-	-	-	-
hy	*8.57*	*12.18*	*3.67*	*14.82*	*14.70*	*13.66*	*14.40*	*14.81*	*14.28*	*9.01*	*20.44*
ol	*11.46*	*9.10*	*8.95*	-	-	-	-	-	-	-	-

TABLE 6. Whole rock chemical analyses (XRF) (continued)

	TEBRUKUNNA DYKE SWARM										
Region	**Mt William area**										
Locality	Purdon B	2.7 km E	3.7 km SSE	5 km S	2.5 km W	3 km NNE	E side of Mt William		W side	Upper Icena Creek	
Field No.	**NJ364B**	**NJ423**	**NJ262**	**ER2**	**EA11**	**63095**	**MW1**	**NJ245**	**MW2**	**ER1**	**NJ401**
other ID	R013304	R013317	R013280	73-636	85/262		73-634	R013279	73-633	73-635	R013312
Analysis No	20080286	20080225	20080200	736631	802656		736627	20080199	736628	736630	20080220
Type	C	T	T	A	T	T	T	T	C	T	T
SiO2 (%)	65.64	49.36	48.10	48.50	49.01	48.29	47.95	47.88	56.68	47.75	47.63
TiO2	0.48	3.03	3.05	2.96	1.84	0.98	1.05	0.96	0.49	1.48	1.43
Al2O3	16.76	14.50	13.64	14.34	15.77	18.83	18.23	18.61	19.04	18.25	18.33
Fe2O3	0.40	1.20	1.83	3.24	1.74	*8.61	1.27	1.24	0.46	2.03	1.79
FeO	2.90	11.80	11.90	10.90	9.24	nd	7.00	6.60	5.60	7.20	7.30
MnO	0.04	0.21	0.22	0.23	0.18	0.13	0.15	0.13	0.11	0.15	0.15
MgO	0.62	4.90	5.54	5.00	7.23	8.40	8.15	7.95	4.58	6.68	6.68
CaO	1.74	8.47	8.83	7.71	9.55	11.13	10.81	10.94	8.93	10.56	10.31
Na2O	3.14	3.47	2.80	3.43	2.24	2.38	2.78	2.42	2.58	2.88	3.04
K2O	6.50	0.62	0.87	0.96	0.34	0.61	0.19	0.72	0.20	0.59	0.25
P2O5	0.34	0.61	0.72	0.36	0.30	0.09	0.11	0.13	0.09	0.20	0.22
H2O+	0.90	1.55	1.55	2.30	2.38		2.31	2.02	1.22	2.34	2.58
H2O-					0.37						
CO2	0.10	0.00	0.10	0.20	0.26		0.10	0.00	0.10	0.10	0.10
SO3	0.01	0.01	0.02	0.06			0.03	0.04	0.01	0.02	0.04
LOI						1.61					
TOTAL	**99.57**	**99.72**	**99.16**	**100.19**	**100.45**	**101.06**	**100.14**	**99.62**	**100.09**	**100.23**	**99.85**
LOI2	0.67	0.24	0.32	1.29			1.64	1.29	0.70	1.64	1.87
FeOt	3.26	12.88	13.55	13.82	10.81	7.75	8.15	7.71	6.01	9.03	8.91
Mg#(0.20)	28.57	44.45	46.25	43.22	58.46	69.51	67.79	68.43	61.57	60.88	61.20
Li (ppm)											
F (ppm)											
S (%)	<0.01	0.1	0.0					0.1			0.1
Cl (ppm)	310	200	190	90			50	110	140	50	80
Sc	<9	41	41	39		29.9	29	26	22	27	27
V	14	284	289	400			190	164	165	220	189
Cr	<5	37	62	23	180		175	165	26	115	120
Co	3	66	45	66	50		42	40	21	40	37
Ni	<2	44	30	43	49		105	102	24	67	61
Cu	5	18	17	37	26		51	48	4	28	26
Zn	96	214	168	175	96		70	63	56	85	75
Ga	23	24	22	24	18		17	16	19	18	17
As	<3	6	6	10			<3	5	8	<3	3
Rb	330	25	50	40	14	99.7	14	93	8	29	10
Sr	145	361	280	280	222	216.4	210	214	550	350	345
Y	62	64	52	54	38	21.8	22	20	11	27	25
Zr	170	273	343	200	120	47.6	67	62	74	110	101
Nb	22	14	14	7	9	1.4	5	4	3	6	6
Mo	<1	2	2	<1			<1	<1	<1	<1	<1
Sn	7	2	3	<2	<12		<2	1	<2	2	<2
Sb	<2	<2	<2	<2			<2	1	2	<2	<2
Cs	13	<3	8	<3			7	45	4	16	7
Ba	960	250	310	200	123	65	58	66	76	115	83
La	100	26	38	14			7	32	<6	17	8
Ce	195	64	67	45			11	10	18	20	20
Nd	94	40	43	27			<7	4	7	13	14
W	<2	<2	<2	<2			<2	2	2	3	<2
Pb	48	5	5	6	12		3	3	2	2	<2
Bi	<1	4	4	3			1	2	<1	2	1
Th	62	1	<2	<2			<2	<2	2	<2	<2
U	13	2	2	2			1	1	<1	<1	<1
Partial CIPW norms at Fe2O3/FeO = 0.20											
Q	*15.95*	*0.30*	*0.39*	-	*1.49*	-	-	-	*12.59*	-	-
C	-	-	-	-	-	-	-	-	-	-	-
ne	-	-	-	-	-	-	-	-	-	-	-
hy	*8.18*	*19.59*	*21.88*	*15.07*	*25.88*	*6.47*	*5.86*	*5.83*	*17.96*	*3.78*	*6.27*
ol	-	-	-	*5.03*	-	*13.18*	*13.57*	*13.03*	-	*12.84*	*11.60*

TABLE 6. Whole rock chemical analyses (XRF) (continued)

	TEBRUKUNNA DYKE SWARM							
Region	Mt William area							
Locality	"Telegraph" area		Musselroe Rd quarry		Musselroe Road area			
Field No.	**NJ406**	**NJ407**	**MUS**	**MR1**	**NJ422**	**MR2**	**NJ420**	**MR3**
other ID	R013313	R013314	C108643	73-605	R013316	73-606	R013315	73-632
Analysis No	20080221	20080222	20010259	736624	20080224	736625	20080223	736626
Type	T	T	C	C	T	T	T	T
SiO2 (%)	48.56	47.23	51.20	52.83	47.60	47.77	48.63	48.10
TiO2	1.76	1.38	2.35	1.63	2.06	1.99	1.86	1.80
Al2O3	15.83	16.52	15.05	15.41	15.97	16.04	16.05	16.20
Fe2O3	1.27	1.66	1.02	1.05	1.22	0.94	0.81	*12.40
FeO	9.40	8.10	10.32	9.00	10.30	10.50	9.70	nd
MnO	0.19	0.17	0.18	0.17	0.21	0.25	0.19	0.18
MgO	6.79	8.58	4.68	5.13	7.01	6.84	7.17	7.10
CaO	9.92	10.42	7.31	7.85	9.22	9.27	9.69	9.30
Na2O	2.93	2.58	3.54	3.02	2.78	3.00	2.29	2.70
K2O	0.30	0.33	0.87	1.07	0.43	0.42	0.49	0.57
P2O5	0.27	0.19	0.62	0.41	0.32	0.28	0.37	0.35
H2O+	2.18	2.50	2.63	2.37	2.45	2.55	2.24	
H2O-								
CO2	0.50	0.20	0.08	0.00	0.00	0.20	0.00	
SO3	0.08	0.02	0.08	0.01	0.04	0.05	0.03	
LOI								1.70
TOTAL	**99.97**	**99.88**	**99.93**	**99.95**	**99.61**	**100.11**	**99.51**	**100.40**
LOI2	1.64	1.80	1.56	1.37	1.31	1.59	1.16	
FeOt	10.54	9.59	11.24	9.95	11.40	11.35	10.43	11.16
Mg#(0.20)	57.52	65.31	46.69	52.04	56.39	55.90	59.11	57.23
Li (ppm)								55
F (ppm)								
S (%)	0.1	0.1	0.2		0.2		0.2	
Cl (ppm)	220	190	130	100	100	50	40	
Sc	33	28	32	30	36	36	38	
V	253	200	270	200	299	290	260	
Cr	160	220	47	110	65	62	97	
Co	36	44	47	36	42	45	81	
Ni	32	94	39	45	52	47	130	58
Cu	17	47	37	21	35	48	34	31
Zn	86	77	150	120	125	120	185	122
Ga	18	16	22	20	21	20	21	
As	4	4	8	10	58	11	34	<4
Rb	8	13	35	44	40	32	63	37
Sr	221	201	340	300	302	300	290	271
Y	30	26	68	48	45	37	58	43
Zr	114	92	240	220	144	140	240	219
Nb	7	5	15	14	7	7	11	
Mo	<1	<1	1	<1	<1	<1	<1	
Sn	1	1	2	<2	6	3	10	9
Sb	<2	<2	<2	<2	2	<2	<2	
Cs	1	5	<3	<3	2	<3	9	
Ba	105	77	220	240	69	93	90	
La	6	5	40	27	8	10	40	
Ce	25	16	83	64	30	26	58	
Nd	14	8	49	34	13	20	51	
W	<2	<2	<2	<2	1	<2	<2	
Pb	1	<2	6	7	8	6	10	27
Bi	2	1	3	2	3	2	1	
Th	<2	<2	<2	3	<2	<2	<2	
U	1	<1	1	2	1	<1	1	
Partial CIPW norms at Fe2O3/FeO = 0.20								
Q	-	-	*2.91*	*5.00*	-	-	*0.46*	-
C	-	-	-	-	-	-	-	-
ne	-	-	-	-	-	-	-	-
hy	*15.17*	*7.64*	*20.64*	*20.51*	*15.99*	*12.08*	*25.12*	*16.90*
ol	*5.38*	*13.80*	-	-	*7.11*	*9.35*	-	*6.69*

TABLE 6. Whole rock chemical analyses (XRF) (continued)

	FURNEAUX ISLANDS DYKES							
Region	**Flinders Island**							
Locality	Pt Reid	East of Lady Barron		Long Pt	Badger Cnr	Cannes Hill	----Stanley Pt----	
Field No.	**FLD1**	**FLD2**	**FLD3**	**77/907b**	**77/908**	**R013341**	**FLD4**	**-**
other ID	R006525	R006526	R006527			R013341	R006528	R014365
Analysis No	990882	990883	990884	20070302	20070303	20080434	990885	20170188
Type	T	T	T	T	T	T	A	A
SiO2 (%)	48.55	48.20	47.02	47.30	49.75	48.93	44.17	44.01
TiO2	1.65	1.39	1.86	1.95	1.20	2.17	2.25	2.21
Al2O3	16.54	17.07	15.35	15.69	18.00	14.71	15.13	15.36
Fe2O3	1.20	1.19	1.50	1.88	0.71	2.70	1.94	*11.92
FeO	8.38	7.74	9.92	9.70	7.40	8.40	9.15	nd
MnO	0.17	0.17	0.19	0.21	0.13	0.20	0.18	0.20
MgO	6.66	8.20	7.84	7.46	6.67	6.71	5.07	5.08
CaO	9.33	10.25	10.30	10.11	10.29	10.36	7.29	6.95
Na2O	3.33	2.09	2.55	2.51	2.28	2.77	3.75	3.94
K2O	0.60	0.19	0.19	0.34	1.36	0.34	2.96	2.96
P2O5	0.36	0.24	0.20	0.25	0.22	0.27	0.93	0.93
H2O+	2.84	3.20	2.72	2.64	1.57	2.42	2.17	
H2O-								
CO2	0.01	0.05	0.02	0.00	0.10	0.10	4.72	3.15
SO3	0.07	0.01	0.06	0.00	0.00	0.04	0.04	
LOI								1.88
TOTAL	**99.69**	**99.99**	**99.72**	**100.04**	**99.67**	**100.12**	**99.75**	**100.59**
LOI2	1.92	2.39	1.64	1.56	0.85	1.59	5.87	5.03
FeOt	9.46	8.81	11.27	11.39	8.04	10.83	10.90	10.75
Mg#(0.20)	59.69	66.19	59.40	57.94	63.58	56.58	49.46	49.91
Li (ppm)								
F (ppm)								
S (%)				0.0	0.2	0.0		0.1
Cl (ppm)	340	670	330	460	280	80	170	
Sc	18	24	28	36	25	32	9	11
V	199	193	208	242	199	277	135	141
Cr	175	220	160	180	220	220	69	72
Co	36	40	42	46	31	38	37	37
Ni	62	80	47	47	99	27	80	74
Cu	29	34	28	40	47	29	40	38
Zn	86	79	94	126	84	85	125	117
Ga	17	16	20	20	17	20	22	22
As	7	5	3	1	24	6	7	5
Rb	28	16	11	22	72	13	75	77
Sr	478	297	203	221	328	262	940	889
Y	26	22	30	33	23	30	24	24
Zr	143	109	114	129	117	154	335	328
Nb	9	6	5	6	7	6	83	79
Mo	<1	<1	<1	<1	<1	<1	7	5
Sn	1	1	2	6	4	1	2	<2
Sb	<2	<2	<2	<2	2	<2	<2	<2
Cs	7	8	5	8	29	2	19	16
Ba	168	54	92	80	150	78	910	1058
La	16	12	5	10	30	5	85	61
Ce	31	18	14	15	25	27	125	97
Nd	20	12	10	12	15	17	50	79
W	<2	1	<2	1	3	<2	<2	<2
Pb	<2	1	<2	3	2	<2	5	8
Bi	1	2	2	3	1	2	3	<1
Th	<2	<2	<2	<2	<2	<2	5	11
U	<1	2	1	<1	1	<1	1	3
Partial CIPW norms at Fe2O3/FeO = 0.20								
Q	-	-	-	-	-	-	-	-
C	-	-	-	-	-	-	-	-
ne	-	-	-	-	-	-	*8.83*	*9.71*
hy	*8.07*	*25.90*	*12.38*	*14.35*	*15.94*	*18.23*	-	-
ol	*10.22*	*0.67*	*9.64*	*8.01*	*3.55*	*1.40*	*14.90*	*15.32*

TABLE 6. Whole rock chemical analyses (XRF) (continued)

	FURNEAUX ISLANDS DYKES					
Region	**Cape Barren Is**					**Mt Chappell Is**
Locality	Apple Orch Pt	Riddles Bay		Nautilus Cve	Puncheon Pt	
Field No.	**BA3**	**BA5**	**BA6**	**BA4**	**BA35**	**77/910**
other ID	R011908	R011910	R011911	R011909	R011928	
Analysis No	20050175	20050177	20050178	20050176	20050192	20070305
Type	C	T	C	C	C	A
SiO2 (%)	49.73	49.72	52.03	54.67	65.09	49.66
TiO2	2.27	1.26	1.21	1.78	0.55	2.85
Al2O3	14.91	16.72	16.41	14.74	16.71	13.91
Fe2O3	2.98	1.32	1.74	1.27	0.81	2.44
FeO	8.92	7.00	6.23	8.28	2.89	10.10
MnO	0.26	0.14	0.13	0.16	0.06	0.22
MgO	3.00	7.75	6.18	4.23	2.13	4.93
CaO	6.74	8.83	7.84	6.26	4.57	7.82
Na2O	3.62	2.61	3.56	3.02	4.35	3.71
K2O	3.38	0.82	1.06	1.70	1.33	0.74
P2O5	1.10	0.24	0.31	0.31	0.22	0.37
H2O+	2.72	2.83	3.10	2.60	0.80	2.94
H2O-						
CO2	0.19	0.13	0.13	0.25	0.08	0.20
SO3	0.02	0.02	0.05	0.01	0.02	0.01
LOI						
TOTAL	**99.83**	**99.39**	**99.98**	**99.25**	**99.60**	**99.90**
LOI2	1.92	2.18	2.54	1.93	0.56	2.02
FeOt	11.60	8.19	7.80	9.42	3.62	12.29
Mg#(0.20)	35.24	66.56	62.50	48.56	53.32	45.75
Li (ppm)						
F (ppm)						
S (%)	0.1	0.2	0.1	0.0	0.0	0.1
Cl (ppm)	110	500	580	240		460
Sc	7	23	25	30	10	33
V	66	182	200	240	72	314
Cr	<5	220	170	19	27	16
Co	24	38	33	31	11	41
Ni	2	71	48	11	11	7
Cu	14	30	20	15	9	9
Zn	190	83	88	116	66	114
Ga	20	17	18	20	19	21
As	7	5	6	8	<20	6
Rb	165	48	52	87	52	42
Sr	760	407	581	340	680	276
Y	68	24	28	40	12	37
Zr	320	141	145	220	190	199
Nb	17	8	10	13	9	8
Mo	3	<1	<1	1	<5	<1
Sn	2	3	1	3	<9	3
Sb	<2	<2	<2	4		<2
Cs	3	2	6	4		2
Ba	1200	184	291	574	520	107
La	48	11	21	23	38	14
Ce	99	30	46	53	56	35
Nd	60	17	20	32	22	20
W	<2	1	<2	1	<10	1
Pb	7	4	2	6	12	1
Bi	3	<1	1	2	<5	2
Th	<2	1	3	4	<10	<2
U	2	2	2	2	<10	2
Partial CIPW norms at Fe2O3/FeO = 0.20						
Q	-	-	*0.35*	*8.80*	*20.65*	-
C	-	-	-	-	*0.34*	-
ne	-	-	-	-	-	-
hy	*1.72*	*23.77*	*20.95*	*18.89*	*9.76*	*18.56*
ol	*10.75*	*1.44*	-	-	-	*0.24*

TABLE 7 ICPMS analyses and comparison with XRF results

Field No.	Maria Is SMD		Lagunta Ck LC3		Cape Tourville Rd NJ477		N of Pretty Marsh MNET12		S side of Mt William NJ245		Lady Barron FLD3	
Type	calc-alkaline		alkalic		alkalic		andesite		tholeiitic		tholeiitic	
	icpms	xrf	icpms	xrf	icpms	xrf	icpms	xrf	icpms	xrf	icpms	xrf
Li (ppm)	48.91		63.46		88.18		19.90		78.49		54.97	
Be	1.43		2.02		1.87		1.92		0.41		0.77	
Sc	26.06	29	26.23	19	28.61	32	21.44	24	26.09	26	33.24	28
Ti	8536	8693	15998	15647	13927	14208	10919	11211	5827	5755	10766	11151
V	168.63	183	213.58	178	260.06	240	134.72	165	165.38	164	242.43	208
Co	28.31	28	45.91	42	39.31	42	18.14	21	40.86	40	45.72	42
Ni	41.14	44	56.24	52	74.63	86	15.18	20	103.73	102	44.76	47
Cu	4.81	8	22.25	20	25.98	26	1.90	7	47.83	48	29.59	28
Zn	143.87	149	109.39	92	123.42	135	106.21	120	58.66	63	93.58	94
Rb	32.23	31	52.80	52	97.59	105	100.27	99	106.42	93	8.34	11
Sr	503.56	485	406.90	363	744.22	720	542.29	550	234.98	214	209.50	203
Y	32.06	31	41.17	36	33.82	33	32.48	33	20.61	20	31.13	30
Zr	146.54	163	294.95	285	280.44	260	287.53	300	42.58	62	120.90	114
Nb	7.43	8	15.34	13	15.41	14	23.84	26	2.30	4	3.64	5
Cs	5.29	5	10.53	7	114.61	<3	9.88	8	43.98	45	3.30	5
Ba	404.40	381	333.35	275	nd	590	528.53	510	54.59	66	87.04	92
La	19.62	17	30.58	30	45.99	63	33.60	39	4.62	32	6.60	5
Ce	44.82	40	69.96	59	100.17	95	72.74	78	11.07	10	17.71	14
Pr	6.07		9.52		11.61		9.34		1.70		2.83	
Nd	26.59	24	41.28	34	50.04	51	38.00	37	8.37	4	14.27	10
Sm	6.19		9.19		9.38		7.75		2.62		4.29	
Eu	1.84		2.62		2.79		2.30		1.04		1.60	
Gd	6.12		8.84		8.02		6.93		3.20		5.17	
Tb	0.97		1.38		1.18		1.05		0.57		0.91	
Dy	5.81		8.00		6.57		6.01		3.60		5.72	
Ho	1.18		1.59		1.29		1.17		0.75		1.20	
Er	3.28		4.32		3.51		3.27		2.14		3.40	
Tm	0.47		0.62		0.50		0.48		0.31		0.49	
Yb	2.98		3.79		3.11		3.01		1.94		3.11	
Lu	0.44		0.55		0.47		0.45		0.29		0.46	
Hf	3.61		6.56		5.92		6.68		1.44		3.10	
Ta	0.46		1.03		0.90		1.51		0.16		0.26	
Pb	17.33	<2	4.75	1	10.13	9	11.70	3	5.51	3	1.84	<2
Th	3.13	<2	2.27	<2	4.18	<2	4.85	2	0.69	<2	0.83	<2
U	0.70	<1	0.51	1	0.94	1	1.16	2	0.17	1	0.17	1

ICPMS analyses: NJ477- HF, H_2SO_4, high pressure digestions. Others- HF, HNO_3 digestion.
Analyst: Ian Little, University of Tasmania

TABLE 8 Summary of $^{39}Ar/^{40}Ar$ dating

Sample	Description	Location	Age type	Apparent age (± 2σ)	Period
NJ245	Dolerite	E side of Mt William	plateau	334.2 ± 7.0	early Carboniferous
MNET2	Dolerite	Gripe Creek	total gas	330.2 ± 5.6	early Carboniferous
FLD3	Dolerite	Yellow Beaches, Lady Barron	total gas	333.0 ± 7.0	early Carboniferous
LC1E	Dolerite	Lagunta Creek, Freycinet Pen.	total gas	258.1 ± 5.0	late Permian

All determinations made on plagioclase separates.

TABLE 9 $^{40}Ar/^{39}Ar$ furnace step-heating analytical results for eastern Tasmanian dolerite samples

Temp (˚C)	Cum.% ^{39}Ar	^{40}Ar	±	^{39}Ar	±	^{38}Ar	±	^{37}Ar	±	^{36}Ar	±	Ca/K	±	$\%^{40}Ar^*$	$^{40}Ar^*/^{39}Ar$	±	Age (Ma)	±
		(x10^{-13} moles)		(x10^{-14} moles)		(x10^{-16} moles)		(x10^{-16} moles)		(x10^{-16} moles)								
Sample NJ245 (R013279); dyke at Forester Kangaroo Drive, via Mt William																		
J-Value = 0.013817 ± 0.000025																		
600	0.33	0.052	0.000	0.004	0.000	0.018	0.013	3.16	2.82	0.149	0.019	15.87	14.161	15.7	23.53	15.75	507.9	296.3
700	3.8	0.186	0.000	0.037	0.000	0.091	0.003	63.26	1.87	0.524	0.055	29.664	0.943	16.7	8.34	4.33	196.8	96.8
800	11.6	0.290	0.001	0.084	0.000	0.109	0.007	390.17	4.3	0.664	0.017	81.66	0.979	32.4	11.25	0.61	260.6	13.1
900	18.76	0.199	0.000	0.077	0.000	0.033	0.023	242.66	3.16	0.299	0.017	55.289	0.748	55.6	14.44	0.66	328.1	13.6
1000	27.18	0.207	0.000	0.090	0.001	0.019	0.011	123.1	1.11	0.259	0.011	23.852	0.266	62.9	14.4	0.38	327.4	8.0
1050	33.88	0.142	0.000	0.072	0.000	0.003	0.012	60.9	0.89	0.111	0.014	14.846	0.23	77	15.28	0.59	345.6	12.1
1100	40.37	0.137	0.000	0.070	0.000	0.004	0.013	59.44	0.83	0.088	0.015	14.951	0.214	81.1	16.01	0.63	360.5	12.8
1150	47.5	0.148	0.000	0.077	0.000	0.026	0.022	61.64	4.81	0.104	0.015	14.103	1.103	79.2	15.32	0.59	346.5	12.2
1200	52.83	0.113	0.000	0.057	0.000	0.028	0.027	57.52	5.51	0.118	0.034	17.62	1.692	69.2	13.66	1.76	311.8	36.9
1250	57.08	0.101	0.000	0.046	0.001	0.000	0.015	60.47	1.7	0.119	0.020	23.174	0.697	65.1	14.35	1.32	326.2	27.4
1350	65.05	0.224	0.000	0.086	0.001	0.069	0.020	313.48	2.27	0.363	0.014	64.185	0.586	52	13.6	0.49	310.7	10.3
1450	76.1	0.337	0.001	0.119	0.000	0.105	0.021	569.98	2.33	0.562	0.015	84.164	0.403	50.7	14.41	0.39	327.5	8.1
1500	85.5	0.236	0.001	0.101	0.001	0.059	0.015	529.99	4.36	0.293	0.020	92.049	0.945	63.3	14.81	0.6	335.9	12.5
1550	100	0.385	0.001	0.156	0.000	0.154	0.041	982.08	7.95	0.494	0.024	110.518	0.944	62.1	15.38	0.45	347.6	9.3
Total															14.09	1.15	320.8	23.9
Sample MNET2 (R001064); dyke at Gripe Creek, via Ansons Bay																		
J-Value = 0.013829 ± 0.000023																		
550	0.03	0.011	0	0.002	0.000	0.004	0.002	0.05	0.05	0.012	0.016	0.419	0.431	69.7	36.01	21.42	729.0	356.7
650	0.86	0.191	0.000	0.069	0.001	0.034	0.011	16.76	2.18	0.334	0.009	4.278	0.557	48.2	13.4	0.42	306.7	8.9
750	4.34	1.133	0.002	0.287	0.001	0.547	0.018	200.13	2.53	2.760	0.027	12.206	0.158	28	11.04	0.29	256.4	6.3
850	11.95	1.570	0.003	0.627	0.001	0.493	0.027	1068.78	5.56	2.424	0.033	29.828	0.165	54.4	13.62	0.17	311.2	3.5
925	18.77	1.065	0.002	0.561	0.001	0.132	0.030	789.45	5.39	0.701	0.019	24.625	0.178	80.5	15.29	0.11	346.0	2.2
1000	28.19	1.450	0.003	0.776	0.001	0.150	0.026	550.99	3.37	0.84	0.016	12.42	0.078	82.9	15.48	0.07	350.1	1.5
1075	44.4	2.320	0.004	1.335	0.002	0.247	0.038	421.58	4.47	1.010	0.015	5.526	0.059	87.1	15.14	0.05	343.0	1.0
1150	55.81	1.624	0.003	0.940	0.001	0.172	0.030	320.15	2.72	0.78	0.017	5.963	0.051	85.8	14.83	0.06	336.6	1.3
1250	67.8	1.903	0.003	0.988	0.001	0.352	0.034	937.12	5.67	1.659	0.023	16.602	0.103	74.2	14.3	0.08	325.6	1.6
1300	74.31	1.116	0.002	0.536	0.001	0.294	0.015	604.85	3	1.217	0.020	19.742	0.102	67.8	14.11	0.12	321.5	2.4
1350	78.87	0.827	0.001	0.376	0.001	0.223	0.020	451.14	5.37	0.957	0.021	21.025	0.252	65.8	14.48	0.17	329.3	3.5
1400	81.9	0.603	0.001	0.249	0.001	0.155	0.010	348.41	1.73	0.787	0.016	24.444	0.173	61.4	14.84	0.2	336.8	4.2
1450	84.14	0.427	0.001	0.184	0.001	0.121	0.015	315.56	3.21	0.433	0.014	29.973	0.315	70.1	16.26	0.24	366.0	4.8
1550	100	3.107	0.005	1.307	0.001	0.948	0.051	3102.43	16.32	3.927	0.045	41.549	0.223	62.7	14.9	0.11	338.0	2.3
Total															14.52	0.13	330.2	2.8

TABLE 9 (continued).

Temp (˚C)	Cum.% ^{39}Ar	^{40}Ar (x10^{-13} moles)	±	^{39}Ar (x10^{-14} moles)	±	^{38}Ar (x10^{-16} moles)	±	^{37}Ar (x10^{-16} moles)	±	^{36}Ar (x10^{-16} moles)	±	Ca/K	±	%^{40}Ar*	^{40}Ar*/^{39}Ar	±	Age (Ma)	±
Sample FLD3 (R006527); dyke east of Lady Barron, Flinders Island																		
J-Value = 0.013806 ± 0.000027																		
600	0.1	0.076	0.000	0.006	0.000	0.035	0.011	3.77	0.96	0.210	0.009	11.521	2.944	18.6	24.74	4.58	530.1	84.9
700	1.94	0.446	0.001	0.107	0.001	0.242	0.008	69.25	2.96	1.081	0.017	11.302	0.487	28.3	11.77	0.47	271.6	10.0
800	9.43	1.185	0.002	0.437	0.001	0.583	0.026	845.7	4.32	2.086	0.027	33.874	0.181	48	13.02	0.19	298.2	4.0
900	21.85	1.302	0.002	0.725	0.001	0.156	0.029	1870.55	9.42	0.805	0.027	45.153	0.236	81.7	14.68	0.12	332.8	2.4
1000	33.57	1.182	0.002	0.683	0.001	0.072	0.021	574.31	3.83	0.514	0.018	14.706	0.1	87.2	15.07	0.09	341.0	1.8
1050	44.25	1.047	0.002	0.623	0.001	0.028	0.021	304.53	3.13	0.397	0.015	8.557	0.089	88.8	14.93	0.08	338.0	1.6
1100	53.44	0.898	0.002	0.536	0.001	0.068	0.021	237.42	3.55	0.400	0.014	7.748	0.117	86.8	14.54	0.09	330.0	1.8
1150	60.99	0.735	0.001	0.441	0.001	0.067	0.018	215.94	2.6	0.394	0.011	8.574	0.104	84.2	14.03	0.08	319.5	1.6
1200	68.26	0.721	0.001	0.424	0.001	0.100	0.016	256.27	2.71	0.435	0.012	10.586	0.115	82.2	13.98	0.1	318.5	2.1
1250	74.37	0.64	0.001	0.357	0.001	0.108	0.015	305.68	2.57	0.499	0.012	14.995	0.132	77	13.81	0.11	314.7	2.3
1350	80.85	0.818	0.001	0.378	0.001	0.272	0.026	576.11	4.76	0.853	0.02	26.691	0.241	69.2	14.99	0.17	339.3	3.5
1450	86.85	0.839	0.003	0.35	0.001	0.218	0.017	691.91	5.27	0.925	0.020	34.597	0.279	67.4	16.18	0.19	363.6	4.0
1500	90.7	0.546	0.001	0.225	0.001	0.155	0.031	488.43	3.3	0.634	0.013	38.011	0.274	65.7	15.96	0.18	359.2	3.6
1550	100	1.260	0.002	0.542	0.000	0.340	0.027	1301.34	7.43	1.379	0.021	41.983	0.242	67.7	15.72	0.12	354.4	2.5
Total															14.69	0.17	333.0	3.5
Sample LC1E (R004469); plagioclase megacryst from dyke at Lagunta Creek, Freycinet Peninsula																		
J-Value = 0.013819 ± 0.000022																		
600	0.14	0.154	0.000	0.015	0.000	0.069	0.014	0.42	1.16	0.438	0.010	0.494	1.365	15.9	16.56	2.04	371.7	41.4
700	1.73	0.420	0.002	0.174	0.002	0.242	0.015	63.26	1.63	0.855	0.040	6.366	0.172	39.9	9.63	0.69	225.3	15.1
800	9.4	1.457	0.003	0.835	0.002	0.597	0.029	565.85	6.08	2.247	0.029	11.86	0.131	54.4	9.5	0.11	222.5	2.4
900	19.99	1.378	0.003	1.153	0.001	0.085	0.035	1159.79	4.68	0.492	0.019	17.609	0.072	89.4	10.69	0.05	248.6	1.2
1000	33.47	1.690	0.003	1.467	0.002	0.040	0.041	653.71	6.58	0.441	0.021	7.798	0.079	92.3	10.63	0.05	247.4	1.1
1050	46.03	1.552	0.003	1.368	0.001	0.000	0.042	391.1	4.18	0.399	0.010	5.003	0.054	92.4	10.48	0.03	244.0	0.7
1100	55.37	1.138	0.002	1.016	0.001	0.072	0.030	258.8	1.21	0.409	0.038	4.457	0.021	89.4	10.01	0.11	233.6	2.5
1150	63.14	0.926	0.002	0.846	0.001	0.057	0.024	199.09	2.34	0.326	0.016	4.117	0.049	89.6	9.81	0.06	229.2	1.4
1200	71.42	1.057	0.002	0.901	0.002	0.079	0.028	308.84	4.29	0.401	0.014	6.001	0.084	88.8	10.43	0.05	242.8	1.2
1250	78.98	1.105	0.002	0.824	0.002	0.121	0.024	400.91	2.46	0.445	0.020	8.52	0.055	88.1	11.82	0.08	272.9	1.7
1350	85.79	1.161	0.002	0.741	0.001	0.222	0.034	523.61	3.13	0.706	0.010	12.368	0.075	82	12.86	0.05	295.0	1.1
1450	91	1.052	0.002	0.568	0.001	0.308	0.033	570.49	5.29	1.126	0.020	17.592	0.166	68.4	12.67	0.11	291.0	2.4
1500	93.93	0.566	0.001	0.319	0.000	0.115	0.025	394.9	3.11	0.522	0.020	21.65	0.172	72.7	12.9	0.19	296.0	4.0
1550	100	1.117	0.002	0.661	0.001	0.163	0.030	937.43	3.93	0.793	0.015	24.834	0.111	79	13.36	0.08	305.6	1.6
Total															11.13	0.11	258.1	2.5

APPENDIX

DETAILED FIELD AND PETROGRAPHIC DESCRIPTIONS

South Maria Island

Stinking Creek (SMD) (Fig. 8l)

A small dyke-like body, a few metres wide with a NNE strike, intrudes Mathinna Supergroup east of the headwaters of Stinking Creek. It is traceable for 60-70 m up to a fault with Permian strata, which it does not intrude (Clarke & Baillie, 1981, 1984). Although described as a microdiorite, a similarity with "the late-stage intermediate dykes associated with granites elsewhere in northeast Tasmania" was suggested (Clarke & Baillie, 1984).

In thin section, a sample (R004379) consists of a coarse-grained, interlocking, locally subophitic intergrowth of zoned plagioclase laths (0.5–3 mm) and largely "uralitised" clinopyroxene, together with equant to skeletal opaque grains and minor interstitial anhedral quartz. Some relict colourless clinopyroxene remains, but most is altered to fibrous actinolite (pleochroic from colourless to pale yellow to pale green) with subordinate pale to dark brown hornblende. Hornblende forms well-crystallised subhedra or remains as relict patches within the actinolite, which is probably retrograde.

Freycinet Peninsula

Lagunta Creek (LC1, LC3)

A conspicuous black dolerite dyke near the mouth of Lagunta Creek, at the southern end of Hazards Beach, has been described in detail by Everard (2001) and only a summary is given here. The dyke is up to 6.5 m wide, strikes 165° and can be traced for about 70 m. It abruptly crosscuts mafic enclaves within the host Bluestone Bay Granodiorite, which also contains aplite and leucogranite veins that are abruptly truncated against the contact and do not extend into the dyke.

Dyke margins are chilled for about 50 mm from sharp, steeply east-dipping but locally irregular contacts, partly controlled by jointing within the host granodiorite. Abrupt changes in direction, such as small dextral offsets, may be associated with offshoots of dolerite into the host rock. Stoped blocks of granodiorite (≤0.5 m) within the dolerite match irregularities in the contact, suggesting dilational emplacement.

These relationships suggest that the granodiorite had already essentially cooled and solidified at the time of dyke emplacement, and there is no sign of magma mingling.

The dolerite contains sparse (<1%) but large (typically 10–30 × 5–20 mm but up to 140 × 50 mm) euhedral to subhedral megacrysts of plagioclase ($An_{64.5}$, microprobe analyses). A sample (LC3; Fig. 8g) from the interior of the dyke consists of a subophitic intergrowth of weakly zoned titaniferous augite granules (≤1 mm), largely altered plagioclase, ragged opaque minerals, and scattered equant pseudomorphs of former olivine (<800 µm). A mineral with high relief and birefringence (possibly titanite) is present as irregular angular grains up to 1.5 mm across, but usually much smaller. Secondary chlorite, serpentine, epidote and actinolite are also present. The chilled margin (LC1; Fig. 8f) is mineralogically similar with an intergranular texture. Minute fragments of probable biotite are associated with chlorite and abundant chlorite-filled amygdales (<500 µm) are present (Everard, 2001).

The dyke has a high magnetic susceptibility (23–25 × 10^{-3} SI), consistent with abundant magnetite.

Graham Creek (FY30)

An area of subrounded to subangular cobble- to boulder-sized float, and some sub-outcrop, of dolerite is located on the main Freycinet Peninsula walking track about 2 km NNE of Mt Graham, near the headwaters of Graham Creek, at the start of the descent to Wineglass Bay. The dolerite is a very tough blue-grey aphanitic rock with sparse small feldspar phenocrysts. It possibly forms a dyke about 10 m wide, striking at ~340°, within typical Freycinet Granite (J. L. Everard, pers. obs.).

In thin section (sample FY30) the rock consists mainly of a seriate intergrowth of interlocking, generally clear plagioclase, ranging up to microphenocrysts 2 mm long; subordinate smaller augite grains; generally strongly elongate opaque grains, and clear interstitial quartz anhedra. Some secondary chlorite, actinolite and rare carbonate are present. A rounded, corroded quartz xenocryst (4 × 2.5 mm) is surrounded by a narrow (150 µm) reaction halo of finely prismatic outwardly radiating augite.

Mt Freycinet (FY31)

Sparse cobble-sized float of fine-grained dolerite is present, amid large talus boulders of pink granite, on the main walking track immediately east of Mt Freycinet (J. L. Everard, pers. obs.).

A thin section (Fig. 8m) contains sparse, generally subhedral, corroded microphenocrysts (≤2.5 mm) and glomerocrysts of plagioclase with numerous inclusions, and rare phenocrysts of possible former olivine (≤1 mm) are replaced by reddish-brown iddingsite. The intergranular groundmass consists mainly of plagioclase

laths (100–400 µm), small granules and prisms of augite, and a little quartz Opaque grains are generally small and elongate (20–40 µm) or less commonly elongate to acicular. Minor secondary carbonate is present, and there is some turbid incipient alteration of augite, but the groundmass is relatively fresh.

Southeast end of Wineglass Bay (FP4, NJ475, CB20, CB21)

On the foreshore about 300 m NNE of the end of the beach, a dyke of black aphyric dolerite striking at ~155–161° intrudes coarse-grained red granite. Much of the dyke is obscured by beach boulders, but near low water mark it is about 2 m wide, whereas ~8 m to the south it narrows to 0.8–0.9 m. Dolerite float was noted on the headland about 100 m inland (FP08323016). Contacts are sharp, but parallel veins of dyke rock are present in the granite, and thin stringers of granite in the dyke (P. L. F. Collins, J. L. Everard field notes).

Sample FP4 consists of a rather coarsely intergranular to slightly subophitic intergrowth of plagioclase laths (500 µm to 2 mm × 150–250 µm) and pink titaniferous augite, partly altered to pale yellow-green fibrous actinolite. Sparse small opaque grains are largely replaced by formless aggregates of titanite.

Samples collected by J. D. Cocker (CB20, CB21) are similar but also contain plagioclase phenocrysts and megacrysts (≥25 mm), and augite is completely replaced ("uralitised") by actinolite.

Another sample (NJ475) is more altered, with turbid plagioclase partly replaced by fine-grained prehnite, abundant pale green chlorite in addition to actinolite, and minor secondary iron oxide. Several plagioclase megacrysts (≤4 mm) with very abundant small melt inclusions ("sieve texture") and slightly corroded margins are present.

Hawksnest Cove (FY32; FP1)

A dyke (described in the field as dolerite) with abundant feldspar phenocrysts intrudes the Bluestone Bay Granodiorite on the foreshore between the north end of Wineglass Bay and Hawksnest Cove. It is about 3 m wide with irregular to lobate margins, but overall strikes at ~100° and dips steeply south. It can be traced from low water mark, up cliffs and disappears inland. (J. L. Everard, field notes).

Collins (1972 field notes) described the same dyke as striking ~100N70, with very irregular margins offset 1.5–2 m by a fault. Veins of quartz, feldspar and minor biotite trending 15–25° cut both the dyke and the host granodiorite.

Thin sections (FY32, FP1; Fig. 8o) show numerous anhedral, corroded xenocrysts of quartz (≤ 3 mm) with narrow reaction rims of pale yellow-green actinolite, and rounded, largely sericitised feldspar phenocrysts, some of which may also be xenocrysts. The groundmass is mineralogically different from the other dykes, and largely consists of a mosaic of abundant brown biotite (100–200 µm), actinolite, plagioclase and anhedral quartz and possibly alkali feldspar. Opaque grains are largely altered to titanite. Irregular patches of coarser-grained actinolite may have formed by the complete digestion of quartz xenocrysts, whereas other actinolite patches have vague crystal outlines and may be pseudomorphs after augite. Rare larger (~1 mm) grains of biotite may also be xenocrysts derived from the host granodiorite.

Mineralogically and chemically, the dyke approximates a biotite microtonalite. The disequilibrium textures, together with geochemical features such as high SiO_2 (~58.7%) and K_2O (~2.8%), suggest incomplete assimilation of granodiorite by a more mafic magma.

Carp Bay (NJ476, FP21)

A massive dark grey dolerite dyke about 10 m wide, striking at about 165° and dipping steeply, transects the cliffy headland between Sleepy Bay and Carp Bay, near the contact between the Bluestone Bay Granodiorite and Coles Bay Granite. The dolerite is hosted by granodiorite, which contains mafic enclaves and exhibits alternating biotite- and feldspar-rich bands. These are cut by aplite veins emanating from a larger sill-like intrusion which extends north towards Cape Tourville and is apparently related to the Coles Bay Granite. The aplite dykes, however, do not cut the dolerite, which appears to be the youngest intrusive phase (P. L. F. Collins, field notes, 1973). These field relationships are similar to those at Lagunta Creek (Everard 2001).

This dyke was re-located by J. L. Everard in 2011. Coarse-grained (~1 mm) black dolerite crops out well near the crest of the headland at (610290mE, 5334570mN), and may extend to a large black crag just off the southern side of the headland.

Both samples are coarse-grained seriate-textured rocks with partly turbid plagioclase phenocrysts (≤3 mm), grading down to smaller laths, intergrown with pseudomorphs of actinolite, with a few relict cores colourless augite. Minor biotite, irregular to elongate

or skeletal opaque grains, accessory apatite and some secondary carbonate are also present.

Sleepy Bay (FP22)

On a large shore platform on the north side of Sleepy Bay and a few hundred metres west of the above locality, aplite and pegmatite, possibly the top of a sill-like intrusion of porphyritic granite, has a subhorizontal contact with overlying granodiorite. The coarsest pegmatite occurs just below the contact, where it occurs as gently dipping bands. The granodiorite hosts a feldspar-phyric mafic dyke, which exhibits flow structure and very irregular margins, suggesting that it was intruded when the granodiorite was still partly mobile. The dyke trends at ~106°, offshore but towards the dolerite dyke on the headland (FP21). However, unlike that dyke, the Sleepy Bay dyke (FP22) is truncated by the aplite and pegmatite, suggesting that it is an earlier intrusion. Marked compositional differences (e.g., 48.1 vs 60.3% SiO_2) also suggest that the two dykes are not consanguineous (P. L. F. Collins, field notes and unpublished data).

A sample (FP22) contains several small (2–3 mm) xenoliths of anhedral polycrystalline quartz and equant rounded subhedral phenocrysts and glomerocrysts of plagioclase (1–2.5 mm) in a fairly even-grained (50–100 µm) mosaic of abundant biotite, subordinate actinolite, plagioclase, anhedral quartz and possibly alkali feldspar. Many of the plagioclase phenocrysts appear corroded and, together with, larger (≤1 mm) ragged anhedra of biotite and aggregates (~500 µm) of actinolite may also be partly reacted xenocrysts of granitic origin. No opaque phase is present, although there is a tenuous interstitial dust of formless titanite.

Petrographically and chemically, the rock resembles the dyke at Hawksnest Cove (FY32, FP1) and probably also formed by partial assimilation by a mafic intrusion of the granodiorite wall rock.

Cape Tourville Road (NJ477, FP24)

A dolerite dyke, 8-10 m wide and striking at ~140°, is poorly exposed near a crest of the road about 1.5 km from the lighthouse. Float and sporadic outcrop can be traced for at least 50 m northwest of the road. The host rock is enclave-bearing Bluestone Bay Granodiorite (P. L. F. Collins, J. L. Everard field notes).

The samples are similar. Both consist of a coarse-grained intergrowth of plagioclase (1–2 mm) and pale yellow to green pleochroic actinolite preserving crystal outlines after pyroxene. Minor biotite, rare relict clinopyroxene and equant to elongate opaque grains are also present, but quartz is apparently absent.

Bluestone Bay (NJ478, FP11, CB7)

A vertical dolerite dyke 2.5–4 m wide and striking at ~175° is exposed on a west-facing coastal cliff about 300m east of Bluestone Bay, Much of the dyke is difficult to reach, but it can be traced for about 30 m and to the north disappears offshore. Contacts are very irregular and "sprout" several narrow crooked fingers or apophyses, 20–100 mm wide and up to 1 m long, into the host Bluestone Bay Granodiorite. The margins of the dyke are very fine-grained, chilled and aphyric, but the interior is coarser-grained and bears abundant small feldspar phenocrysts (≤5 mm) (P. L. F. Collins, J. L. Everard, field notes).

The freshest of the samples (NJ478) contains plagioclase phenocrysts to 3 mm, grading down to groundmass plagioclase (typically 300–600 µm) with intergranular pale pink titaniferous augite granules (~150–400 µm) partly replaced by actinolite and subordinate orange-brown biotite, together with equant to slightly elongate opaque grains and minor quartz.

The other samples (FP11, CB7) are similar but more altered. FP11 is a medium-grained, intergranular to seriate-textured dolerite, containing large (≤3 mm), roughly equant, variably altered plagioclase subhedra. These grade down to a groundmass largely of finer-grained plagioclase (~500 µm-1 mm), augite pseudomorphs replaced by pale green actinolite, and subordinate brown biotite. Some of the actinolite is oxidised to brown alteration products, but generally equant and angular (≤100 µm) to elongate opaque grains are little altered. A few small quartz anhedra are present.

Sample CB7 has been cut across the contact with the granite country rock. The dolerite contains a quartz xenocryst (~2 mm) with a narrow reaction rim of fibrous actinolite, numerous relatively fresh plagioclase phenocrysts and a relatively altered groundmass. The grain size of the dolerite decreases about 10 mm from the contact, which is sharp to within a few hundred µm, but there is no obvious mineralogical change right up to the contact. The country rock is distinctly banded adjacent and parallel to the contact and consists of interlocking turbid feldspar subhedra (~200–500 µm), minor interstitial chlorite and rare quartz. About 10 mm inside the contact, the grain size increases and biotite as well as chlorite is present, but quartz remains relatively uncommon. There is little evidence for magma mingling,

but quartz and possibly feldspar from the granitic country rock have been partly digested by the dolerite, and the granite may have been locally remelted within a few mm of the contact.

The samples resemble those from the dyke at Carp Bay (NJ476, FP21) except for the presence of quartz, which probably reflects their slightly higher SiO_2 content (Table 6)

Friendly Beaches area

Several NNW-trending dolerite dykes were mapped by D. J. Jennings intruding Coles Bay Granite (but not the overlying Permian sedimentary strata) south of the Friendly Beaches (Jennings, 1984; Bacon, 1984, 1991). The dykes crop out poorly inland and no coastal outcrops are known.

Freshwater Lagoon (NJ438)
Sporadic cobbles and small boulders of weathered grey-green dolerite, together with pink medium- to fine-grained granite country rock occur about 1.3 km west of Freshwater Lagoon (~606110mE, 5341720mN).

A sample (NJ438) is a coarsely ophitic intergrowth of turbid plagioclase (≤3 mm), pink titaniferous augite partly replaced by finely fibrous yellow-green actinolite and dark green chlorite, and large (≤1 mm), equant or irregular to elongate opaque grains. Interstitial patches of black glass, containing microlites of augite replaced by actinolite, between coarse plagioclase grains, suggest that slow cooling was followed by sudden quenching.

Middleton Creek tributary (NJ442)
Weathered dolerite float was also noted on the eastern side of a small tributary of Middleton Creek (FP06604019).

A thin section is a coarsely ophitic dolerite, closely resembling sample NJ438. Some fresh augite remains, and the larger opaque grains (≤2 mm) appear little affected, but plagioclase is completely altered, and chlorite and actinolite are partly oxidised. Epidote is also present.

Bicheno area

Three mafic dykes in the Bicheno area were previously mapped and sampled by Cocker (1977), but no further details were given.

Cape Lodi NJ440, NJ441, B15a, B15b, B36)
Near coastal cliffs about 300m north of Cape Lodi (FP09395799)(~609390mE, 5357990mN), an in-weathering dolerite dyke about 1 m wide and trending at 180W75 occupies a deep cleft, 2–4 m deep, within Bicheno Granite. The dyke extends northward to the base of the hill slope (FP09395801), where it has a more NNW-trend and a chilled margin was observed at its western contact. To the south it traverses the shore platform for about 50 m to disappear offshore at FP09395796, but the same dyke almost certainly reappears on the north side of Cape Lodi (FP09385782). Here, although largely concealed by granite boulders, it is probably also ~1 m wide with irregular margins. On the south side of the Cape (FP09365765), a prominent joint within the granite is present along strike, suggesting that the dyke pinches out, but sporadic dolerite cobbles suggest that it is at least locally present (J. L. Everard, field notes).

Samples (NJ440, NJ441) are coarse-grained dolerites with turbid plagioclase laths typically 250 µm to 1 mm, but ranging up to phenocrysts of 3 mm; a very large (~14 mm) rounded tabular, largely altered plagioclase megacryst is probably a xenocryst derived from the host granite. Intergranular prisms (≤400 µm long) and granules of pink titaniferous augite are partly altered. Some interstitial patches (~1 mm) of dark green chlorite show distinct crystal outlines and are probably pseudomorphs after olivine, whereas others appear to be subspherical amygdales. Finely acicular opaque grains (100–200 µm long) are partly altered to fine-grained titanite. A large (10 mm) irregular amygdale is filled with well crystallised pale yellow epidote, a finely granular isotropic mineral (possibly hydrogrossular) and minor carbonate.

Samples collected by J. D. Cocker (B15a, B36) are similar, slightly finer-grained dolerites with zoned plagioclase megacrysts (≤12 mm in B36) in an intergranular groundmass of plagioclase, titaniferous augite and abundant chlorite. Sample B15b is a chilled dolerite with aligned plagioclase phenocrysts (≤1 mm, sparse) and plagioclase laths (~200–500 × 20–50µm) and equant aggregates (50–150 µm) of strongly pleochroic (green to yellow) chlorite, which grade down to a very fine-grained mesostasis probably of plagioclase, actinolite, chlorite and titanite.

An analysis (sample NJ441) is noteworthy mainly for its rather high K_2O (2.70%) and Rb (287 ppm) contents.

Bicheno Blowhole (BD2A)
An in-weathering black dolerite dyke occupies a deep cleft in the shore platform about 110 m south of the

blowhole. The host rock is coarse-grained, porphyritic to megacrystic Bicheno Granite. Most of the exposure is subject to strong wave action and partly obscured by granite boulders, but the dyke is at least 2.5 m but less than 4 m wide, and trends offshore at about 155°. Inland, it tapers and probably pinches out beneath beach boulders. The total exposed strike length is ~30 m. Contacts, where exposed, are sharp with chilled margins and locally follow joints in the host rock, at one place forming an irregular tapering finger extending for about 2 m into granite. Sparse feldspar phenocrysts (≤ 10 mm) are present. (J. L. Everard, field notes). This dyke has also been described by Hunns (1982).

In thin section (sample BD2A; Fig. 8i) it consists of a seriate but mostly medium-grained, slightly subophitic intergrowth of plagioclase laths (≤3 mm but mostly 500 µm to 1 mm), titaniferous augite platelets, pale green chlorite probably partly after olivine, and numerous small acicular opaque grains (50–200 µm) partly altered to titanite. It resembles the Cape Lodi dyke petrographically and chemically, except for minor textural differences and lower K_2O and Rb.

Governor Island (The Gulch) (B1, B33)

Cocker (1977) indicated a N- to NNW-trending mafic dyke within granite on the western side of Governor Island at Bicheno. Although not re-visited by the present authors, it is clearly visible from the Esplanade (about 250m away) as a black body a few metres wide, about 200m from the northern tip of the island (~608780mE, 5363370mN).

In thin section, a sample (B1) collected by P. L. F. Collins consists of a rather altered intergranular to subophitic intergrowth of turbid plagioclase (≤ 2 mm but mostly ~1 mm long), titaniferous augite, pale green chlorite (partly after olivine) and finely acicular opaques partly altered to titanite. Prehnite is identifiable as an alteration of plagioclase, and some secondary carbonate is present. A similar sample (B33) collected by J. D. Cocker contains corroded plagioclase phenocrysts (≤3 mm) and a large (~10 mm) corroded K feldspar xenocryst with reaction rims of chlorite and epidote. A large (0.5 mm) possibly xenocrystal opaque grain is surrounded by well-crystallised titanite.

It closely resembles, both petrographically and chemically, the dolerite at the Bicheno Blowhole about 1 km to the SSW, but is unlikely to be same dyke unless it is offset by unrecognised faults.

St Helens area

Arm Creek (B135, NJ480)

At Arm Creek, about 8 km northwest of Scamander, a dolerite dyke striking at about 050° has intruded along the line of the Orieco Fault, a sinistral wrench displacing the Mathinna Supergroup (Worthing & Woolward 2010).

Both thin sections (Fig. 8h) are of coarse- and fairly even-grained dolerite consisting of mainly interlocking (consertal) turbid plagioclase and partly uralitised clinopyroxene. Some plagioclase occurs as large (≤ 2 mm), roughly equant plagioclase grains, but mostly it forms broad laths (500 µm to 1.5 mm × 200–400 µm). It invariably contains numerous tiny inclusions of, or is partly replaced by, prehnite and possible epidote. Clinopyroxene occurs as colourless subhedra (typically 200–400 µm) across, which range to pale purplish to brown when incipiently altered; about 40% is replaced by yellow-brown to khaki-green actinolite. Opaque minerals are large (400–800 µm) equant angular anhedral, less commonly skeletal or elongate. Small (≤ 200 µm) interstitial anhedral of clear quartz are also present. Green chlorite, minor epidote and minute grains of titanite are also present as secondary minerals.

In the same area, dolerite dykes were mapped near the Orieco Mine (~599900mE, 5413500mN) by McClenaghan et al. (1987), and mentioned at (~602400mE, 5415900mN) by Walker (1957), but attempts to re-sample them have been unsuccessful. These occurrences correspond to an ENE-trending magnetic lineament and may represent a single dyke subparallel to and ~1 to 1.5 km SE of the Arm Creek dyke.

Dianas Basin (NJ446)

South of St Helens, about 1.2 km north of the outlet of Dianas Basin, a mafic dyke about 1 m wide and striking about 080° discordantly intrudes southwest dipping and facing (~132SW70) medium-bedded fine-grained siltstone and sandstone of the Mathinna Supergroup. Dyke margins are locally irregular. The rock (sample NJ446) is dark grey to black with abundant (several per cm2) small (1–3 mm) feldspar phenocrysts (J. L. Everard, field notes).

In thin section, the rock has a microgranitic rather than doleritic texture. Numerous large (1–3 mm) broad corroded phenocrysts of turbid plagioclase lie in a very fine-grained groundmass (~10–20 µm), which appears to consist mainly of brown biotite, plagioclase and at least some quartz. There are some large patches of fine-

grained biotite, several millimetres across, which are probably recrystallised biotite phenocrysts. A few larger (50–150 µm) laths of plagioclase are present. There are also abundant, formless blebs (10–20 µm) of turbid titanite, minor anhedral apatite and accessory finely acicular apatite. The chemical composition (Table 6) is consistent with a mineralogy dominated by plagioclase and biotite, with minor quartz and potash feldspar.

Onion Creek (NJ447)

On a small headland about 300 m further north, just south of the mouth of Onion (formerly Stinking) Creek another, wider (~4 m) dolerite dyke trends northeast (~040°). It has chilled margins against both east-dipping (~010E45) Mathinna Supergroup and a small apophysis of granodiorite, and is therefore younger than both. To the southwest, on the inland side of the headland, it terminates abruptly close to a major generally north-trending contact between the Mathinna Supergroup (to the east) and the main body of George River Granodiorite (to the west). This dyke contains abundant small (≤ 500 µm) feldspar microphenocrysts (J. L. Everard, field notes).

The rock is a rather fine-grained and altered dolerite, consisting mainly of a meshwork of turbid feldspar laths (~200 µm) intergranular yellow to khaki-green granules of uralitised clinopyroxene, abundant generally equant opaques (typically 50–100 µm, but rarely over 1 mm across) and clear interstitial quartz anhedra. Possible relict unaltered clinopyroxene is rare. Some secondary titanite and carbonate is present. There are also a few amygdales up to 1 mm across, filled with carbonate and sometimes euhedral quartz.

This dyke was briefly mentioned by Walker (1957), and a previous major element analysis (sample 41701) published by Cocker (1977, p. 143) is probably also from this body.

Burns Bay, via St Helens Point (SHP)

A vertical dyke of black aphyric dolerite, about 14 m wide and trending at 020º, intrudes the Akaroa Granodiorite on the foreshore about 70 m northeast of the boat ramp at St Helens Point (McClenaghan et al. 1987, 1992). A strong linear aeromagnetic anomaly with the same trend suggests that the dyke extends SSW across the peninsula to Maurouard Beach (~611900mE, 5427300mN). It may continue, partly offshore and offset by several cross-faults, to the Arm Creek locality (see above), as samples are compositionally very similar (Table 6).

The rock consists mainly of interlocking broadly oblong grains of slightly turbid plagioclase (≤ 2 mm long), generally smaller subhedra and glomerocrysts of clear to slightly brownish augite (mostly ≤ 500 µm), together with abundant pale green to pale yellow pleochroic chlorite (≤500 µm). There a few clear interstitial anhedra of quartz (generally ≤ 200 µm) and a very little mesostasis of turbid possible potash feldspar or perthite. Abundant relatively large (mostly 150- 300 µm, but one ~3 mm × 1 mm) opaque grains are equant to less commonly skeletal, generally fresh or less commonly show marginal alteration to turbid titanite. Plagioclase generally contains numerous tiny splintery inclusions of probable prehnite. Other secondary minerals, usually associated with chlorite, include finely fibrous actinolite, a few small grains of epidote (≤100 µm) and traces of secondary carbonate. A veinlet, 150 µm wide, of well-crystallised prehnite transects the thin section.

Grant Point (NJ508, MSH91, MSH172)

A dolerite dyke intruding the Grant Point Granite is exposed on the foreshore, about 2 km east of Binalong Bay (McClenaghan et al. 1992). The dyke, which occupies an in-weathering cleft in the granite, is subvertical, about 1.6 m wide and can be traced for about 20m with an overall strike of ~005°. To the north, where it disappears offshore, the strike veers to 170/350°, and to the south it diverges to about 160E85 before disappearing beneath granite boulders. The dolerite is black and aphyric, and contacts are sharp with chilled margins against the granite, with no sign of mingling. Within the dolerite, a set of rather poorly developed joints 100 - 200 mm apart tends to parallel to dyke walls, but also locally diverge or anastomose, and there is also a perpendicular set of cross-cutting joints perpendicular (J. L. Everard, field notes). There is apparently no associated aeromagnetic anomaly.

In thin section, samples (NJ508, MSH91) display a fine-grained, dominantly intergranular texture, and consist mainly of interlocking unoriented laths of plagioclase (typically 150–500 × ~100 µm) and clinopyroxene granules (typically 50–200 µm across), partly replaced by sericite and “uralite” respectively, together with equant to elongate opaques and a brown turbid altered mesostasis. In some slightly coarser-grained areas, a relict ophitic texture is preserved, with plagioclase laths enclosed by platelets of uralitised clinopyroxene. Sparse “ghost” phenocrysts up to 2 mm across, probably after clinopyroxene, are largely replaced by very fine-grained yellow-green actinolite. Composite glomerocrysts, up to 1 mm across, consist of several (typically 5–10) grains of

mostly fresh clinopyroxene and plagioclase. Scattered plagioclase phenocrysts (500 µm–1.5 mm), more equant in form than the groundmass plagioclase and typically have mottled cores with abundant melt inclusions and narrow clear rims. A few anhedral and embayed quartz xenocrysts (1 - 3 mm across) are surrounded by narrow (~100µm) reaction coronas. The quartz and feldspar xenocrysts are probably derived from the granite country rock.

Roses Tier area

East of Cascade Creek (R1084)

At least two outcrops, up to 10 m wide, of a dark to medium grey massive dolerite dyke were noted on a small ridge about 700 m south of the Upper Blessington Road. The dolerite is finer-grained towards the contact with the coarse-grained granite country rock (Russells Road Granite), and a dyke trending approximately 080° for at least 350 m is inferred. Sparse small feldspar phenocrysts, rare large crystals of black amphibole (up to 20 × 5 mm) and irregular xenoliths of granite are present (M. P. McClenaghan, field notes; McClenaghan et al., 1993). It may be associated with a weak linear magnetic anomaly with a similar orientation (~070°), resolvable for about ~4 km on the first vertical derivative image.

In thin section, a sample (R1084; Fig. 8t) contains a few slightly corroded megacrysts (≤4 mm) of plagioclase and possible orthoclase in a fairly even-textured groundmass of interlocking euhedral to subhedral hornblende prisms (≤3 mm long), tabular and strongly zoned plagioclase and orthoclase (typically 500 µm to 2 mm × 150–500 µm), subordinate ragged biotite (≤400 µm), minor quartz and sparse small (50–150 µm) equant to irregular, angular opaques. Hornblende is optically negative and pleochroic (α and β pale yellow-brown, γ medium-brown or sometimes dark olive-green at rims), whereas biotite displays pleochroism from very dark brown to pale yellow-brown.

Mount Scott area

South of Valentine Rivulet (SB27)

A small patch of spheroidally weathered “basalt” was noted a small hill ~1.6 km ESE of Mt Scott and just south of Valentine Rivulet (M. P. McClenaghan, field notes). Although not shown on geological maps, the locality is just west of the contact of the western contact of the Russells Road Granite, within a 2–3 km-wide screen of hornfelsed Mathinna Supergroup separating the Diddleum Granodiorite from the rest of the Scottsdale Batholith. There is no clearly associated magnetic anomaly, although there are a series of poorly defined ENE-SSW (~070–080°) trending magnetic lineaments throughout much of the southern part of the Scottsdale Batholith.

In thin section (SB27), the rock contains plagioclase phenocrysts (≤3 mm × 500 µm) grading down to an altered, dominantly intergranular groundmass of plagioclase laths (typically ≤ 200–400 µm long), relict pale purplish-brown clinopyroxene largely replaced by a fine-grained aggregate of pale yellow actinolite, abundant acicular opaque grains (typically 100–250 × 10–20 µm) and minor interstitial anhedral quartz. There are also a few altered pseudohexagonal phenocrysts of possible former olivine, now replaced by finely fibrous talc.

Pyengana area

North George River (AJ807)

A probable dyke of very tough, fine- to medium-grained massive dolerite crops out in a small steep gorge of the North George River, about 3 km northeast of Seaview Hill. Contacts with the country rock, medium- to coarse-grained hornblende-biotite granodiorite (Pyengana Granodiorite) are irregular, but the dyke possibly strikes at ~50°, roughly parallel to the local direction of the river.

There is no clear associated magnetic anomaly on the 2008 survey. A strong negative anomaly related to Eocene basalt to the south, weaker anomalies related to the commonly magnetite-bearing Pyengana Granodiorite, and possibly the ruggedness of the terrain may have obscured any response.

In thin section, abundant laths of plagioclase (mostly about 500 × 150 µm, but grading to microphenocrysts (≤1.5 mm × 200 µm) are generally turbid, but multiple twinning is commonly preserved. The altered fine- to medium-grained groundmass also contains intergranular, largely uralitised clinopyroxene, now brownish-yellow to green actinolite. Some pseudomorphs after probable clinopyroxene microphenocrysts (≤500 µm) are recognisable. Narrowly elongate to acicular opaque grains (100–300 × 10–50 µm) are abundant and show slight to incipient marginal alteration to titanite. There are rare small (~50 µm) anhedra of clear quartz.

Waratah Creek tributary (AJ914)

A small outcrop of tough dark blue-grey medium- to coarse-grained dolerite was located in the bed of a

steeply descending minor tributary of Waratah Creek, about 4.5 km NNW of Pyengana. Contacts with the host Poimena Granite, which crops out a short distance upstream, are not exposed. Although there is no clear corresponding magnetic anomaly, there are several weak to moderate linear anomalies with a trend of about 50° in the immediate area, some of which are associated with mapped dolerite dykes.

In thin section, the rock has a well-preserved subophitic texture, and consists of large (500 µm to 1.5 mm × 150–300 µm) fairly fresh plagioclase laths, intergrown with more equant grains of pale pink augite (≤ 1 mm across), which are 60–70% uralitised to pale yellow-brown to green actinolite. Equant angular opaque grains (≤ 500 µm) are abundant, but under strong illumination are seen to be largely (~95%) replaced by turbid titanite.

Blue Tier area

Crowther Creek (NJ455)

Float of well-jointed blue-grey dolerite, together with granite, occurs in a disturbed area on Blue Tier, about 1.2 km NNW of Poimena near the confluence of Crowther Creek and the Wyniford River. In thin section it is a medium-grained dolerite consisting of mainly of tabular plagioclase (0.5–1.5 mm long) and intergranular "uralitised" pseudomorphs after clinopyroxene, now wholly replaced by yellow to green pleochroic actinolite, in turn partly oxidised to orange-brown alteration products. There are also small ragged flakes or orange-brown pleochroic biotite intergrown with, or marginal to, former clinopyroxene, elongate to acicular opaque grains (~250 µm to 1 mm long) and traces of interstitial quartz.

Weldborough Pass (NJ454, JR66, JR26)

Float of dark grey dolerite occurs in cuttings of the Tasman Highway about 900 m northeast of Weldborough Pass. In thin section (NJ454) it is a medium-grained dolerite consisting of interlocking (consertal) to subophitic tabular plagioclase (typically 0.5–1.5 mm × 150–500 µm), largely altered, more-or-less equant clinopyroxene (~ 500 µm), elongate to acicular opaques (typically 0.5–1 mm × 30–100 µm) and traces of interstitial quartz. Some fresh pale pink clinopyroxene (titaniferous augite) is present, but most is "uralitised" to actinolite.

At least two samples were also collected from this locality by J. McClenaghan. No section of the analysed sample (JR66) is available, but JR26 (74/518) is a "uralitised" coarse-grained dolerite closely resembling NJ454. Unaltered clinopyroxene is rare and traces of quartz are also present.

Mt Paris Road (MR136)

Collected near the western contact of the Pyengana Granodiorite, this rather altered dolerite consists mainly of plagioclase laths (~0.5–1.5 mm long) with a fine-grained interstitial mesostasis of finely fibrous actinolite and small, rather sparse opaque grains. There are also scattered equant phenocrysts (~0.5–1 mm across) with crystal outlines suggesting former clinopyroxene, which is now replaced by an intergrowth of pale red-brown pleochroic biotite and colourless tremolite-actinolite.

East of Lottah (MBT210, MBT219, MBT220)

These samples, none of which were analysed, are relatively coarse-grained, ophitic textured dolerites with completely "uralitised" clinopyroxene. They resemble NJ454 and NJ455, although their opaque phase is generally equant to skeletal, and none appear to contain any quartz.

Sample MBT220 is an ophitic-textured dolerite consisting mainly of incipiently altered, randomly oriented, slightly sericitised plagioclase laths (≤3 mm) and completely altered clinopyroxene, replaced by fibrous yellow-green pleochroic actinolite ("uralite") with some margins of brown hornblende. Angular, equant to finely skeletal opaques (≤400 µm long) are present. Samples MBT210 and MBT219 are similar, although ophitic texture is less well-developed.

Rocky Creek, northern Blue Tier (JR65, JR13)

Several NE-trending dolerite dykes and isolated outcrops of uncertain trend are mapped in the McGoughs Lookout area on the northern part of Blue Tier. An analysed sample was collected from Rocky Creek (JR65), and a thin section (JR13, 74/510) from the same locality is a medium-grained dolerite with an intergranular to subophitic texture. Randomly oriented blocky plagioclase phenocrysts (≤2 × 1 mm) grade downward to more elongate laths (typically 400 µm to 1 mm × 50–100 µm). Sparse corroded phenocrysts (≤2.5 mm) of former clinopyroxene and/or possibly olivine are completely replaced by very fine-grained actinolite. Interstitial clinopyroxene is also almost completely uralitised to pale yellow to pale green pleochroic actinolite, which varies in grain size from relatively coarsely fibrous (≤200 µm) to almost cryptocrystalline. Colourless unaltered clinopyroxene is rare. Opaques are equant (~80–200

µm) across, or less commonly irregular, skeletal or somewhat elongate. No quartz is identifiable.

South of Sun Flats Road (MBT225- Jurassic)
This sample, collected about 2.7 km northeast of Lottah, is assigned a Jurassic age on petrographic criteria. It consists of subhedral platelets (≤1.5 mm) of essentially unaltered colourless clinopyroxene (both biaxial augite and virtually uniaxial pigeonite), much smaller plagioclase laths (~200–400 µm) and dark poorly crystalline interstitial patches rich in fine-grained opaques ("black glass"). Clinopyroxene ophitically encloses some of the plagioclase laths. Possible lag deposits containing boulders of similar Jurassic dolerite are mapped a short distance away in the Sun Flats Road area.

Tebrakunna Road area

In this area about 10 km east of Pioneer, at least eight parallel dykes, with a trend of 035–040°, intrude the Poimena Granite, the Gardens Granodiorite and a narrow screen of Mathinna Supergroup hornfels. Seven thin sections, three of analysed samples, show considerable textural variation. This may due to different cooling rates between dyke margins and centres, but is difficult to demonstrate, as all samples have been collected from float. Hand specimens and thin sections for the two other analysed samples (BT28 and BT31) may have been lost.

MNET38, MNET 37 (Fig. 8b)
This fine-grained dolerite (MNET38) has a well-developed micropoikilitic texture. The groundmass consists of finely intergrown rather turbid, interlocking plagioclase subhedra (500 µm to 1.5 mm long but usually smaller), some strongly zoned alkali feldspar and numerous patches of polycrystalline quartz, typically 200–400 µm across with locally development of micrographic texture. Plagioclase in particular contains very abundant inclusions of pale pink clinopyroxene, typically as tiny prisms (100–200 µm long by 20–40 µm across). Acicular opaques (300 µm to 1.5 mm long × 10–40 µm wide) are abundant throughout. There is minor replacement of clinopyroxene by pale green actinolite and chlorite.

Sample MNET37, collected from the same dyke along strike about 650 m to the northeast, is virtually identical.

MNET36
This relatively coarse-grained dolerite has a well-developed subophitic to ophitic texture. Plagioclase laths (500 µm to 2 mm × 150–400 µm) are partly enclosed by platelets (1–2 mm across) of pale pink clinopyroxene (biaxial positive augite). Scattered equant angular opaque grains, typically 150–400 µm across, and rare interstitial quartz, are also present. There is some replacement and oxidation of augite to fine-grained khaki green-brown to orange-red alteration products.

NJ453
A small area of Tertiary basalt is indicated near this locality, about 400 m north of Tebrakunna Road, on the Blue Tier 1:50 000 sheet (McClenaghan & Williams 1985). On re-investigation in 2010, only cobble float of dark grey fine-grained aphanitic dolerite, together with granite, was located. It is likely that the rock was originally misidentified.

In thin section (NJ453; Fig. 8a) the rock displays a microporphyritic texture. Euhedral to less commonly embayed phenocrysts and microphenocrysts of plagioclase, up to 3 mm × 0.5 mm with melt inclusions, but more typically narrow laths (~1 mm × 300 µm), show a preferred orientation to define a flow lamination. Subordinate, generally euhedral microphenocrysts of clinopyroxene, up to 500 µm but usually 100–200 µm across are sometimes fresh but commonly replaced by a pale yellow-green finely fibrous intergrowth of actinolite and chlorite. The very fine-grained felted groundmass probably consists of plagioclase microlites (~20–50 µm) and fuzzy fibrous actinolite aggregates after clinopyroxene, speckled with abundant equant opaque blebs (2–5 µm). This sample may be from the marginal, chilled part of a dyke.

MNET35
Although collected from very close (~20 m) to NJ453, this sample is texturally quite different. Fewer, larger (≤2.5 mm) and more turbid plagioclase phenocrysts and rare altered pseudomorphs (≤1 mm) of yellow-green chlorite and actinolite, possibly after clinopyroxene, lie in a turbid, less fine-grained groundmass. This consists of plagioclase laths (mostly ≤500 µm long), intergranular pale pink clinopyroxene granules (50–100 µm), equant opaques (~40–80 µm), pale yellow-green chlorite and traces of quartz as rare interstitial anhedra (≤100 µm).

MNET34
Collected about 120 m northeast of MNET35 and NJ453, this sample is a much coarser-grained, and may be from the interior of the same dyke. Relatively clear, corroded plagioclase phenocrysts (≤4 mm) with melt inclusions grade down to a coarse-grained subophitic groundmass of tabular plagioclase (typically 0.5–1.5

mm long), completely uralitised pyroxene (now fibrous yellow-green actinolite) and generally equant, angular (often pseudohexagonal) to skeletal opaques (typically 150–300 µm). Quartz appears to be absent.

MNET33

This sample, collected from a parallel dyke about 200 m to the east, contains turbid plagioclase phenocrysts (≤4 mm), clinopyroxene phenocrysts (≤2 mm) now largely replaced by green chlorite and/or yellow-green actinolite, but with rare fresh cores; and a few very corroded quartz xenocrysts (≤1 mm) with reaction halos. The rather turbid, relatively fine-grained groundmass consists of plagioclase laths (mostly ≤500 µm), almost completely uralitised clinopyroxene, more-or-less equant opaques (mostly ≤100 µm) and relatively abundant interstitial anhedral quartz.

Ansons River-Ansons Bay area

At least two petrographic types, dolerite and "andesite", are present in this area.

Dolerites

The first type is usually coarse-grained and consists of a subophitic to ophitic intergrowth of very pale pink clinopyroxene (titaniferous augite?) and plagioclase, with minor opaque grains and rare interstitial quartz. Some variants are finer-grained with a mainly intergranular texture. Clinopyroxene shows varying degrees of "uralitisation" to fine-grained actinolite and chlorite. This type is doleritic in composition (~47–49 % SiO2). Most of the NE-trending dykes appear to consist predominantly or wholly of this type.

Bark Hut Marsh area (MNET17, MNET32, MBT44)

Although no dyke is mapped in this area, several boulders (≤1 m) of dolerite float were noted from three localities on cleared land, together with granodiorite country rock (M. P. McClenaghan, field notes). A NNE-trending (~030°) linear positive magnetic anomaly, similar to those coincident with mapped dolerite dykes elsewhere, lies about 350 m to the southeast. Two dolerite occurrences are approximately coincident with a small ellipsoidal (~450 × 250 m) negative magnetic anomaly. However, basanite float (with much higher magnetic susceptibility, ~32 × 10^{-3} vs ~0.6 × 10^{-3} SI) was also noted in the area, and therefore a Cainozoic plug is a more plausible source of the anomaly.

The freshest dolerite sample (MNET17) contains nearly euhedral to slightly corroded subhedral plagioclase phenocrysts (≤5 mm), grading down to a generally intergranular groundmass of plagioclase laths (mostly ≤500 µm), narrowly elongate clinopyroxene prisms (mostly ≤400 µm) and granules, mostly elongate opaque grains (≤600 × 60 µm), rare interstitial quartz and minute needles of apatite (typically a few hundred µm long but only 5–10 µm wide). The groundmass minerals are locally aligned to define a crude "fluidal" flow lamination of inconsistent direction. The section intersects a single corroded clinopyroxene phenocryst, 3.5 mm across, bearing numerous melt inclusions ("sieve texture"). Minor interstitial pale yellow-green actinolite and chlorite are present.

MNET32 is a similar rock with a more turbid intergranular groundmass with mostly incipiently altered plagioclase and clinopyroxene, with only minor yellow-green actinolite and pale green chlorite. The groundmass also contains elongate opaques (typically 250–500 × 20–50 µm) and traces of interstitial quartz and minute acicular apatite. In addition to plagioclase phenocrysts (≤4 mm, typically 2 × 1 mm), former olivine or clinopyroxene phenocrysts (1–2.5 mm across) are now completely replaced by finely fibrous khaki yellow-green "bowlingite(?)", possibly actinolite, chlorite and iron oxides.

MBT44 is a coarse-grained dolerite, similar to MBT32, characterised by aligned plagioclase laths (fluidal texture). A few large plagioclase phenocrysts lie in a turbid plagioclase-rich groundmass with fine-grained interstitial clinopyroxene, elongate opaque grains and traces of quartz. This sample was analysed (~51.6% SiO_2), and it may be petrographically and chemically transitional between the two types; i.e., a weakly contaminated dolerite.

Sampsons Creek area (MBT74, MNET16) (Fig. 8j)

A NE-trending (~045°) dyke is mapped for a strike length of ~4 km. The associated magnetic anomaly extends further southwest for at least 6 km, but to the northeast it is less well-defined.

A 'substantial' outcrop beside Ansons Bay Road, just north of Last River, is in thin section (sample MBT74) a coarse-grained consertal to subophitic dolerite. It consists of fresh pale pink clinopyroxene platelets (typically 1–2 mm across), interlocking with and partly enclosing turbid plagioclase laths (mostly ≤1 mm long), together with equant, angular to skeletal opaques (typically 200–400 µm) across, and interstitial pale green chlorite and minor actinolite.

Fairly abundant but small float fragments were noted beside a logging road near Sampsons Hill, along the anomaly 2 km to the northeast. A sample (MNET16) is, however, markedly different from MBT74. Narrow crudely aligned plagioclase microphenocrysts (≤1 mm × 200 µm) lie in a fine-grained intergranular groundmass of smaller plagioclase laths (typically 50–200 µm) long, ragged fragments of actinolite and possible chlorite, and opaque blebs (~5–10 µm) partly altered to titanite. Clinopyroxene and traces of quartz, ilmenite and mica were also detected by X-ray diffraction (Table 4). It closely resembles sample MBT73 (see below) and is probably also a chilled dolerite.

Pretty Marsh Hill (NNET13, MBT71)

A large dyke is mapped for a strike length of ~5.5 km northeast and southwest of Pretty Marsh Hill. Aeromagnetic data suggests that it extends further southwest for at least ~11 km, where boulders of dolerite (samples MBT30 and MBT176) were collected from two localities, although a continuous dyke was not evident from the initial field mapping.

Sample MNET13 is a coarse-grained dolerite with a subophitic texture. Pink titaniferous augite platelets (≤1.5 mm) are partly uralitised to yellow-green actinolite and pleochroic chlorite (α pale yellow, β and γ green). Rather turbid, commonly zoned plagioclase laths (≤2 mm) may be partly enclosed by augite platelets. Equant to irregular, angular to skeletal opaque grains (≤500 µm), minor interstitial quartz and accessory acicular apatite are also present. Actinolite is partly oxidised to khaki-brown alteration products.

Sample MBT71 was collected nearby, from outcrop on the southern spur of Pretty Marsh Hill. It is similar but slightly coarser-grained (particularly in plagioclase) and displays a consertal to slightly subophitic texture. Clinopyroxene platelets (≤1.5 mm) and large blocky plagioclase crystals (≤2.5 mm) with numerous melt inclusions are intergrown with smaller plagioclase laths (≤2.5 mm), equant opaque grains (≤500 µm) and rare small interstitial quartz anhedra. Plagioclase is locally turbid and secondary chlorite, actinolite and rare epidote are also present. The sample is slightly weathered with some oxidation.

Near Kangaroo Flat (MBT132)

Collected from the same dyke ~2.2 km along strike from Pretty Marsh Hill, this is a similar coarse-grained subophitic to ophitic dolerite. It consists of clinopyroxene platelets (≤2.5 mm); some blocky plagioclase (≤2 mm) with melt inclusions, grading to narrower plagioclase laths (500 µm to 2 mm long); equant to elongate, mostly skeletal opaques (mostly ≤500 µm) and minor quartz. Clinopyroxene is largely fresh, but plagioclase is extensively altered and secondary chlorite and actinolite are abundant.

Near Janeys Creek (MBT73)

The same dyke crops out here, ~1.6 km SSW of Pretty Marsh Hill. The contact with the Gardens Granodiorite is exposed and trends 040° vertical (M. P. McClenaghan, field notes). A thin section cut across the sharp contact shows a chilled dolerite with narrow plagioclase laths (~300–800 × 30–70 µm), aligned parallel to the contact. The groundmass is dark grey and cryptocrystalline within about 2 mm of the contact, but further away is slightly paler and fine-grained, fibrous, partly oxidised actinolite (≤50 µm) and tiny opaque blebs (≤5 µm) are resolvable. The adjacent granodiorite is a relatively fine-grained (~2 mm) equigranular of anhedral quartz, sericitised feldspar and altered and oxidised biotite. Within 0.5–1 mm of the contact, it has recrystallised to a finer-grained granophyric aggregate, presumably because of thermal effects.

Spurrs Rivulet tributary (MBT30)

Aeromagnetic data suggest that bouldery float at this locality, 5 km southwest of MBT73, is derived from the same dyke. In thin section it displays a coarse-grained, consertal to slightly subophitic texture. Clinopyroxene grains (≤1 mm) are mostly fresh, but plagioclase laths are large (1–4 mm) and very turbid and contrast with clear interstitial quartz anhedra (≤400 µm) which comprise 2–3% of the rock. Opaque grains are relatively large (~400 µm to 1 mm) and mostly equant but skeletal. Ragged grains of secondary actinolite, chlorite and epidote are abundant.

Northwest of Cliffords Road (MBT176)

Boulders of granite at this locality, a further 4 km southeast, represent the same dyke, which here has intruded the Poimena Granite. In thin section it is a rather altered and slightly oxidised coarse-grained dolerite with a predominantly intergranular texture, resembling MBT30. Some clinopyroxene is fresh, but plagioclase is very turbid. Large equant angular to skeletal opaques (400 µm to 1 mm), partly oxidised chlorite and actinolite and a few per cent quartz are also present.

West of Gripe Creek headwaters (MBT76)

Several outcrops of both dolerite and granodiorite were noted in this area, near a small stream draining

into Big Creek (M. P. McClenaghan, field notes). Four of the five "dolerite" samples collected belong to the andesite group (see below). Sample MBT76, however, is of a rather weathered, coarse-grained, subophitic dolerite, similar to many other dykes. It consists mostly of interlocking pale pink titaniferous augite platelets (≤ 1 mm), elongate plagioclase laths (≤1.5 mm), mostly equant and angular to skeletal opaques (≤200 µm) and minor quartz. Although the sample is rather oxidised, some fresh clinopyroxene is present. Elongate to acicular opaque grains are less abundant. There is some alteration of augite to finely fibrous actinolite and pale green chlorite, which in turn may be oxidised to bright orange alteration products.

Gripe Creek (MBT82)

Another large dyke lies about 800 m northwest of, and parallel to, the Pretty Marsh Hill dyke. Field mapping has demonstrated it continuity for ~1800m in the Gripe Creek- Big Creek area, but aeromagnetic data indicates its continuity southwestward for ~3 km along strike to a float occurrence south of Pretty Marsh (NJ471), and potentially for another ~13 km toward Blue Tier.

Toward the northeast end, the dyke crops out in Gripe Creek, intruding granodiorite. In thin section, a sample (MBT82) is a coarse-grained subophitic metadolerite with little-altered plagioclase laths (≤2 mm), but clinopyroxene is largely replaced by ("uralitised" to) a fine-grained aggregate of pale yellow to pale green actinolite. Opaque grains are mostly equant (≤400 µm) and angular to skeletal, or less commonly elongate to acicular. Quartz appears to be absent.

Big Creek area (MNET10)

This coarse-grained, ophitic to subophitic dolerite consists of pale pink titaniferous augite platelets (≤2 mm) partly enclosing plagioclase laths (≤2.5 mm long but more typically 0.5–1 mm; commonly strongly zoned) and mostly equant, angular to skeletal opaque grains (≤500 µm), together with rare interstitial quartz and possible alkali feldspar. Clinopyroxene is partly altered to fine-grained pale yellow-green actinolite and chlorite, and minor orange-brown biotite.

South of Pretty Marsh (NJ471)

Numerous boulders (≤1 m) and suboutcrop of very coarse-grained dolerite contains large blocky plagioclase phenocrysts (≤10 mm), grading down plagioclase laths (typically 0.5–1.5 mm) ophitically intergrown with very pale pink titaniferous augite platelets (≤2 mm), together with equant angular opaques (≤400 µm) and rare interstitial quartz. Plagioclase is commonly turbid and there is extensive replacement of augite by pale green chlorite, actinolite and their brown to orange-red oxidation products.

Lower Gripe Creek-lower Big Creek (MNET2, MNET 4)

These samples probably lie on another dyke 150–250 m to the northwest of the Gripe Creek-Big Creek dyke (MBT82-MNET10).

Sample MNET2 is a coarse-grained seriate to ophitic textured dolerite, consisting of plagioclase (0.3–3 mm), pinkish titaniferous augite platelets (≤1.5 mm) and large (≤4 mm) equant to irregular or skeletal opaque (ilmenite) grains. Augite is partly replaced by tremolite-actinolite, intergrown with minor biotite. XRD indicates that quartz is present (<2 wt %), although it was not identified in thin section.

MNET4 is a medium-grained, intergranular to subophitic-textured dolerite, consisting mainly of plagioclase laths (300–600 µm), pale pink titaniferous augite granules (200–400 µm), equant angular to skeletal opaques (ilmenite; mostly ≤100 µm), pale yellow to green tremolite-actinolite and minor pale green chlorite. Numerous round vugs (1–1.5 mm across) are filled with calcite or finely fibrous tremolite-actinolite. Quartz is absent.

Near tributary of Boggy Creek (MBT143)

Fragmentary float of dolerite here may be indicate a poorly exposed dyke, although there is no well-defined aeromagnetic anomaly. A sample (two thin sections) is a fine- to medium-grained intergranular dolerite with pale pink titaniferous augite prisms (≤500 µm long and 100–200 µm across), very turbid plagioclase laths (~500 µm to 1 mm long) and abundant equant opaques (~50–100 µm). One of the sections partly intersected two largely sericitised plagioclase phenocrysts, at least 4 mm long and up to 1.5 mm wide. Quartz is absent or nearly so. (However, one of the thin sections shows strong orange-brown staining due to oxidation, and the other is far too thin.)

Andesites

The second type contains sparse small phenocrysts of quartz, plagioclase and less commonly alkali feldspar and biotite in a fine-grained quartzofeldspathic ground-mass with actinolite and/or biotite. Many of the phenocrysts, particularly quartz, are strongly resorbed and surrounded by reaction haloes. This type is broadly andesitic in composition (typically 57–59 % SiO_2). Some of these samples are from small bodies, 50–200

m across, mapped as andesite ("Dn" on the Blue Tier 1:50 000 map; "Dgra" on the 1:25 000 digital coverage), but others are from NE-trending dykes, some of which also contain dolerite of the first type. It seems possible that the andesites are hybrid rocks related to the first type by assimilation of granitic country rock.

Northeast of Pretty Marsh (MNET12, MBT165)

Sample MNET12 (Fig. 8s) contains sparse small phenocrysts and xenocrysts of plagioclase, quartz, and alkali feldspar in a fine-grained foliated groundmass. Quartz anhedra (≤500 µm) are rounded, resorbed and surrounded by a narrow biotite-rich haloes. Plagioclase phenocrysts are mostly subhedral, weakly resorbed narrow to tabular laths (mostly ≤500 µm) long. Ragged, elongate to almost acicular fragments of dark red-brown biotite (≤1 mm) may be altered to chlorite. The groundmass mineralogy is difficult to resolve, but it appears to consist mainly of small narrow (50–150 µm) laths of plagioclase, pale brown to pale green splinters of actinolite, subordinate pale green chlorite and weakly pleochroic red-brown biotite, together with small equant (~20–50 µm) to less commonly more elongate opaque blebs. X-ray diffraction (Table 4) indicates that 5–10 % relict clinopyroxene is also present.

MBT165

This sample was collected within about 100m of, and resembles, MNET12. Plagioclase microphenocrysts (~200–600 µm) lie in a fine-grained groundmass bearing subspherical polycrystalline aggregates (≤400 µm across) of interlocking ~5–10 quartz anhedra. These structures have irregular margins and appear to be late stage segregations. The rest of the groundmass consists of plagioclase laths (typically ~100 µm), pale greenish-brown actinolite splinters, opaque blebs (~5 -10 µm) partly replaced by titanite, and minor chlorite.

Near headwaters of Gripe Creek (MBT75, MNET5, MBT77, MNET9, MBT97)

Sample MBT75 (Fig. 8r) contains sparse euhedral, blocky to elongate plagioclase phenocrysts (≤1 mm × 300 µm) and very turbid, equant oblong to elongate microphenocrysts (≤400 µm) of a former opaque phase, now finely granular titanite. The uneven felted groundmass contains diffuse very fine-grained bands or zones and ill-defined slightly coarser zones. It consists mainly of mainly narrow plagioclase laths (~100–200 µm) and narrow pale yellow-brown to pale green actinolite prisms (100–250 × 10–20 µm) which grade to brown hornblende. Small clinopyroxene granules, ragged fragments of pale green chlorite, minor biotite and interstitial quartz are also present.

Sample MNET5 from the same locality contains deeply embayed or corroded quartz xenocrysts (≤3 mm) as well as sparse microphenocrysts of plagioclase (≤1 mm × 150 µm) in a similar but slightly coarser-grained groundmass of plagioclase, actinolite, pale green chlorite, turbid opaques largely replaced by titanite, and interstitial quartz. Minor clinopyroxene was also detected by x-ray diffraction (Table 4).

Sample MBT77 from about 100 m away resembles the coarser-grained parts of MBT75. The quartz segregations are larger (≤1 mm across) and commonly irregular in outline. Sparse stubby plagioclase microphenocrysts (≤600 µm) lie in a similar groundmass of plagioclase laths, actinolite splinters, chlorite, interstitial quartz and small irregular to elongate opaque blebs largely replaced by titanite. Quartz veinlets are present.

Sample MNET9, from about 100 m southwest, is similar. Small plagioclase phenocrysts (≤ 1 mm), elongate former opaque phenocrysts (≤1 mm), now replaced by very fine-grained titanite, and chlorite microphenocrysts (≤700 × 140 µm) lie in a groundmass of plagioclase, actinolite, chlorite, turbid former opaques, interstitial quartz, possible alkali feldspar and possible granules of relict clinopyroxene.

Sample MBT97 was collected from a mapped dyke about 350 m further southwest. Sparse small corroded xenocrysts of quartz (≤200 µm) are surrounded by reaction halos, typically ~100 µm wide, of pale yellow-green to yellow-brown finely fibrous actinolite. The rest of the rock displays a weakly developed fluidal texture, with crudely aligned plagioclase laths (mostly 200–400 µm long) and actinolite fibres, together with fragments of chlorite, opaque grains largely replaced by titanite, and interstitial quartz. Plagioclase (≤1 mm), chlorite (500µm to 1 mm) and narrow former opaques (≤300 µm) locally attain microphenocryst dimensions.

Near Big Creek (MNET11, MBT98)

Sample MNET11 is a fine-grained, nearly aphyric rock, containing sparse small phenocrysts of plagioclase (≤1.5 mm) and chlorite (≤1 mm), which grade down to a groundmass also containing tremolite-actinolite, pale green chlorite, quartz and opaques (ilmenite) partly replaced by titanite.

Sample MBT98 (Fig. 8q) differs texturally from the other andesites, and is probably a chilled phase. Euhedral to slightly embayed subhedral plagioclase phenocrysts (≤2 mm, but mostly <1 mm) grade down to a groundmass of abundant plagioclase laths (typically 200–500 µm) with a very fine-grained mesostasis. A few small lath-like microphenocrysts of actinolite, possibly pseudomorphs after clinopyroxene, can be distinguished in the mesostasis, which probably largely consists of very fine-grained actinolite, together with small equant angular blebs (10–50 µm) and more elongate (rarely ≤500 µm) opaque grains. This is also a large (~4 mm) deeply embayed xenocryst of turbid plagioclase, mottled with numerous small altered melt inclusions, and partly enclosing two ragged fragments of red-brown biotite. The xenocryst is probably a fragment of the granodiorite country rock.

Pretty Marsh (MNET14)

This rather weathered sample contains a few small (≤250 µm) corroded quartz xenocrysts with narrow reaction halos, and rare microphenocrysts of pale green chlorite (≤1.5 mm × 250 µm). The rather oxidised groundmass consists largely of turbid feldspar, actinolite fibres, chlorite, elongate opaques replaced by very fine-grained titanite, and clear interstitial quartz.

Gripe Creek (MBT167)

Sample MBT 167 has a curious mottled appearance, with equidimensional but irregular darker and paler patches 5–10 mm across. The paler patches are granitic in composition, and consist of anhedral quartz (500 µm to 1 mm) and turbid, strongly zoned feldspar. The quartz grains are commonly corroded, and surrounded by reaction haloes of finely fibrous actinolite or biotite (?), now strongly oxidised to orange-red alteration products. The darker patches are finer-grained and doleritic, consisting of plagioclase laths (≤1 mm) and intergranular very turbid dark green to yellow-brown actinolite and abundant small (~50–100 µm) mostly equant opaques.

Coast ~2 km S of Policemans Point (NJ511)

Grey porphyry with rather sparse (<5%) and small (rarely 10 mm, mostly ≤5 mm) phenocrysts of quartz and feldspar crops out near high water mark at the end of a long sandy beach south of Ansons Bay (508255mE, 5451495 mN). Contacts with Mathinna Supergroup hornfels to the south and apparently on offshore rocks are not exposed, but body appears to be at least 20 m wide. On the Blue Tier 1:50 000 and 1:25 000 map sheets, derived from field work circa 1980, the outcrop is depicted as a dyke of Devonian quartz feldspar porphyry ~500 m long and trending at 020°. This could not be substantiated in 2016, possibly due to increased sand cover.

In thin section (sample NJ511; Fig. 8n), the fine- to medium-grained groundmass consists of randomly oriented, strongly zoned stubby plagioclase laths (≤2 mm but typically ~500 µm long), anhedral quartz, minor potash feldspar, ragged grains of tremolite-actinolite (nearly colourless or pleochroic from pale yellow to pale green), red-brown biotite and generally elongate small opaque grains. Corroded xenocrysts of quartz (0.5–5 mm, but typically 1–2 mm across) are surrounded by mostly narrow fine-grained reaction coronas of tremolite-actinolite, subordinate biotite and locally carbonate. Mottled, embayed xenocrysts (≤5 mm) of perthitic potash feldspar and plagioclase have partly reacted to biotite or are partly replaced by carbonate. The quartz and feldspar xenocrysts are probably of granitic origin. Secondary carbonate is also present adjacent to the quartz xenocrysts and within the groundmass.

The rock differs petrographically from the other andesites in the abundance of biotite and the slightly coarser-grained groundmass. An analysis (Table 6), with 55% SiO_2, has higher MgO, Ni and Cr suggesting a greater component of mafic material.

Other samples

Eddystone Road near source of Reeves Creek (MBT144) – Jurassic

The sample was taken from one of two large dolerite boulders beside Eddystone Road, not far from outcropping granite (M. P. McClenaghan, field notes). In thin section, the rock is a coarse-grained dolerite, consisting of fresh plagioclase and pyroxene, and some interstitial black glass. It texturally resembles Jurassic dolerite, which is also consistent with the presence of pigeonite. It seems possibly that the boulders have been transported, although the nearest outcropping Jurassic dolerite is more than 10 km away in the Rushy Lagoon-Cape Portland area.

Mt William area

North end of Purdon Bay (NJ364)

An unusual dyke with textures suggestive of inter-mingling of mafic and felsic magmas is exposed in the intertidal zone near the north end of Purdon Bay, intruding the Ansons Bay Granite. The body is about

2.8 m wide, trends at ~070°, and possibly dips steeply (70–80°) south. Contacts are sharp but slightly wavy on a scale of a few centimetres. The adjacent granite is very coarse-grained and equigranular-seriate, with feldspars up to 60 mm and abundant biotite, and contains rare finer-grained and more leucocratic autoliths, a few tens of centimetres across, with biotite-rich selvages. The margins of the dyke, inward for 50–200 mm from the contacts, are dark grey to black, very fine-grained to almost black, but the dyke rock generally becomes paler inward. Sporadic feldspar megacrysts, probably derived from the granite country rock, are present, particularly near the dyke margins. The interior of the dyke is very inhomogeneous, with diffuse irregular to wavy banding defined by darker finer-grained and paler less fine-grained zones. In places, textures within the dyke resemble those of soft sediment deformation, such as convolute bedding, scouring and flame structures. On the Eddystone 1:50 000 map (Baillie et al., 1984), the dyke is depicted as a raft of Mathinna Group ("SDs") within the granite.

In thin section, a sample (NJ364B) from the interior of the dyke contains abundant ragged flakes, typically 200–500 µm long, of biotite (pleochroic from very dark brown, through red-brown to very pale yellow-brown) within an uneven-textured (but typically 0.5–1.5 mm) quartzofeldspathic groundmass of subhedral microcline, anhedral quartz and minor subhedral plagioclase. Both quartz and microcline commonly enclose poikilitic inclusions of each other, and biotite, and there are interstitial micrographic intergrowths of quartz and feldspar. Rare flakes and ragged fragments of muscovite and accessory zircon, apatite and opaque minerals (rare, small and equant) are present.

Petrographically and geochemically (Table 6), the felsic component is dominant and the rock probably represents a minor late intrusive phase of the Eddystone Batholith. It is quite unlike the much more mafic dolerites of the Tebrakunna Dyke Swarm.

2.7 km E of Mt William (NJ423)

Sparse float of tough fresh blue-grey dolerite was noted near a former fence-line track within Mount William National Park. In thin section (Fig. 8d), it consists of a relatively clear, coarse-grained consertal to slightly subophitic intergrowth of plagioclase (1–3 mm), completely uralitised clinopyroxene (i.e., now actinolite), and abundant acicular opaques (typically 500 µm to 1 mm × 20–50 µm), together with a few per cent dark to very pale orange-brown biotite as ragged flakes intergrown with actinolite. Quartz and unaltered pyroxene are absent.

3.7 km SSE of Mt William (NJ262)

Scattered small boulders of pervasively weathered, dark maroon, fairly coarse-grained aphyric dolerite form a patch no more than a few tens of metres across, just north of a firebreak in the Mount William National Park.

In thin section, the rock consists of a coarse-grained interlocking (consertal) intergrowth of plagioclase (1–3 mm), partly oxidised uralitised pyroxene and abundant large (1–2 mm) equant to elongate opaques, with minor biotite and interstitial quartz. It resembles NJ423, but is more altered, opaque grains are larger and broader, and quartz is present.

These samples (NJ423 and NJ262) are petrographically and chemically similar (Table 6), strongly fractionated tholeiitic dolerites, lying ~3.4 km apart on the same weak NNE-trending magnetic anomaly, and may be from the same dyke. It is not clear why quartz is present in NJ423 only.

5 km S of Mt William (ER2)

This dolerite sample was collected in 1973 by P. Collins near Telegraph Creek. Attempts to re-locate the occurrence in 2008 were unsuccessful, although a 200 mm cobble of medium-grained aphyric dolerite was noted about 370 m to the west (~599550mE, 5465480mN).

In thin section, the rock (ER2) is a rather coarse-grained metadolerite with a turbid, consertal to slightly subophitic texture, consisting of partly altered plagioclase laths (500 µm to 1 mm), uralitised granules of former clinopyroxene (up to 2 mm, but usually smaller), now replaced by pleochroic pale yellow to deep green actinolite and minor chlorite, and angular to skeletal opaques. Traces of brown biotite are present, associated with actinolite and as small isolated grains. Quartz is absent.

Chemically, the rock is a strongly fractionated dolerite similar to NJ262 and NJ423, although it plots in the alkalic field due to slightly higher alkalis, and aeromagnetic data clearly indicates that it is from a separate dyke.

East side of Mt William (NJ245, MW1)

Sparse small angular boulders of dark grey to blue-green porphyritic dolerite lie beside Forester Kangaroo Drive, northeast of Mt William. Plagioclase phenocrysts up to 10 mm long are present.

Sample NJ245 (Fig. 8e) contains numerous plagioclase phenocrysts (up to 8 × 2 mm) grading down to an ophitic groundmass with largely uralitised clinopyroxene. The phenocrysts may be fresh and clear, but commonly are riddled, particularly around their cores, with numerous inclusions of fine-grained tremolite-actinolite, possibly originally melt inclusions. The groundmass consists of unoriented plagioclase laths (typically 300–600 µm long), partly or wholly enclosed in platelets (500 µm to 1 mm) of former clinopyroxene, now largely replaced by pleochroic, pale yellow to pale green, tremolite-actinolite, grading to brown hornblende. Some clear colourless unaltered clinopyroxene remains. Equant angular to skeletal opaque grains (100–150 µm) are also present. Quartz is apparently absent, nor was it detected by x-ray diffraction.

Another sample (MW1), collected by P. Collins 2.5 km to the SSW, lies on the same magnetic anomaly and is probably from the same dyke. In this section, it contains abundant euhedral to subhedral phenocrysts (≤8 mm) and glomerocrysts of plagioclase, with slightly ragged margins and numerous melt inclusions, in a subophitic to intergranular groundmass of pale pink clinopyroxene, largely altered to actinolite, plagioclase and opaques.

Both samples are similar unfractionated tholeiitic dolerites, although NJ245 has much higher K_2O and Rb (Table 6).

West side of Mt William (MW2)

This sample, collected by P. Collins, consists mainly of a relatively coarse-grained intergrowth of plagioclase laths (400 µm to 1 mm) and former clinopyroxene (≤2 mm), replaced by amphibole (fibrous colourless to pale yellow-green tremolite-actinolite with some better crystalllised pale brown hornblende) and colourless chlorite. Minor red-brown biotite is usually intergrown with tremolite-actinolite. Interstitial quartz (≤1 mm) is common. Sparse small (≤100 µm) equant to scaly opaques are partly replaced by finely granular titanite.

Upper Icena Creek (ER1, NJ401)

Scattered boulders (≤1 m) of dolerite lie beside a farm track on the "Telegraph" property, together with float of hornfelsed Mathinna Supergroup and granite (the latter possibly brought in). The dolerite consists of plagioclase phenocrysts (≤8 mm), some at least as calcic as An_{66}, in a blue-grey medium-grained aphanitic groundmass. In thin section (samples ER1, NJ401), the phenocrysts are seen to be subhedral, commonly with ragged margins, and grade down to a subophitic groundmass of smaller and narrower plagioclase laths (typically 500 µm to 1.5 mm long), pale pink clinopyroxene partly (~50%) replaced by actinolite, and opaque grains (≤500 µm) partly replaced by titanite. Minor chlorite and traces of secondary carbonate are also present.

Eddystone Road near "Telegraph" (NJ406, NJ407)

Granodiorite and dolerite crops out sporadically in paddocks on the southwest side of Eddystone Road, near and opposite the entrance to the "Telegraph" property.

A sample (NJ406) from a dolerite outcrop is very coarse-grained, consisting of plagioclase crystals (typically 1–3 mm long but up to 5 × 1 mm) subophitically intergrown with platelets of clinopyroxene (≤5 mm), now partly altered ("uralitised") to yellow-green actinolite. Opaque grains are typically angular or skeletal to somewhat elongate, mostly ≤5 mm long. A few plagioclase crystal show partial alteration to fine-grained prehnite, and more altered parts of the section contain some chlorite and fine-grained talc.

A more strongly porphyritic variant of the dolerite (NJ407) contains 5–10% megacrysts and glomerocrysts of plagioclase (≤ 10 mm) and subordinate, largely altered clinopyroxene and olivine (1–2.5 mm) in a fine- to medium-grained subophitic groundmass of plagioclase, clinopyroxene, actinolite and opaques. The plagioclase megacrysts are euhedral to subhedral, commonly slightly embayed, and fresh apart from numerous small altered inclusions, possibly melt inclusions. Although some are zoned, their optical properties indicate that some are at least as calcic as bytownite (i.e., $An_{>70}$). Some clinopyroxene and olivine megacrysts are fresh, but most are surrounded by reaction coronas of, and largely altered to, a very fine-grained aggregate of talc (?) and opaque dust, with a few fresh cores. Some "ghost' megacrysts consist entirely of this material, but have crystal forms suggesting former olivine. A few pseudomorphs, however, are now composed of actinolite and have crystal outlines clearly indicating former clinopyroxene. The groundmass consists of randomly aligned narrow laths of plagioclase (200–400 µm long), subophitically intergrown with granules and platelets of pink clinopyroxene (100–200 µm across), of which about 60-70% is replaced by pale yellow to pale green pleochroic fibrous actinolite. Equant to irregular of scaly opaques (≤80 µm) are common. Minor chlorite and traces of red-brown biotite (as shreds associated with actinolite) are also present.

Musselroe Road quarry (MUS, MR1)

A large dolerite dyke, possibly about 40 m wide, crops out in a disused quarry on the eastern side of Musselroe Road, northwest of Mt William. Deeply weathered dolerite, now a sticky orange clay, contains fresh rounded kernels, 0.5–1 m in diameter, of coarse-grained dolerite with sparse feldspar phenocrysts. Fine-grained sandstone (Mathinna Supergroup country rock) crops out on the northern edge and south-eastern corner of the quarry.

A thin section (MUS) shows sparse phenocrysts of plagioclase (≤4 mm) in a relatively clear intergranular groundmass of plagioclase, elongate prisms of former pyroxene (1–2 mm), equant to elongate or skeletal opaque grains, and minor quartz. Pyroxene is replaced to yellow-green "uralite", opaque grains partly altered to titanite or oxidised to dark red hematite, and pale yellow-green secondary chlorite is also present.

A second sample (MR1) is similar but coarser-grained, with plagioclase laths typically 1–1.5 mm but up to 3 mm long. Minor chlorite and traces of pale brown biotite and quartz are also present.

~2.5 km west of Mt William (EA11)

This sample, collected by P. W. Baillie, is a markedly porphyritic dolerite. Abundant large (≤4 mm) euhedral to slightly resorbed phenocrysts of plagioclase, commonly with melt inclusions, comprise about 25 vol % of the rock. They grade down through smaller (~1 mm) narrower laths, to groundmass plagioclase. Smaller (1–2 mm) and less abundant, equant to irregular phenocrysts of chlorite (pleochroic from pale yellow-green to colourless) are probably pseudomorphs after resorbed olivine. The chlorite contains aligned feathery elongate to dendritic inclusions of an opaque phase (magnetite?). There are also a few microphenocrysts (≤500 µm) of uralitised clinopyroxene. All lie in a fine-grained groundmass with a relict intergranular texture of plagioclase laths (typically 150–250 µm), pleochroic yellow-green actinolite after clinopyroxene, minor chlorite, and abundant equant angular (50–150 µm) to elongate opaques, partly replaced by titanite. Unaltered clinopyroxene and quartz are absent.

The locality lies about 2 km south of and approximately along strike from the Musselroe quarry outcrop (MUS, MR1), but in view of the petrographic and chemical differences (Table 6) with those samples, it is doubtful that this sample is from the same dyke.

Musselroe Road ~4 km south of Musselroe Bay township (NJ420, MR3, MR2, NJ422, EE6)

Several subparallel N- to NNE-trending dolerite dykes are mapped in this area, although outcrop is poor. The orientation of several dykes is inferred from aeromagnetic data, but survey resolution and anomaly magnitude are insufficient to resolve and separate them with confidence

Sporadic cobble-sized float of blue-grey medium-grained dolerite containing sparse feldspar phenocrysts occurs on the southern side of a small spur road (~599230mE, 5474260mN). In thin section (sample NJ420), plagioclase laths (typically 500 µm to 1.5 mm × 150–300 µm) are subophitically intergrown with former clinopyroxene platelets (mostly 300–800 µm) across, now largely (~80%) "uralitised" to pale yellow to pale green finely fibrous actinolite, which is intergrown with minor brown biotite. There is some relict but turbid pale pink clinopyroxene. Opaque grains (mostly 100–200 µm but up to 500 µm) are equant to ragged and irregular. Sample MR3, collected from the vicinity by P. Collins and probably from the same dyke, is similar but slightly coarser-grained with some plagioclase grains up to 3 mm long.

A poorly located sample (EE6 = 85/274) from this area similarly consists of sparse plagioclase phenocrysts in a coarse-grained subophitic groundmass of slightly sericitised plagioclase (≤1 mm), uralitised clinopyroxene and relatively large (100–200 µm) equant to skeletal opaques. It resembles NJ420 and MR3, but is more weathered with some orange brown oxidation of actinolite.

Another dyke is mapped about 200 m to the east. Sample MR2, collected by P. Collins, is a coarse-grained metadolerite with a relict subophitic to ophitic texture, largely consisting of uralitised clinopyroxene partly enclosing plagioclase laths (≤2 mm), and equant to skeletal opaques. Some rather turbid, relict clinopyroxene is preserved. A large plagioclase megacryst (~7 mm) has ragged margins, but lacks reaction rims.

A further 200 m to the east (~5996400mE, 5474140mN), float boulders (≤0.5 m) of similar blue-grey dolerite lie in paddocks and adjacent scrub, and probably indicate another subparallel dyke. In thin section (sample NJ422), the rock is a medium-grained dolerite with a predominantly intergranular texture, consisting of plagioclase laths (400 µm to 1 mm), almost completely uralitised clinopyroxene and elongate to acicular

opaques. A fine-grained part of the section grades into a poikilitic-textured zone, in which abundant disoriented acicular fibres of actinolite, several hundred µm long but only 5–20 µm wide, are enclosed in large (several mm) platelets of plagioclase.

George Rocks (GR6 = 43954; PE11 = 85/281)

This series of low lying islets, located about 8 km north of Eddystone Point and ~3 km offshore, consist predominantly of granite which, on the largest islet, is intruded by a "lamprophyre dyke" (Baillie 1984, 1986).

A sample collected by J. D. Cocker (GR6; Fig. 8v) contains sparse small phenocrysts of clinopyroxene (≤ 1 mm, mostly ≤0.5 mm) in a rather turbid intergranular groundmass of aligned, largely altered, plagioclase laths (200–500 µm × 50–100 µm), colourless clinopyroxene granules and granules and prisms of pleochroic (colourless to deep yellow-brown) hornblende. Equant angular opaque grains (25–75 µm) are abundant. There are a few irregular amygdales (≤0.5 mm across) of carbonate and much interstitial very fine-grained dark brown alteration.

Sample PE11 is similar but in parts less oxidised, with some interstitial finely granular pale green chlorite and finely fibrous actinolite.

Baillie (1984, 1986) correlated this body with Cretaceous dykes ("lamprophyres"), lavas and small intrusions at Cape Portland and elsewhere in northeast Tasmania, which are of shoshonitic composition (Jennings & Sutherland, 1969; McDougall & Green, 1982). The samples described above are, however, atypical of the shoshonites, e.g., in lacking large hornblende phenocrysts. Zwingmann et al. (2004) reported a K/Ar date of 40.6 ± 0.8 Ma from a "basanite" from George Rocks. However, these samples are also petrographically atypical of Tasmanian Cenozoic basalts, and it is uncertain if the date is from the same occurrence. A whole rock analysis may be needed to resolve the question.

Flinders Island

Point Reid, Lady Barron (FLD1)

Boulders of grey to bluish-green, massive dolerite are present on the west side of Point Reid at Lady Barron, and the eastern end of the adjoining beach. The dolerite is massive with pyroxene up to 2–3 mm, but mostly finer-grained. Although the magnetic field in the vicinity is affected by likely Cainozoic basalt just offshore, the locality lies on the extrapolation of a linear anomaly, well defined between about 1 km (near Vinegar Hill) and 4 km to the northeast. This probably represent a dyke trending at about 050°.

A thin section (sample FLD1) is a nearly aphyric, fine- to medium-grained dolerite with a subophitic texture. The primary mineralogy consisting of laths of turbid plagioclase (mostly 200–500 µm) partially enveloped by granules of pinkish titaniferous augite, together with abundant small equant angular opaque granules (≤80 mm). One or two percent brown hornblende is present, mostly as marginal replacements of augite, which is more commonly partly replaced by pale green chlorite, actinolite and possible epidote. Titanite partly replaces the opaque grains. Some anhedral aggregates of chlorite, up to 1 mm across, more resemble amygdale fillings rather than pseudomorphs after olivine.

Yellow Beaches, east of Lady Barron (FLD3, 43943)

A large (15–20 m wide) dyke of black, aphyric and coarse-grained dolerite (≤5 mm at the dyke centre) intrudes the Lady Barron Granite on the headland between Yellow Beaches and White Beach. Diffuse banding is discernible within the dyke for up to 0.3 m from, and parallel to, the western contact, which is sharp, straight and strikes 025° vertical. A subvertical aplite dyke, 25–30 mm wide and striking~105° but slightly wavy, originates in the granite and transects the dolerite. A few narrower (5–10 mm) aplite veinlets, more irregular in direction, also cut the dolerite, but do not extend far into the granite. These features may suggest some re-melting of the granite by the dolerite, but elsewhere the contacts are sharp and lack associated aplite.

The locality lies on a strong linear aeromagnetic anomaly with the same trend (~025°), traceable for about 4 km. Inland (NNE) the dyke is likely to be concealed beneath sand cover, but offshore (SSE) it may outcrop on Little Green Island. In both directions the anomaly becomes lost in short wavelength anomalies probably due to Cainozoic basalt.

A thin section (sample FLD3) from the main dyke consists mainly of a very coarsely ophitic intergrowth of stubby plagioclase laths (500 µm to 3 mm × 200–500 µm; up to An_{80}) and large platelets of titaniferous augite up to 5 mm across. Some of the augite is replaced by a finely fibrous pale yellow-green aggregate of actinolite and chlorite. Equant, angular opaque grains (≤500 µm) are mostly unaltered, but some fine-grained anhedral titanite is also present.

A sample (43943) collected by J. D. Cocker from "east of Lady Barron township" is probably from the cross-cutting aplite dyke. In hand specimen it consists of sparsely distributed small (≤ 2 mm) cream phenocrysts of feldspar in a slightly greenish pale grey fine-grained groundmass. A faint wavy anastomosing hair-line foliation is defined by a dark mineral.

In thin section, this is a feldspathic rock with a few subhedral phenocrysts of plagioclase (≤2 mm) in a mosaic (~100–250 µm) of plagioclase, potash feldspar, rare glomerocrysts of epidote and scattered grains of well-crystallised titanite. The foliation is due to shreds of finely fibrous, turbid (?) actinolite.

White Beach, east of Lady Barron (FLD2)

About 200 m to the east, and 80 m from the northern end of White Beach, a narrower (0.5–0.6 m) dyke of dolerite strikes ~175° vertical within equigranular medium- to coarse-grained biotite granite (Lady Barron Granite). The dyke locally displays chilled margins against sharp contacts, which are slightly wavy on a scale of 50–200 mm over 1–2 m. Elsewhere the dolerite is aphyric, black with a purplish to greenish weathering patina, and well-jointed. The main joint set (055SE77) is oblique to the trend of the dyke. Any associated aeromagnetic anomaly is not resolvable from that caused by the thicker dyke (FLD3) and given the divergent trends, this dyke may be a minor offshoot.

In thin section (sample FLD2) is a medium-grained dolerite, mineralogically similar to FLD1, but lacking hornblende. It consists of a generally intergranular intergrowth of plagioclase laths (≤1 mm), titaniferous augite partly replaced by chlorite and actinolite, and small opaque grains largely replaced by titanite.

Badger Corner (77/908)

Two dolerite dykes, each about 1–2 m wide, intrude the Mathinna Supergroup on the foreshore near the boat ramp at Badger Corner (~601450mE, 5545660mN and ~601380mE, 5545720 mN), and a third dyke of similar dimensions crops out on the foreshore about 400 m further north (~601300mE, 5546100mN) (M. J. Vicary, pers. comm.). There are no clearly associated aeromagnetic anomalies, although short wavelength anomalies, probably due to Cainozoic basalt, lie just offshore.

A sample (77/908) was collected by D. J. Jennings in 1977, probably from the dyke nearest the boat ramp. In thin section, it is a coarse-grained dolerite with a porphyritic to seriate texture. Phenocrysts of plagioclase (up to 4 mm × 2 mm) grade into a meshwork of smaller plagioclase laths (typically 1 mm × 200 µm), subophitically intergrown with actinolite and pale finely fibrous reddish-brown pleochroic biotite. Some relict, turbid augite is present. Opaque grains are ragged to skeletal but little altered. A small xenolith (~5 mm) of polycrystalline quartz is present.

Although classified as a tholeiitic dyke, the potassium content (1.36% K_2O) is higher than other dykes of this type, and is consistent with the presence of biotite.

Cannes Hill (3 km NNE of Whitemark) (R013341)

A sample collected by T. Methorst from this locality, although described as Tertiary basalt, has the petrographic and geochemical characteristics of dolerite. The locality lies directly over one of several well-defined, parallel, slightly arcuate NE- to NNE-trending (~015°–040°) linear aeromagnetic anomalies, up to 25 km long, that transect central Flinders Island, almost coast-to-coast, and are therefore attributed to dykes of this rock type.

The sample (R013341) is a coarse- to very coarse-grained dolerite with an intergranular to slightly subophitic texture. A few plagioclase phenocrysts (up to 7 × 1.5 mm) grade down to laths (typically 500 µm to 2 mm long), between which are platelets of titaniferous augite (typically 1–2 mm across). Plagioclase is slightly turbid, and about 30% of the augite is altered to fibrous yellow-green actinolite and darker green chlorite, but equant, angular to somewhat elongate opaque grains are little altered. Probable melt inclusions in the plagioclase phenocrysts are replaced by fine-grained actinolite (?). Minor secondary carbonate is present.

Long Point (77/907)

This sample was collected by D. J. Jennings from near the tip of Long Point, about 3.5 km west of Flinders Island airport. No field observations are recorded, but the local country rock is Mathinna Supergroup. A weak linear aeromagnetic anomaly trending at about 015º through the locality suggests a dyke. Much stronger short wavelength anomalies due to Cainozoic basalt lie to the west, south and east.

In thin section, the sample (77/907; Fig 8c) is a coarse-grained dolerite resembling sample FLD3 from near Lady Barron, although more altered. Stubby plagioclase laths typically 1–2 mm long, but grading to microphenocrysts 3–5 mm long, are ophitically to subophitically intergrown with titaniferous augite platelets 1–3 mm across. Plagioclase is slightly turbid, but 50–60% of the

augite is replaced to a finely fibrous intergrowth of pleochroic yellow to green actinolite and subordinate chlorite. Opaque grains are generally equant to angular, 400 µm to 1 mm across, with only slight alteration to titanite.

Stanley Point (FLD4, R014365)
Near the northern tip of Flinders Island, a vertical dyke about 0.7 m wide striking ~095° lies subparallel to joints in the enclosing Palana Granite. The dyke locally jumps sinistrally by up to 2 m, and at its western end it narrows, diverges to ~230°, anastomoses and pinches out. Another narrower (~0.2 m) subparallel dyke (~100°) lies about 2.5 m north of the main dyke, and pinches out to the east.

The host granite is medium- to coarse-grained, sparsely to variably porphyritic with potash feldspar phenocrysts (≤40 mm) locally defining a foliation at ~015°, and is cut by occasional aplite dykes. Enclaves, some of which are gneissic and probably metasedimentary, tend to have long axes aligned to the phenocryst foliation.

The dyke (sample FLD4; Fig. 8k) contains randomly oriented narrow plagioclase laths (200 µm to 1 mm long) and euhedral olivine phenocrysts (≤1 mm but commonly 150–500 µm), now almost entirely altered to a fibrous length-slow, moderate birefringence secondary mineral, possibly anthophyllite. The groundmass contains very abundant small prisms of deep pink titaniferous augite (≤500 µm but more commonly 100–200 µm) and abundant small (50–100 µm) opaque grains in a base of plagioclase and possibly alkali feldspar. Some of the titaniferous augite grains are partly (at their margins) or wholly replaced by deep orange-red kaersutitic amphibole. A few small (≤1 mm) irregular patches of very fine-grained poorly crystalline and partly altered material are present within the groundmass. Minor secondary carbonate is present.

Another sample (R014365) is similar, with larger (≤1.5 mm) and less altered olivine phenocrysts in a slightly coarser-grained groundmass.

This dyke is petrographically distinct from other dolerite dykes, and also differs in its strongly alkalic chemistry, particularly high Nb. It has similarities to certain Tasmanian Cenozoic alkali basalts (e.g., some nepheline hawaiites), but the characteristics of low MgO and Mg#, high K_2O and K_2O/Na_2O, and relatively high Al_2O_3 are, taken together, difficult to match with any known basalt. In addition, none are known to contain kaersutite. An affinity to the Cenozoic basalts of the nearby Killiecrankie area (Sutherland & Kershaw, 1971) cannot be excluded, but it is more likely that this dyke belongs to a different suite of unknown age.

Cape Barren Island

In addition to five samples from the eastern part of the Cape Barren Island collected in 2005, thirteen samples of mafic dykes, mainly from the western part, were collected by J. D. Cocker but described only in general terms (Cocker, 1980). Thin sections of the latter, where available, have been retrieved from the University of Tasmania collection and are described below, but no geochemical data are available from them.

The coordinates quoted by Cocker (1980) are approximate, due to inaccuracies in the topographic base map, but in most cases sample locations can be reliably identified with particular mafic dykes shown on Cocker's map, his figure E1.

Apple Orchard Point (BA3)
Dark to pale grey pelite and very fine-grained sandstone, assigned to the Mathinna Supergroup, are sporadically exposed on the north-west coast of Cape Barren Island from Apple Orchard Point to about 2 km east of Kenneth Point. The sequence is folded into a series of upright, gently NNE-plunging anticlines and synclines with a half wavelength of 500–1500 m.

On the south side of Apple Orchard Point, a poorly outcropping, sparsely porphyritic dolerite dyke and a small body of quartz feldspar porphyry intrude gently W- to NW-dipping, thick- to medium-bedded dark grey spotted siltstone. There is no obvious aeromagnetic anomaly associated with the dolerite, although there are numerous short wavelength anomalies in the area, probably caused by Cainozoic basalt just offshore.

The dolerite (sample BA3; Fig. 8p) is relatively fresh and fine-grained with a microporphyritic texture. Abundant narrow laths of fresh to slightly altered plagioclase (typically 300–600 µm × 50–100 µm) and generally slightly smaller (200–400 µm) prisms of pinkish titaniferous augite are locally aligned to define a flow lamination. There are also small rhombic microphenocrysts (≤200 µm) across of probable former olivine, now replaced by finely granular yellow-green chlorite. Rather sparsely disseminated, equant angular opaque grains (≤50 µm) are partly replaced by turbid titanite. The groundmass consists of smaller (~50 µm) prisms of similar titaniferous augite and a feldspathic mesostasis. Some potash feldspar is probably present.

Riddles Bay (BA5, BA6)

At least two dolerite dykes crop out poorly on the foreshore near the mid-point of Riddles Bay. On images derived from aeromagnetic data, the area coincides with a rather diffuse anomaly which lies on a rather weak linear trending offshore for about 3 km at ~010°. Several similar subparallel lineaments cross the coast further east (notably near FR065343), but are not known to be associated with dykes.

The larger dyke is about 6 m wide, but poorly exposed. About 150 m further west another, marked mainly by a line of rounded boulders, appears to be a few metres wide and striking at about 010°, roughly parallel to the regional fold axes.

In thin section, the larger dyke (sample BA5) is a relatively fresh coarse-grained dolerite with a well-developed subophitic to ophitic texture. Plagioclase ranges from oblong phenocrysts up to 3 mm long, to a meshwork of stubby laths (mostly 200–500 µm long), enveloped or partly enveloped by platelets of mostly clear to somewhat turbid colourless augite up to 2 mm across. Sparse (six or seven in the thin section) possible phenocrysts (≤1.5 mm) after olivine are now replaced by pale yellow-green chlorite and turbid carbonate. Scattered, generally ragged opaque grains range from equant and angular (50–200 µm) across to strongly elongate. Secondary actinolite, prehnite and titanite (in addition to chlorite and carbonate) are also present.

The other dyke (sample BA6) is aphyric, more metamorphosed and has a less well-developed ophitic texture. It consists of augite granules (≤500 µm), partly altered to clear, brown to pale green pleochroic hornblende or more fibrous actinolite; turbid plagioclase (mostly 500 µm to 1 mm); pale yellow-green chlorite; small equant to skeletal opaque grains, mostly replaced by titanite; and minor interstitial clear quartz (≤300 µm). Secondary epidote and carbonate are also present. The presence of quartz is consistent with the high SiO_2 content (52.0 vs 49.7%) and crustally contaminated character of this dyke.

Nautilus Cove (BA4)

About 500 m WSW of the western headland of Nautilus Cove, a narrow (300 mm) dyke of fine-grained, dark grey to bluish-green dolerite, trending ~130°, intrudes white, sparsely porphyritic biotite granite.

The locality roughly coincides with a long (~26 km) NW–SE-trending (mean ~140°) linear magnetic anomaly extending from Passage Island, across Cape Barren Island to Franklin Sound, where it is obscured by short wavelength anomalies attributable to Cainozoic basalt.

A thin section (sample BA4) consist of an altered intergrowth of randomly aligned turbid feldspar (probably 500 µm to 1 mm), dark very turbid prisms (≤200 µm long) of altered ferromagnesian material, and elongate to acicular opaque grains (500 µm to 1.5 mm × 30–150 µm), together with numerous interstitial patches of clear anhedral quartz (≤200 µm across). The ferromagnesian mineral or minerals, possibly former clinopyroxene, is completely altered to pale green chlorite and fine-grained indeterminate material, possibly a mixture of actinolite and titanite.

Opposite Puncheon Island (BA35, 43940)

On the northeast coast of Cape Barren Island, opposite Puncheon Island, several dark grey in-weathering dykes intrude the Puncheon Point Granite. The main dyke trends at ~085°, is traceable for ~10 m, and has sharp contacts, slightly undulose on a 5–10 cm scale, with several narrow irregular offshoots into the country rock. Rare small granite xenoliths are present. About 8 m to the east are two narrower (0.7 m and 1.2 m wide) parallel dykes, with an attitude of ~085S60, separated by a 0.8 m wide screen of granite.

In thin section, a sample (BA35; Fig. 8u) from the main dyke is a seriate-textured rock with euhedral prisms (≤7 mm × 1 mm) of hornblende (α pale yellow, β and γ sea-green); tabular and strongly zoned phenocrysts (≤2 mm) of plagioclase and orthoclase, and a few microphenocrysts of titanite (≤400µm). Dark to very pale red-brown biotite may be marginal to, or form glomerocrysts with hornblende, but also occurs as separate ragged fragments. All these mineral grade downward in size to a poorly defined groundmass of about 100 µm, which also contains abundant quartz. Feldspars are fresh or very slightly turbid. Notably, opaque minerals are absent. The rock is a microgranodiorite (analysis, Table 6) and clearly belongs to a different suite.

A similar sample (43940) collected by J. D. Cocker is probably also from this locality. It consists of subhedral prisms of hornblende (α and β brown to green, γ bluish-green) up to 3 mm long and strongly zoned phenocrysts of plagioclase (≤ 2 mm) lie in a groundmass (~100–200 µm) of dark brown splinters of biotite, feldspar and quartz.

~2 km E of The Settlement (43933)

The thin section displays an intergranular texture,

consisting of unoriented plagioclase laths (~400 µm to 1 mm), pinkish titaniferous augite granules partly replaced by tremolite-actinolite and generally small (40–80 µm) equant opaques. Quartz is apparently absent.

Thunder and Lightning Bay (43934)
This fairly coarse-grained altered dolerite probably originally had a subophitic texture. Plagioclase laths (1–2 mm) are largely replaced by very fine-grained sericite ± prehnite and clinopyroxene is completely replaced by tremolite-actinolite. Large (≤500 µm) equant to irregular opaques are present, but apparently not quartz.

West of Whittling Office Bay (43935)
A sample from a dyke trending at ~050° contains rare corroded xenocrysts of quartz (≤2.5 mm) and rare possible pseudomorphs after olivine (≤500 µm), now fine-grained pale green nearly isotropic chlorite. The fine-grained intergranular feldspathic groundmass consists of plagioclase laths (typically 150–400 µm long), rather turbid pale pink titaniferous augite, titanite, small elongate to acicular opaques, and quartz.

Head of Battery Bay (43936)
This fairly coarse-grained seriate-textured rock contains plagioclase phenocrysts (≤2.5 mm), sometimes strongly zoned, and rare possible clinopyroxene phenocrysts (≤1.5 mm) now replaced by tremolite-actinolite. These grade down to a feldspathic groundmass of rather turbid plagioclase laths (typically 400 µm to 1 mm), intergranular clinopyroxene partly replaced by tremolite-actinolite, chlorite, equant to somewhat elongate opaques and common interstitial quartz.

Southeast flank of Petticoat Ridge (43937)
This relatively fresh, coarse-grained dolerite, from a dyke mapped trending ~ 075°, displays an ophitic texture. Clinopyroxene platelets, crystallographically continuous for up to 4 mm, enclose numerous plagioclase laths (typically 500 µm to 1 mm long); plagioclase also occurs as phenocrysts (≤3.5 mm) and glomerocrysts. Some large patches (≤3 mm) of fine-grained pale green ± isotropic chlorite may be pseudomorphs after olivine. Clinopyroxene shows some alteration to tremolite-actinolite, which together with very fine-grained chlorite also occurs as a mesostasis. Opaque grains (mostly 100–300 µm) are irregular to skeletal or elongate. Quartz appears to be absent.

Near Dyas Creek (?) (43938)
Sparse pseudomorphs after olivine (≤3.5 mm) are now replaced by fine-grained nearly isotropic chlorite. Turbid plagioclase phenocrysts (≤3 mm), some with mottled mantles (probably altered melt inclusions) grade to a subophitic groundmass of incipiently to partly sericitised plagioclase laths (typically 400 µm to 1 mm), partly enclosed by colourless clinopyroxene platelets (500 µm to 1.5 mm across). Equant angular opaques (~250–500 µm), interstitial very fine-grained pale green chlorite and minor actinolite are also present.

The sample location may be uncertain, as no dyke is shown on Cocker's map at the quoted coordinates.

Near Dover Point (43939)
This altered dolerite with a consertal to subophitic texture consists of turbid plagioclase (~500 µm to 1 mm), interlocking with or partly enclosed by clinopyroxene platelets (≤400 µm). Abundant equant angular opaques (mostly 100–200 µm) and interstitial quartz anhedra, pale green chlorite, minor actinolite and epidote are also present.

The coordinates quoted by Cocker (FR063363) plot offshore, but (FR063343) corresponds to a mapped dyke on the coast east of Dover Point.

North flank of Phils Hill (?) (43941)
This fine- to medium-grained dolerite contains quartz xenocrysts (≤2.5 mm) with reaction haloes, sparse plagioclase phenocrysts (≤1 mm) and probable chloritized olivine phenocrysts. These grade to an intergranular groundmass of rather turbid plagioclase laths (~250–500 µm), clinopyroxene, actinolite, chlorite, skeletal to acicular opaques partly altered to titanite, and interstitial quartz. Note that no dyke is shown on Cocker's map at his quoted coordinates.

Long Island

Eastern Long Island (43948)
This dolerite has a coarse-grained consertal texture and consists of rather turbid plagioclase laths (~1–3 mm), partly uralitised titaniferous augite, large mostly equant opaques (200–400 µm) and minor interstitial quartz.

Western Long Island (43949)
This rather coarse-grained seriate- to ophitic-textured dolerite contains a few plagioclase phenocrysts (≤4 mm) partly replaced by prehnite, which grade down to a groundmass of slightly turbid plagioclase laths (≤500 µm), ± fresh nearly colourless clinopyroxene platelets (≤1.5 mm) and mostly equant opaques (~100–200 µm).

Clarke Island

Three samples from two locations were collected by J. D. Cocker (1980).

N of Lookout Head, western Clarke Island (43951)
This porphyritic dolerite consists of scattered phenocrysts and glomerocrysts of tabular plagioclase (≤2 × 0.4 mm) and equant clinopyroxene (0.5–1 mm across, very pale yellow-green to slightly pink, biaxial positive) in a very-fine-grained groundmass of clinopyroxene rods (~100 × 10 µm), plagioclase laths (~50–100 µm long), orange-brown biotite flakes (≤ 30 µm) and abundant equant opaques (~10–15 µm across).

The glomerocrysts consist of 5–10 crystals, and may be composite with subophitically intergrown clinopyroxene and plagioclase. Plagioclase is partly sericitised, but zoning is visible in some phenocrysts. Clinopyroxene is fresh or partly altered to khaki brown-green actinolite and chlorite.

Kangaroo Bay, eastern Clarke Island (43952, 43953)
Sample 43952 contains a few corroded and deeply embayed quartz xenocrysts (≤5 mm) with reaction haloes of fine-grained clinopyroxene with some secondary carbonate, in a fine-grained feldspathic groundmass of turbid plagioclase (≤ 600 µm), sparse rod-like prisms of clinopyroxene, small equant opaques, chlorite and a trace of epidote.

Sample 43953 contains a single plagioclase phenocryst (~2 × 0.5 mm), numerous narrow crudely aligned plagioclase laths (≤500 µm long) and rare small (~200 µm) rod-like grains of clinopyroxene in a very fine-grained, almost unresolvable mesostasis, probably crystallites of plagioclase, clinopyroxene and opaques.

No dyke is shown on Cocker's map at this locality, although the quoted coordinates (FR022157) plot on the coast.

Other islands in the Furneaux Group

Mt Chappell Island (77/910)
A sample (77/910) collected by D. J. Jennings from the north coast consists of a coarse-grained intergrowth of mostly very turbid plagioclase (500 µm to 1.5 mm) and augite grains, often with very turbid brown margins, partly altered to chlorite, actinolite and minor epidote. Large (~100–250 µm) equant to elongate, sometimes skeletal opaque grains are little altered. Some interstitial clear anhedral quartz and minor secondary carbonate are present.

Northeastern Badger Island (43966, 43967, 43968)
At least three dykes with strikes of ~055° to 070° intrude the Badger Head Granodiorite (Cocker 1980).

Sample 43966 is an aphyric, even-textured, intergranular to subophitic rock consisting of very turbid plagioclase laths (≤1 mm), mostly unaltered clinopyroxene (200–500 µm) and interstitial chlorite, epidote, quartz and fairly large (150–400 µm) irregular to equant opaques.

Sample 43967 is similar but finer-grained; equant opaques are altered to finely granular titanite.

Sample 43968 contains sparse plagioclase phenocrysts (≤3 mm), partly replaced by carbonate, in a similar fine-grained intergranular groundmass of turbid plagioclase, pinkish titaniferous augite, chlorite and equant opaques largely replaced by titanite.

Western Badger Island (43969)
Cocker (1980) shows a dyke, trending ~ 020°, intruding the Mathinna Supergroup. The thin section displays a consertal to intergranular texture of turbid altered plagioclase laths (≤2 mm, usually smaller), interlocking pale pink to nearly colourless clinopyroxene and irregular to skeletal or elongate opaques, with interstitial chlorite, tremolite-actinolite and quartz.

South of Lucy Point, southeastern Badger Island (43970, 43972)
A dyke trending ~035° intrudes the Badger Island Granodiorite, and another at ~050° the Mathinna Supergroup near the granite contact (Cocker, 1980). Both consist of turbid plagioclase, relatively clear clinopyroxene, opaques, chlorite, tremolite-actinolite and traces of quartz and epidote, similar to the other dykes on the island.

Additional samples from Cape Barren Island

Prior to finalisation of this report, the following three previously unregistered and undocumented samples, collected by D. J. Jennings, were noticed in the MRT collection. Thin sections have been prepared, but geochemical data are not available at the time of publication.

Eastern side of Cone Point (R014343) (~618600mE, 5517300mN)
This dark grey aphyric dolerite intrudes granite on the southeastern coast of Cape Barren Island. In thin section it displays a dominantly seriate to intergranular texture, but with considerable variations in grain size. It consists mainly of slightly to moderate turbid plagioclase laths (≤800 µm long), largely fresh titaniferous augite prisms (up to 800 µm long but more commonly <250 µm), abundant equant angular opaque grains (mostly 40–80 µm), and abundant fine-grained khaki-brown to green

interstitial alteration products, probably mostly chlorite and actinolite, and possibly in part replacing olivine. Small angular to pseudohexagonal grains of pleochroic dark red-brown kaersutitic amphibole (≤50 µm across) are mostly associated with augite and opaque grains.

This specimen resembles those of the dyke from Stanley Point near the northern tip of Flinders Island (samples FLD4, R014365; Fig. 8k), although it lacks unaltered olivine. It is probably also an alkali dolerite and may belong to the same suite.

The location is coincident with one of at least four NE-SW-trending magnetic lineaments that extend across eastern and central Cape Barren Island (Fig. 3a). This sample, however, is dissimilar to sample BA4 from Nautilus Cone, which is coincident with another anomaly of similar trend.

Cape Sir John, eastern dyke (R014344) (584500mE, 5524800mN)

This massive grey coarse-grained aphyric dolerite intrudes Mathinna Supergroup sedimentary rocks on a shore platform. This is probably the same dyke mapped by Cocker (1980).

In thin section it displays a medium- to coarse-grained subophitic texture, and consists mainly of fresh to slightly altered laths (typically 1–4 mm long) and zoned subhedra of plagioclase, mostly altered clinopyroxene grains (typically 1–2 mm across), and sparse, elongate to skeletal or irregular opaque grains (~0.5–1.5 mm long). Some fresh cores of colourless augite, surrounded by colourless to pale brown prismatic tremolite-actinolite, are present, but clinopyroxene is largely replaced by fine-grained pale yellow-green "uralite." Quartz is absent.

Cape Sir John, western dyke (R014345) (584000mE, 5525000mN)

A pale grey-green medium-grained dolerite intrudes granodiorite on the shore platform about 500 m west of the eastern dyke (R014344). In thin section it displays a subophitic to intergranular texture, consisting mostly of plagioclase laths (mostly 0.5–1 mm long), largely uralitised clinopyroxene grains (mostly ≤1 mm) with some relict pale pink weakly titaniferous augite, and scattered, equant and angular to elongate or skeletal opaque grains (~200–500 µm). A few round possible amygdales (≤1 mm across) are also filled with "uralite." There are a few resolvable patches of pale green, nearly isotropic chlorite. Quartz is absent.

Both dykes at Cape Sir John (R014344 and R014345) are petrographically similar to tholeiitic dykes from elsewhere in the Furneaux Group and northeastern Tasmania.